

AN INVESTIGATION OF THE GROWTH AND FEEDING RESPONSES OF  
OLIGOTRICH CILIATES TO FOOD TYPES AND CONCENTRATIONS: AN APPROACH  
TO ASSESSING THE POTENTIAL OF MARINE PLANKTONIC CILIATE BLOOMS

by

DAVID JOSEPH SELWYN MONTAGNES

B.Sc., The University of Guelph, 1983  
M.Sc., The University of Guelph, 1986

A THESIS SUBMITTED IN PARTIAL FULFILLMENT OF  
THE REQUIREMENTS FOR THE DEGREE OF  
DOCTOR OF PHILOSOPHY

in

THE FACULTY OF GRADUATE STUDIES  
(Department of Oceanography)

We accept this thesis as conforming  
to the required standard

THE UNIVERSITY OF BRITISH COLUMBIA

September 1993

©David Joseph Selwyn Montagnes, 1993

In presenting this thesis in partial fulfilment of the requirements for an advanced degree at the University of British Columbia, I agree that the Library shall make it freely available for reference and study. I further agree that permission for extensive copying of this thesis for scholarly purposes may be granted by the head of my department or by his or her representatives. It is understood that copying or publication of this thesis for financial gain shall not be allowed without my written permission.

(Signature)

Department of Oceanography

The University of British Columbia  
Vancouver, Canada

Date SEPT 28<sup>TH</sup> 93

## ABSTRACT

Planktonic ciliates consume small phytoplankton and can be important in the transfer of carbon through food webs. This study examined the impact of clonal ciliate populations on short term algal blooms. Numerical and functional responses (growth and grazing rates with varied food concentration) were established for 5 marine planktonic ciliates and were used in a model to examine predator-prey dynamics of ciliates and 8  $\mu\text{m}$  algae. The ciliates *Strombidinopsis acuminatum*, *Strobilidium spiralis*, *Strobilidium* sp., *Strombidium acuminatum*, and *Strombidium capitatum* were isolated from British Columbian waters and maintained in culture. Ciliates were fed the flagellates *Isochrysis galbana*, *Chroomonas salina*, *Rhodomonas lens*, and the diatom *Thalassiosira pseudonana*, individually or in combinations. Numerical responses were obtained by keeping ciliates in semi-continuous culture, measuring growth rates and fitting them to a modified Michaelis-Menten function; this provided both growth and mortality rates. Species specific differences existed in numerical response parameters. Functional responses were measured by observing the uptake of fluorescently labeled *C. salina* or 5  $\mu\text{m}$  beads. This was a poor method: when measured grazing rates were compared to those predicted by a bioenergetic formula, the measured rates either over or underestimated predicted rates by several fold. Functional responses were determined using 1) the bioenergetic formula  $\text{Ingestion} = (\text{growth} + \text{respiration}) / \text{assimilation efficiency}$ , and 2) volume specific respiration rates.

Ciliate functional and numerical responses from this and other studies were compared, and 3 responses were established. These were used in a model which simulated ciliate-algal population dynamics in a non-steady state, where ciliates and copepods encountered a patch of water with a defined initial algal concentration. The model indicated: 1) ciliates bloom over 10-20 d, when copepods are rare ( $< 1 \text{ L}^{-1}$ ) and algae are initially abundant ( $> 10^3 \text{ mL}^{-1}$ ); 2) ciliate blooms can provide 40-50% of the carbon available to copepods, but when copepods are abundant and initial algal levels low, ciliates are not an important carbon source; 3) under "typical" conditions ( $10^3$  algae  $\text{mL}^{-1}$ , 1 copepod  $\text{L}^{-1}$ ), ciliates are a link to copepods, but primary production is low; 4) bloom dynamics and carbon flow through the food web are dependent on the ciliate species present. In general, ciliates may be, under transient conditions, important as both links and sinks of carbon, but under "typical" coastal conditions, ciliates are not important components of food webs.

## TABLE OF CONTENTS

ABSTRACT	ii
TABLE OF CONTENTS	iii
LIST OF TABLES	vii
LIST OF FIGURES	viii
ACKNOWLEDGMENTS	xii
CHAPTER 1	INTRODUCTION: OLIGOTRICH CILIATES AS FEAST AND FAMINE ORGANISMS
	1
CHAPTER 2	THE SALIENT FEATURES OF ONE UNDESCRIBED SPECIES AND REDESCRIPTION OF FOUR SPECIES IN THE CLASS SPIROTRICHEA (CILIOPHORA, OLIGOTRICHIA) WITH NOTES ON THE CULTURING AND BEHAVIOUR OF THESE SPECIES
	5
	Introduction
	5
	1.0 Materials and Methods
	6
	1.1 Isolation and General Culturing
	6
	1.2 Fixation and Staining
	7
	1.3 Measurements
	7
	2.0 Results and Discussion
	7
	2.1 General Taxonomy
	7
	2.2 Description of Species
	8
	2.2.1 Strobilidiid Ciliates
	8
	2.2.2 Strombidiid Ciliates
	12
	2.2.3 Strombidinopsid Ciliates
	14
CHAPTER 3	GROWTH AND GRAZING RATES OF <i>Strombidinopsis acuminatum</i> STRAIN SPJSC AS A FUNCTION OF FOOD CONCENTRATION
	26
	Introduction
	26
	PART I GROWTH RATES: Estimating the Numerical Response
	26
	1.0 General Methods
	26
	1.1 First Set of Experiments
	28
	1.1.1 Methods
	28
	1.1.2 Results and Discussion
	29
	1.1.2.1 Consistency of Growth Rate
	29
	1.1.2.2 Consistency of Prey Concentration
	29
	1.1.2.3 Numerical Response
	29
	1.2 Second Set of Experiments
	30
	1.2.1 Methods
	30
	1.2.2 Results and Discussion
	30
	1.3 Third Set of Experiments
	31
	1.3.1 Methods
	31
	1.3.2 Results and Discussion
	31
	2.0 Conjugation of Strain SPJSC
	33
	3.0 An Estimate of the Inheritance of Growth Rate
	34
	3.1 Methods
	34



	3.2 Results and Discussion	34
	4.0 Sources of Bias and Explanations of Methods	37
	4.1 Mortality	37
	4.2 Handling of Ciliates	37
	4.3 Food Quality	38
	5.0 Aspects of the Growth Rates and their Ecological Relevance	38
	6.0 A Numerical Response Model	39
	PART II GRAZING RATES: Estimating the Functional Response	40
	7.0 General Methods	40
	7.1 Results and Discussion	41
	7.2 Modeling the Response	42
	CONCLUDING REMARKS	42
CHAPTER 4	GROWTH AND GRAZING RATES OF <i>Strobilidium spiralis</i> STRAIN IA AS A FUNCTION OF FOOD CONCENTRATION	52
	Introduction	52
	PART I GROWTH RATES: Estimating the Numerical Response	52
	1.0 General Methods	52
	2.0 Results	53
	3.0 Change in Culture Growth Rate Over Time	54
	4.0 Examining the Growth Estimates and Developing a Numerical Response Model	56
	5.0 Aspects of the Growth Rates and Their Ecological Relevance	57
	PART II GRAZING RATES: Estimating the Functional Response	57
	6.0 General Methods	57
	7.0 Results, Discussion and Modeling the Response	59
	CONCLUDING REMARKS	59
CHAPTER 5	GROWTH AND GRAZING RATES OF <i>Strobilidium</i> sp. STRAIN JERC AS A FUNCTION OF FOOD CONCENTRATION	67
	Introduction	67
	PART I GROWTH RATES: Estimating the Numerical Response	67
	1.0 General Methods	67
	2.0 Results and Discussion	68
	2.1 General	68
	2.2 Numerical Response	69
	3.0 Aspects of the Growth Rates and Their Ecological Relevance	70
	PART II GRAZING RATES: Estimates of the Functional Response	70
	4.0 General Methods	70
	5.0 Results and Discussion	72
	CONCLUDING REMARKS	73
CHAPTER 6	GROWTH AND GRAZING RATES OF <i>Strombidium acuminatum</i> Strain BJSCH AS A FUNCTION OF FOOD CONCENTRATION	78
	Introduction	78

	PART I GROWTH RATES: Estimating the Numerical Response	78
	1.0 General Methods	78
	2.0 Results and Discussion	80
	2.1 General	80
	2.2 Numerical Response	80
	3.0 Aspects of the Growth Rates and Their Ecological Relevance	80
	PART II GRAZING RATES: Estimating the Functional Response	81
	4.0 General Methods	81
	5.0 Results and Discussion	82
	6.0 Swimming Behaviour	82
	CONCLUDING REMARKS	83
CHAPTER 7	GROWTH RATES OF <i>Strombidium capitatum</i> STRAIN APAG AS A FUNCTION OF FOOD CONCENTRATION	89
	Introduction	89
	PART I GROWTH RATES: Estimating the Numerical Response	89
	1.0 General Methods	89
	2.0 Results and Discussion	90
	3.0 Aspects of the Growth Rates and Their ecological Relevance	90
	PART II GRAZING RATES	91
	4.0 A Discussion of Grazing Experiments.	91
CHAPTER 8	AN EXAMINATION OF THE FUNCTIONAL AND NUMERICAL RESPONSES OF OLIGOTRICHS	95
	Introduction	95
	1.0 Reasons for Response Variation	95
	1.1 Methodological Biases and the Use of Steady State Measurements	95
	1.1.1 Methodological biases	95
	1.1.2 The Use of Steady State Measurements	96
	1.2 Use of Surrogate Particles to Determine Grazing Rates	98
	1.3 Physiological-Behavioural Variables	100
	1.4 Species Differences	103
	2.0 Ciliate Growth and Grazing Responses for Food Web Modeling	103
CHAPTER 9	A MODEL OF CILIATE AND PHYTOPLANKTON POPULATION DYNAMICS	116
	Introduction	116
	1.0 The Model (see Appendix 4)	117
	1.1 General Description	117
	1.2 Constraints	118
	1.3 Parameters and Rate Equations	118
	1.3.1 Ciliates	118
	1.3.2 Copepod	118
	1.4 Variables	120
	1.5 A Summary of Assumptions	120
	1.6 Equations	120

2.0 Results of the Model and Discussion of their Implications	122
2.1 Ciliate Blooms Control Blooms of Small Phytoplankton	122
2.2 Ciliates can Bloom Over 10 to 20 Day Periods	124
2.3 Ciliates Are Both a Link and Sink, and Ciliates Can Compete With Copepods	125
2.4 Species Differences Are Important	128
2.5 How Ciliate Blooms Influence Carbon Flow to Copepods	129
CONCLUDING REMARKS	130
LITERATURE CITED	143
APPENDIX 1	THE GROWTH MEDIUM USED IN THIS STUDY TO GROW BOTH CILIATES AND PHYTOPLANKTON 153
APPENDIX 2	CONSUMPTION AND FILTRATION: Their Derivation and Application. 155
APPENDIX 3	THE ANNUAL CYCLE OF OLIGOTRICHS AND $< 10 \mu\text{M}$ PHYTOPLANKTON IN SECHELT INLET, A BRITISH COLUMBIAN FJORDAL SYSTEM 158
APPENDIX 4	THE CODE FOR A BASIC MODEL TO INVESTIGATE THE ROLE OF CILIATES AS GRAZERS OF SMALL PHYTOPLANKTON 172

## LIST OF TABLES

Table 3.1. Growth and grazing data for <i>Strombidinopsis acuminatum</i> strain SPJSC; parameters and estimates of error of the numerical and functional response equations presented in Figs. 3.3-3.6.	44
Table 3.2. The increase in cell numbers and survival of cell lines of <i>Strombidinopsis acuminatum</i> strain SPJSC.	45
Table 4.1. The relative growth rate of <i>Strobilidium spiralis</i> strain IA over a 2 and a 4 day period when fed on all the combinations of the three prey: <i>Isochrysis galbana</i> , <i>Chroomonas salina</i> and, <i>Rhodomonas lens</i> .	61
Table 4.2. Growth and grazing parameters for <i>Strobilidium spiralis</i> strain IA; parameters and estimates of error of the numerical and functional response curves presented in Figs. 4.1 and 4.4.	62
Table 5.1. The relative growth rate of <i>Strobilidium</i> sp. strain JERC over a 5 day period when fed on all the combinations of the three prey: <i>Isochrysis galbana</i> , <i>Chroomonas salina</i> , and <i>Rhodomonas lens</i> .	74
Table 5.2. Growth and grazing parameters for <i>Strobilidium</i> sp. strain JERC; parameters and estimates of error of the numerical and functional response curves presented in Figs. 5.1 and 5.2.	75
Table 6.1. The relative growth rate of <i>Strombidium acuminatum</i> strain BJLSC over a 4 day period when fed on all the combinations of the three prey: <i>Isochrysis galbana</i> , <i>Chroomonas salina</i> , and <i>Rhodomonas lens</i> .	84
Table 6.2. Growth and grazing parameters for <i>Strombidium acuminatum</i> strain BJLSC; parameters and estimates of error of the numerical and functional response curve presented in Figs. 6.1 and 6.2.	85
Table 7.1. The relative growth rate of <i>Strobilidium capitatum</i> strain APAG over a 7 day period when fed on all the combinations of the three prey: <i>Isochrysis galbana</i> , <i>Chroomonas salina</i> , and <i>Rhodomonas lens</i> .	92
Table 7.2. Growth parameters for <i>Strombidium capitatum</i> strain APAG; parameters and estimates of error of the numerical response curve presented in Fig. 7.1.	93
Table 8.1. A comparison of numerical response constants for 10 oligotrichs.	105
Table 8.2. A comparison of functional response constants for 8 oligotrichs.	106
Table 8.3. A comparison of error estimates of numerical and functional responses (coefficients of variation) from data of the five species presented in Chapters 3-7.	107
Table 8.4. Parameters used to establish ciliate numerical response curves for use in the model of ciliate-prey population dynamics in Chapter 9.	108
Table 9.1. Parameters and variables used in the model of ciliate-phytoplankton interactions.	133

## LIST OF FIGURES

Fig. 2.1. Schematic diagram of <i>Strobilidium spiralis</i> (Leegaard, 1915) Lynn and Montagnes, 1988 strain IA from protargol stains and augmented by electron microscope observations.	17
Fig. 2.2. Electron micrographs of <i>Strobilidium spiralis</i> (Leegaard, 1915) Lynn and Montagnes, 1988 strain IA.	18
Fig. 2.3. Schematic diagram of <i>Strobilidium</i> sp. strain JERC from protargol stains and augmented by electron microscope observations.	19
Fig. 2.4. Electron micrographs of <i>Strobilidium</i> sp. strain JERC.	20
Fig. 2.5. Schematic diagram of <i>Strombidium capitatum</i> (Leegaard, 1915) Montagnes <i>et al.</i> 1988.	21
Fig. 2.6. Schematic diagram of <i>Strombidium acuminatum</i> , (Leegaard, 1915) Kahl, 1932 strain BJSC from protargol stains and augmented by electron microscope observations.	22
Fig. 2.7. Electron micrographs of <i>Strombidium acuminatum</i> , (Leegaard, 1915) Kahl, 1932 strain BJSC.	23
Fig. 2.8. Schematic diagram of <i>Strombidinopsis acuminatum</i> Fauré-Fremiet, 1924 strain SPJSC from protargol stains and augmented by electron microscope observations.	24
Fig. 2.9. Electron micrographs of <i>Strombidinopsis acuminatum</i> Fauré-Fremiet, 1924 strain SPJSC.	25
Fig. 3.1. The variability of growth rate of <i>Strombidinopsis acuminatum</i> strain SPJSC at nine prey concentrations over a nine day period.	46
Fig. 3.2. An indication of the variability of food concentration during growth experiments on <i>Strombidinopsis acuminatum</i> strain SPJSC, over a five day period.	47
Fig. 3.3. The numerical response of <i>Strombidinopsis acuminatum</i> strain SPJSC from three separate experiments.	48
Fig. 3.4. The change in growth rate with number of generations for <i>Strombidinopsis acuminatum</i> strain SPJSC grown on saturating food concentrations.	49
Fig. 3.5. The numerical response of <i>Strombidinopsis acuminatum</i> strain SPJSC from a combination of three experiments; the distribution of the residuals for the Michaelis-Menten fit to all the data in Fig. 3.5a; and the distribution of the residuals for the Michaelis-Menten fit to a subset of the data in Fig. 3.5a.	50
Fig. 3.6. The change in number of fluorescent beads ingested by <i>Strombidinopsis acuminatum</i> strain SPJSC over time (at two bead concentrations), and the functional response of strain SPJSC ingesting fluorescent beads.	51

Fig. 4.1. The numerical response of <i>Strobilidium spiralis</i> strain IA grown on the prey flagellate <i>Chroomonas salina</i> .	63
Fig. 4.2. The change in culture growth rate of <i>Strobilidium spiralis</i> strain IA over time.	64
Fig. 4.3. The number of beads ingested by <i>Strobilidium spiralis</i> strain IA over time.	65
Fig. 4.4. The functional response of <i>Strobilidium spiralis</i> strain IA ingesting a 1:1 ratio of 5 $\mu$ m fluorescent beads and <i>Chroomonas salina</i> .	66
Fig. 5.1. The numerical response of <i>Strobilidium</i> sp. strain JERC growing on a 1:1 ratio of the prey flagellates <i>Chroomonas salina</i> and <i>Isochrysis galbana</i> .	76
Fig. 5.2. The functional response of <i>Strobilidium</i> sp. strain JERC ingesting a 1:1 ratio of stained and live <i>Chroomonas salina</i> .	77
Fig. 6.1. The numerical response of <i>Strombidium acuminatum</i> strain BJLSC growing on two different diets: 1) the diatom <i>Thalassiosira pseudonana</i> and 2) a 1:1:1 combination of the three flagellates <i>Isochrysis galbana</i> , <i>Chroomonas salina</i> , and <i>Rhodomonas lens</i> .	86
Fig. 6.2. The functional response of <i>Strombidium acuminatum</i> strain BJLSC grazing on a 1:1 mixture of the diatom <i>Thalassiosira pseudonana</i> and 5 $\mu$ m fluorescent beads.	87
Fig. 6.3. The change in position (in the water column vs. on a surface) of <i>Strombidium acuminatum</i> strain BJLSC at different prey ( <i>Thalassiosira pseudonana</i> ) concentrations.	88
Fig. 7.1. The numerical response of <i>Strombidium capitatum</i> strain APAG growing on a 1:1 ratio of the two flagellates <i>Isochrysis galbana</i> and <i>Chroomonas salina</i> .	94
Fig. 8.1. The growth rate (numerical response) of 10 oligotrichs in response to varied prey concentration, as prey numbers and prey carbon.	109
Fig. 8.2. The grazing rate (functional response) of eight oligotrichs in response to varied prey concentration, as numbers and prey carbon.	110
Fig. 8.3. A comparison of observed grazing rates and those predicted from equation 3 (Chapter 8), using growth rates predicted by values presented in Chapters 3-6, equation 1 (Chapter 3), and equation 3 (Chapter 8).	111
Fig. 8.4. A comparison of gross growth efficiencies based on observed growth and grazing data and those based on observed growth and predicted grazing rates (predicted grazing rates were determined using equation 3 in Chapter 8 and growth rates predicted by values presented in Chapters 3-6 and equation 1, Chapter 3).	112
Fig. 8.5. The growth rate of 10 oligotrichs in response to varied prey concentration, corrected for differences in cell volume and ambient temperature.	113

Fig. 8.6. The grazing rate of eight oligotrichs in response to varied prey concentration, corrected for differences in cell size and ambient temperature.	114
Fig. 8.7. Three growth responses used to represent different ciliate types (A-C). These responses were used to model ciliate-nanoplankton prey interactions in Chapter 9.	115
Fig. 9.1. A schematic diagram of the food web model described in Appendix 4.	134
Fig. 9.2. Output from the model of ciliate-phytoplankton dynamics (Appendix 4): the effect of variations in initial algal concentration and constant copepod abundance on the formation and peak magnitude of ciliate blooms.	135
Fig. 9.3. Output from the model of ciliate-phytoplankton dynamics (Appendix 4): five examples of bloom development over 20 days and the flow of carbon during those 20 days.	136
Fig. 9.4. Output from the model of ciliate-phytoplankton dynamics (Appendix 4): the effect of variations of initial algal concentration and constant copepod abundance on gross ciliate production and gross primary production over a 20 day simulation.	137
Fig. 9.5. Output from the model of ciliate-phytoplankton dynamics (Appendix 4): the effect of variations in initial algal concentration and constant copepod abundance on four bloom parameters measured over the 20 day simulation: 1) (algae consumed by copepods)/(algae produced); 2) (algae consumed by ciliates)/(algae produced); 3) (ciliates consumed by copepods)/(ciliates produced); and 4) (ciliates consumed by copepods)/(ciliates consumed by copepods + algae consumed by copepods).	138
Fig. 9.6. Output from the model of ciliate-phytoplankton dynamics (Appendix 4): the effect of variations in initial algal concentration and constant copepod abundance on algae carbon eaten by copepods and algae carbon eaten by ciliates over the 20 day simulation.	139
Fig. 9.7. Output from the model of ciliates-phytoplankton dynamics (Appendix 4): the effect of variations in initial algal concentration and constant copepod abundance on the formation and peak magnitude of ciliate blooms when only one species of ciliate was included in the model.	140
Fig. 9.8. Output from the model of ciliate-phytoplankton dynamics (Appendix 4): the separate effects of the three ciliate species on bloom development over 20 days and the flow of carbon during those 20 days.	141

Fig. 9.9. Output from the model of ciliate-phytoplankton dynamics (Appendix 4): the effect of initial algal concentration and constant copepod abundance on four bloom parameters: 1) total (algae + ciliates) carbon eaten by copepods over the 20 day simulation; 2) total (algae + ciliates) carbon eaten by an individual copepod over the 20 day simulation; 3) ciliate carbon eaten by copepods over the 20 day simulation; and 4) ciliate carbon eaten by an individual copepod over the 20 day simulation.



## ACKNOWLEDGEMENTS

Over the last five years there have been a myriad of people who have helped me. If you are missed in these acknowledgments I apologize; accredit it to my poor memory and not my lack of appreciation. Thank you: M. Adamson, W. Coats, T. de Haan, P. Franks, L. Greenway, R. Haigh, N. Haigh, R. Johnson, D. Jones, E. Lessard, D. Lynn, C. Mewis, D. McPhail, T. Parsons, T. Pedersen, E. Simons, D. Stoecker, T. Sutherland, A. Wait, M. Watt, and M. Weis. I also thank the committee of professors who aided me in conducting this work: J. D. Berger, P. J. Harrison, A. G. Lewis, W. Neil, F. J. R. Taylor, and C. F. Walters and my external examiner P. G. Verity.

There were several grad' students and post-docs' without whom I would not have survived this study. They were always there to listen, encourage, and criticize. I can't thank you enough: Peter Arthur, John Berges, Philip Boyd, Rob Golblatt, Katriona Hurd and Peter Thompson.

Finally, there are three people who I would like to dedicate this work to. The first is Ramona who takes me to see Shakespeare. The other two are Cheryl Jerome and Alan Martin, who gave me the chance to learn and teach.

This study and my living expenses were partially funded by an NSERC graduate fellowship, a University of British Columbia Graduate Fellowship, and NSERC funding awarded to F. J. R. Taylor.

## CHAPTER ONE

### INTRODUCTION: OLIGOTRICH CILIATES AS FEAST AND FAMINE ORGANISMS

Blooms of planktonic ciliates are primarily the result of asexual reproduction and are largely clonal populations. It is therefore important to understand the population dynamics of clones, and "to follow the history of a clone accurately, it is essential to study isolated individuals in small volumes of medium; this was Maupas' fundamental technical achievement" (Bell 1988). The purpose of this dissertation was to investigate small scale planktonic ciliate blooms and determine their potential impact on carbon flow in food webs, by examining ciliates in culture.

If we know ciliate and prey biomass and growth rates and the grazing rates of the ciliates, then we can determine the impact of ciliates on a prey population over time. Both growth and grazing rates change with food concentration, typically as rectangular hyperbolic functions (referred to as numerical and functional responses, respectively, see Appendix 2). I have investigated the growth rate of ciliates under steady state conditions at a number of prey concentrations (Chapters 3-7). These experiments provided numerical response curves which indicated not only the growth rates of the ciliates but also the mortality rates at sub-threshold concentrations. I also measured grazing rates at a number of prey concentrations, by observing the uptake of fluorescently labeled beads and/or flagellates (Chapters 3-7). This method proved unsatisfactory, as it either under or over estimated feeding rates (see Chapter 8). I therefore used the numerical response data and a bioenergetic formula to determine functional responses (Chapter 8). However, I have presented the grazing rate data, measured by labeled prey uptake, to indicate that this method, which is often used to estimate ciliate grazing rates, is inaccurate. The numerical and functional responses were used to determine the impact of ciliates on prey populations (Chapter 9).

In the last 150 years it has been established that ciliates are a dominant component of the microzooplankton (20-200  $\mu\text{m}$ ) and may shunt a substantial portion of energy through planktonic food webs (Lynn and Montagnes 1991). Studies have provided information on a

number of aspects of marine planktonic ciliate biology, for example: *biomass* (Lynn and Montagnes 1991); *grazing* (Scott 1985, Gifford 1988); *growth rate* (Rassoulzadegan 1982, Smetacek 1984, Verity 1991a); *mixotrophy* (Blackbourn *et al.* 1973, Stoecker *et. al.* 1988, Putt 1990); *behaviour* (Buskey and Stoecker 1988, 1989, Fenchel and Jonsson 1988); *nutrient flux* (Johannes 1965, Stout 1980, Taylor 1982, Verity 1985); *distribution* (Lynn and Montagnes 1991); *migration* (Jonsson 1989); *food for zooplankton* (Jonsson and Tiselius 1990, Gifford and Dagg 1991); and *taxonomy* (Laval-Peuto and Brownlee 1986, Montagnes and Lynn 1991). Many of these studies indicate that ciliates are an important component of planktonic trophodynamics.

However, Banse (1982) suggested that, in the open ocean, on average ciliates consume little food relative to copepods because the concentrations of suitable food particles tend to be too low. A similar situation may also arise in coastal waters if food concentrations are low there too. Thus, ciliates may not normally be important in the flow of carbon in some marine food webs. Banse (1982) argued that the maximum growth and grazing rates of ciliates are so high that, if they grew and fed at these rates, they would rapidly deplete their prey. Thus, the potential impact of ciliates on phytoplankton would be rarely realized, and ciliate ingestion and specific growth rates would be typically low. Under these conditions, ciliates could only reach their potential rates when encountering a short term bloom of small algae, as long term blooms (e.g. the spring bloom) would be exploited by mesozooplankton. During short term algal blooms, ciliates could graze down the algae unless the ciliates are grazed down by mesozooplankton.

Others have also indicated that planktonic ciliates act as feast and famine organisms over a few days, as Banse suggested (Blackbourn 1974, Ibanez and Rassoulzadegan 1977, Grice *et al.* 1980, Smetacek 1984, Andersen and Sorensen 1986, Fenchel 1987, Lynn and Montagnes 1991), and that under some conditions ciliates are not an important carbon source to upper trophic levels (Montagnes *et al.* 1988a). Thus, ciliates may only be important for brief periods in some planktonic ecosystems.

Many non-marine ciliates exhibit a feast-famine existence related to temporal and spatial patches (Fenchel 1987). They can remain dormant in cysts (Corliss and Esser 1974), at reduced metabolic rates (Fenchel 1987), or at very low numbers (Taylor and Shuter 1981), during a famine. Then, at times when food is abundant, ciliates rapidly exploit the resource. Presumably, marine planktonic ciliates also act in this fashion, as some species make cysts (Reid and John 1978, 1983, Paranjape 1980, Reid 1987).

In the plankton, food for ciliates may become abundant in small patches, as phytoplankton bloom in localized regions. Such phytoplankton blooms appear as rapid increases in numbers or biomass, visible as transient peaks, and can be stimulated by a number of factors: tidal or wind mixing events, changes in irradiance, or by allochthonous inputs from terrestrial run off (Mackas *et al.* 1985, Legendre 1990). These blooms can be meters to kilometers in size and exist for 10-20 days, when mixing processes (e.g. wind and tides) dissipate them (Haury *et al.* 1978, Mackas *et al.* 1985). In contrast, during large persistent blooms of phytoplankton, mesozooplankton populations will respond. Thus, short term phytoplankton blooms represent conditions where ciliates might bloom and where ciliates would have a selective advantage over mesozooplankton, due to their rapid growth rates.

Unfortunately, the logistics of sampling marine systems prevent most studies from detecting the genesis and following the development of short term blooms. Therefore, our knowledge of such bloom-dynamics in the field is limited, and most food web analyses have not acknowledged that short term phytoplankton blooms may be grazed down by ciliates. One way to circumvent this problem is to use laboratory data to model blooms. This approach provides a means to estimate the potential occurrence of such blooms. Further, if we can establish the conditions under which blooms may occur, then we may reduce our effort searching for them.

Lynn and Montagnes (1991) developed a simple model of the ciliate *Strobilidium spiralis* grazing on small flagellates. Their study was based on functional and numerical response data obtained from work on *S. spiralis* (Jonsson 1986). This model indicated that ciliate blooms occur over <20 days and can graze down prey populations.

My goal was to improve the data-base used to model planktonic ciliate blooms, and then employ it to: 1) further substantiate that field observations of these ciliate blooms are due to the rapid growth rates of ciliates and 2) show that small scale phytoplankton blooms may be grazed down by ciliate blooms. To do this I have: 1) cultured and identified 5 different ciliates (Chapter 2); 2) obtained functional and numerical responses from these ciliates (Chapters 3-7); 3) compared my data to that obtained in other studies and established 3 "typical" ciliate responses (Chapter 8); and 4) used the functional and numerical response data to develop a simple model which illustrates that short term ciliate blooms can occur and indicates conditions under which blooms may exist (Chapter 9). Finally, I have investigated the dynamics of these blooms in terms of carbon flow through a phytoplankton-ciliate-copepod food web (Chapter 9).

## CHAPTER 2

### **THE SALIENT FEATURES OF ONE UNDESCRIBED SPECIES AND REDESCRIPTION OF FOUR SPECIES IN THE CLASS SPIROTRICHEA (CILIOPHORA, OLIGOTRICHIA) WITH NOTES ON THE CULTURING AND BEHAVIOUR OF THESE SPECIES**

#### **Introduction**

The "oligotrichs" have been recognized as a distinct assemblage of ciliates, beginning with Butschli's classification scheme of the 1880's and continuing up to the present (Small and Lynn 1985, Montagnes and Lynn 1991, Lynn and Corliss 1991, Petz and Foissner 1992). Corliss (1979) noted in his chapter on the "often neglected oligotrichs" that the literature on this group, excluding the monographic works on the tintinnines (e.g. Kofoed and Campbell 1939), is not very extensive. He commented that a major modern treatise is long overdue. Recently, there have been a number of works that have begun this arduous task (Maeda and Carey 1985, Maeda 1986, Grim 1987, Foissner *et al.* 1988, Lynn and Montagnes 1988, Lynn *et al.* 1988, Montagnes *et al.* 1988b, Krainer 1991, Montagnes and Lynn 1991, Petz and Foissner 1992, Martin and Montagnes 1993). Still, it is typical that in routine sampling of marine waters new ciliate species are found (e.g. Martin and Montagnes 1993). This suggests that work on the oligotrichs is far from finished.

Most of the taxonomic work conducted on the oligotrichs has used field samples to describe morpho-species and has assumed that variation in these samples would be sufficient to appraise the variability within a species. Further, field based taxonomy assumes that a species can be identified (morphologically) from a single cell. Consequently, species descriptions from field samples may on one hand underestimate the variability of a species and on the other, lump species together. Thus, taxonomic studies on cultured isolates will help to indicate the variability within and between species.

In this chapter, I present the salient features of five species (my experimental organisms) obtained from examining protargol stained, scanning electron micrographed and

live specimens. With the salient features, I have included some remarks on the culturing and behaviour of the ciliates.

## 1.0 Materials and Methods

### 1.1 Isolation and General Culturing

Oligotrichs have been cultured during the past 20 years (e.g. Gold 1970) and in the last 10 years explicit methods have been developed (see Gifford 1985). I have roughly followed the procedures of these authors (see Chapters 3-7).

Strains of marine planktonic oligotrichs were collected in bottles from coastal subsurface waters of British Columbia. Then, 5-10 mL of the sample water was placed in 20-mL plastic culture plates (Falcon, 3046, Becton Dickinson & Co., Lincoln Park, NJ, USA). Samples were enriched with natural seawater (Appendix 1) and the putative prey: *Chroomonas salina* NEPCC 275, *Isochrysis galbana* NEPCC 633, *Rhodomonas lens* NEPCC 588, and sometimes *Thalassiosira pseudonana* NEPCC 58 (species were obtained from the Northeast Pacific Culture Collection, NEPCC, Department of Oceanography, University of British Columbia, Vancouver, British Columbia). Ciliate and phytoplankton cultures were maintained at 16-17°C on a 14:10 light:dark cycle at 30-70  $\mu\text{mol photons m}^{-2} \text{ s}^{-1}$ .

Following enrichment, if ciliate numbers increased, some ciliates were removed (using finely drawn Pasteur pipettes), transferred through 3-4 washes of sterile culture medium and placed in medium containing defined prey species in tissue culture plates. After several generations, the above process was repeated to ensure there were no contaminating eukaryotes (cultures were never made bacteria free). Then, cultures were maintained by serial transfers, either to 50 mL of medium and defined prey in 125-mL flasks or to 10 mL of medium in 20 mL tissue plates.

At a later date, after cultures had been well established, clonal cultures were made by isolating single ciliates. The single cells were allowed to divide several times and then a second single-cell isolation was repeated; this procedure ensured the cultures were clonal.

## 1.2 Fixation and Staining

For light microscopy, the ciliates were fixed in 5-10% Bouin's solution (volume/volume) (Lee *et al.* 1985) and protargol silver stained (Montagnes and Lynn 1987, 1993). For scanning electron microscopy, the ciliates were fixed in 5% Bouin's or 2% acid Lugol's iodine, subsequently dehydrated in ethanol, critical point dried in a Balzers CPD 020, mounted on aluminum stubs, gold coated (25 nm) in a Nanotech SEMPREP 2 sputter coater, and viewed with a Cambridge 250T SEM.

## 1.3 Measurements

Examination of cells followed the recommendations of Montagnes and Lynn (1991). Longitudinally oriented, protargol stained specimens were examined. The following features were measured: *somatic length* as the maximum longitudinal linear distance, excluding cilia; *somatic width* as the maximum linear distance (diameter) across the cell at right angles to the longitudinal axis; *macronuclear diameter*; *number of polykinetids in the anterior or external polykinetid zone*; and *number of polykinetids in the ventral or internal polykinetid one*. All anterior, external and internal polykinetid counts were made on polar orientated cells except for *Strombidium acuminatum* strain BJSCH in which polar orientation was extremely rare. Counts of the ventral and internal polykinetids may be highly variable due to the orientation of cells, which often obscured the smaller polykinetids in the cytostomal region. Further, the dimensions given are based on Bouin's-fixed and protargol-stained material, which are ~0.85 of live measurements (Jerome *et al.* 1993). Also, fixation, by inducing some contraction in the ciliates, may also distort the natural path of structures.

## 2.0 Results and Discussion

### 2.1 General taxonomy

The five ciliate species presented below belong to the class Spirotrichea, subclass Oligotrichia (following Lynn and Corliss 1991), and are in the Order Oligotrichida, family Strombidiidae and Order Choreotrichida, families Strobilidiidae and Strombidinopsidae (Small and Lynn 1985).



Oligotrichs are often the dominant ciliates in the marine plankton (Montagnes and Lynn 1991). This subclass is typically conical or ovoid in shape with specialized oral polykinetids used mainly for locomotion and feeding. The somatic ciliature is specialized and may be reduced to non-ciliated kinetids. The Oligotrichida are distinguished by the oral polykinetids being divided into anterior polykinetid (APZ) and ventral polykinetid zones (VPZ), while the Choreotrichida are distinguished by the oral external polykinetids (EPZ) forming a complete circle that encloses the internal polykinetid zones (IPZ) (Fauré-Fremiet 1969, Small and Lynn 1985). *Note* that different diagnostic features have been used to characterize the oligotrichs (see Petz and Foissner 1992).

I have been conservative in the identification of these strains of oligotrichs from the eastern north Pacific, attributing to them the names of species from the north Pacific, eastern north Atlantic and North Sea, whenever appropriate.

## 2.2 Description of species

### 2.2.1 Strobilidiid ciliates

*Strobilidium spiralis* (Leegaard, 1915) Lynn and Montagnes, 1988 strain IA

(Choreotrichida, Strobilidiidae)

(Figs. 2.1, 2.2)

#### *Salient features.*

Cell shape, subspherical, although flattened on one side due to the characteristic structure of kinety 2. Cell length, 40  $\mu\text{m}$  (range, 33-57) and width, 45  $\mu\text{m}$  (38-55). External polykinetidal zone (EPZ) composed of 38 (40-36) external polykinetids (EPk). Internal polykinetidal zone (IPZ) composed of 13 (9-20) internal polykinetids (IPk). IPk's and EPk's usually contiguous but those further from the cytostome may be continuous. The IPZ sit above an acentric concavity that leads to the cytostome. Cytopharyngeal fibers present. Paroral kinety begins parallel to the last IPk (near the cytostome) and lies internal to the EPk's. Cilia of the paroral kinety lie on the oral surface inside the region defined by the EPK. Five somatic kineties (K) present, whose cilia (2-3  $\mu\text{m}$  long) are directed to the right (when viewed aborally). The somatic kineties are partially covered by a cytoplasmic flap. K1 is

slightly dexterally spiralled and extends from the posterior of the cell to just below the EPZ. K2 describes an arc that encloses a space between K1 and K2 by extending from the posterior of the cell to a position half way along K1; at this point K2 reflects away from K1 and produces a small (2-4  $\mu\text{m}$ ) "crook". K3 and K4 are simple; they originate perpendicular to and near the aboral third of K2 and extend anteriorly to just below the EPZ. K5 originates one-third of the cell length from the aboral end and runs anteriorly, paralleling K1. One C-shaped macronucleus, positioned anteriorly around the oral cavity and below the EPZ, has its opening near the cytostome. Two micronuclei (not always visible) are indented into the macronucleus 180° around from the cytostome. Cell surface often covered by 2-4  $\mu\text{m}$  rods (possibly extrusomes) which stain darkly with protargol.

#### *Time and locality of isolation*

Early March, Indian Arm, British Columbia, Canada, (122°53'W, 49°21'N,) at a depth of 2 m, temperature of 8 °C, and salinity of 16 ‰.

#### *Discussion of species*

Before discussing strain IA specifically, I will provide a brief definition of the genus *Strobilidium*. The family Strobilidiidae *sensu stricto* exhibit the following characters: somatic kineties with short cilia overlain by a cytoplasmic flap and a closed circle of external polykinetids; the genus *Strobilidium* possesses these same characters (Lynn and Montagnes 1988). Following these criteria Lynn and Montagnes (1988) made *Lohmanniella spiralis*, Leegaard, 1915 (a commonly referred to marine ciliate) a junior synonym for *Strobilidium spiralis*. More recently, Petz and Foissner (1992) have placed a number of species of *Strobilidium* in the genus *Rimostrombidium* Jankowski, 1978. Their arguments for doing this however are in conflict with the criteria proposed by Lynn and Montagnes (1988) and resurrection of the "desk genus" *Rimostrombidium* for this group creates unnecessary etymological confusion. I therefore have maintained the genus *Strobilidium* for my identifications.

Strain IA is identical to *Strobilidium spiralis* (Leegaard, 1915) Lynn and Montagnes, 1988 except for two features: 1) *S. spiralis* has only one micronucleus indented into the

macronucleus (180° around from the cytostome), while strain IA has two, and 2) K5 on *S. spiralis* originates anteriorly, extends posteriorly, and then curves anteriorly around to describe a partial circle; but K5 on strain IA originates one-third of the cell length from the aboral end and runs anteriorly, paralleling K1. These two differences may denote a new species.

However, I have been conservative and considered strain IA to be *Strobilidium spiralis*.

#### *Remarks on culturing and behaviour*

Strain IA was grown on three flagellates in culture: *Chroomonas salina*, *Isochrysis galbana*, and *Rhodomonas lens*. However, it first was grown on a mixed culture of natural prey; ciliates isolated from these cultures had ingested 30-40 µm pennate diatoms (likely *Nitzschia*). Strain IA was also used to estimate the effect of Bouin's and Lugol's fixatives and Protargol staining on cell size (see Jerome *et al.* 1993).

*Strobilidium* sp. strain JERC

(Choreotrichida, Strobilidiidae)

(Figs. 2.3, 2.4)

#### *Salient features*

Cell subspherical with flat anterior and round posterior, 14-40 µm long and 15-45 µm wide. External polykinetid zone (EPZ) and internal polykinetid zone (IPZ) not completely separate. EPZ comprised of 22-23 polykinetids of 35 µm long cilia, surrounding anterior end. Inner portion of each external polykinetid ends with 4 ciliated kinetosomes; the cilia are 3-4 µm long and directed inward. Oral cavity acentrically placed within the circle of external polykinetids (EPK). 1-3 inner polykinetids (IPK) lie in oral cavity; 1-2 IPK are completely separate, the others are extensions of EPK. Ten (range, 6-12) somatic kineties, equally spaced around cell, extend from 5-10 µm below oral region to near posterior pole. Each somatic kinety composed of continuous row of cilia directed to the right when viewed from the aboral end. A rudimentary flap covers the base of the somatic cilia. Macronucleus, typically C-shaped but often fragmented, lies below EPZ, with arms of "C" near cytostome. Faintly staining micronucleus positioned in a depression of macronucleus opposite the cytostome.

### *Time and locality of isolation*

Late April, from surface waters (top meter, temperature of 10 °C, salinity 22 ‰) at Jericho Pier, English Bay, Vancouver, British Columbia, Canada, (123°10'W, 49°17'N).

### *Discussion of species*

In shape, strain JERC is superficially similar to four *Strobilidium* species: *S. multinucleatum* Lynn and Montagnes, 1988, *S. sphaericum* Lynn and Montagnes, 1988, *S. spiralis* (Leegaard, 1915) Lynn and Montagnes, 1988, and *S. undinum* Martin and Montagnes, 1993. However, there are differences between strain JERC and all four of these species: 1) *S. multinucleatum* has 5 somatic kineties, 18-20 EPK and 11 spherical macronuclei; 2) *S. sphaericum* has no IPK, 24-30 EPK and many oral fibers that spiral into a central cytostome; 3) *S. spiralis* has a characteristic asymmetrical distribution of somatic kineties, 33-39 EPK and 8-20 IPK; and *S. undinum* has 6 somatic kineties, 21-24 EPK, and 4-6 IPK. In contrast, strain JERC has 10 to 12 symmetrically arranged somatic kineties (although these stain poorly at times and may appear as 6-9 asymmetrically placed kineties); 22 EPK; 1-3 IPK; one C-shaped macronucleus and an acentric cytostome not heavily supported by fibers. Further, strain JERC is 14-40 µm long and 15-45 µm wide which is smaller than *S. sphaericum* (40-70 µm long and 40-60 µm wide) and *S. spiralis* (40-60 µm long and 40-52 µm wide) but in the same range as *S. undinum* (16-29 µm long and 15-23 µm wide). Considering the above differences, strain JERC likely represents a distinct and undescribed species.

### *Remarks on culturing and behaviour*

Strain JERC was maintained in culture for 2-3 months on a mixture of *Isochrysis galbana*, *Chroomonas salina*, and *Rhodomonas lens*. Observations of this species in 10 mL of culture medium in 20 mL tissue plates indicated that the ciliates typically remained in the water column (i.e. they were planktonic). When disturbed either by motion of the container or when hitting a suspended particle, they very rapidly "jumped" approximately 1-3 cell lengths and then reoriented themselves and continued swimming.

### 2.2.2 Strombidiid ciliates

*Strombidium capitatum* (Leegaard, 1915) Montagnes *et al.*, 1988 strain APAG

(Oligotrichida, Strombidiidae)

(Fig. 2.5)

#### *Discussion of species*

Several isolates of *Strombidium capitatum* have been used to redescribe this species (Montagnes *et al.* 1988b); strain APAG fits the criteria for the species.

#### *Time and locality of isolation*

April, from surface waters (temperature of 8 °C, salinity of 28 ‰) at Agamemnon Channel, British Columbia, Canada, (124°5'W, 49°40'N).

*Strombidium acuminatum*, (Leegaard, 1915) Kahl, 1932

strain BJSC

(Oligotrichida, Strombidiidae)

(Figs. 2.6, 2.7)

#### *Salient features*

Cell conical, 80-138  $\mu\text{m}$  long and 13-31  $\mu\text{m}$  wide. The posterior tapers to a fine point that is curved in fixed material. Anterior polykinetid zone (APZ) and ventral polykinetid zone (VPZ) not distinctly separate. The inner 2-3 polykinetids of the VPZ are continuous or contiguous with the first 2-3 of the APZ. Anterior polykinetid zone comprised of 20 (range, 18-26) polykinetids, surrounding anterior end. Ventral polykinetid zone comprised of 7 (6-11) polykinetids which lie in a shallow oral groove. One ciliated paroral kinety on right side of oral groove. The girdle begins just below the oral groove, spirals dexterally (when viewed from anterior) to dorsal surface, continues around to ventral surface where it angles posteriorly, spirals to the dorsal surface and extends to ~10  $\mu\text{m}$  from posterior. The "ventral" kinety, situated on the dorsal surface, begins 10-20  $\mu\text{m}$  from the posterior, runs adjacent to, and on the right (dorsal view) of, the descending girdle for 5-10  $\mu\text{m}$  and then continues to the cell posterior. Descending portion of the girdle and ventral kinety possess 2-3  $\mu\text{m}$  long cilia

spaced 2-3  $\mu\text{m}$  apart. One ovoid, anteriorly positioned, macronucleus, 17 (13-24)  $\mu\text{m}$  long, 6 (4-8)  $\mu\text{m}$  wide. Lightly staining "trichites" insert along and perpendicular to girdle and extend internally ~10  $\mu\text{m}$  into cell. Dark staining (tear shaped) extrusomes lie below girdle.

Extruded, moniliform, extrusomes often intertwined with cilia extend 10-15  $\mu\text{m}$ .

#### *Time and locality of isolation*

July, from Sechart Inlet, British Columbia, Canada, 1 m depth, temperature of 20 °C, and salinity of 20 ‰ (123°45' W, 49°40'N).

#### *Discussion of species*

There are four species of *Strombidium* which, like strain BJLSC, are elongate, conical and ~100  $\mu\text{m}$  long: *S. cornucopiae* Wailes, 1929; *S. pulchrum* Leegaard, 1915; *S. rhyticollare* Corliss and Snyder, 1986; and *S. acuminatum* Leegaard, 1915.

*Strombidium cornucopiae* is larger than the typical range of strain BJLSC (97-200 vs. 80-138  $\mu\text{m}$ ) and has prominent striations which strain BJLSC lacks. *Strombidium pulchrum* has a spiraling ventral kinety like strain BJLSC, but it is slightly larger (167  $\mu\text{m}$  long) and has a more extensive zone of oral polykinetids than strain BJLSC. *Strombidium rhyticollare* is similar in size to strain BJLSC but differs from it in three ways: *S. rhyticollare* has 32 oral polykinetids while strain BJLSC has 27 (20+7); *S. rhyticollare* has a groove around its anterior end (posterior to the oral ciliature) which strain BJLSC lacks; and *S. rhyticollare* has a pair of ventral kineties that run one-third the cell length (from the posterior) while the ventral kinety and the extension of the girdle of strain BJLSC run together for one-quarter or less of the cell.

Of the above species, strain BJLSC is most similar to *S. acuminatum*, although *S. acuminatum* is smaller (60-88  $\mu\text{m}$ ). Leegaard (1915) illustrated three views of *S. acuminatum*, two of which (her Fig. 12 a and b) are similar to strain BJLSC while the third (Fig. 12c) is not. Figures 12a and b (Leegaard 1915) depict a ciliate with indications of a girdle similar to that of strain BJLSC and a similar number of oral polykinetids. Further, the nuclear shape and position of *S. acuminatum* are similar to that of strain BJLSC.

Any of the older descriptions by Wailes or Leegaard could be used to describe strain BJLSC, but the description of *S. acuminatum* appears most fitting. Further, Wailes (1943) observed *S. acuminatum* in British Columbian waters. Therefore, I consider strain BJLSC to be *Strombidium acuminatum*.

#### *Remarks on culturing and behaviour*

Observations of this species, in 10 mL of culture medium and the prey *Thalassiosira pseudonana* in 20 mL tissue plates, indicated that the ciliate is not strictly planktonic: at *T. pseudonana* concentrations ranging from 0 to  $5 \times 10^4$  cells mL<sup>-1</sup>, ~15% of the ciliates were in the water column while the others swam along the surfaces. After maintaining strain BJSC for prolonged periods in culture (> 15 days) the prey, *T. pseudonana*, became clumped. When this occurred, ciliates were typically associated with these clumps. This species may be pseudo-planktonic and associated with suspended particles (marine snow).

### 2.2.3 Strombidinopsid ciliates

*Strombidinopsis acuminatum* Fauré-Fremiet, 1924 strain SPJSC

(Choreotrichida, Strombidinopsidae)

(Figs. 2.8, 2.9)

#### *Salient features*

Cell round or cylindrical with tapering posterior, 35-82  $\mu$ m long and 29-49  $\mu$ m wide. External polykinetid zone and internal polykinetid zone not completely separate. External polykinetid zone comprised of 15-16 polykinetids with ~25  $\mu$ m long cilia, surrounding anterior end. Deep oral cavity acentrically placed within the circle of external polykinetids. Internal polykinetid zone comprised of 6-10 polykinetids which lie in oral cavity; 4-5 internal polykinetids are completely separate; the rest are extensions of external polykinetids. Somatic kineties, 13-19, equally spaced around cell, composed of dikinetids (both with 3-5  $\mu$ m cilia), extend from oral region to posterior pole. Macronuclei, typically 2 (range, 1-6) semi-spherical (10  $\mu$ m in diameter).

### *Time and locality of isolation*

June from 1 m depth, temperature of 20 °C, and salinity of 20 ‰ in Sechart Inlet, British Columbia, Canada. (123°45' W, 49°40' N).

### *Discussion of species*

Lynn *et al.* (1991) have rediagnosed the Strombidinopsidae as: free swimming aloricate ciliates with many (usually > 10) ciliated somatic kineties, extending the entire length of the cell, composed of dikinetids. They also typically have two similarly-shaped spherical to ovoid macronuclei; the genus *Strombidinopsis* has characters of the family. Strain SPJSC possess these characters and consequently has been placed in the genus *Strombidinopsis*.

Strain SPJSC is similar to two previously described species: *Strombidinopsis spiniferum* (Leegaard, 1915) Lynn *et al.*, 1991 and *Strombidinopsis acuminatum* Fauré-Fremiet, 1924. All three species exhibit characters with ranges that overlap; these are size, oral cilia length, number of external polykinetids, number of somatic kineties, number of kinetids in somatic kineties and macronuclear number. However, the one character that distinguishes strain SPJSC from the two described species is inner polykinetid number; the new isolate has 4-5 independent polykinetids while the other two species have only 3.

*Strombidinopsis spiniferum* has a thin tapering posterior which strain SPJCH lacks. The differences in shape between strain SPJSC and *Strombidinopsis acuminatum* are marginal since Lynn *et al.* (1991) indicate that the latter species may be long and thin or short and fat; the latter shape is similar to strain SPJSC.

It is possible that strain SPJSC is a new species since it has one more IPK than *Strombidinopsis acuminatum*. Rather than diagnosing a new species based on a single inner polykinetid, I have been conservative and identified strain SPJSC as *Strombidinopsis acuminatum*.

### *Remarks on culturing and behaviour*

*Strombidinopsis* SPJSC was initially cultured on a mixture of prey: *Chroomonas salina*, *Isochrysis galbana*, and *Rhodomonas lens*. It grew well ( $\sim 1$  division  $d^{-1}$  at concentrations  $> 10^4$  cells  $mL^{-1}$ ) on *Chroomonas salina*, or *Rhodomonas lens* as monocultures. It was later



cultured on *Thalassiosira pseudonana* on which it also grew at a maximum rate (see Chapter 3).

Observations of this species in 10 mL of culture medium in 20 mL tissue plates indicated that the ciliates typically remained in the water column (i.e. it was planktonic). However some ciliates "grazed" along the surface. The ciliate typically swam in a straight line with a helical movement, analogous to that described for a species of *Strombidium* (Fenchel and Jonsson 1988). Fenchel and Jonsson (1988) however, attributed this motion to the asymmetric positioning of oral polykinetids, and such an arraignment does not exist for *Strombidinopsis*; possibly another mechanism controls its swimming behaviour.

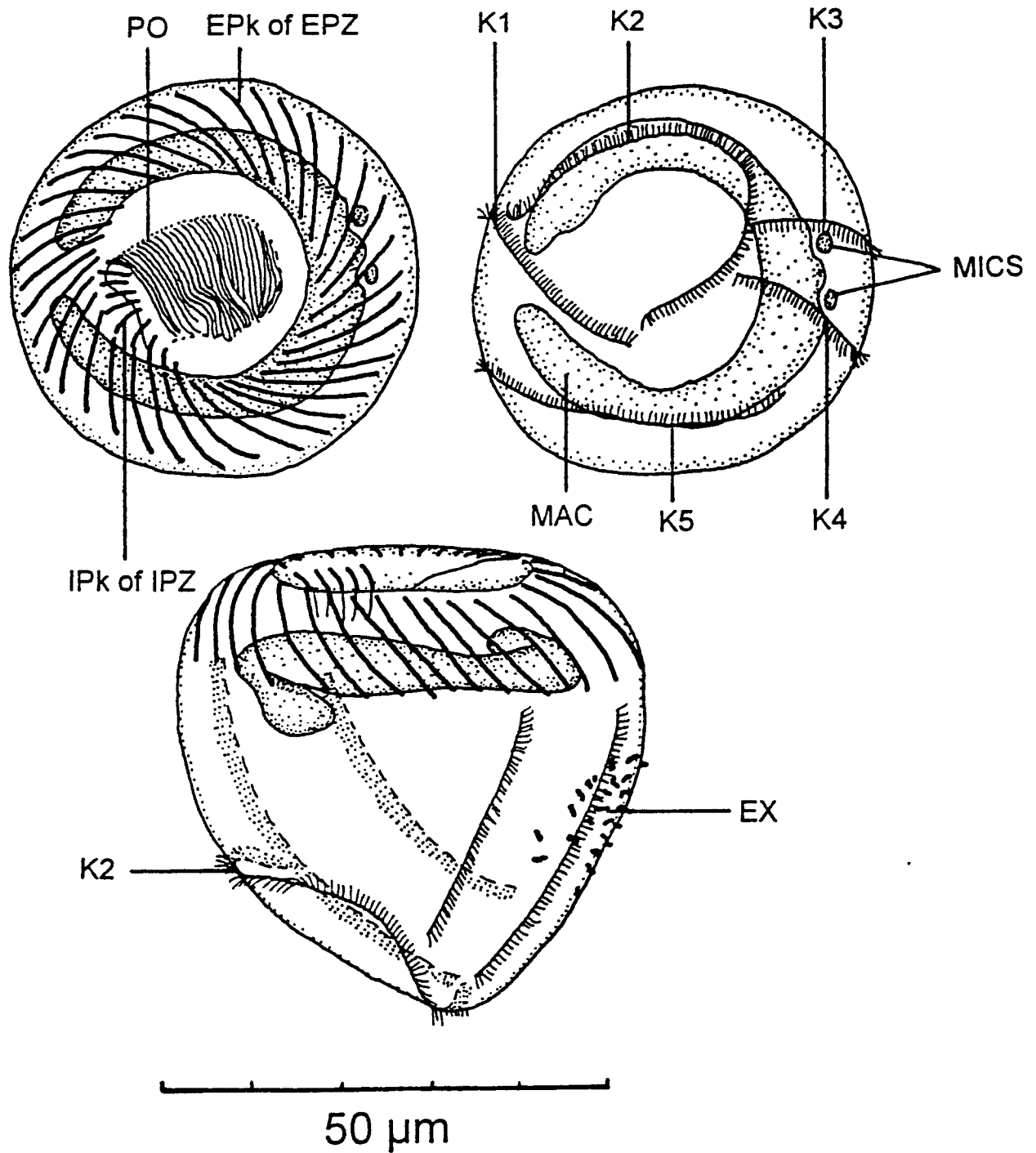
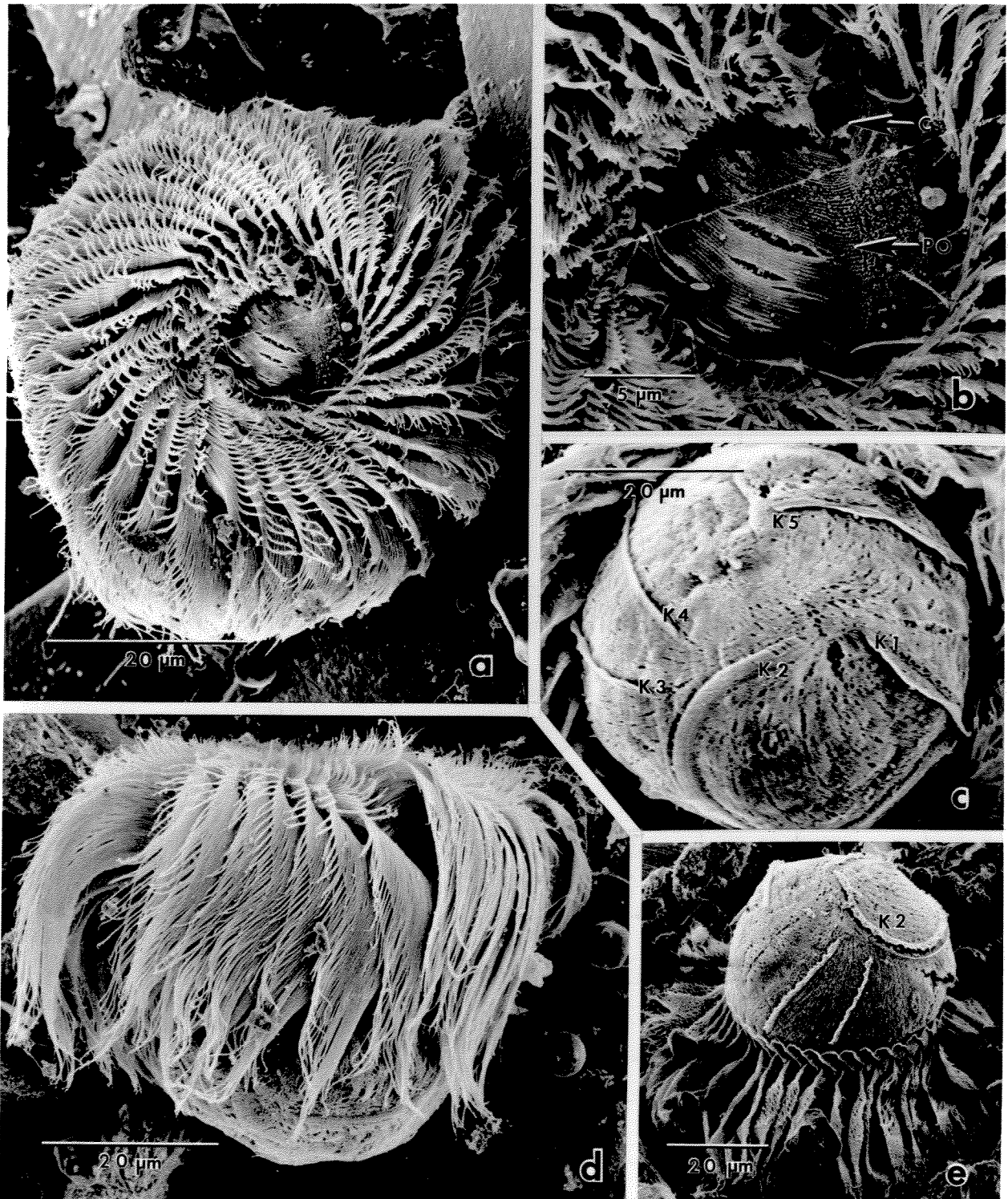


Fig. 2.1. Schematic diagram of *Stribilidium spiralis* (Leegaard, 1915) Lynn and Montagnes, 1988 strain IA from protargol stains and augmented by electron microscope observations. Paroral cilia, PO; external polykinetid of external polykinetidal zone, EPk of EPZ; internal polykinetid of internal polykinetidal zone, IPk of IPZ; kineties 1-5, K1-K5; macronucleus, MAC; micronuclei, MICS; extrusomes (only shown for a small portion of the cell), EX.

Fig. 2.2. Electron micrographs of *Strobilidium spiralis* (Leegaard, 1915) Lynn and Montagnes, 1988 strain IA. a, anterior view; b, detail of oral region with cytostome (C) and paroral cilia (PO); c, posterior view showing somatic kineties (K1-K5); d, lateral view; e, lateral view showing the curved second somatic kinety (K2).



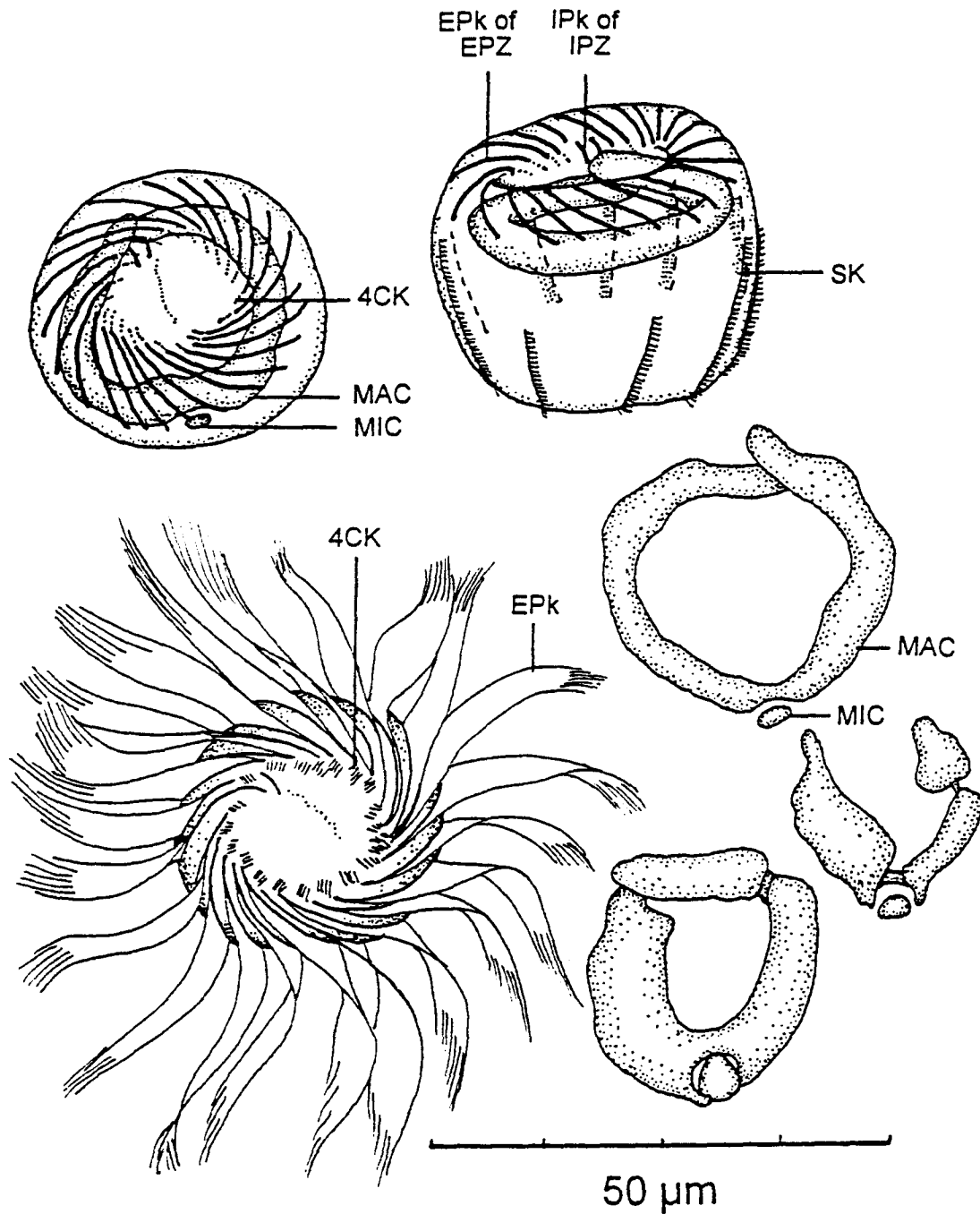
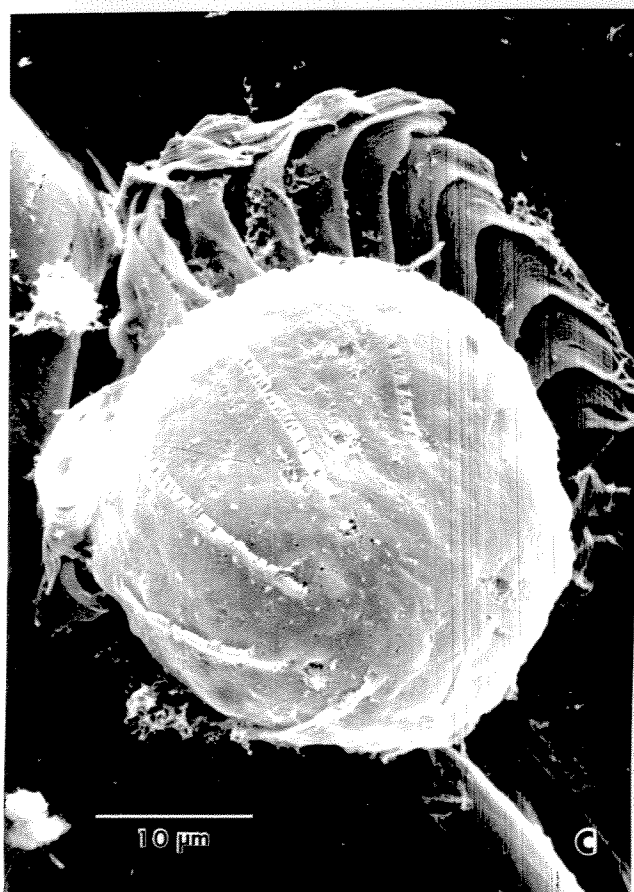
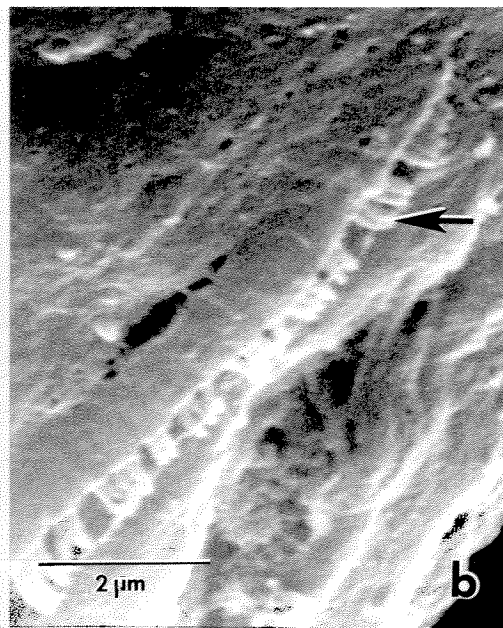
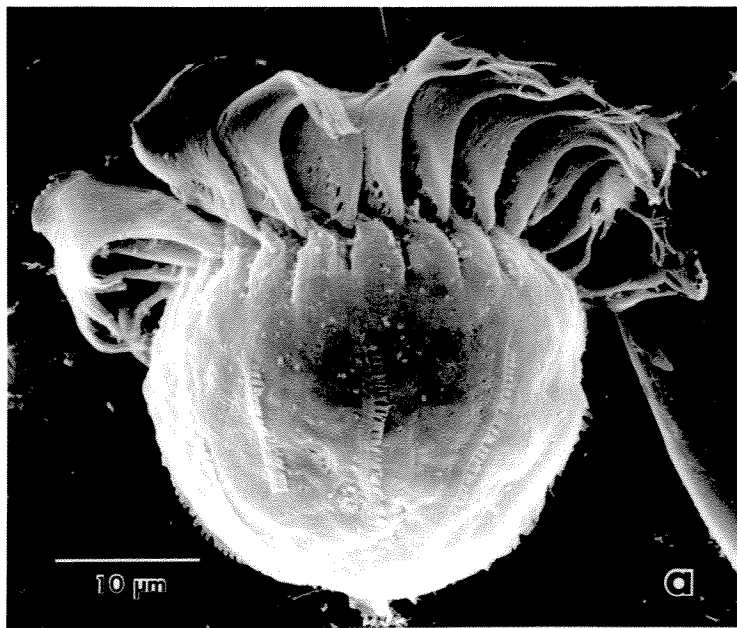


Fig. 2.3. Schematic diagram of *Strobilidium* sp. strain JERC from protargol stains and augmented by electron microscope observations. Four ciliated kinetosomes internal to each external polykinetid, 4CK; external polykinetid of external polykinetidal zone, EPk of EPZ; internal polykinetid of internal polykinetidal zone, IPk of IPZ; one of 10 somatic kineties, SK; macronucleus, MAC; micronucleus MIC.

Fig. 2.4. Electron micrographs of *Strobilidium* sp. strain JERC. a, lateral view; b, detail of a somatic kinety showing somatic cilia (arrow); c, posterior view showing position of somatic kineties; d, lateral and anterior views of two ciliates.



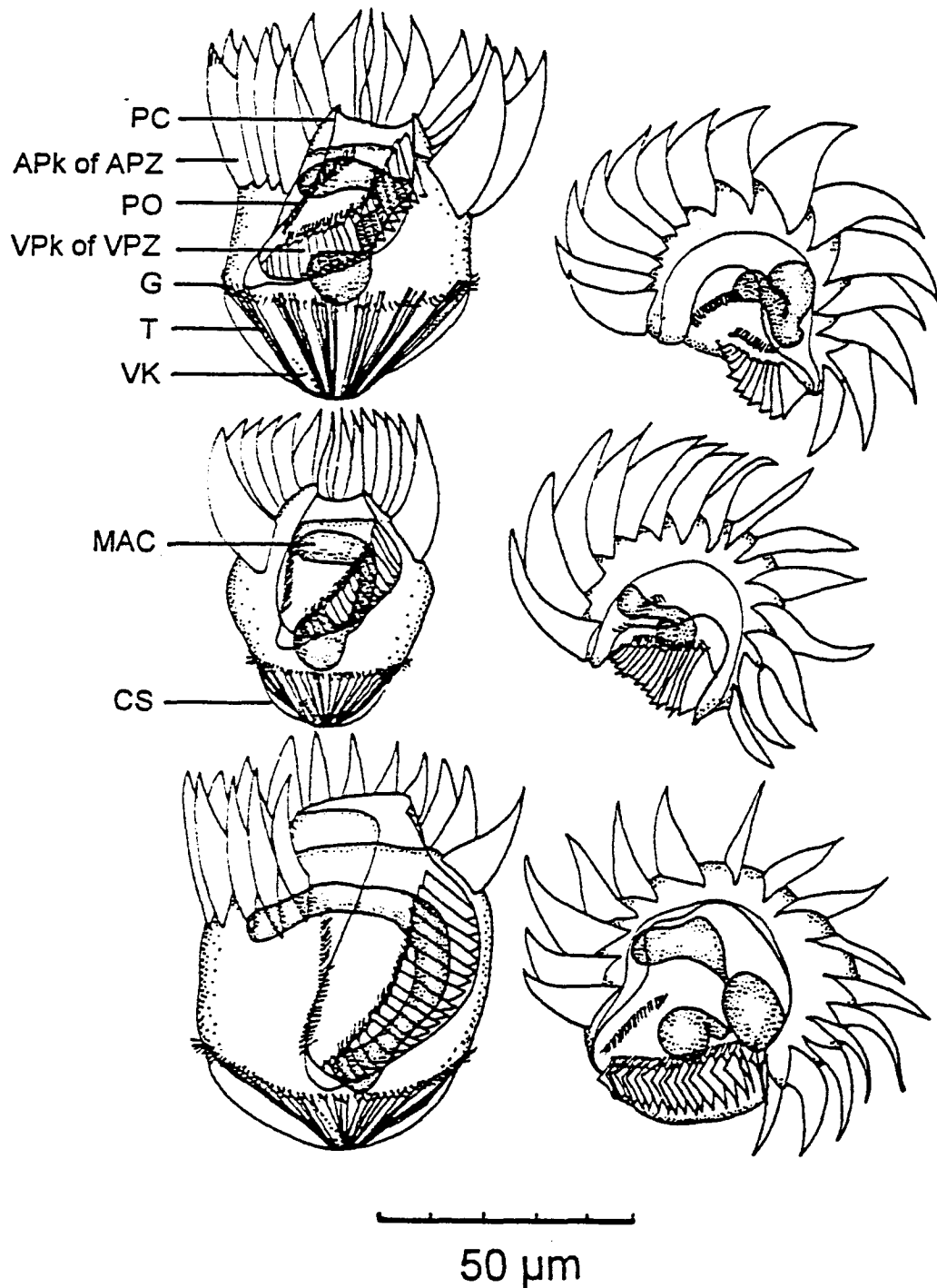


Fig. 2.5. Schematic diagram of *Strombidium capitatum* (Leegaard, 1915) Montagnes *et al.*, 1988 modified from Montagnes *et al.* (1988b). Peristomial collar, PC; anterior polykinetid of anterior polykinetidal zone, APk of APZ; ventral polykinetid of ventral polykinetidal zone, VPk of VPZ; paroral cilia, PO; girdle cilia, G; trichites, T; ventral kinety, VK; macronucleus, MAC; distended cell surface, CS.



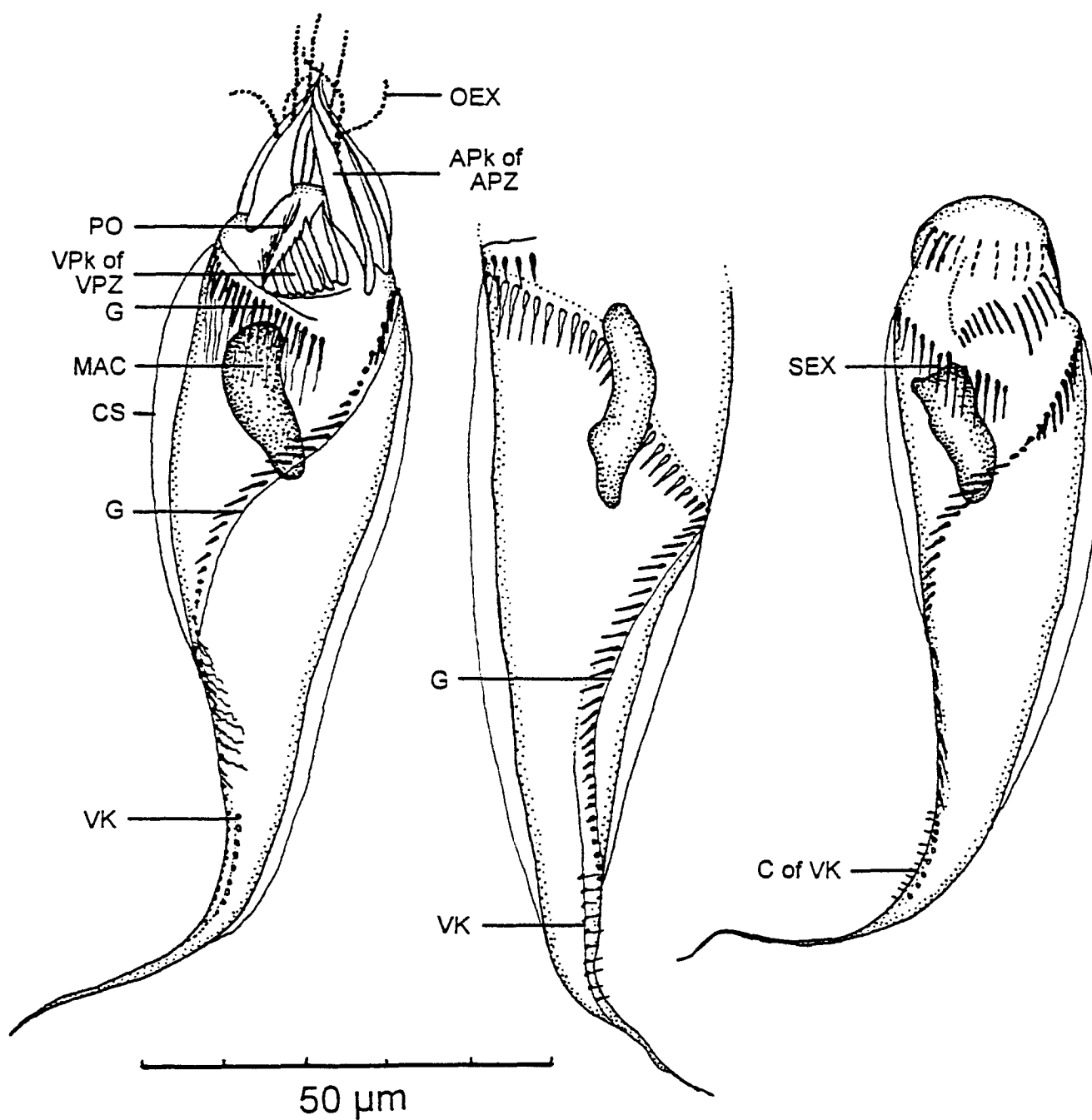


Fig. 2.6. Schematic diagram of *Strombidium acuminatum*, (Leegaard, 1915) Kahl, 1932 strain BJSC from protargol stains and augmented by electron microscope observations. Anterior polykinetid of anterior polykinetidal zone, APk of APZ; ventral polykinetid of ventral polykinetidal zone, VPk of VPZ; paroral cilia, PO; girdle, G; ventral kinety, VK; cilia of ventral kinety, C of VK; macronucleus, MAC; distended cell surface, CS; oral trichites (discharged), OEX; somatic trichites, SEX.

Fig. 2.7. Electron micrographs of *Strombidium acuminatum*, (Leegaard, 1915) Kahl, 1932 strain BJSC. a, antero-ventral view showing oral ciliature and girdle (G); b, ventral view showing ventral and oral ciliature and girdle (G) algal prey, *Thalassiosira pseudonana* (TP); c, lateral view showing inclined orientation of oral ciliature; d, ventro-lateral view showing curved posterior and cilia of ventral kinety (arrow).



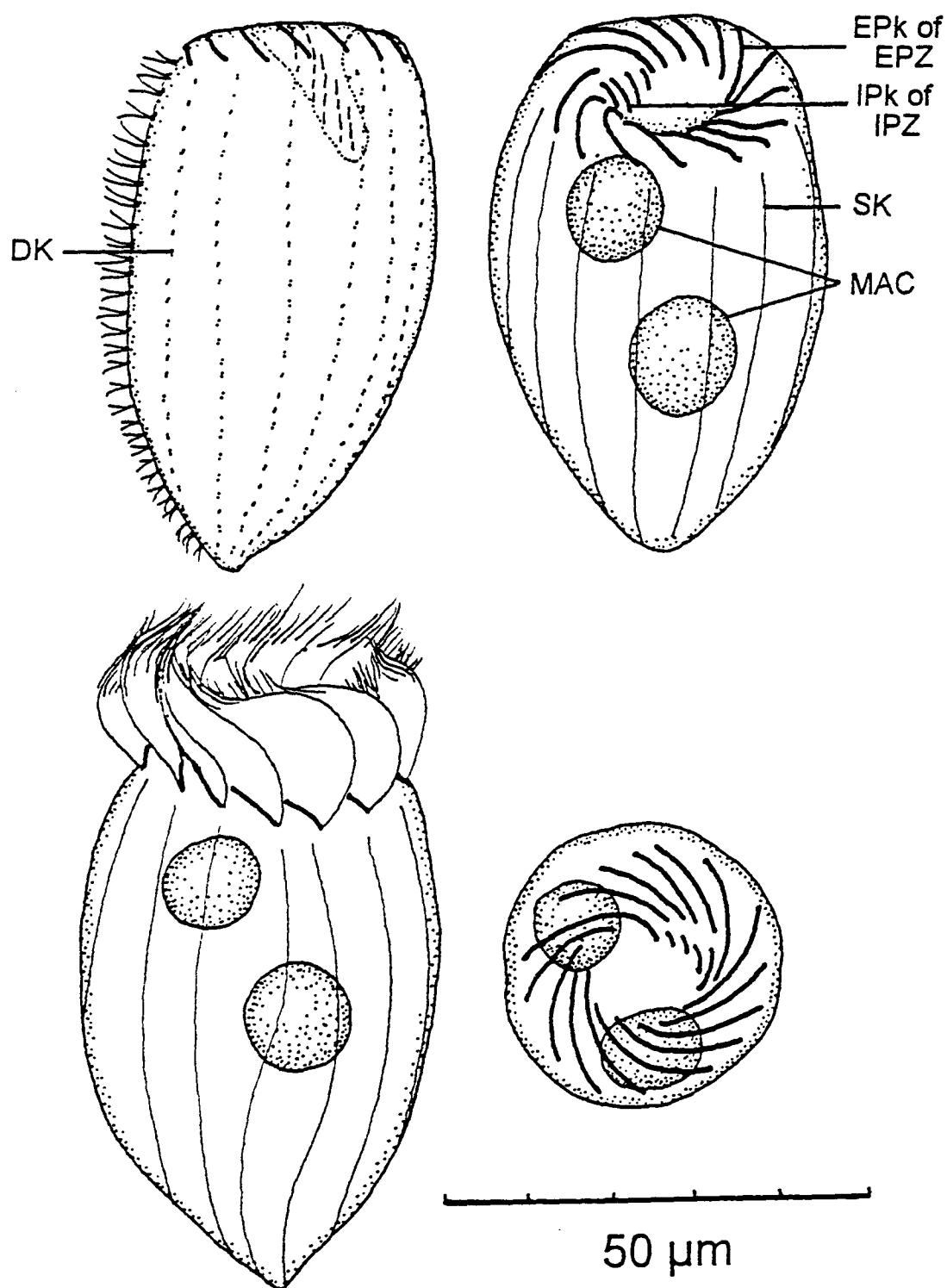
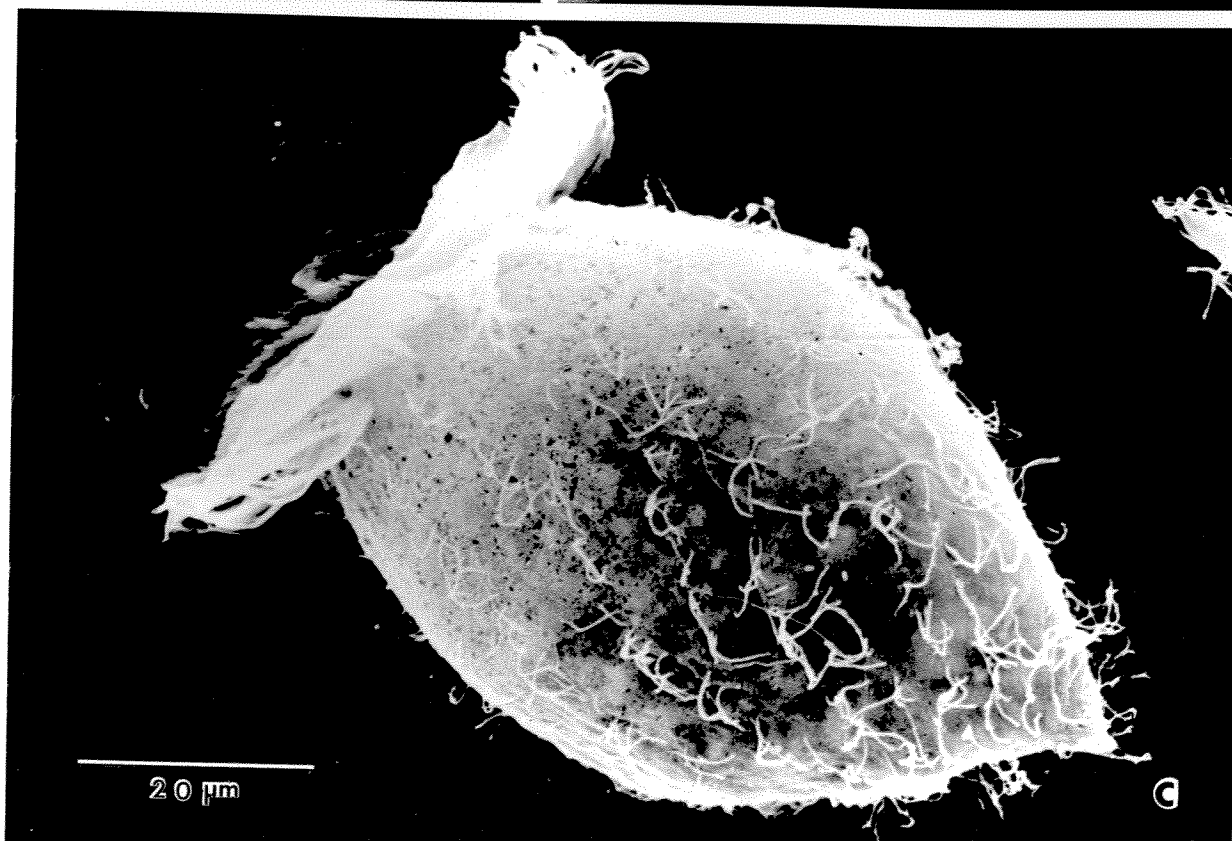
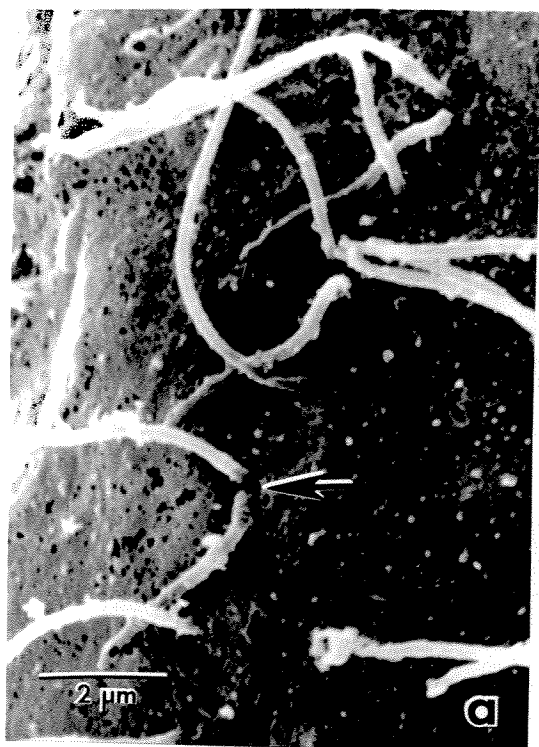


Fig. 2.8. Schematic diagram of *Strombidinopsis acuminatum* Fauré-Fremiet, 1924 strain SPJSC from protargol stains and augmented by electron microscope observations. External polykinetid of external polykinetidal zone, EPk of EPZ; internal polykinetid of internal polykinetidal zone, IPk of IPZ; a somatic kinety, SK; macronucleus, MAC; a somatic dikinetid DK.

Fig. 2.9. Electron micrographs of *Strombidinopsis acuminatum* Fauré-Fremiet, 1924 strain SPJSC. a, detail of somatic dikinetids with cilia (arrow); b, anterior view; c, lateral view.



## CHAPTER 3

### GROWTH AND GRAZING RATES OF *Strombidinopsis acuminatum* STRAIN SPJSC AS A FUNCTION OF FOOD CONCENTRATION

#### Introduction

In this chapter I examine *Strombidinopsis acuminatum* strain SPJSC, the first ciliate that I cultured for an extended period. This ciliate became the "test" organism for a number of methods that were used for ciliates in later chapters. These methods are presented in detail here and only referred to later.

Strain SPJSC was unusual in a number of ways. Most remarkably, it was kept in culture for almost a year while the other ciliates I studied were maintained only for weeks to months. Thus, a detailed study of SPJSC was possible, but problems arose. In the process of determining growth and grazing response curves, it became apparent that sub-clones had different growth and grazing responses. Several experiments were devised to determine the effect and nature of these differences. Consequently, the studies on this ciliate became diversified beyond the original focus on growth and grazing rates.

#### PART I GROWTH RATES: Estimating the Numerical Response

##### 1.0 General Methods

A series of experiments was conducted to determine the numerical response of strain SPJSC grazing on the diatom *Thalassiosira pseudonana* at food concentrations ranging from 0 to  $10^5$  cells mL<sup>-1</sup>. The ciliates and prey were maintained in a semi-continuous culture by transferring the ciliates to new prey and medium on a daily basis. The details of this method follow.

Prey cultures of *T. pseudonana* were maintained at a constant nutritional quality (see Harrison *et al.* 1990), in a 500 mL glass turbidostat at  $2.5 \times 10^5$  cells mL<sup>-1</sup> at 16-17°C with continuous irradiance of 100  $\mu$ mol photons m<sup>-2</sup> s<sup>-1</sup>. Prior to the experiments, strain SPJSC was maintained in enriched natural seawater with *T. pseudonana* (medium modified from that of Harrison *et al.* 1980, see Appendix 1) in 150 mL glass flasks at 16-17°C on a 14:10 h light:dark cycle at 20  $\mu$ mol photons m<sup>-2</sup> s<sup>-1</sup>. Ciliates were collected during log or stationary

phase; prey concentrations, which the ciliates were collected from, were not controlled and ranged from  $10^3$ - $10^5$  prey mL<sup>-1</sup>.

During the experiments, ciliates were grown in the dark (to prevent mixotrophic autotrophy) in 6-well, 20 mL plastic tissue culture plates containing 10 mL of prey and medium. Prey concentrations were made by diluting prey and medium, collected from the turbidostat, with unenriched, pasteurized natural seawater (heated at 80°C for > 12 h and filtered with Whatman GF/A glass fiber filters, 1.6 µm retention). Prey concentrations were measured using a Coulter Counter (Model TAI). Typically, each concentration was replicated three times.

For any one prey concentration (treatment), the semi-continuous culturing method was as follows: ciliates were collected from stock cultures and 10 ciliates were placed in each of 3 wells in a 6-well tissue plate (thus, n=3), using a finely drawn Pasteur pipette (the 10 mL volume of water was altered by < < 0.01 % by this procedure). The tissue plate was then placed in the dark for 24 h at 16-17°C. After 24 h, the prey concentration was remade (as described above) and allocated to 3 wells in a new tissue plate. Then, from an old well, 10 randomly chosen ciliates were removed and transferred to a new well. If more than 10 ciliates were in an old well (i.e. population growth was positive), the excess was counted and removed. If less than 10 ciliates were in a well (i.e. population growth was negative), all the ciliates were transferred. It was thus possible to determine a daily change in ciliate numbers and establish a growth rate at a defined prey density. Growth rate ( $\mu$ ) was calculated as  $\mu = (\ln \text{cells}_{t+1} / \ln \text{cells}_t)$ , where t = time in days (i.e. exponential growth was assumed over 24 h).

The numerical response data were fitted to a modified Michaelis-Menten model (Eq. 1). This model was chosen since it is a good predictor of both functional and numerical responses and is based on theoretically sound mechanisms (see Holling 1959, Spain 1982, Fenchel 1986, Taniguchi and Takeda 1988, Appendix 2).

$$\mu = \{\mu_{\max} * ([P] - x')\} / \{k + ([P] - x')\} \quad (1)$$

where,



$\mu$  = growth rate ( $d^{-1}$ ) =  $(\ln \text{cells}_{t+1} / \ln \text{cells}_t)$ ,  $t = 24 \text{ h}$

$\mu_{\max}$  = the maximum growth rate ( $d^{-1}$ )

[P] = prey concentration ( $\# \text{ mL}^{-1}$ )

$x'$  = the x intercept (the prey concentration where  $\mu = 0$ ) ( $\# \text{ mL}^{-1}$ )

$k$  = the half saturation constant (i.e. [P] at  $0.5 \mu_{\max}$ ) ( $\# \text{ mL}^{-1}$ )

Curves were fitted to the data using the Marquardt-Levenberg algorithm (Sigmaplot, Jandel Scientific, CA.). This is an iterative fit which minimizes the sum of squares of differences between the dependent variables in the equation and the observed data. At very high prey concentrations growth rate of the ciliate was often negative. Curves were not fitted to data above  $7 \times 10^4 \text{ prey mL}^{-1}$ .

The methodology, described above, was followed for three separate sets of experiments. As experiments were performed, modifications were made in the procedure to determine the cause of unanticipated variation in the growth response. The methods, results and discussion for each of the three sets of experiments are outlined in three sections below.

## **1.1 First Set of Experiments**

### **1.1.1 Methods**

A total of 25 treatments (prey concentrations) were examined in 5 experiments, since it was not logistically possible to run 25 treatments simultaneously. Treatments ranged from  $2 \times 10^3$ – $10^5 \text{ prey mL}^{-1}$ . The 5 experiments were similar in their execution, but they were run days to weeks apart, on different "batches" of prey and on different "batches" of ciliates (ciliates from the same original clone but different sub-clones). At the time, it was assumed that combining these experiments would not bias the results.

Two tests of methodology were made: 1) One of the experiments was run for 9 days while the others were run for 5 days. The 9-day experiment was used to determine the variation of growth rate over the 9 days. 2) One of the 5-day experiments was used to determine the stability of the prey concentrations; the prey concentrations were measured prior to adding the ciliates and after the ciliates had been removed (24 h later). Otherwise, the

experimental procedure of the 5 experiments followed the semi-continuous culture methodology described in section 1.0.

## **1.1.2 Results and Discussion**

### **1.1.2.1 Consistency of Growth Rate**

For all prey concentrations, of the 9-day experiment, there was an increase in growth rate of strain SPJSC over the first 1-2 days. This was followed by a relatively constant growth rate between days 3-5. After day 5, in several treatments, growth rate decreased (Fig. 3.1a-i). Typically, a replicate (10 cells) which began to decline in growth rate continued to do so, but other replicates at the same treatment concentration often maintained a constant rate (e.g. Fig. 3.1e).

Thus, I decided that growth rate did not stabilize until after day 2, and that after day 5 there was a potential bias, possibly caused by the experimental procedure or by stochastic extinction (see sections 3.2 and 4.1). Growth rates reported for all experiments use the mean growth rate from days 3-5 exclusively.

### **1.1.2.2 Consistency of Prey Concentration**

Data from one experiment were used to assess the day-to-day precision of maintaining prey stocks at a predetermined concentration. The *T. pseudonana* concentration typically increased over the 24 h dark period. Higher concentrations remained relatively constant but lower concentrations ( $< 10^3$  cells mL<sup>-1</sup>) were, at times, 50% higher than the desired treatment level (Fig. 3.2). It is likely that "background noise" added to the imprecision of lower counts. Prey concentrations, used for the numerical response, were the average concentrations determined from the tissue plate wells over days 3-5.

### **1.1.2.3 Numerical Response**

The growth rate followed a rectangular hyperbolic response from  $2 \times 10^3$  to  $7 \times 10^4$  prey mL<sup>-1</sup> (Fig. 3.3a). At concentrations above  $7 \times 10^4$  prey mL<sup>-1</sup>, the response was less predictable: some replicates lay near the asymptote predicted by the hyperbolic function, but others lay well below it. The variance of the treatment response increased as prey

concentration increased. At prey concentrations below  $3 \times 10^3 \text{ mL}^{-1}$ , ciliate net mortality (henceforth referred to as mortality) occurred, presumably due to starvation.

Equation 1 was fitted to the data between  $2 \times 10^3$ - $7 \times 10^4 \text{ prey mL}^{-1}$  (Fig. 3.3a). The parameters and estimates of error of the equation are presented in Table 3.1. The data were not evenly scattered around the predicted curve. Variation between treatments existed and was related to the different experimental runs (i.e. over a range of similar prey concentrations, experimental runs yielded different values from each other). I speculated that this was due to changing experimental conditions (e.g. food quality); this was examined next.

## 1.2 Second Set of Experiments

### 1.2.1 Methods

In the first set of experiments there was variation in growth response within and between treatments (see section 1.1.2.3). I hypothesized that the variation between treatments was due to combining the 5 separate experiments. To test this, a single experiment was run with 20 treatments using only one "batch" of prey and one "batch" of ciliates. If inter-treatment variation was due to combining experiments, this procedure would reduce the amount of variation. Because the growth response was asymptotic by  $4 \times 10^4 \text{ prey mL}^{-1}$  (Fig. 3.3a), this experiment was conducted over a smaller prey range than the previous experiment: from  $0$ - $4 \times 10^4 \text{ mL}^{-1}$ .

### 1.2.2 Results and Discussion

The growth rate followed a rectangular hyperbolic response between  $0$ - $3.7 \times 10^4 \text{ prey mL}^{-1}$  (Fig. 3.3b). There was a decrease in the variance of the treatment response as the prey concentration increased (Fig. 3.3b). At concentrations below  $10^3 \text{ prey mL}^{-1}$  mortality occurred, presumably due to starvation. Equation 1 was fitted to all the data (Fig. 3.3b). At  $7$ - $8 \times 10^2 \text{ prey mL}^{-1}$  growth rate was 0. The parameters and estimates of error for the curve fitted to this data are presented in Table 3.1.

There was less variation between treatments than in the previous experiment (section 1.1) but variation existed within treatments (Fig. 3.3b). This suggested that the variation seen in the previous experiment was not caused by changes in culturing but was due to some

intrinsic factor of the ciliate culture. I speculated that the variation was due to different ciliate strains within the harvested "batch" culture. This prediction was supported by what appeared to be three distinct numerical response curves formed by the data (Fig. 3.3b); these may have represented three genotypes (or phenotypes) which expressed different growth rates. The next experiment examined the differences in growth rate between cell lines.

### **1.3 Third Set of Experiments**

#### **1.3.1 Methods**

The modifications made in the second set of experiments did not reduce the variation within treatments. Thus, a third set of experiments was performed to test if the variation was due to differences in ciliate cell lines (see section 2.0 and 3.2 for an explanation of how different genetic lines could occur).

A single ciliate was placed in each of 24 tissue plate wells containing 10 mL of medium with saturating prey ( $10^4 \text{ mL}^{-1}$ ) and allowed to grow (at  $\sim 1$  division  $\text{d}^{-1}$ , this provided sufficient numbers of progeny, from a single cell, to perform experiments within 8-10 days).

In the first experiment of this type, two clones were grown in 6 treatments ranging between  $4 \times 10^2$ - $1.8 \times 10^4$  prey  $\text{mL}^{-1}$ . Some ciliates in one of these clones were conjugating on day 10 of the isolation period. Only non-conjugating individuals were used from this culture, but these may have been exconjugants.

In the second run of this experiment, the progeny of one of the isolated cells produced  $> 360$  cells within 8 days (sufficient numbers to perform 6 replicates at 6 concentrations).

*Note:* an increase from 1 to 360 cells indicated that this clone had an average growth rate ( $\mu$ ) of  $0.74 \text{ d}^{-1}$  for the first 8 days. For this run, the 6 replicate clones were grown in 6 treatments ranging between  $3.7 \times 10^2$ - $1.9 \times 10^4$  prey  $\text{mL}^{-1}$ .

#### **1.3.2 Results and Discussion**

Only 2 of 24 cells isolated for the first run of this experiment and 1 of 24 cells isolated for the second run survived and divided over the 8-10 day isolation period. This suggests a survival rate of only 4-8% for ciliates in the culture flasks. Since these experiments were run

well into the first year of the life of this culture it may be that these low survival rates were due to ageing of the culture (see section 3.0).

Of the three cell lines examined, two exhibited positive growth at some of the prey concentrations. The other exhibited negative growth at all treatment levels. In the cell line that exhibited maximum growth (open circles, Fig. 3.3c) ~20% of cells were conjugating when the cells were harvested. This alone is remarkable since it indicated that strain SPJSC was capable of selfing conjugation.

Equation 1 was fitted to all the data in the two data sets that exhibited positive growth (open circles and triangles, Fig. 3.3c, Table 3.1). For both growth curves, the growth rate followed a rectangular hyperbolic response between  $4 \times 10^2$ - $2 \times 10^4$  prey  $\text{mL}^{-1}$ . For the fast growing clone (open circles, Fig. 3.3c), the variance within replicates was considerably lower than that observed in previous experiments. Below  $1.8 \times 10^3$  prey  $\text{mL}^{-1}$  mortality occurred, presumably due to starvation. For the slower growing clone (triangles, Fig. 3.3c), the variance within replicates was greater than that of the fast growing clone, but lower than that observed in previous experiments. For this clone, mortality occurred below  $1 \times 10^4$  prey  $\text{mL}^{-1}$ .

The clone that was conjugating prior to the experiment produced cells that grew as fast as the maximum rates determined from previous experiments and the three replicates showed a higher level of precision than replicates from the other clones (cf. Figs. 3.3a, b and c). Assuming that the isolated cells were exconjugants, these data suggest there was a genetic influence on growth rate.

During clonal growth there are a number of mechanisms which reduce the quality of the macronucleus and reduce clonal vitality (see Smith-Sonneborn 1981, Bell 1988 and section 3.0 below). Conjugation in ciliates results in the generation of a new macronucleus from the micronucleus. Since the macronucleus mediates cell growth, and thus fission rate, it follows that conjugation, which "rejuvenates" the macronucleus should both increase the fission rate and decrease the variability in fission rates in a culture; this is precisely what was observed.

These data suggest some of the variation presented in sections 1.1 and 1.2 was due to genetic variation in clonal lines.

The data from this experiment also suggest that over short incubation periods (5-10 days) experimental manipulation was not the cause of high variation of growth rates within a single treatment. Instead, intrinsic features, likely genetic infirmity (loaded with mutations), caused the variation. If reduced growth rates were due to genetic infirmity (caused by maintaining small populations in culture), then the maximum growth rates (observed in previous experiments) may have been representative of natural populations (assuming that natural populations regularly conjugate).

These findings are important in analyzing the data of the previous experiments since they provide criteria for "editing" the data, prior to constructing a population model (see Chapters 8 and 9). If natural populations grow at near maximal rates then, much of the data obtained in previous experiments may be ignored (however, see section 3.0).

## **2.0 Conjugation of Strain SPJSC**

Occasionally, during routine culturing of strain SPJSC, conjugating pairs were observed. Since all the sub-cultures were the descendents of a single cell, this strain must have been capable of selfing conjugation. Routinely, when conjugating pairs were observed in cultures, they were isolated. All attempts to maintain and isolate exconjugants were fruitless; all cells died while joined, or possibly shortly after separating.

Why did all these cells die? Possibly the number of heterozygotic mutations in the ciliate was sufficient to result in mortality of most exconjugants. However, this type of mortality typically occurs after several post-conjugation divisions due to phenotypic (cytoplasmically or genetically induced) lag (Berger 1976). Alternatively, it may be that the observed cells were genetically infirm or that culturing conditions were poor, and the process of conjugation caused mortality.

### 3.0 An Estimate of the Inheritance of Growth Rate

Growth rate varied between different sub-clones raised for ~10 generations, and these disparate growth rates may have been caused by genetic differences. If this were so, then the progeny of a fast growing clone should also be fast growing. Further, if a fast growing clone was "genetically healthy" (i.e. lacked mutations) then, fast growth should be constant for many (>50) generations (Nanny 1980, Bell 1988, and discussion below). The following experiment was conducted to test this hypothesis.

#### 3.1 Methods

One hundred and two cells of strain SPJSC were isolated from stock cultures and placed in separate 20 mL wells containing 10 mL of culture medium (as described in section 1.0 above) and saturating levels of *T. pseudonana* ( $3 \times 10^4 \text{ mL}^{-1}$ ). The ciliates were left in these containers at 16-17°C on a 14:10 light:dark cycle at  $10 \mu\text{mol photons m}^{-2} \text{ s}^{-1}$  for 9 days. On day 4 and day 9 the number of cells in each well was estimated.

After 9 days only 17 of the 102 wells had ciliates in them (i.e. ~17%). Three of these clones were used to repeat the experiment: from each of the three clones 34 cells (a total of 102) were isolated and maintained for 10 days under the conditions described above. Again, on day 4 and day 10 the cell number in each well was estimated. Finally, after 10 days only 1 of the 102 wells had ciliates in it (i.e. <1%). Sixty-six cells were isolated from this sub-clone, maintained for 9 days under the conditions described above, and on day 4 and day 9 the number of cells in each well was determined.

#### 3.2 Results and Discussion

If growth rate was strictly an inheritable trait for strain SPJSC, then the progeny of the fast growing cells would also be fast growing, but this was not so. The mean and maximum growth rate of sub-clones decreased over 20 generations (Fig. 3.4, Table 3.2). This was also observed in section 1.3 where the growth rate of one clone decreased from 0.74 to  $<0.5 \text{ d}^{-1}$  over 10-15 days. The fast growing cells typically represent 1-15% of the population (Table 3.2). This agrees with the 4-8% survival rate observed in section 1.3.2. Thus, when these

experiments were performed, culture growth may have been by a small percentage of the population surviving and growing relatively rapidly.

The reductions in growth rate may have been the result of experimental manipulation (external sources) but also could be due to intrinsic (genetic) factors. Both empirical and theoretical evidence suggests that if growth rate was inheritable then the progeny of a fast growing clone should also be fast growing and this trait should be constant for  $> 100$  generations after conjugation.

Bell (1988) has reviewed the literature and emphasized what others have shown: typically, isolated cells will maintain a constant growth rate for  $> 100$  generations, but by  $\sim 200$  generations after conjugation, most ciliate clones are extinct. However, the older the parent at the time of conjugation, the shorter the life span of the progeny line (Smith-Sonneborn 1981). Thus, in a population, a series of delays in the onset of conjugation would reduce the number of viable generations, post conjugation (i.e. clonal lines would maintain a constant growth rate for  $< 200$  generations).

There are 5 reasons for the decrease in vitality in small populations: 1) *random assortment in the macronucleus* causes a dilution and/or change of frequency of functionally haploid genetic fragments (i.e. heterozygosity verges to homozygosity or a loss of a gene); 2) *repeated automixis or selfing conjugation* fractions a heterozygotic population into homozygotic lines; 3) *recessive mutations in the micro- and macronuclei* become expressed through *random assortment in the macronucleus* and/or *repeated automixis and selfing* (1 and 2 above); 4) *Muller's ratchet* (the accumulation of deleterious mutations) works on the micro- and macronuclei in small populations; and 5) *probability of extinction from stochastic processes* occurs in small cultures (i.e. for a finite population growing exponentially there is always a probability that the population will go extinct; this probability increases exponentially with decreasing population size).

These processes increase the likelihood of: 1) expression of lethal or sublethal recessive genes; 2) homozygosity, which may reduce hybrid vigor; 3) the accumulation of mutations; and 4) dilution out of healthy stock from cultures. All of these would increase the likelihood



of a culture becoming extinct and help to explain why so many ciliates do not survive well in culture (see Nanney 1980, Smith-Sonneborn 1981, and Bell 1988 for reviews of these concepts).

The biological solution to these degenerative processes is sex. Conjugation in ciliates generally replaces the macronucleus which controls somatic growth (Lynn and Corliss 1991). Thus, the progeny after conjugation will grow faster than their parents. However, if the parental lines are old, the number of transmittable mutations increases and the progeny will still have a retarded growth rate. This may be what was happening in the cultures of strain SPJSC.

Strain SPJSC was maintained in culture for >250 days. If the ciliate grew near the maximum rate in stock cultures ( $1\text{-}2\text{ division d}^{-1}$ ), then it exceeded the 200 generations typical of viable lab cultures. Since conjugation occurred in cultures, the life of the culture may have been prolonged. However, conjugation may not have entirely rejuvenated the culture. When the experiment described in this section was conducted, strain SPJSC was near the end of its life; a month later it was dead. Possibly, the reason that 1-5% of the population grew rapidly while the rest died was that, a few cells underwent undetected conjugation which stimulated rapid growth for several generations.

Since the results of these experiments were conducted on "old" cultures it would be imprudent to directly apply them to natural populations. However, the data can be used to interpret variation in earlier numerical response experiments. Previous results suggested that growth rate was inheritable: 1) groups of 10 ciliates maintained a constant growth rate for 5-8 generations (Fig. 3.1); 2) some isolated cells grew to form large numbers (up to 360) in 8 days while others died off; and 3) cells that were likely post conjugates grew at maximum rates. The data from this section do not support the notion that growth rate was strictly inheritable unless I invoke the notion that undetected conjugation occurred. Possibly, both inheritable and non-inheritable factors affected the growth rate.

## 4.0 Sources of Bias and Explanations of Methods

### 4.1 Mortality

Equation 1 was fitted to all prey concentrations, including lower prey concentrations where mortality occurred. However, this procedure may be incorrect since mortality rate in food deprived cultures may not be constant (Jackson and Berger 1985). In the semi-continuous culturing method a healthy, non-starving, population should (and typically did, Fig. 3.1) maintain a constant growth rate over the experimental period. This is an assumption for the exponential model. However, mortality rate was likely not constant over the same period. Two reasons this may be so are: 1) If the ciliates were dying due to starvation (low food) or the accumulation of "toxic" material (possibly the cause of mortality at high food conditions), mortality would be time dependent. Since, for negative growth rates, the same cells were observed each day, cumulative effects could change the mortality rate; thus, it would not be constant. 2) The negative growth rate would not be constant for strictly stochastic reasons. Since ciliates were not added to wells where numbers dropped below 10 (see section 1.0), the likelihood of the population becoming extinct would increase as the cell number decreased (i.e. the probability (P) of a population of n cells becoming extinct is:  $P(0,n) = 1$ , if  $b \leq d$ , and  $P(0,n) = (d/b)^n$ , if  $b > d$ , where  $d$  = death rate and  $b$  = birth rate, Bell 1988).

With these biases in mind, I have still used the exponential growth model to estimate mortality rates and have used the data range where the ciliates were likely starving to establish numerical response curves; this is similar to methods adopted by others (e.g. Jackson and Berger 1984, Turley *et al.* 1986). The negative growth rates, established in the above sections, may be interpreted as 3-day averages. When modeling the response to food for this ciliate and others (in Chapter 8 and 9), mortality rate was estimated with these biases in mind; both biases overestimate mortality rate.

### 4.2 Handling of Ciliates

Daily transfer of ciliates with finely drawn pipettes may have delayed division and biased the growth rate estimates. Others have found similar transfers to cause 10 min delays in fission rate (e.g. Adl and Berger 1991, for *Paramecium tetraurelia*). Such delays in fission

would cause a small ( $< 1\%$ ) reduction in generation time, assuming that similar effects occurred for strain SPJSC, and they were ignored in the analysis.

### 4.3 Food Quality

For the growth experiments on strain SPJSC, all the prey were grown in a turbidostat. This was done to provide food of a constant biochemical quality, thus removing one source of potential variation. In retrospect, there was considerable variation due to the ciliate and not the food. In subsequent work, on other ciliates, I did not use a turbidostat to grow the food but kept the food in exponential growth phase by serial dilutions of batch cultures.

### 5.0 Aspects of the Growth Rates and their Ecological Relevance

Although there was variation in the data, both within and between treatments, 4 pieces of information can be procured from the numerical response data: 1) The threshold concentration of *T. pseudonana* for strain SPJSC (i.e. the prey concentration below which the ciliates cannot survive) was  $\sim 10^3 \text{ mL}^{-1}$ ; 2) the major increase in growth rate occurred between  $10^3$ - $10^4$  prey  $\text{mL}^{-1}$ ; 3) the maximum growth rate was  $\sim 1.4$  divisions  $\text{d}^{-1}$  (Fig. 3.3c, Fig. 3.5a, broken line); and 4) strain SPJSC was capable of selfing.

During the summer in the Sechelt fjordal system (Appendix 3), where strain SPJSC was collected, average numbers of phytoplankton of similar size to *T. pseudonana* ( $5\text{-}10 \mu\text{m}$ ) ranged from  $200\text{-}44000 \text{ cells mL}^{-1}$  (Appendix 3) and more relevantly, small diatoms ( $4\text{-}5 \mu\text{m}$ ) ranged from  $0\text{-}2000 \text{ cells mL}^{-1}$  (data not shown). This means that on average natural levels of food could be sufficient to support strain SPJSC, and for short periods this ciliate could be growing at its maximum rate, potentially forming blooms.

The occurrence of selfing in strain SPJSC indirectly supports the notion that it forms monoclonal blooms. The following scenario may occur if: 1) selfing conjugation is a trait acquired to allow conjugation when ciliates are unable to find other clones, and 2) starvation stimulates conjugation (Nanney 1980): a bloom develops from a single cell finding itself in optimum-food conditions, the progeny of this ciliate then deplete the food and starvation

ensues. This in turn stimulates conjugation. However, the bloom would be monoclonal and selfing would result.

This scenario requires that both ciliate abundance and prey patch size are such that only one mating type of a species will find a prey bloom. In Indian Arm (British Columbia), in the late winter, *Strombidinopsis* abundance was rare (Martin and Montagnes 1993). It was found at only 1 of 6 sites that were 1-5 km apart. Although this does not indicate *Strombidinopsis* forms monoclonal blooms, it does suggest a patchy distribution or that this species is rare in the winter.

## 6.0 A Numerical Response Model

Initially, the goal of these studies was to establish a numerical response curve for strain SPJSC with which to model blooms. But, the expression and evaluation of variance in growth response retarded the development of this curve. The variance suggested that many of the low growth rate data resulted from genetically unhealthy lines. Assuming that natural populations grow at near maximal rates, much of the lower growth rate data may be ignored. Accordingly, some editing was conducted.

Equation 1 was fitted to a compilation of the data presented in sections 1.3-3.3, (Fig. 3.5a, solid line). The residual sum of squares (calculated by the Sigmaplot curve fitting function) were plotted against prey concentration (Fig. 3.5b, all data). The residuals were not evenly distributed around zero. To adjust for this, points below - 0.4 were omitted (Fig. 3.5b, open circles); these points were assumed to represent genetically unhealthy lines. Equation 1 was then fitted to the remaining data (Fig. 3.5a solid circles, broken line; 3.5b, solid circles); the residuals of this fit appeared (by eye) to be evenly distributed around zero (Fig. 3.5c), suggesting a better fit. The second curve (Fig. 3.5a, broken line) provided a higher numerical response with a more rapid response to food concentration than the fit to all the data. This upper response has been used in Chapters 8 and 9 to predict the growth response of a "genetically healthy" population of strain SPJSC. The parameters and estimates of error for the solid and broken curves in Fig. 3.5 are presented in Table 3.1.

## PART II GRAZING RATES: Estimating the Functional Response

### 7.0 General Methods

A series of experiments ( $n = 16$ ) was conducted to determine the effect of prey concentration on the grazing rate of strain SPJSC. Fluorescently labeled,  $5\ \mu\text{m}$ , latex beads (Seradyn, Particle Tech. Div., Indianapolis IN, USA) were used to simulate the diatom *Thalassiosira pseudonana*, on which the ciliate was cultured. The experiments were run at "food" concentrations ranging from  $1.8 \times 10^3$  to  $1.1 \times 10^5$  beads  $\text{mL}^{-1}$ .

The beads, which were suspended in a "toxic" surfactant, were rinsed with distilled water using a  $3\ \mu\text{m}$  filter, suspended in a 5% bovine serum albumen-distilled water solution for  $>24$  h (up to a month) to reduce clumping (Pace and Bailiff 1987) and refrigerated ( $5^\circ\text{C}$ ) for storage. Prior to use, the beads were rinsed with prefiltered seawater with a  $3\ \mu\text{m}$  Millipore filter and resuspended by sonication (50/60 Hz bath sonicator). Beads were also sonicated prior to counting with a Coulter Counter (Model TA II).

Prior to the experiment, ciliates were maintained as described in section 1.0. To standardize the nutritional history of the ciliates prior to experimentation, ciliates were placed in filtered seawater to starve for 4-5 h. Then,  $4\text{-}5 \times 10^2$  ciliates were transferred in a drop of seawater (0.1 mL) to a 20 mL plastic tissue culture well containing 10 mL of treatment solution (enriched seawater containing  $5\ \mu\text{m}$  fluorescent beads at a known concentration). The bead solution was previously sonicated for 30 s to ensure mono-dispersion. The experiments were run at  $16\text{-}18^\circ\text{C}$ .

Every 5 min, for 30 min, after the ciliates were added to the bead solution (time 0) 30-60 ciliates were removed from the container, using a finely drawn pipette and fixed in 5% (volume/volume) Bouin's fluid on coverslips with petroleum jelly on the edges. These were then placed on a microscope slide, the petroleum jelly sealing the edges. Some ciliates were lost during this manipulation; for each time interval, 20-40 ciliates were observed. The ciliates were examined using fluorescent microscopy (100-200 X; Zeiss filters blue excitation, BP 450-490, FT 510, LP 520). To estimate bead ingestion rate, the mean number of beads

ciliate<sup>-1</sup> was visually determined and plotted against time. The grazing rates were fitted to a Michaelis-Menten function (Eq. 2, see Appendix 2).

$$G = (G_{\max} \times [B]) / (k + [B]) \quad (2)$$

where,

$G$  = grazing rate (beads ciliate<sup>-1</sup> h<sup>-1</sup>)

$G_{\max}$  = the maximum grazing rate (beads ciliate<sup>-1</sup> h<sup>-1</sup>)

$[B]$  = beads concentration (# mL<sup>-1</sup>)

$k$  = the half saturation constant (i.e.  $[B]$  at  $0.5G_{\max}$ )

## 7.1 Results and Discussion

For all treatments (bead concentrations) the mean number of beads ciliate<sup>-1</sup> increased linearly with time (Fig. 3.6a). Grazing rate ranged from 0.48 to 27 bead ciliate<sup>-1</sup> h<sup>-1</sup> and increased with bead concentration, but an asymptotic response, as predicted by Eq. 2, did not exist (Fig. 3.6b). If feeding and growth were linearly correlated, this response would asymptote after  $2 \times 10^4$  prey mL<sup>-1</sup> (see Fig. 3.5).

Why did grazing not follow a hyperbolic response? Here are four possibilities: 1) The nutritional history of the ciliates may have influenced their ingestion rate (i.e. the 4-5 h starvation period was an inadequate method of standardizing nutritional history). The ciliates used for the experiment at  $7.5 \times 10^4$  beads mL<sup>-1</sup> were isolated from a dense culture of prey ( $> 10^5$  prey mL<sup>-1</sup>), and the points at this concentration appear to be anomalous (open circles, Fig. 3.6b). Further, the starvation period may have caused elevated grazing rates. 2) The variation in feeding may have been due to clonal variation (as seen in Part I). 3) Higher variation of feeding data occurred  $> 7 \times 10^4$  beads mL<sup>-1</sup>. Possibly there was grazing inhibition at high concentrations; this parallels the growth response (Fig. 3.5). 4) The ciliates selected against the beads. This last reason is the simplest and may be the most reasonable, as several ciliates did not eat beads (see Chapter 8).

Since the 3-4 h starvation period and a diet of only beads may have biased grazing rates, I modified grazing experiments (on other ciliates, see following chapters) by 1) using a

1:1 combination of live prey with fluorescent surrogates and 2) acclimating the ciliates to the prey concentrations used during the grazing experiments.

## 7.2 Modeling the Response

Although there was no asymptotic response in the grazing rate with food concentration, there was a good fit of the data to Eq. 2 (Fig. 3.6b, solid line). However, given that the points at  $7.5 \times 10^4$  beads  $\text{mL}^{-1}$  (Fig. 3.6b open circles) may be poor estimates of grazing rate, I refit the response without them (Fig. 3.6b, broken line). For the reasons discussed above, the data may be biased, but I have still used the upper curve in Fig. 3.6b to compare grazing rates in Chapter 8.

## CONCLUDING REMARKS

The genus *Strombidinopsis* is found in many coastal marine waters (Fauré-Fremiet 1924, Gifford 1985, Lynn *et al.* 1991, Snyder and Ohman 1991, Putt 1991, Sime-Ngando *et al.* 1992). This genus has never been reported at high densities, suggesting that it rarely, if ever, forms blooms. However, the data from this study suggest that *Strombidinopsis* has the potential to bloom over short periods, as it can grow rapidly when exposed to high prey concentrations. The growth response of this species has been used in Chapters 8 and 9 to model one potential ciliate response to changing prey concentrations.

Gifford (1985) cultured *Strombidinopsis* (cf. *acuminatum*) on several prey and maintained it on a combination of *Heterocapsa triquetra* and *Chroomonas salina* for almost a year. Although her *Strombidinopsis* culture was not monoclonal, it was the only one of 21 isolated oligotrichs that conjugated. Possibly these cultures were selfing or were at least predisposed to conjugating in culture. Thus, *Strombidinopsis* may be a useful organism to culture for future research on oligotrich mating.

Gifford (1985) also supported Blackburn's (1974) assertion that oligotrichs, and specifically *Strombidinopsis*, do not grow well on *Thalassiosira* species, arguing that  $\beta$ -chitan threads on the frustule render them inaccessible to ciliates.  $\beta$ -chitan threads also inhibited

growth of tintinnids fed *T. pseudonana*, but when stirred or shaken the diatoms lost their threads and supported ciliate growth (Verity and Villareal 1986).

My cultures of *T. pseudonana*, which supported *Strombidinopsis*, were stirred and were therefore likely "thread-free". This study may therefore represent an "unnatural" situation as some *Thalassiosira* species possess  $\beta$ -chitan threads *in situ*. However, the presence of threads is variable in field samples (F. J. R. Taylor, pers. comm.), and field observations indicate that ciliates do eat small centric diatoms (unpublished data). Further, natural populations of ciliates were attracted to *T. pseudonana*, suggesting that it may be a beneficial prey species (Verity 1991b). *Thalassiosira pseudonana* could stimulate ciliate blooms, as it does bloom in some coastal waters (Guillard and Ryther 1962). However, blooms of *T. pseudonana* have not been reported in British Columbian waters. Even if *T. pseudonana* is not a typical food for ciliates, my data will be useful for modeling potential responses. Assuming that there is a relation between organic carbon and growth rate, these data can be used to estimate a general growth response of this ciliate (see Chapter 9).



Table 3.1. Growth and grazing data for *Strombidinopsis acuminatum* strain SPJSC; parameters and estimates of error of the numerical and functional response equations presented in Figs. 3.3-3.6. See section 1.0 in this chapter for the equations used. Values are in units of numbers  $\text{mL}^{-1}$  for concentrations ( $k$ ,  $x'$ ), and  $\text{d}^{-1}$  for growth rate ( $\mu_{\text{max}}$ ).

	value	standard deviation	coefficient of variation
-----			
Michaelis-Menten fit from Fig. 3.3a			
$\mu_{\text{max}}$	0.9769	0.0765	7.840
$k$	4993	1628	32.60
$x'$	3026	426.6	14.10
Michaelis-Menten fit from Fig. 3.3b			
$\mu_{\text{max}}$	0.731	0.071	9.664
$k$	1674	505.5	30.20
$x'$	7739	201.1	25.99
Michaelis-Menten fit from open circles in Fig. 3.3c			
$\mu_{\text{max}}$	1.179	0.167	14.13
$k$	4063	1208	29.73
$x'$	1753	265.0	15.12
Michaelis-Menten fit from triangles in Fig. 3.3c			
$\mu_{\text{max}}$	0.1992	0.1642	82.45
$k$	1.349E4	4521	33.52
$x'$	1.067E4	4266	39.99
Michaelis-Menten fit from solid and open circles in Fig. 3.5a			
$\mu_{\text{max}}$	0.7286	0.07747	10.63
$k$	4843	1255	25.92
$x'$	2531	4515	17.84
Michaelis-Menten fit from solid circles in Fig. 3.5a			
$\mu_{\text{max}}$	0.9845	0.04613	4.686
$k$	4091	614.5	15.02
$x'$	1567	157.4	10.04
Michaelis-Menten fit from all circles in Fig. 3.6b			
$G_{\text{max}}$	28670	286900	1001
$k$	1.669E8	1.671E9	1001
Michaelis-Menten fit from solid circles in Fig. 3.6b			
$G_{\text{max}}$	101	184.8	182.9
$k$	426300	924600	2169



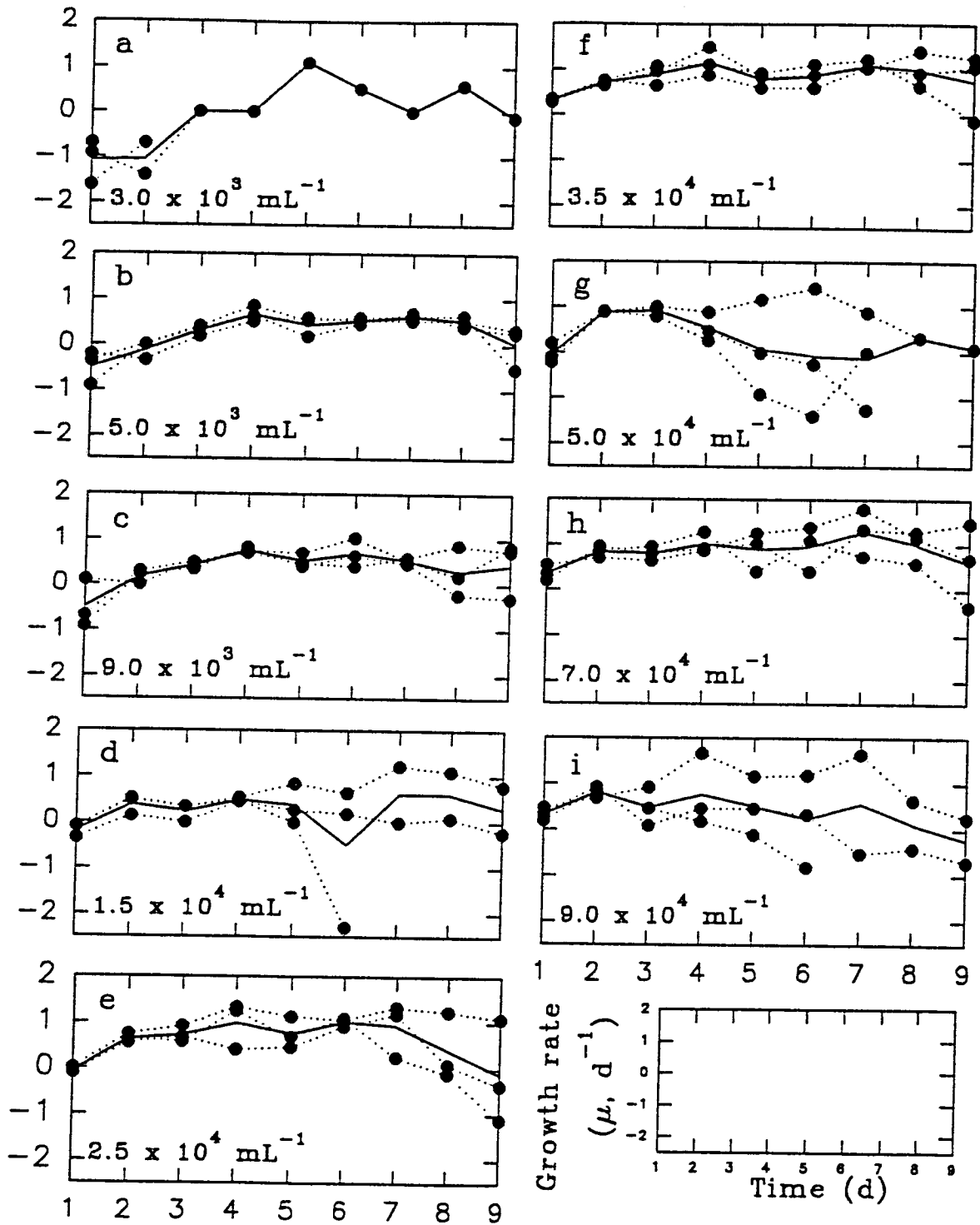


Fig. 3.1. The variability of growth rate of *Strombidinopsis acuminatum* strain SPJSC at nine prey concentrations (cells  $mL^{-1}$  as depicted in panels a-i), over a 9 day period (for 1 of the 5 experiments presented in section 1.1). Data represented by circles and connected by a broken line are the growth rate of each replicate (n = 3). The solid lines represent the average growth rate.

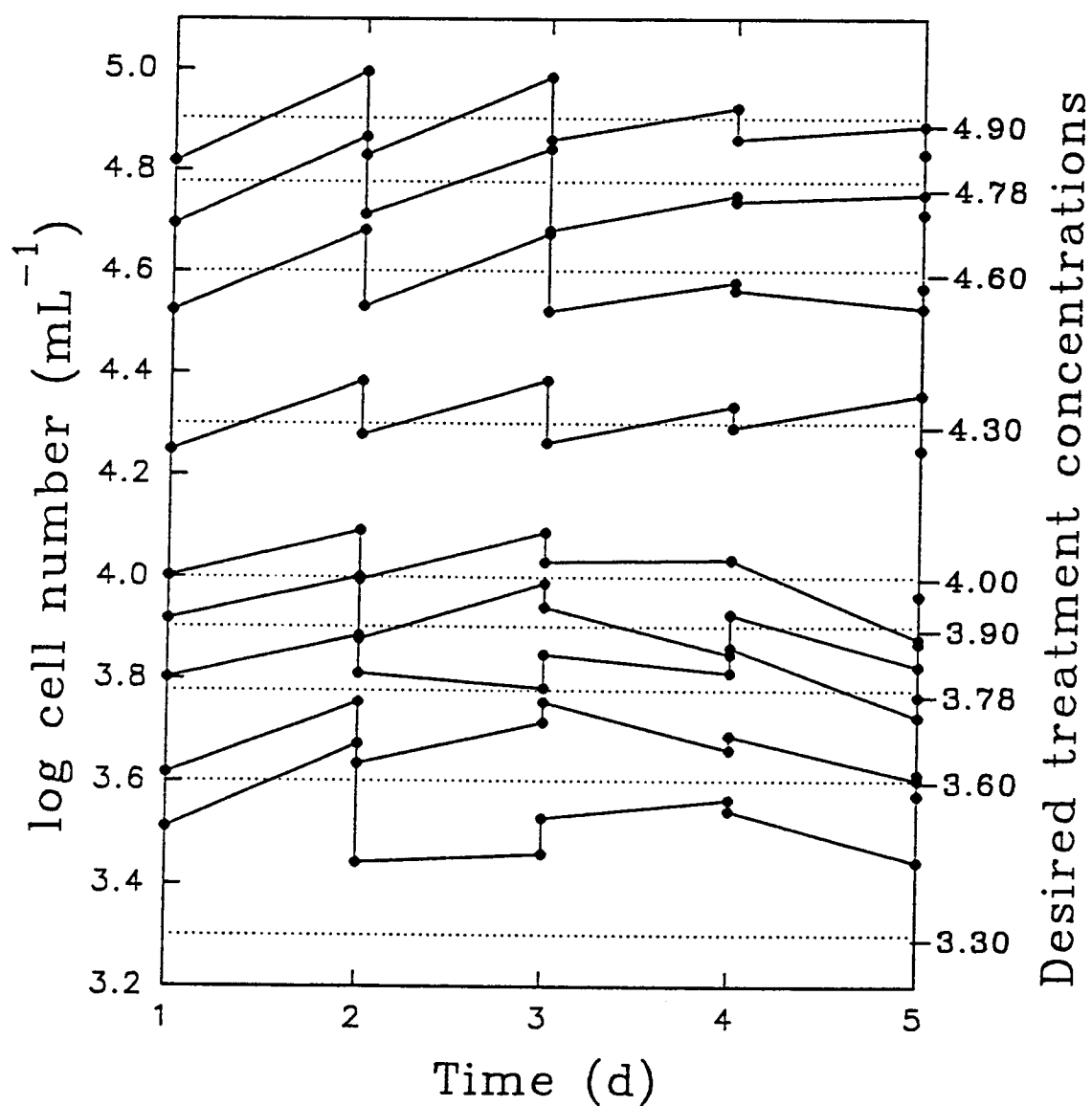


Fig. 3.2. An indication of the variability of food concentration during growth experiments on *Strombidinopsis acuminatum* strain SPJSC, over a 5 day period (for 1 of the 5 experiments presented in section 1.1). Data represented by circles and connected by solid lines are the log concentration of prey (*Thalassiosira pseudonana* mL<sup>-1</sup>). The broken lines represent the desired concentration of cells.

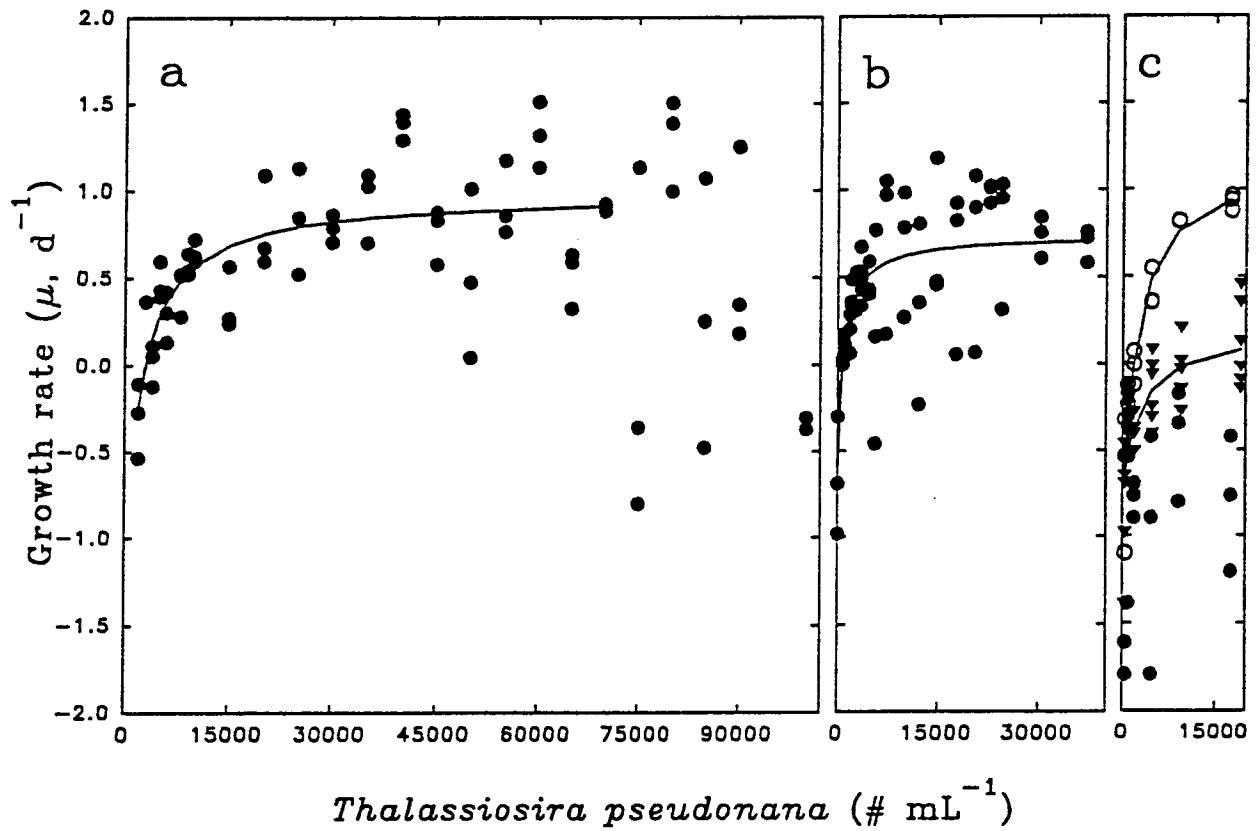


Fig. 3.3. The numerical response of *Strombidinopsis acuminatum* strain SPJSC from 3 experiments (for details see section 1.1.2.3 for panel a; 1.2.2 for panel b; and 1.3.2 for panel c). All data points represent growth rates. The open circles, triangles and solid circles in panel c represent different sub-clones (see section 1.3 for details). The curves in all figures are the modified Michaelis-Menten fit (Eq. 1 in text) to the data (see Table 3.1 for the parameters associated with these curves).

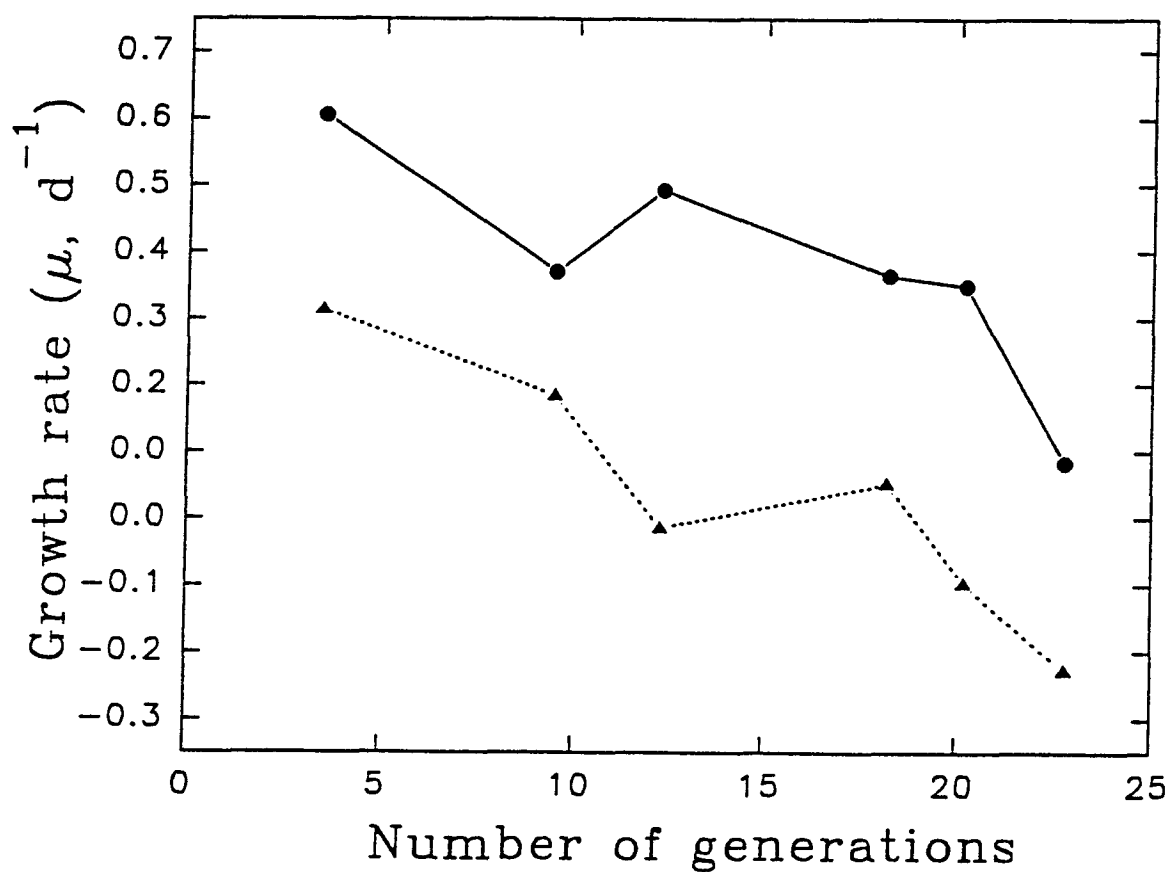


Fig. 3.4. The change in growth rate ( $d^{-1}$ ) with number of generations for *Strombidinopsis acuminatum* strain SPJSC grown on saturating food concentrations (see section 3.0 for details). The solid circles, connected by a solid line, represent the maximum growth rate, which was exhibited by 1-6% of the population. The triangles, connected by a broken line, represent the average growth rate of the experimental population.

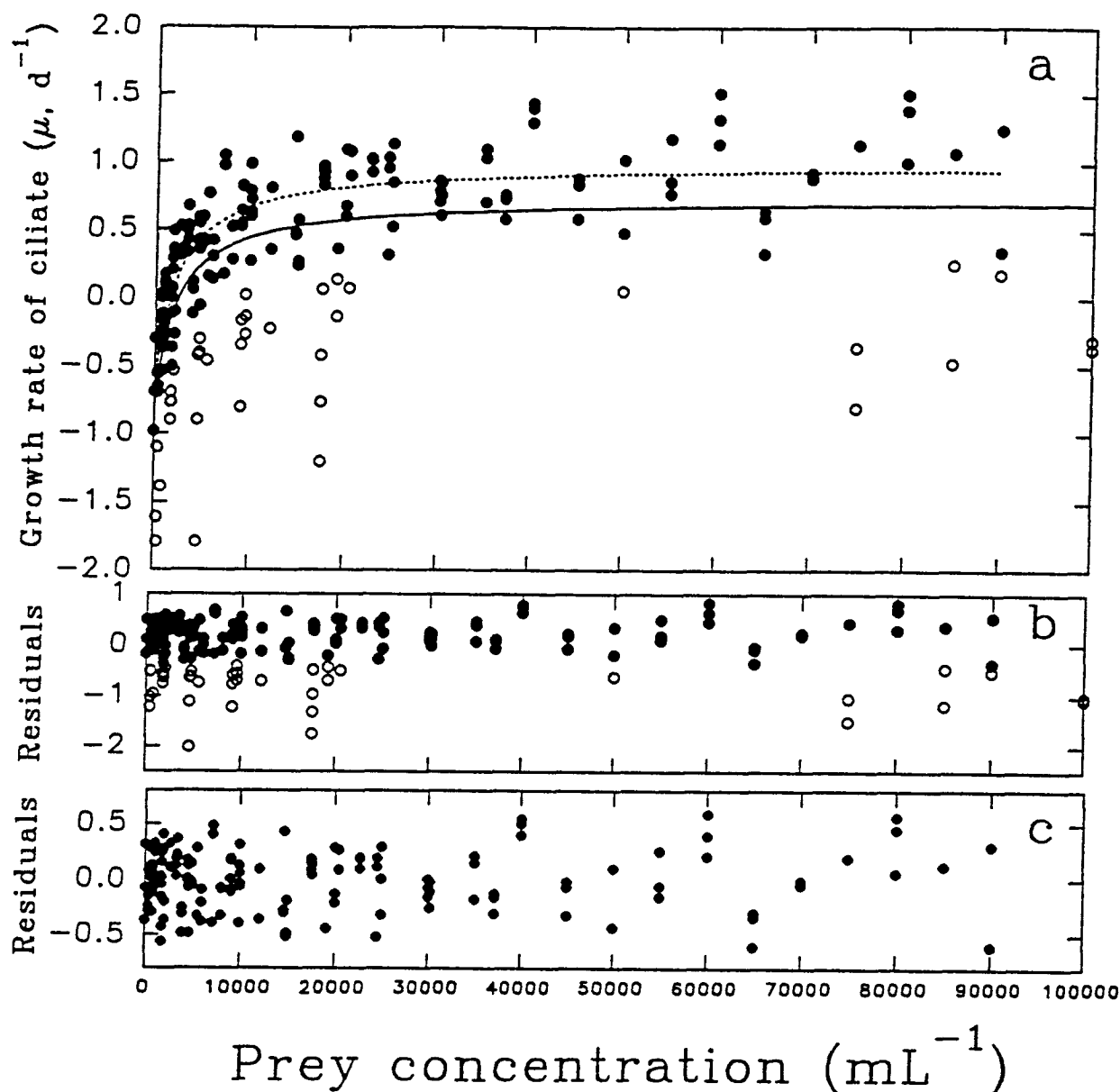


Fig. 3.5. Panel a, The numerical response of *Strombidinopsis acuminatum* strain SPJSC from a combination of 3 experiments (sections 1.1-1.3). All data points represent growth rates. The solid line represents the modified Michaelis-Menten response (Eq. 1 in text) between  $0-1 \times 10^5$  prey  $\text{mL}^{-1}$  using data represented by both open and solid circles. The broken line represents the modified Michaelis-Menten response between  $0-9 \times 10^4$  prey  $\text{mL}^{-1}$  using only data represented by the solid circles (see section 6.0 for details on how outliers were removed). See Table 3.1 for the parameters associated with the curves. Panel b, The distribution of the residuals for the Michaelis-Menten fit to all the data in Fig. 3.5a (open and solid circles, solid line). Panel c, The distribution of the residuals for the Michaelis-Menten fit to a subset (solid circles, broken line) of the data in Fig. 3.5a (see section 6.0).

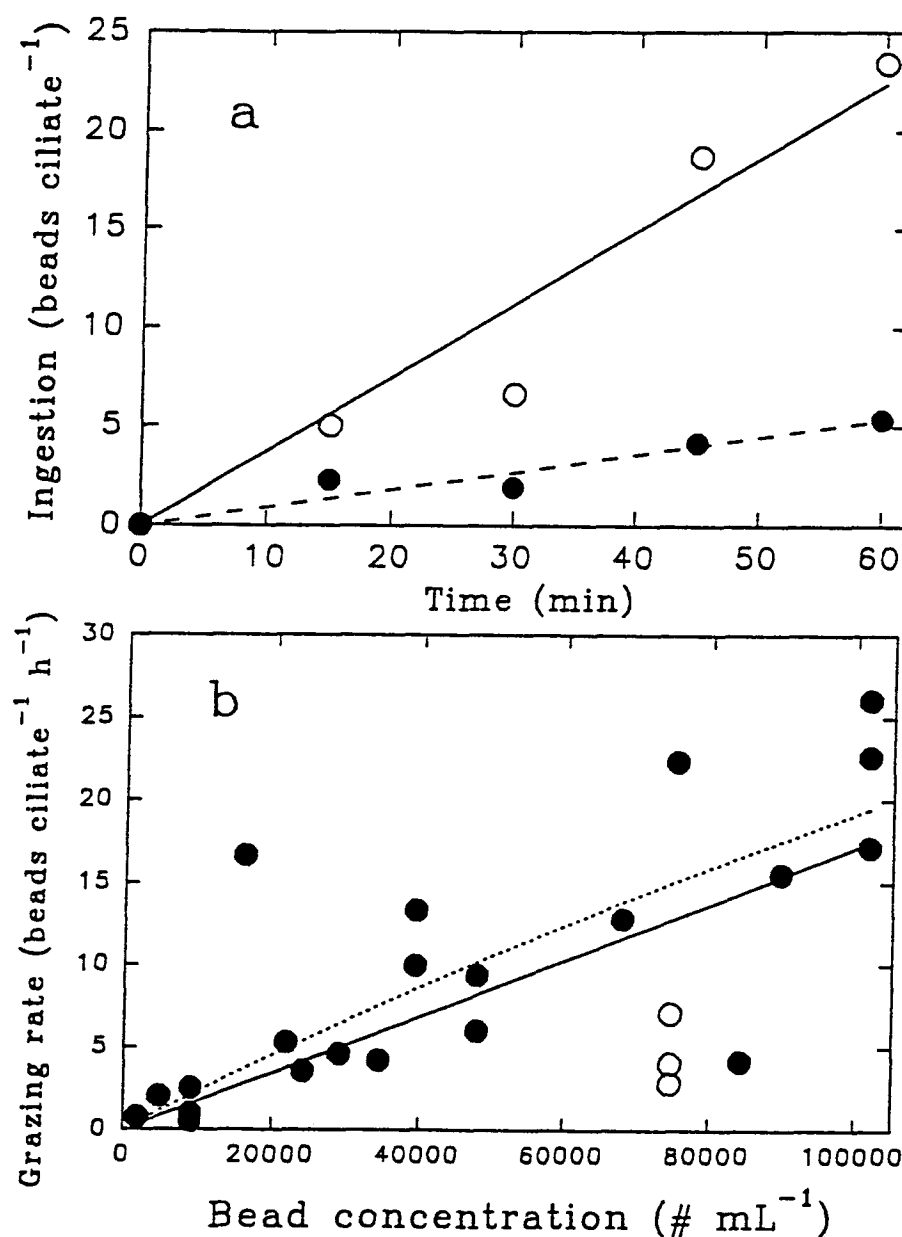


Fig. 3.6. Panel a, The change in number of fluorescent beads ingested by *Strombidinopsis acuminatum* strain SPJSC over time at two bead concentrations (open circles and solid line,  $4 \times 10^4$  beads mL<sup>-1</sup>; solid circles and broken line,  $1 \times 10^4$  beads mL<sup>-1</sup>). Both lines are linear regressions forced through the origin. *Note:* these two examples were measured every 15 min over an hour while most estimates were made by measurements made every 5 min over 30 min (see section 7.0). Panel b, The functional response of stain SPJSC ingesting 5  $\mu$ m fluorescent beads (section 7.0 for details). All data points represent grazing rates. The solid line is the Michaelis-Menten fit (Eq. 2 in text) to all the data between  $0-1.1 \times 10^5$  beads mL<sup>-1</sup>, and the broken line is the same fit but does not include the open circles (see section 7.2 for details). See Table 3.1 for the parameters associated with these curves.



## CHAPTER 4

### GROWTH AND GRAZING RATES OF *Strobilidium spiralis* STRAIN IA AS A FUNCTION OF FOOD CONCENTRATION

#### Introduction

*Strobilidium spiralis* was the last ciliate I maintained in culture. Therefore, experiments conducted on it were refined, compared to those described in the previous chapter. Unlike *Strombidinopsis acuminatum* (Chapter 3) which was maintained for almost a year, this ciliate was only maintained for 3 months before the culture died. This was typical for many of the ciliates I isolated, and I was often not able to perform a complete suite of experiments before the clones were lost. This will become apparent in later chapters where data are either missing or unsatisfactory. I was however, able to obtain estimates of grazing and growth rates for *S. spiralis*. Further, I documented the change in culture viability during the period the ciliate was maintained. This provided criteria to evaluate the growth and grazing response data.

#### PART I GROWTH RATES: Estimating the Numerical Response

##### 1.0 General Methods

Experiments were conducted to determine the numerical response of *Strobilidium spiralis* strain IA grazing on the prey flagellate *Chroomonas salina*, at food concentrations ranging from 0 to  $9.5 \times 10^4$  cells mL<sup>-1</sup>. The ciliates were maintained in semi-continuous cultures by transfers to new prey and medium on a daily basis, as outlined in Chapter 3. Modifications of this method follow.

After *S. spiralis* was isolated (see Chapter 2), it was fed 3 prey flagellates (*Chroomonas salina*, *Isochrysis galbana*, and *Rhodomonas lens*). The ciliate grew on all 3 prey individually and in combinations, but it grew faster on some prey (Table 4.1). *Strobilidium spiralis* grew well on *C. salina* alone, often as well as it grew on combinations of 2 or 3 prey. Since a major goal of this study was to determine the impact of a mono-clonal

ciliate bloom on a single prey species bloom (see later chapters), experiments were conducted using *C. salina* alone to determine the ciliate's numerical response.

*Chroomonas salina* was maintained in log phase, in 300 mL flasks, by serial dilution, on a 14:10 light:dark cycle with irradiance of  $50\text{--}100\ \mu\text{mol photons m}^{-2}\ \text{s}^{-1}$  at  $16\text{--}17^\circ\text{C}$ . Prior to the experiments, *S. spiralis* was maintained in 20 mL tissue culture wells containing enriched natural seawater with *C. salina* on a 14:10 light:dark cycle with lighting of  $25\text{--}50\ \mu\text{mol photons m}^{-2}\ \text{s}^{-1}$  at  $16\text{--}17^\circ\text{C}$ . For experiments, the ciliates were collected during log growth phase; prey concentrations, from which the ciliates were collected, were not controlled.

During the experiment, ciliates were grown in the dark in 20 mL tissue culture plates containing 10 mL of prey and medium. Prey concentrations were prepared and enumerated as described for *Thalassiosira pseudonana* in Chapter 3 (section 1.0). Typically, each concentration was replicated 3 times. The semi-continuous culture method was similar to that described in Chapter 3 (section 1.0), for *Strombidinopsis acuminatum* grown on *T. pseudonana*, except that daily transfers were continued for 7 days rather than 5 and the average growth rate was determined for days 3-7 (days 1 and 2 were an acclimation period after which growth rate was relatively constant, data not shown). The numerical response data were fitted to a modified Michaelis-Menten model using an iterative fit (Eq. 1, Chapter 3).

A total of 32 treatments (prey concentrations) were examined in two consecutive experiments; treatments ranged from 0 to  $9.5 \times 10^4$  prey  $\text{mL}^{-1}$ . Prey concentrations were measured before and after each transfer of the ciliates to examine the stability of the prey concentrations. Typically prey concentrations varied in a manner similar to that seen for *T. pseudonana* in Chapter 3: prey number increased slightly over the 24 h period and lower concentrations varied, on a relative scale, more than higher ones. Growth rates were plotted against the average prey concentration during the incubation period (5 days).

## 2.0 Results

Growth rate followed a rectangular hyperbolic response between  $0\text{--}9.5 \times 10^4$  prey  $\text{mL}^{-1}$  (Fig. 4.1). At concentrations  $< 6 \times 10^3$  prey  $\text{mL}^{-1}$  mortality occurred within the first 48 h (the

acclimation period). After the acclimation period, at concentrations  $< 1.0 \times 10^4$  prey  $\text{mL}^{-1}$ , mortality occurred, presumably due to starvation. Equation 1 (Chapter 3) was fitted to points from  $0$ - $9.5 \times 10^4$  prey  $\text{mL}^{-1}$  (Fig. 4.1). The parameters and estimates of error of this equation are presented in Table 4.2.

### 3.0 Change in Culture Growth Rate Over Time

*Strobilidium spiralis* was collected in early March. By early April it was being maintained as a monoclonal culture grown on a single prey: *C. salina*. At 3 times, between early April and mid May, the culture growth rate was measured. Ciliates were acclimated to  $5 \times 10^4$  *C. salina*  $\text{mL}^{-1}$ . Then, 70-100 ciliates were removed from the cultures and placed in separate wells in a 24 well tissue culture plate (well size = 3.5 mL). Each well contained 2 mL of culture medium plus  $5 \times 10^4$  *C. salina*  $\text{mL}^{-1}$  (a concentration yielding maximum growth rate, see Fig. 4.1). The ciliates in tissue culture plates were placed in conditions similar to those in which the ciliates had been previously maintained (see section 1.1). After 24 h the number of ciliates  $\text{well}^{-1}$  was determined.

In the first of these isolations, more than a month after the ciliates were collected, the modal number of progeny from a single cell was 4 and some cells produced up to 8 progeny. Nineteen days later, in the second isolation, the modal number of progeny was 2 and in no cases were  $\geq 5$  cells produced. Eight days later, in the final isolation, many cells had died, few were dividing and the maximum number of progeny was 2 (Fig. 4.2). Two weeks later the culture was dead. These results indicate how the culture vitality decreased over 2 months.

The reason for this decrease in growth rate was not determined. This was a trend for not only this ciliate but for several others I isolated (data not presented). In fact, it is a feature typical of most cultured oligotrichs (Gifford 1985). In the last chapter I argued that genetic deterioration was the primary cause of culture decline, but other reasons may exist for this persistent feature of oligotrich culturing.

As mentioned in Chapter 3, growth rate in most ciliate cultures decreases over time due to genetic changes (Bell 1988). Such reductions in growth rate are typical over several

months, but *S. spiralis* stopped growing after several weeks. Possibly one of the genetic infirmities, that plague isolated cultures, already existed in the collected *S. spiralis*. This would have escalated the culture's deterioration. Alternatively, it may have been inadequate culturing methods that caused the decline of the ciliates.

Lack of essential nutrients in the food supply may cause a decline in ciliate culture vitality. For a nutrient to be virtually diluted out of *S. spiralis* by the number of observed fissions (20-40), its initial concentration would need to be  $<2^{20}\text{-}2^{40}$  ( $= 10^5\text{-}10^{12}$ )  $\text{cell}^{-1}$ . The likelihood of a nutrient being diluted out of the *S. spiralis* culture was high. For example, the carbon content of *S. spiralis* is only  $6 \times 10^{16}$  atoms  $\text{cell}^{-1}$  (assuming a cell  $\sim 50 \mu\text{m}$  in diameter and  $0.19 \text{ pg carbon } \mu\text{m}^{-3}$ , Putt and Stoecker 1989). Since most essential nutrients have concentrations far below that of carbon, the depletion of a nutrient was plausible in my cultures. In fact, empirical data support this reasoning. Growth rate of the ciliate *Didinium nasutum* decreased due to "poor" food quality over 20 days ( $<40$  fissions), and the ciliate was revitalized by the introduction of "good" food (Beers, summarized in Bell 1988). It appears then that growth rate can be depressed over an extended period by poor food quality. Several substances (e.g. amino acids, purines, pyrimidines, lipids and trace elements) are required for *Paramecium* (Wichterman 1986), trace metals (either in the medium or prey) appear to be required for oligotrichs (Gifford 1985), and chloroplasts are required in the diet of *Strombidium capitatum* (Stoecker and Silver 1990). Possibly one of these was depleted in my culture of *S. spiralis*.

An alternate scenario, still within the confines of culturing technique, would be to invoke the role of some sub-lethal toxin. Such a substance could accumulate in the ciliates over time and eventually reach lethal levels. Trace metals may also act in this manner (Gifford 1985, Stoecker *et al.* 1986).

Regardless of the cause of growth rate decline, its impact has bearing on the results of this chapter. The growth rate experiments (section 1.0) were conducted from March 30 to April 9 during which time growth rate was high (Fig. 4.2). Possibly though, growth rate was even higher prior to these experiments. The grazing rate experiments (section 6.0) were

conducted on April 18-20 by which time growth rate had likely declined. Assuming that growth and grazing rates are correlated, the grazing rates of the ciliates that were used to determine growth rates may have been higher than those described in section 6.0.

#### 4.0 Examining the Growth Estimates and Developing a Numerical Response Model

The problems associated with the methods used in this chapter parallel those discussed in Chapter 3 (section 4.0). For instance, mortality was likely over-estimated and handling of ciliates was probably not an important bias. As discussed above, genetic degradation or culturing methods may also have effected growth rate, but this was not explored.

In general, the results of the numerical response of *S. spiralis* were consistent with the model (Eq. 1, Chapter 3). Some deviation occurred between  $5 \times 10^3$ - $1.5 \times 10^4$  prey  $\text{mL}^{-1}$  (Fig. 4.1). A change from rapid growth to mortality occurred over a narrow prey concentration. Then, mortality was almost constant for a range of prey concentration that were inconsistent with those predicted by the model. This may indicate switching behaviour on the part of the ciliate that is not consistent with the simple Michaelis-Menten dynamics. Possibly reduced activity (either physiological or physical) occurred below mortality-inducing concentrations. Weight specific respiration can decrease over starvation periods for protozoa (Fenchel 1982, Caron *et al.* 1990). Further, starvation reduces cell size in protozoa, and this may alter the growth rate (Fenchel 1982, 1990).

The change in cell size with food concentration was measured for strain IA, to determine if this might explain the anomalous mortality rates. In these experiments, the ciliates cultured at concentrations at  $< 1.8 \times 10^4$  *C. salina*  $\text{mL}^{-1}$  died, and there was no trend in the change of cell volumes between  $1.8 \times 10^4$ - $1 \times 10^5$  prey  $\text{mL}^{-1}$ . However, these experiments were made in mid-May near the end of the culture's life, and thus the results are suspect. There may, in fact, have been a change in cell volume with food concentration in the experiment in section 1.0. Alternatively, the mortality rate data may be misleading since, as mentioned above (Chapter 3, section 4.1), they are likely overestimated. Such an overestimation could cause the jump in response seen at the concentration where mortality

occurred. With these potential deviations from the model in mind, I have still used Eq. 1 for estimating the response curve.

## 5.0 Aspects of the Growth Rates and Their Ecological Relevance

In general, the data for this species provided a good description of the numerical response. There are 4 useful pieces of information provided by the above experiments: 1) the threshold concentration of *C. salina* for *S. spiralis* was  $\sim 10^4$  mL<sup>-1</sup>; 2) the maximum increase in growth rate was between  $10^4$ - $2 \times 10^4$  prey mL<sup>-1</sup> but may actually be over a narrower range near  $1.5 \times 10^4$  prey mL<sup>-1</sup>; 3) the maximum growth rate was  $\sim 2.5$  divisions d<sup>-1</sup> but was as high as 3 d<sup>-1</sup> (Fig. 4.1 and 4.2); and 4) the growth rate of this culture declined to zero over a period of three months (Fig. 4.2), suggesting either culture conditions were inadequate, genetic deterioration was rapid or a combination of both.

During the late winter, when strain IA was collected in Indian Arm (see Chapter 2), the abundance of phytoplankton, of a similar size to *C. salina* (3-10  $\mu$ m), was typically  $< 10^2$  mL<sup>-1</sup> (Martin and Montagnes 1993). These prey levels would not sustain the ciliate, suggesting that either *S. spiralis* grows much better on other prey, the ciliates were in a reduced metabolic state (winter temperatures are 4-10°C), or the prey were distributed in small concentrated patches. However, other numerical response-curve estimates for *S. spiralis* indicate that it is able to survive at much lower food levels (see Chapter 8, Fig. 8.1, Table 8.1); possibly my estimates are erroneous or this clone is distinctly different from previously studied (Atlantic) strains (see Chapter 2).

## PART II GRAZING RATES: Estimating the Functional Response

### 6.0 General Methods

Initially, to determine if *S. spiralis* consumed fluorescently labeled prey (Gonzalez *et al.* 1990, Sherr and Sherr 1993) the ciliates were fed a 1:1 mixture of stained and live *C. salina* at  $10^5$  particles mL<sup>-1</sup>. The ciliates died after  $< 45$  min in this treatment. However, the ciliates lived and consumed fluorescent beads in experiments using a 1:1 mixture of beads

(used in Chapter 3) and live *C. salina* at  $\sim 10^5$  particles  $\text{mL}^{-1}$ . Hence, beads were used as a surrogate food to estimate grazing rates.

Fluorescent beads and *C. salina* were fed to strain IA over an 80 min period at  $5 \times 10^4$  prey  $\text{mL}^{-1}$ . Bead ingestion was measured at 2 to 10 min intervals and followed a rectangular hyperbolic response. Over the first 20 min, this response was virtually linear (Fig. 4.3). Thus, a 20 min incubation period was used for subsequent experiments, assuming that grazing rate was constant from when beads were added to 20 min later.

An experiment was conducted to determine the effect of prey concentration on the grazing rate of the ciliate *S. spiralis*. Fluorescent beads (see Chapter 3) were fed to the ciliates in a 1:1 ratio with live *C. salina*. The experiments were run at particle concentrations ranging from  $10^3$  to  $9.5 \times 10^4$  prey (beads plus *C. salina*)  $\text{mL}^{-1}$ . Live prey concentrations were made by diluting a culture of *C. salina* (maintained as described in section 1.0) with natural pasteurized sea water. After diluting the *C. salina* culture to the desired concentrations, the treatments were counted using a Coulter Counter. Twenty-two concentrations (treatments) were made this way. Five mL of each prey treatment were placed in tissue culture plate wells. Each treatment was replicated 3 times, making a total of 66 wells.

The ciliates were grown on *C. salina* prior to the experiments and harvested when the cultures were in log growth phase. Ciliates (40-50) were transferred, using finely drawn pipets, to the wells containing the live-treatments and acclimated to these treatments for 4 h at  $16-17^\circ\text{C}$  at  $5 \mu\text{mol photons m}^{-2} \text{s}^{-1}$ . During the acclimation period, bead treatments that equalled the prey treatments were prepared (following methods similar to those described in Chapter 3) and counted on the Coulter Counter. After the acclimation period, 5 mL of bead-treatments were added to the appropriate live treatment, thus exposing the ciliates to 10 mL of 1:1 beads:live prey at 22 concentrations. The mixtures were incubated at  $16-17^\circ\text{C}$ ,  $5 \mu\text{mol photons m}^{-2} \text{s}^{-1}$  for 20 min and agitated every 5 min to reduce settling of beads and prey.

After 20 min, the 10 mL in each well were transferred to a vial, fixed with acid Lugol's iodine (final concentration 2% volume/volume) and later bleached with concentrated sodium thiosulphite (since Lugol's masks fluorescence). Some ciliates were lost during this

manipulation; typically 20-40 ciliates were observed. The ciliates were examined using 10 mL settling chambers and an inverted fluorescent microscope (see Chapter 3). The mean number of beads ciliate<sup>-1</sup> was determined and ingestion rate estimated; ingestion rate was approximately twice the number of beads in the ciliates (depending on the actual ratio of beads:live prey at each treatment level). I assumed no preference for beads or prey and no egestion of prey due to fixation, both of which may underestimate grazing rates (Sieracki *et al.* 1987, Stoecker 1988).

## 7.0 Results, Discussion and Modeling the Response

Grazing rates ranged from 3 to 60 beads ciliate<sup>-1</sup> h<sup>-1</sup> and increased with prey concentration, but there was variation in the grazing rate at single concentrations (Fig. 4.4, all data). The grazing rate data were fitted to a rectangular hyperbolic response using an iterative fit (Eq. 2, Chapter 3) between 0-9.5x10<sup>4</sup> prey mL<sup>-1</sup> (Fig. 4.4, solid line). At concentrations <3x10<sup>3</sup> prey mL<sup>-1</sup> grazing rate dropped.

The relation determined above did not give a good fit to the grazing rates above 4.5x10<sup>4</sup> prey mL<sup>-1</sup>. Possibly the data were not accurately represented by Eq. 2 (Chapter 3). However, assuming that gross growth efficiency was constant (at concentrations eliciting maximum growth rates), the notion that grazing rates >4.5x10<sup>4</sup> prey mL<sup>-1</sup> were elevated, is not supported by the growth data (Fig. 4.1) since a corresponding increase in growth rate did not occur above 4.5x10<sup>4</sup> prey mL<sup>-1</sup>. Thus, I have used the curve based on Eq. 2 (Chapter 3) as an estimate of the functional response, to examine grazing rates in Chapter 8. The parameters of the equation, from the line depicted in Fig. 4.4, and its estimates of error are presented in Table 4.2.

## CONCLUDING REMARKS

*Strobilidium spiralis* (= *Lohmanniella spiralis*, see Chapter 2) is found in many coastal marine waters (Smetacek 1981, 1984, Rassoulzadegan 1982, Sheldon *et al.* 1986, Lynn and Montagnes 1988, Verity 1991a). This genus has been reported at high densities, suggesting



that it forms blooms (Smetacek 1981, 1984). The data from my studies also suggest that *S. spiralis* has the potential to form blooms over short periods, as it grows rapidly under optimal conditions. My estimates and those of Smetacek (1984) indicate that *S. spiralis* can undergo up to 3 divisions  $\text{d}^{-1}$  and likely has a maximum sustainable growth rate of 2.5 divisions  $\text{d}^{-1}$  (see Chapter 8, Table 8.1). The ubiquitous nature of this ciliate, its large size and its rapid growth and grazing rates undoubtedly make it one of the more important components of the microzooplankton.

Table 4.1. The relative growth rate of *Strobilidium spiralis* strain IA over a 2 and a 4 day period. The ciliates were grown on a 14:10 light:dark cycle at 16-17°C on all the combinations of the three prey: *Isochrysis galbana*, *Chroomonas salina*, and *Rhodomonas lens* (the initial combined prey concentrations was  $\sim 3 \times 10^4$  cells mL<sup>-1</sup>). Growth rates were qualitative estimates of increase in numbers: cells died, -; cells grew slowly, +; cells grew, ++; cells grew quickly +++.

PREY CONCENTRATION	GROWTH RATE					
	REPLICATE #1		REPLICATE #2		REPLICATE #3	
	day2	day4	day2	day4	day2	day4
<i>R. lens</i>	+	-	++	-	++	-
<i>I. galbana</i>	+	+	+	+	+	+
<i>C. salina</i>	+	+++	++	+++	++	+++
<i>I. galbana</i> & <i>R. lens</i>	++	++	++	++	+++	++
<i>I. galbana</i> & <i>C. salina</i>	+++	++	+++	+++	+++	+++
<i>C. salina</i> & <i>R. lens</i>	++	+++	+++	+++	+++	+++
<i>I. galbana</i> & <i>C. salina</i> & <i>R. lens</i>	+++	++	+++	++	+++	+++

Table 4.2. Growth and grazing parameters for *Strobilidium spiralis* strain IA; parameters and estimates of error of the numerical and functional response curves presented in Figs. 4.1 and 4.4. See section 1.0 in Chapter 3 for the equations used. Values are in units of numbers  $\text{mL}^{-1}$  for concentrations ( $k$ ,  $x'$ ), and  $\text{d}^{-1}$  for growth rate ( $\mu_{\max}$ ).

	value	standard deviation	coefficient of variation
-----			
Michaelis-Menten fit for Fig. 4.1			
$\mu_{\max}$	1.845	0.2572	13.94
$k$	19070	2866	15.03
$x'$	10230	919.8	8.989
Michaelis-Menten fit for Fig. 4.4, solid line			
$G_{\max}$	45.45	2.751	6.052
$k$	4028	1359	33.74
Michaelis-Menten fit for Fig. 4.4, broken line			
$G_{\max}$	50.21	3.869	7.706
$k$	4473	1951	43.62

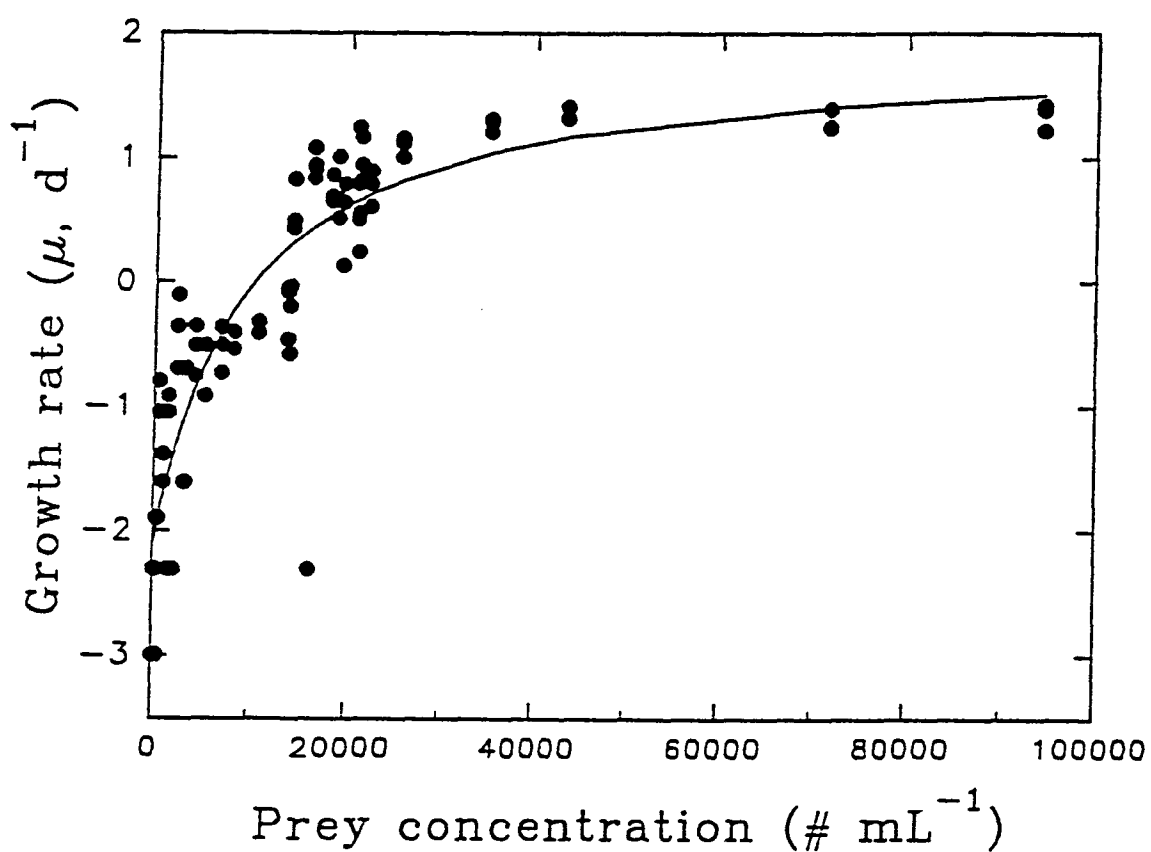


Fig. 4.1. The numerical response of *Strobilidium spiralis* strain IA grown on the prey flagellate *Chroomonas salina*. The circles represent growth rates and the line represents the modified Michaelis-Menten fit to the data (Eq. 1, Chapter 3). See Table 4.2 for the parameters and estimates of error associated with this curve.

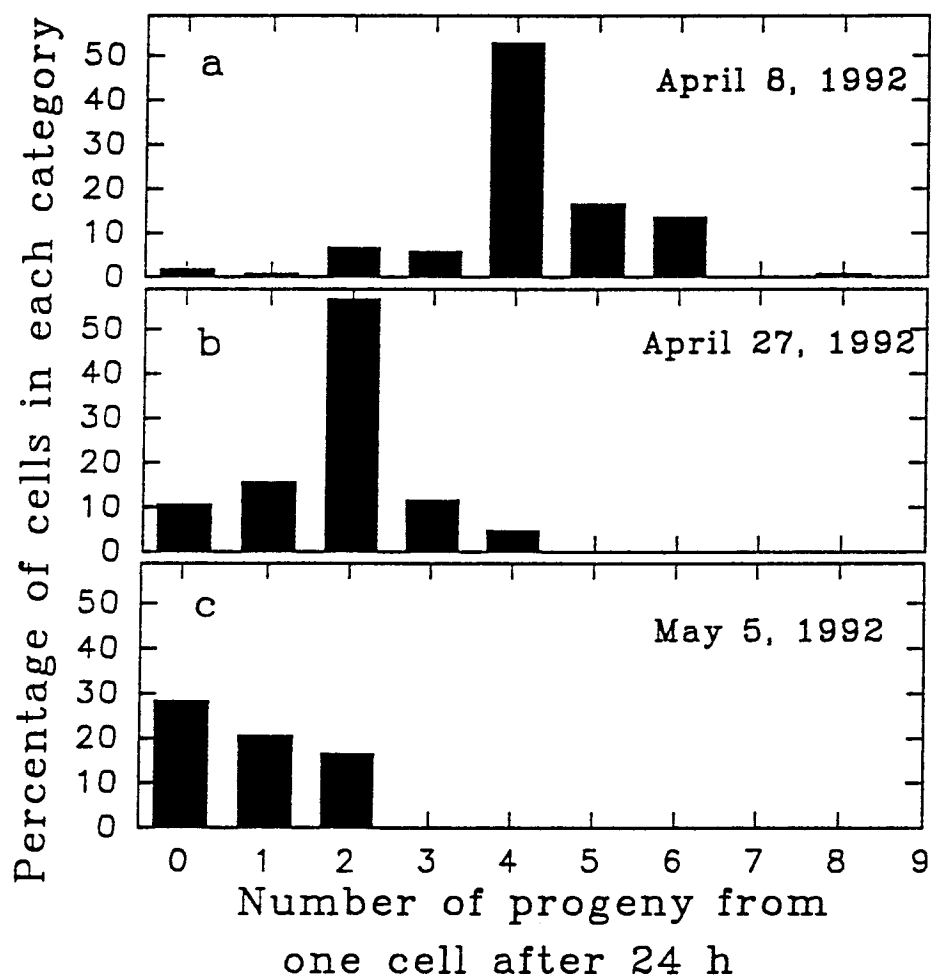


Fig. 4.2. The change in culture growth rate of *Strobilidium spiralis* strain IA over time. Each panel is the distribution of progeny from 70 to 100 single cell isolates after 24 h. (see section 3.0 for details).

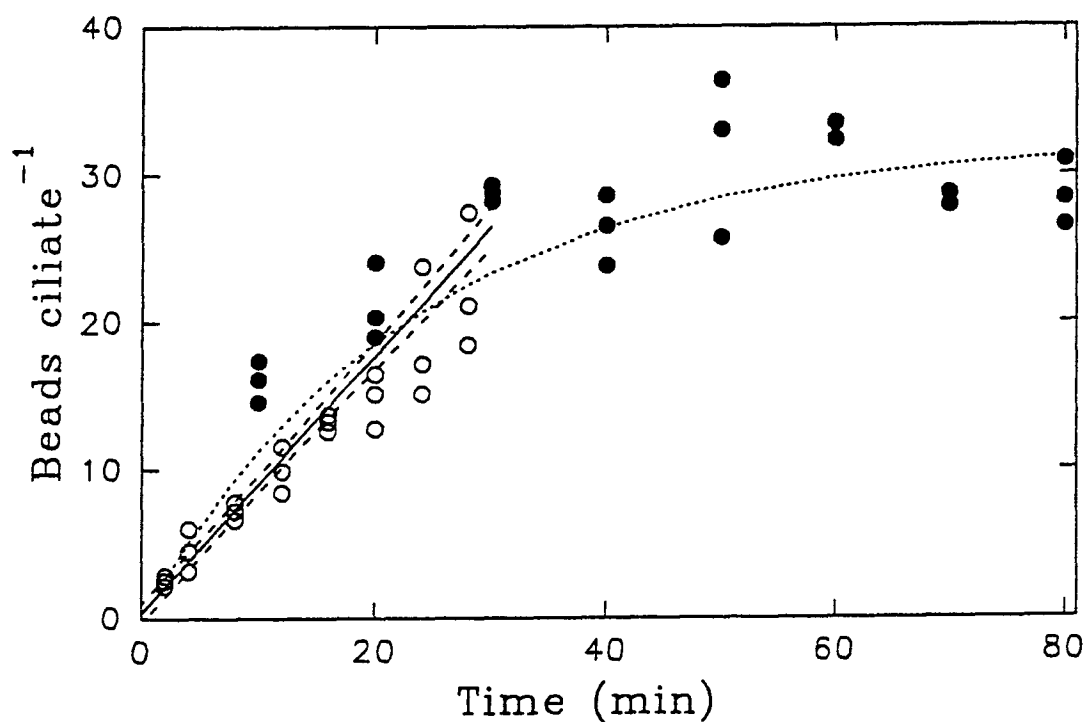


Fig. 4.3. The number of beads ingested by *Strobilidium spiralis* strain IA over time. At two different times, ciliates were fed beads and prey, as described in section 6.0, at 2 concentrations:  $4.7 \times 10^4$  beads  $\text{mL}^{-1}$  (solid circles) and  $4.4 \times 10^4$  beads  $\text{mL}^{-1}$  (open circles). The dotted line was fit to the function  $(\text{beads ciliate}^{-1}) = 3.2(1 - e^{-0.043 \cdot \text{min}})$  using a combination of both data sets. The solid line is the linear regression fitted to only the open circles; it is bound by the 95% confidence intervals around the linear regression (dashed lines).

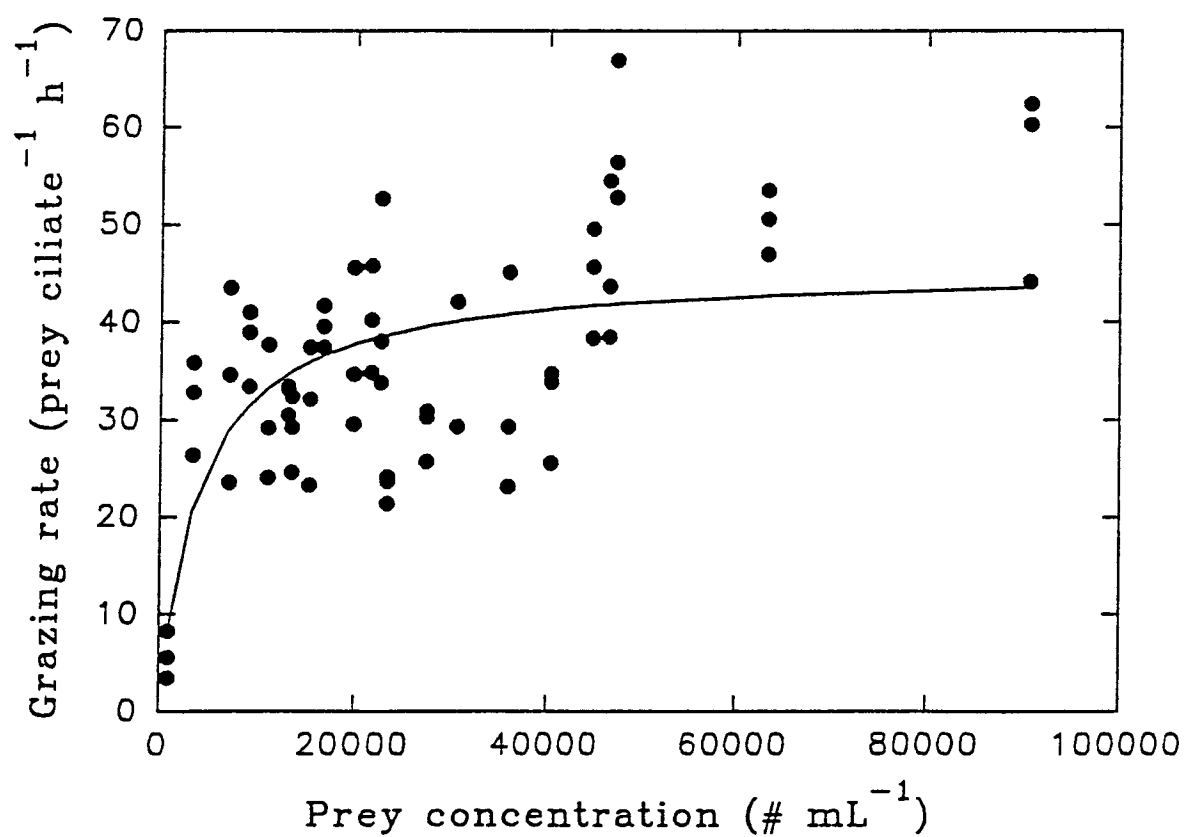


Fig. 4.4. The functional response of *Strobilidium spiralis* strain IA ingesting a 1:1 ratio of 5  $\mu\text{m}$  fluorescent beads and *Chroomonas salina* (see section 6.0 for details). The curve is the Michaelis-Menten fit (Eq. 2, Chapter 3) to the data. See Table 4.2 for the parameters and estimates of error associated with these curves.

## CHAPTER 5

### GROWTH AND GRAZING RATES OF *Strobilidium* sp. STRAIN JERC AS A FUNCTION OF FOOD CONCENTRATION

#### Introduction

This chapter is placed here to offer, by its proximity, a comparison to the last one (a detailed comparison of species is presented in Chapter 8). Both chapters examine species in the genus *Strobilidium*, but the growth and grazing rates of the two species differ considerably. There are also differences in the methodologies used to study the two species. These differences stem from logistic problems and differences in the ciliate's behaviour. Still, comparisons can easily be made between the two species.

#### PART I GROWTH RATES: Estimating the Numerical Response

##### 1.0 General Methods

Experiments were conducted to determine the numerical response of *Strobilidium* sp. strain JERC grazing on a combination of two flagellates, *Isochrysis galbana* and *Chroomonas salina* at concentrations ranging from 0 to  $9.2 \times 10^4$  cells mL<sup>-1</sup>. The prey were maintained, in log phase, by serial dilution, in 150 mL flasks at 50-100  $\mu$ mol photons m<sup>-2</sup> s<sup>-1</sup> on a 14:10 h light:dark cycle at 16-17°C. Prior to the experiments, *Strobilidium* sp. was maintained in enriched natural seawater with *I. galbana* and *C. salina* in 6-well 20 mL plastic tissue culture plates at 16-17°C and on a 14:10 h light:dark cycle at 25-50  $\mu$ mol photons m<sup>-2</sup> s<sup>-1</sup>.

For these experiments, prey concentrations were prepared and quantified as described in Chapter 3, but the prey concentrations were made by combining the two species, *I. galbana* and *C. salina*, in a 1:1 ratio. Although the initial food concentrations were in this 1:1 ratio, it was not determined if they remained this way over the experimental period.

For the growth experiments, ciliates were collected during log or early stationary phase. Then, 10-25 ciliates were transferred to tissue-plate wells containing 10 mL of prey at treatment-concentrations and acclimated in the dark for 24 h. After 24 h, the ciliates were transferred to new prey, at the same concentrations they were acclimated to, and allowed to grow for 96 h, for most treatments. This was too long a period for starving ciliates (usually all died after <96 h), and the concentrations below  $4 \times 10^3$  prey mL<sup>-1</sup> were left for only 24 h



after the initial 24 h acclimation period. Growth rate was estimated as the change in numbers over the incubation period; exponential growth was assumed over the 24-96 h (i.e. growth rate was calculated as  $\mu = 1/t \ln [\text{cells}_{t+1}/\text{cells}_t]$ , where  $t$  = time in days).

Typically, each treatment was replicated 3 times. The prey concentrations used to determine the numerical response were estimated, for each well, prior to the addition of, and after the removal of the ciliates; these two values were then averaged for each "replicate". But, prey were often depleted to different extents in each of the 3 "replicate" wells (which were initially the same concentration). Thus, the "replicates" did not have the same final, or average, concentration and were not considered true replicates. Typically, prey concentrations dropped to 5-35% of the initial concentration over the 96 h, but at times the prey levels increased (~15%) while at one extreme there was an 80% decrease. There was a negative correlation between initial food concentration and percent change (i.e. low concentrations decreased more than higher ones). However, there did not appear to be any relation between change in prey concentration and growth rate. Since the rate of change over the 96 h was not monitored, these differences were ignored. This procedure could alter the precision of estimates of prey concentration and therefore overestimate the threshold concentration by ~15-20%. Further, if the two prey species were not grazed equally (a parameter which could not be determined by Coulter Counter enumeration), this overestimation could be higher.

Growth rate for each well was plotted against the average prey concentration of that well. The numerical response data were fitted to a modified Michaelis-Menten model (Eq. 1, Chapter 3) using an iterative fit.

## **2.0 Results and Discussion**

### **2.1 General**

At first, semi-continuous growth rate experiments, like those described in Chapters 3 and 4, were attempted for Strain JERC. However, this ciliate was smaller than the other species and tended to "jump" when a finely drawn pipette tip was brought near it (see Chapter 2). It was therefore not possible to collect and transfer the ciliates on a daily basis and the

method described above was adopted to estimate growth rate. This long incubation method was not as satisfactory as the semi-continuous method because it did not ensure that food concentration remained constant (on a daily basis) for the duration of the experiment and it did not allow repeated measurements.

Strain JERC was initially cultured on a combination of *I. galbana*, *C. salina* and *R. lens*. Later it was grown on all combinations of these species; the ciliate grew on a number of prey combinations (Table 5.1). Although a diet of *R. lens* alone induced maximum growth (Table 5.1), later experiments indicated that this growth rate was not sustainable (data not shown). Consequently, the numerical response was conducted using a 1:1 mixture of the prey *I. galbana* and *C. salina*, which also gave a maximum sustained growth rate (Table 5.1).

## 2.2 Numerical Response

A total of 76 treatments with no replication (see section 1.0) were run in 3 consecutive experiments (as described in section 1.0). The growth rate followed a rectangular hyperbolic response between  $1.7 \times 10^3$ - $5.7 \times 10^4$  prey  $\text{mL}^{-1}$  (Fig. 5.1). The threshold concentration of prey was  $\sim 4 \times 10^3$  prey  $\text{mL}^{-1}$ . At concentrations above  $5.7 \times 10^4$  prey  $\text{mL}^{-1}$  growth rate was inhibited, and these data were not used to estimate the numerical response. Equation 1 (Chapter 3) was fitted to points between  $1.7 \times 10^3$ - $5.7 \times 10^4$  prey  $\text{mL}^{-1}$  (Fig. 5.1). The parameters of the equation and their estimates of error are presented in Table 5.2.

The calculation of mortality rate in these experiments differs from that described in previous chapters. In Chapters 3 and 4 mortality, was the average rate over several days, after a 2 day acclimation period. Here, the mortality was typically estimated over 24 h, after a 24 h acclimation period. This would give relatively lower mortality rates than those obtained by the previous methods, assuming mortality rate due to starvation is not constant (see Chapter 3). Consequently, the mortality response, presented in Fig. 5.1, might have a different shape if it was obtained by previous methods.

### 3.0 Aspects of the Growth Rates and Their Ecological Relevance

The data for this species provide a good prediction of the numerical growth response. There are 3 pieces of information provided by the above experiment: 1) the threshold concentration of prey for strain JERC was  $\sim 4 \times 10^3 \text{ mL}^{-1}$ ; 2) the maximum increase in growth rate was between  $4 \times 10^3$ - $1.5 \times 10^4 \text{ prey mL}^{-1}$ ; and 3) the maximum growth rate was one division  $\text{d}^{-1}$ .

During May when this ciliate was collected at Jericho Pier in Vancouver Harbour, potential prey ( $\leq 10 \mu\text{m}$  in diameter) concentrations in British Columbian coastal waters ranged from  $10^2$ - $10^3 \text{ cells mL}^{-1}$  (Appendix 3). Thus on average, natural levels of food could be sufficient to support strain JERC but would be unlikely to support it at its maximum growth rate.

## PART II GRAZING RATES: Estimates of the Functional Response

### 4.0 General Methods

Initially to determine if strain JERC consumed fluorescently labeled beads, (see Chapters 3 and 4) the ciliates were fed a 1:1 mixture of beads and *C. salina* at  $3 \times 10^4 \text{ particles mL}^{-1}$ . Virtually no beads were ingested after an hour, indicating a "reluctance" of the ciliate to eat beads. Hence, a different surrogate food was tested: fluorescently stained *C. salina* (Gonzalez *et al.* 1990, Sherr and Sherr 1993). The ciliate consumed fluorescently labeled *C. salina* at concentrations of  $2 \times 10^4 \text{ mL}^{-1}$  and prey uptake was linear over 1 h, sampled at 10 min intervals (data not shown). Thus, a 1 h incubation period was used for subsequent experiments.

Two identical (replicate) experiments were conducted to determine the effect of prey concentration on the grazing rate of strain JERC. Fluorescently stained *C. salina* were used as tracers of ingestion in a 1:1 ratio with live *C. salina*. The experiments were run at food concentrations ranging from  $1.0 \times 10^2$ - $4.8 \times 10^4 \text{ prey mL}^{-1}$  (open circles, Fig. 5.2) and  $2.5 \times 10^2$ - $4.1 \times 10^4 \text{ prey mL}^{-1}$  (solid circles, Fig. 5.2).

The stained prey were prepared as described by Sherr and Sherr (1993), and concentrations of live and stained prey were made up as described for live cells and beads in Chapter 3 and 4. Prior to estimating their concentration, the stained prey were forced through a 10  $\mu\text{m}$  Nitex mesh to insure monodispersion. Stained prey were made the day of the experiment and no preservatives were used (see Sherr and Sherr 1993).

Live-prey concentrations were made by diluting a log phase culture of *C. salina*, grown at 50  $\mu\text{mol photons m}^{-2} \text{ s}^{-1}$  in enriched culture medium, with pasteurized natural seawater. After diluting the stock culture to the desired treatment concentrations, they were counted using a Coulter Counter and allocated to 20 mL wells (5 mL well<sup>-1</sup>) in tissue culture plates. For both experiments, 20 live *C. salina* concentrations (treatments) were made this way and each was replicated 3 times making a total of 60 wells.

Prior to the experiments, the ciliates were grown on *I. galbana* and *C. salina*. Both ciliates and prey were harvested when the cultures were actively growing (log phase). To remove all prey, ~3000 ciliates were transferred (using finely drawn pipettes) through 3-4 rinses of pasteurized natural seawater. Subsequent to rinsing, 30-50 ciliates were transferred to the wells containing the live-prey treatments. The ciliates were acclimated in these live-prey treatments for 4-5 h at 16-17°C and 5  $\mu\text{mol photons m}^{-2} \text{ s}^{-1}$ .

During the 4-5 h acclimation period, stained-prey treatments were made up to concentrations equaling those of the live-prey; these were also counted on the Coulter Counter. After the 4-5 h period, 5 mL of the appropriate stained-prey were added to the ciliate and live-prey mixtures. Thus, the ciliates were exposed to 1:1 stained:live prey at 20 concentrations. The mixtures were left at 16-17°C and 5  $\mu\text{mol photons m}^{-2} \text{ s}^{-1}$  for 1 h, with agitation every 10 min to reduce prey settling. After 1 h, the 10 mL were transferred to vials and processed by a method similar to that used for *Strobilidium spiralis* in Chapter 4; typically 20-40 ciliates were observed.

## 5.0 Results and Discussion

Grazing rate ranged from 0 to 24 prey ciliate<sup>-1</sup> h<sup>-1</sup> and showed a trend to increase with prey concentration from 0 to 5-7x10<sup>3</sup> prey mL<sup>-1</sup>, but there was a steady decline in grazing rate above 5-7.5x10<sup>3</sup> prey mL<sup>-1</sup> (Fig. 5.2, both data sets). The grazing rates, for both data sets depicted in Fig. 5.2, were fitted to rectangular hyperbolic functions using an iterative fit (Eq. 2, Chapter 3) between 0 and the maximum grazing rates. At concentrations above the maximum grazing rate, an asymptotic response, not in accordance with the data, was assumed for both curves.

The rectangular hyperbolic response, typically invoked to explain a functional response (see Appendix 2), did not fit the data in Fig. 5.2. The reasons for this are unclear; possibly food concentrations above a certain level inhibited feeding. However, a concomitant decrease in growth rate would then be expected (assuming growth and grazing are positively correlated); this was not seen (Fig. 5.1). Alternatively, there may have been something in the stained-prey preparation that inhibited feeding and as the concentration of this "substance" increased, its effect increased. In the absence of an inhibitor, feeding rates would have presumably continued to increase and/or become asymptotic as food concentration increased. Consequently, I have used Eq. 2 (Chapter 3) for the first part of the curves depicted in Fig. 5.2 and have predicted an asymptote for the remainder of the curves; these asymptotes would then be minimum responses.

A second anomalous trend, exhibited by the data in Fig. 5.2, is the difference in responses between experiments (solid vs. hollow circles). These two data sets were from experiments performed 10 days apart but ~45 days after the growth rate experiments (section 1.0) and several months after the ciliate was isolated. The experiments used different "batches" of ciliates but were otherwise identical. The difference between the two curves may have been due to a genetic difference between batches (as discussed in Chapter 3) or uncontrolled differences in technique between the experiments (i.e. more of the "inhibitory substance", proposed above, may have reduced the grazing rate). In either of these cases, the upper response curve (solid circles, Fig. 5.2) would be the more accurate representation of

natural conditions. Hence, I have used this upper curve when comparing grazing rates in Chapters 8. The parameters and estimates of error of both curves are presented in Table 5.2.

## CONCLUDING REMARKS

Species of *Strobilidium* in the size range of strain JERC are found in many coastal marine waters (Smetacek 1984, Andersen and Sorensen 1986, Lynn and Montagnes 1988, Martin and Montagnes 1993). Such species have been reported at high densities and have high growth rates, suggesting that they form blooms (Smetacek 1984, Andersen and Sorensen 1986). The data from my studies also suggest that strain JERC has the potential to form blooms. This is further supported by the model presented in Chapter 9. Often species of *Strobilidium* (= *Lohmanniella*) are lumped together in field studies. This likely misrepresents the ciliate assemblage since the differences between two species of *Strobilidium*, strains IA (Chapter 4) and JERC, were pronounced (see Chapter 8).

Table 5.1. The relative growth rate of *Strobilidium* sp. strain JERC over 5 days. The ciliates were grown on a 14:10 light:dark cycle at 16-17°C on all the combinations of the three prey: *Isochrysis galbana*, *Chroomonas salina* and *Rhodomonas lens* (the initial combined prey concentrations was  $3 \times 10^4$  cells mL<sup>-1</sup>). Growth rates were qualitative estimates of increase in numbers: cells grew slowly, +; cells grew, ++; cells grew quickly, +++.

PREY	GROWTH RATE		
CONCENTRATION	REPLICATE #1	REPLICATE #2	REPLICATE #3
<hr/>			
<i>R. lens</i>	+++	+++	+++
<i>I. galbana</i>	+	+	+
<i>C. salina</i> +	+	+	
<i>I. galbana</i> & <i>R. lens</i>	+++	++	++
<i>I. galbana</i> & <i>C. salina</i>	+++	+++	+++
<i>C. salina</i> & <i>R. lens</i>	+++	+++	+++
<i>I. galbana</i> & <i>C. salina</i> & <i>R. lens</i>	++	++	++

Table 5.2. Growth and grazing parameters for *Strobilidium* sp. strain JERC; parameters and estimates of error of the numerical and functional response curves presented in Figs. 5.1 and 5.2. See section 1.0 in Chapter 3 for the equation used. Values are in units of numbers mL<sup>-1</sup> for concentrations ( $k$ ,  $x'$ ), and d<sup>-1</sup> for growth rate ( $\mu_{\max}$ ).

	value	standard deviation	coefficient of variation
-----			
Michaelis-Menten fit for the line depicted in Fig. 5.1			
$\mu_{\max}$	0.7212	0.1097	15.22
$k$	10580	3473	32.83
$x'$	4075	545.8	13.39
Michaelis-Menten fit for the solid line depicted in Fig. 5.2 between 100-4000 particles mL <sup>-1</sup> after which $G_{\max} = 12$			
$G_{\max}$	12.38	0.921	7.436
$k$	711.687	159.7	21.96
Michaelis-Menten fit for the broken line depicted in Fig. 5.2 between 200-5000 particles mL <sup>-1</sup> after which $G_{\max} = 23$			
$G_{\max}$	41.21	5.918	14.39
$k$	3865	903.0	23.36



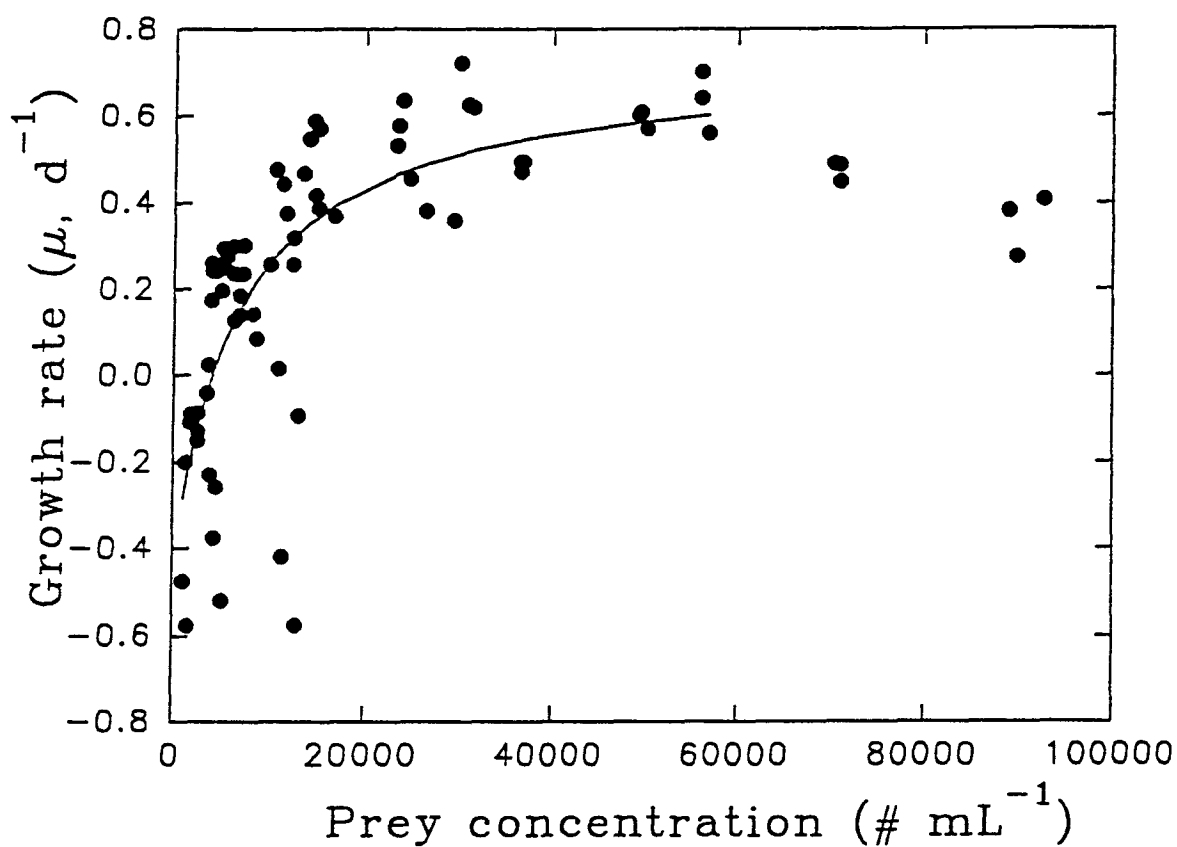


Fig. 5.1. The numerical response of *Strobilidium* sp. strain JERC grown on a 1:1 ratio of the prey flagellates *Chroomonas salina* and *Isochrysis galbana*. The circles represent growth rates and the line represents the modified Michaelis-Menten fit to the data (Eq. 1, Chapter 3). See Table 5.1 for the parameters and estimates of error associated with this curve.

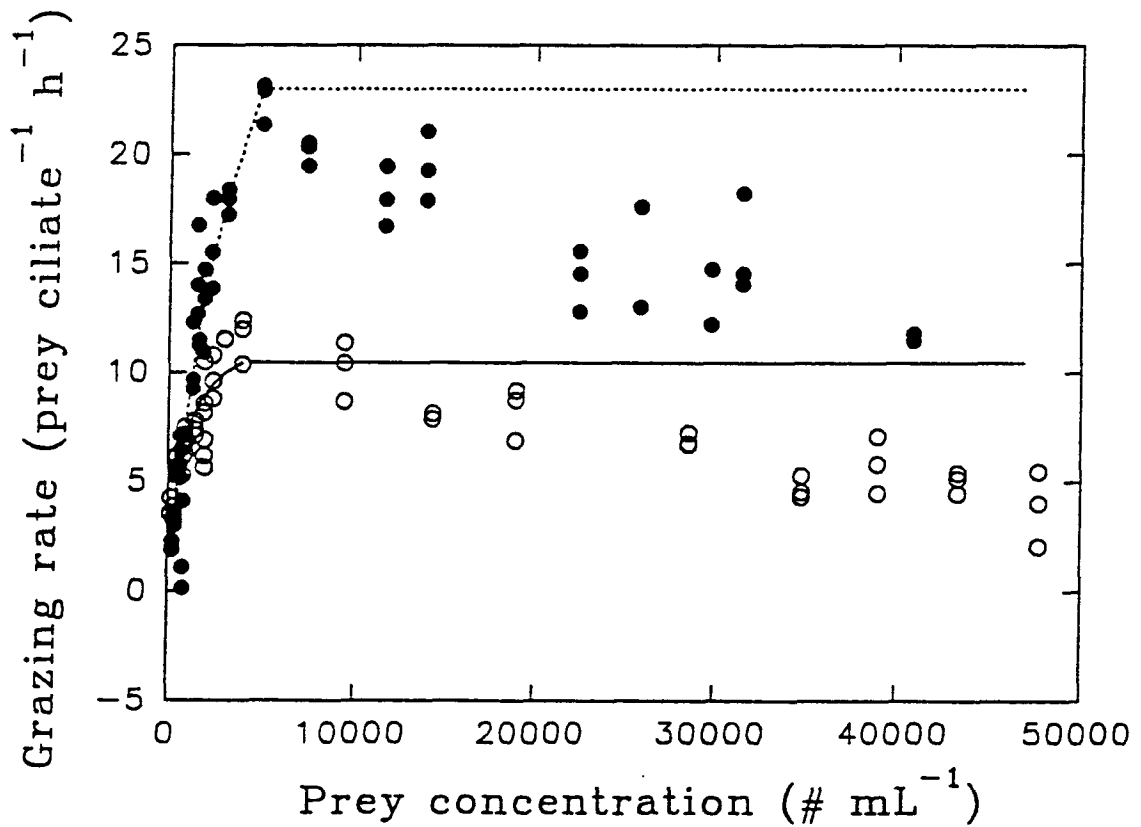


Fig. 5.2. The functional response of *Strobilidium* sp. strain JERC ingesting a 1:1 ratio of stained and live *Chroomonas salina*. The solid and open circles represent two separate experiments (see section 4.0). The two lines are fitted to these data using the modified Michaelis-Menten model (Eq. 2, Chapter 3) and assuming that grazing rate becomes asymptotic after maximum grazing rates were reached (see section 5.0). See Table 5.2 for the parameters and estimates of error associated with these curves.

## CHAPTER 6

### GROWTH AND GRAZING RATES OF *Strombidium acuminatum* Strain BJSCH AS A FUNCTION OF FOOD CONCENTRATION

#### Introduction

Although *Strombidium acuminatum* strain BJSCH was collected from the plankton, its behaviour indicated that it was semi-benthic (see Chapter 2). As well as swimming in the water column, it "crawled" along the bottom of the culture dishes. This made conducting semi-continuous growth experiments impossible and the technique for growth rate measurement described in Chapter 5 was used.

As indicated earlier, I have not presented the experiments chronologically. Strain BJSCH was one of the first species that I examined. Hence, some methods in this chapter may seem poorly designed compared to those previously described. This species is presented near the end since it is semi-benthic and therefore less comparable to the other planktonic forms. However, both the grazing and growth responses were obtained for strain BJSCH and an estimate of growth using two different prey was made. Further, the semi-benthic nature of this species suggested that it may be linked to suspended detritus (marine snow), and therefore it might be used to illustrate grazers in regions of dense suspended material.

#### PART I GROWTH RATES: Estimating the Numerical Response

##### 1.0 General Methods

The numerical response experiments conducted on strain BJSCH were similar to those in Chapter 5 but, in this case, two diets were examined: 1) the diatom *Thalassiosira pseudonana* at food concentrations ranging from  $10^2$  to  $2.5 \times 10^4$  cells  $\text{mL}^{-1}$  and 2) a 1:1:1 combination of 3 flagellates, *Isochrysis galbana*, *Chroomonas salina*, and *Rhodomonas lens*, at combined concentrations ranging from  $2.5 \times 10^2$  to  $4.3 \times 10^4$  cells  $\text{mL}^{-1}$ .

Prior to the 3-flagellate numerical-response experiment, strain BJSCH was cultured on a combination of *I. galbana*, *C. salina*, and *R. lens*. Later it was grown on all combinations of these species; the ciliate grew on a number of prey combinations, but all 3 flagellates

combined gave the maximum growth rate (Table 6.1). Consequently, the numerical response was conducted using a 1:1:1 mixture of these 3 flagellates.

*Thalassiosira pseudonana* was cultured as described in Chapter 3. The three flagellates were cultured separately in 150 mL flasks at 16-17°C on a 14:10 h light:dark cycle at 50-100  $\mu\text{mol photons m}^{-2} \text{ s}^{-1}$ . Prior to the experiments, strain BJSCH was maintained in enriched natural seawater in 6-well 20 mL plastic tissue culture plates at 16-17°C and collected during log or stationary phase.

As in previous experiments, the ciliates were grown in the dark in tissue culture plates (with 10 ciliates and 10 mL of prey-concentration well<sup>-1</sup>); treatments were performed in triplicate. The ciliates were acclimated, at the various prey concentrations, in the wells for 24 h. Then, the ciliates were transferred to new prey concentrations and allowed to grow for 124 h (for the diatom experiment) and 96 h (for the 3-flagellate experiment). All prey concentrations were measured using a Coulter Counter.

As described in Chapter 5, there were changes in prey concentration over the incubation period, but the changes were not monitored in the same manner. The initial prey concentration was the same for all 3 replicates of a single treatment. However, prey concentrations were not measured in each well after the incubation period. Instead, the average of the 3 wells was measured (by mixing the three). Prey concentrations, used to determine the numerical response, were averages of the initial and final (mixed) concentrations.

Growth rate was estimated as the increase in numbers over the incubation period; exponential growth was assumed (i.e. growth rate was calculated as  $\mu = 1/t \ln [\text{cells}_{t+1}/\text{cells}_t]$ , where  $t$  = time in days). The numerical response data were fitted to a modified Michaelis-Menten model (Eq. 1, Chapter 3) using an iterative fit.

## 2.0 Results and Discussion

### 2.1 General

At first, semi-continuous growth rate experiments, like those described in Chapter 3, were attempted for strain BJSCH but this ciliate was small and tended to "hug" the bottom (see Chapter 2). Consequently, it was not possible to collect and transfer the ciliates and the method described above was adopted to estimate growth rate. As mentioned in Chapter 5, this method has disadvantages, but given that the semi-continuous method was not feasible, it provided an estimate of the numerical response.

### 2.2 Numerical Response

*The T. pseudonana experiment:* The growth rate followed a rectangular hyperbolic response between  $1 \times 10^2$ - $2.5 \times 10^4$  prey  $\text{mL}^{-1}$  (Fig. 6.1, solid circles). At concentrations below  $2.7 \times 10^3$  prey  $\text{mL}^{-1}$  mortality occurred, presumably due to starvation. Equation 1 (Chapter 3) was fitted to points between  $9.3 \times 10^2$ - $2.6 \times 10^4$  prey  $\text{mL}^{-1}$  (Fig. 6.1, solid line). The parameters of the equation and their estimates of error are presented in Table 6.2.

*The 3-flagellate experiment:* The growth rate followed a rectangular hyperbolic response between  $2.5 \times 10^2$ - $4.3 \times 10^4$  prey  $\text{mL}^{-1}$  (Fig. 6.1, open circles). At concentrations below  $7.5 \times 10^2$  prey  $\text{mL}^{-1}$  mortality occurred, presumably due to starvation. Equation 1 (Chapter 3) was fitted to points between  $2.5 \times 10^2$ - $4.3 \times 10^4$  prey  $\text{mL}^{-1}$  (Fig. 6.1 broken line). The parameters of the equation and their estimates of error are presented in Table 6.2.

### 3.0 Aspects of the Growth Rates and Their Ecological Relevance

In general, strain BJSCH divided less than once a day ( $-0.88 \text{ d}^{-1}$ ) at saturating prey concentrations, had a threshold concentration of  $7.5 \times 10^2$ - $2.7 \times 10^3$  prey  $\text{mL}^{-1}$ , and the maximum numerical response was between  $1 \times 10^3$ - $5 \times 10^3$  prey  $\text{mL}^{-1}$ . However, these parameters varied with prey type; the 3 flagellates gave a lower mortality rate, more rapid numerical response and lower maximum growth rate than the diatom.

Food type and quality affect ciliate growth (Blackbourn 1974, Repak 1983, Gifford 1985, Verity and Villareal 1986, Skogstad *et al.* 1987, this study Tables 4.1, 5.1, 6.1, and

7.1). The differences in growth rate response (Fig. 6.1) could be due to physical (Gifford 1985) or algal biochemical composition (Thompson and Harrison 1992, Verity 1991a) differences of the prey or they may be due to sub-clonal differences of the ciliate (as seen in Chapter 3). However, the relation of the two curves changes when viewed in terms of carbon rather than cells  $\text{mL}^{-1}$ . The two curves are similar, but ciliates fed *T. pseudonana* reached a higher growth rate than those fed the 3 flagellates (see Fig. 6.1, inset), but given the error estimates of the parameters associated with these curves (Table 6.1.), there may be no difference in these responses.

## **PART II GRAZING RATES: Estimating the Functional Response**

### **4.0 General Methods**

An experiment was conducted to determine the effect of prey concentration on the grazing rate of strain BJSCH. Fluorescently labeled 5  $\mu\text{m}$  beads were used as a tracer of ingestion rate. Ciliates were fed beads and *T. pseudonana* in a 1:1 ratio at combined concentrations ranging from  $4.5 \times 10^2$  to  $5 \times 10^4 \text{ mL}^{-1}$ .

For two days prior to the feeding experiment, strain BJSCH was grown in tissue-plate wells containing 18-20 mL of pasteurized natural seawater and *T. pseudonana* at 12 concentrations. After two days the ciliates were removed from the wells. Then, 3-6 mL of the growth medium was used to estimate the well's abundance of prey, with a Coulter Counter. The remaining 15 mL of the medium were allocated to 3 wells in a tissue plate (5 mL well<sup>-1</sup>). The ciliates were replaced in the medium and allowed to sit for 30 min. The beads, were prepared as described in Chapter 3 and the 1:1 ratio of beads to *T. pseudonana* was established as described in Chapter 4. Beads were added to the medium and the ciliates incubated for 30 min. The ciliates were kept at 16-17°C for all stages of the experiment. The samples were processed as described in Chapter 4. Typically, 20-40 ciliates were observed.

## 5.0 Results and Discussion

Grazing rate ranged from 0 to 7 particles ciliate<sup>-1</sup> h<sup>-1</sup> and showed a trend to increase with prey concentration between  $4.5 \times 10^2$ - $3 \times 10^4$  prey mL<sup>-1</sup> (Fig. 6.2). Although there was considerable scatter in the data, they were fitted to the Michaelis-Menten model (Eq. 2, Chapter 3) using an iterative fit, and this curve was used to compare grazing rates in Chapter 8.

## 6.0 Swimming Behaviour

Strain BJSCH grazed along the bottom of the tissue plates as well as swimming in the water column. Some benthic ciliates tend to swim into the water column when food concentration is high (unpublished data) while a semi-benthic species of *Strombidium* moves off the bottom when food becomes depleted (Fenchel and Jonsson 1988). I thought that strain BJLSC might alter its swimming behaviour at varied food concentrations, affecting its feeding rate and/or acting as a mechanism for dispersal. Therefore, I conducted an experiment to determine the effect of food concentration on the swimming behaviour of strain BJLSC.

Eight concentrations of *T. pseudonana*, ranging from  $10^3$  to  $5 \times 10^4$  mL<sup>-1</sup>, were prepared with natural pasteurized seawater, as described in previous sections. These 8 treatments were allocated to 20 mL tissue plate wells (10 mL well<sup>-1</sup>), with 3 replicates treatment<sup>-1</sup>. Ciliates (50 well<sup>-1</sup>) were placed in the treatments and acclimated for 2 h at 16-17°C and 50  $\mu$ mol photons m<sup>-2</sup> s<sup>-1</sup>. Then, the number of ciliates swimming in the water column was microscopically (10-20x) observed (after a 3 min acclimation period on a dissection microscope stage); ciliates not seen in the water column were assumed to be on a surface.

Food concentration had no effect on the ciliate's position in the water column (Fig. 6.3). Typically 15% of the ciliates were in the water column regardless of food concentration. Apparently, change in food concentration does not change the swimming behaviour of strain BJSCH and can not be invoked as a dispersal mechanism.

## CONCLUDING REMARKS

This work is the first study of the grazing and growth responses of an elongate, semi-benthic species of *Strombidium*. There have been other studies on what are likely semi-benthic species of *Strombidium* (e.g. Rivier *et al.* 1985, Fenchel and Jonsson 1988, Bernard and Rassoulzadegan 1990, Ohman and Snyder 1991), but these were all done on truncated forms (often referred to as *Strombidium sulcatum* but see Montagnes *et al.* 1990). The shape difference of strain BJSCH may be related to its feeding and swimming behaviour, as this species differed from others (see section 6.0 and Chapter 8). Further, this elongate morph seems to be a common but poorly examined type (see Chapter 2). Thus, this study adds new insight into the adaptive diversity of the genus *Strombidium*. Further, since semi-benthic ciliates may be important links in the formation and mineralization of ocean sinking detritus (Silver *et al.* 1984, Lochte 1991), this species and its response curves could be used to investigate the impact of ciliates on marine snow.



Table 6.1. The relative growth rate of *Strombidium acuminatum* strain BJLSC over a 4 day period. The ciliates were grown on a 14:10 light:dark cycle at 16-17°C on all the combinations of the three prey: *Isochrysis galbana*, *Chroomonas salina*, and *Rhodomonas lens* (the initial combined prey concentrations was  $3 \times 10^4$  cells mL<sup>-1</sup>). Growth rates were qualitative estimates of increase in numbers: cells died, -; cells grew slowly, +; cells grew, ++; cells grew quickly, +++.

PREY CONCENTRATION	GROWTH RATE		
	REPLICATE #1	REPLICATE #2	REPLICATE #3
<hr/>			
<i>R. lens</i>	-	-	-
<i>I. galbana</i>	-	+	+
<i>C. salina</i>	-	-	-
<i>I. galbana</i> & <i>R. lens</i>	++	-	-
<i>I. galbana</i> & <i>C. salina</i>	+	++	-
<i>C. salina</i> & <i>R. lens</i>	-	-	-
<i>I. galbana</i> & <i>C. salina</i> & <i>R. lens</i>	++	+++	++

Table 6.2. Growth and grazing parameters for *Strombidium acuminatum* strain BJLSC; parameters and estimates of error of the numerical and functional response curves presented in Figs. 6.1 and 6.2. See section 1.0 in Chapter 3 for the equation used. Values are in units of numbers  $\text{mL}^{-1}$  for concentrations ( $k, x'$ ), and  $\text{d}^{-1}$  for growth rate ( $\mu_{\max}$ ).

	value deviation	standard of variation	coefficient
-----			
Michaelis-Menten fit for the solid line in Fig. 6.1			
$\mu_{\max}$	0.6118	0.07112	11.62
$k$	5812	1224	21.05
$x'$	2709	335.9	12.40
Michaelis-Menten fit for the broken line in Fig. 6.1			
$\mu_{\max}$	0.4169	0.02959	7.098
$k$	1247	327.1	26.22
$x'$	753.4	112.5	14.94
Michaelis-Menten fit for the line in Fig. 6.2			
$G_{\max}$	4.214	0.7463	17.71
$k$	3401	2758	81.08

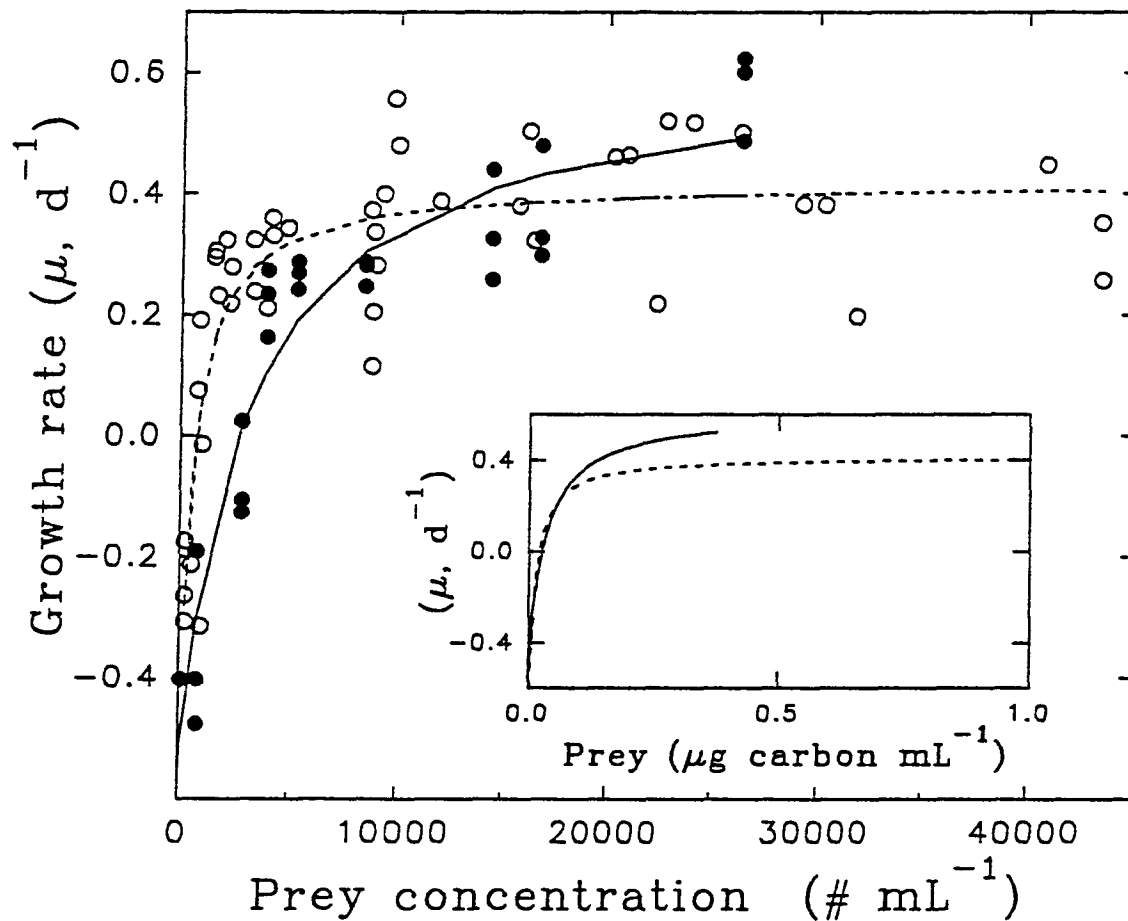


Fig. 6.1. The numerical response of *Strombidium acuminatum* strain BJLSC grown on 2 diets: 1) the diatom *Thalassiosira pseudonana* (solid circles) and 2) a 1:1:1 combination of the three flagellates *Isochrysis galbana*, *Chroomonas salina* and *Rhodomonas lens* (open circles). The lines represent the Michaelis-Menten fit (Eq. 1, Chapter 3) to the two data sets: the diatom (solid line) and the three flagellates (broken line). See Table 6.1 for the parameters and estimates of error associated with these curves. Inset, same as above but the prey concentrations have been converted to carbon using: carbon (pg) =  $0.109 \times \text{live cell volume}(\mu m^3)^{0.991}$  (Montagnes *et al.* submitted).

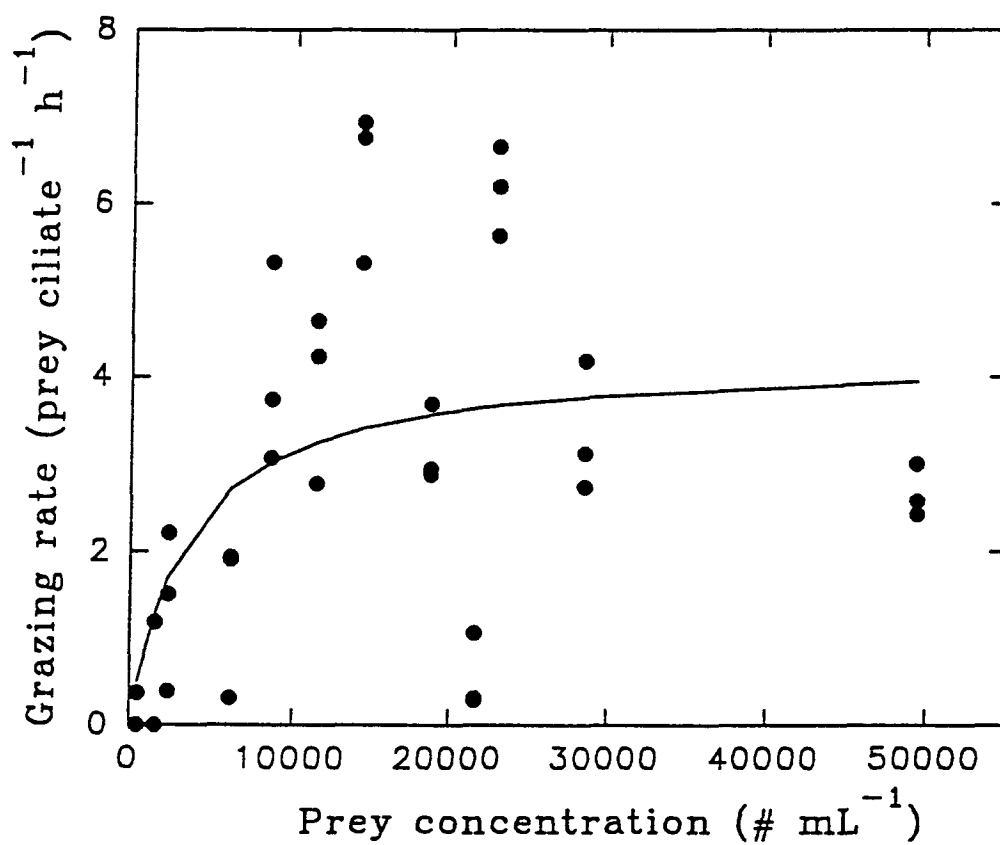


Fig. 6.2. The functional response of *Strombidium acuminatum* strain BJLSC grazing on a 1:1 mixture of the diatom *Thalassiosira pseudonana* and 5  $\mu\text{m}$  fluorescent beads. The line is the Michaelis-Menten fit to the data (Eq. 2, Chapter 3). See Table 6.1 for the parameters and estimates of error associated with this curve.

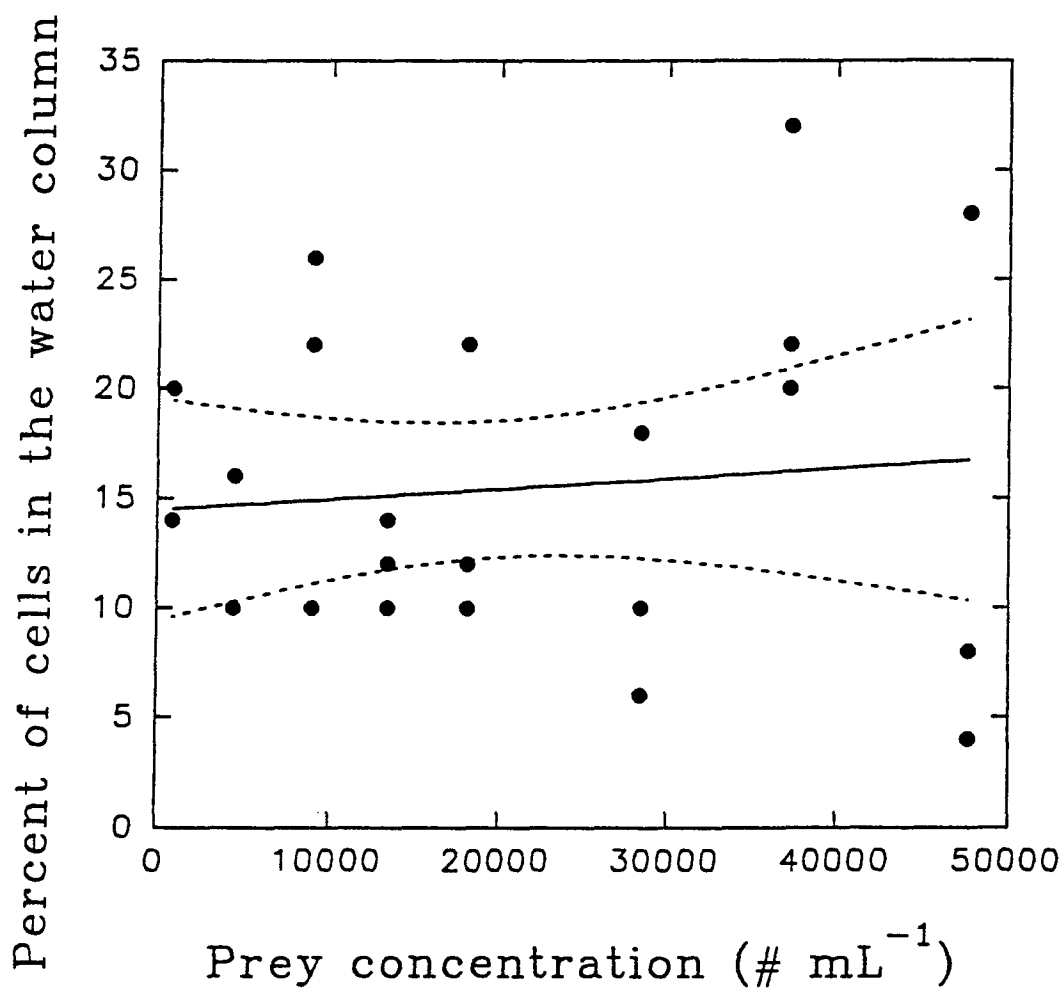


Fig. 6.3. The change in position (in the water column vs. on a surface) of *Strombidium acuminatum* strain BJLSC at different prey (*Thalassiosira pseudonana*) concentrations. The solid line is the regression through the data and the broken lines are the 95% confidence intervals around the regression.

## CHAPTER 7

### GROWTH RATES OF *Strombidium capitatum* STRAIN APAG AS A FUNCTION OF FOOD CONCENTRATION

#### Introduction

This species is presented last because only growth rate data were obtained for it. Although *S. capitatum* was isolated on two separate occasions, neither culture ingested surrogate particles. However, a reasonable numerical response was obtained for it.

#### PART I GROWTH RATES: Estimating the Numerical Response

##### 1.0 General Methods

*Strombidium capitatum* strain APAG was cultured on all combinations of *I. galbana*, *C. salina* and *R. lens*. The ciliate grew on a number of prey combinations but did not survive on single species (Table 7.1). An experiment was conducted to determine the numerical response of *S. capitatum* grazing on a 1:1 ratio of the two flagellate species *Isochrysis galbana* and *Chroomonas salina* (which gave maximum growth rates, Table 7.1), at food concentrations ranging from 0 to  $10^5$  cells mL<sup>-1</sup>. The ciliates were maintained by the semi-continuous culture method described in Chapters 3 and 4.

*Isochrysis galbana* and *C. salina* were maintained in log phase in 150 mL flasks by serial dilution at an irradiance of 50-100  $\mu\text{mol photons m}^{-2} \text{s}^{-1}$  at 16-17°C. Prior to the experiments, *S. capitatum* was maintained in enriched natural seawater with *I. galbana* and *C. salina* at 16-17°C on a 14:10 light:dark cycle at 25-50  $\mu\text{mol photons m}^{-2} \text{s}^{-1}$ . The ciliates were collected during log or stationary phase; prey concentrations, which the ciliates were collected from, were not maintained at a constant concentration.

During the experiment, ciliates were grown in 6-well 20 mL tissue culture plates containing 10 mL of prey medium. Prey concentrations were prepared and enumerated as described in Chapter 3. Typically, each concentration was replicated three times. The semi-continuous culture method was similar to that described in Chapter 3 except for the following modifications.

After the ciliates were placed in the tissue plate they were kept in the dark for 48 h (rather than 24 h) at 16-17°C to allow the ciliates to acclimate. After the acclimation period daily transfers were continued for 5 days, and growth rate was calculated as the 5-day average. The numerical response data were fitted to a modified Michaelis-Menten model (Eq. 1, Chapter 3) using an iterative fit.

A total of 22 treatments (prey concentrations) were examined in two consecutive experiments; treatments ranged from 0-10<sup>5</sup> prey mL<sup>-1</sup>.

A test of methodology was conducted to determine the stability of the prey concentrations. Prey concentration was measured after the initial dilution (prior to adding the ciliates) and after the ciliates had been removed (24 h later). Prey concentrations varied little (~15%) over the 24 h period. Thus, the semi-continuous culture method described above appeared to maintain constant prey levels.

## 2.0 Results and Discussion

The growth rate followed a rectangular hyperbolic response between 1x10<sup>4</sup>-6x10<sup>4</sup> prey mL<sup>-1</sup> (Fig. 7.1). At concentrations below 10<sup>4</sup> (0 and 5x10<sup>2</sup>) and above 6x10<sup>4</sup> (8x10<sup>4</sup> and 10<sup>5</sup>) prey mL<sup>-1</sup> mortality occurred within the first 48 h (the acclimation period). After the acclimation period at concentrations below 1.4x10<sup>4</sup> prey mL<sup>-1</sup>, mortality occurred, presumably due to starvation. Above concentrations of 4x10<sup>4</sup> growth was also inhibited. Similar inhibition of growth at high concentrations was seen in Chapters 3 and 5 and by Verity (1985). Equation 1 (Chapter 3) was fitted to points from 10<sup>4</sup>-6x10<sup>4</sup> prey mL<sup>-1</sup> (Fig. 7.1). The parameters of this equation and their estimates of error are presented in Table 7.2.

## 3.0 Aspects of the Growth Rates and Their Ecological Relevance

In general, *S. capitatum* divided more than once a day (1.5 d<sup>-1</sup> if the curve in Fig. 7.1 is extended beyond the data) at saturating prey concentrations; its threshold concentration was 1.4x10<sup>4</sup> prey mL<sup>-1</sup>; and it had a maximum numerical response between 2x10<sup>4</sup>-3x10<sup>4</sup> prey

$\text{mL}^{-1}$ . There was also a decrease in growth rate with food concentration above  $4 \times 10^4$  prey  $\text{mL}^{-1}$ .

This ciliate is typically mixotrophic (Montagnes *et al.* 1988b, Stoecker and Silver 1990). However, since growth rate was positive in the dark, it is not an obligate mixotroph, like *Laboea strobila* (Stoecker *et al.* 1988, Putt 1990). This seems to contradict the findings of Stoecker and Silver (1990) who suggested that *S. capitatum* requires chloroplasts for continued growth. However, I constantly provided the ciliate with new autotrophic prey, which had been grown in the light. Thus, *S. capitatum* may not be an obligate mixotroph but may require chloroplasts in its diet, as has been suggested by Stoecker and Silver (1990). Possibly, the ciliates would have survived at lower prey concentration if they had been grown in the light.

## PART II GRAZING RATES

### 4.0 A Discussion of Grazing Experiments.

Grazing experiments using  $5 \mu\text{m}$  latex beads, similar to those described in Chapter 4, were conducted with strain IA. However, this ciliate did not ingest beads at any of 8 concentrations ranging from  $1.7 \times 10^4$  to  $7 \times 10^4 \text{ mL}^{-1}$ ; these concentrations covered the range in which *S. capitatum* grew. Further, at a later date, a second clone of *S. capitatum* was established and grown on *I. galbana* and *C. salina*. It was fed fluorescently stained *C. salina* (see Chapter 5), but it did not eat this food analog either. It is not known why this ciliate did not ingest the beads or stained prey. Regardless, no grazing rate measurements were possible.



Table 7.1. The relative growth rate of *Strobilidium capitatum* strain APAG over a 7 day period. The ciliates were grown on a 14:10 light:dark cycle at 16-17°C on all combinations of the three prey: *Isochrysis galbana*, *Chroomonas salina*, and *Rhodomonas lens* (the initial combined prey concentration was  $3 \times 10^4$  cells mL<sup>-1</sup>). Growth rates were qualitative estimates of increase in numbers: cells died, -; cells grew slowly, +; cells grew, ++; cells grew quickly, +++.

PREY	GROWTH RATE
<hr/>	
CONCENTRATION	DAY 7
<i>I. galbana</i>	-
<i>R. lens</i>	-
<i>C. salina</i>	-
<i>I. galbana</i> & <i>R. lens</i>	+
<i>I. galbana</i> & <i>C. salina</i>	+++
<i>C. salina</i> & <i>R. lens</i>	-
<i>I. galbana</i> , <i>C. salina</i> & <i>R. lens</i>	++

Table 7.2. Growth parameters for *Strombidium capitatum* strain APAG; parameters and estimates of error of the numerical response curve presented in Fig. 7.1. See section 1.0 in Chapter 3 for the equation used. Values are in units of numbers  $\text{mL}^{-1}$  for concentrations ( $k, x'$ ), and  $\text{d}^{-1}$  for growth rate ( $\mu_{\max}$ ).

	value	standard deviation	coefficient of variation
-----			
Michaelis-Menten fit			
$\mu_{\max}$	1.074	0.983	92.53
$k$	12370	6410	51.81
$x'$	13860	898.7	6.483

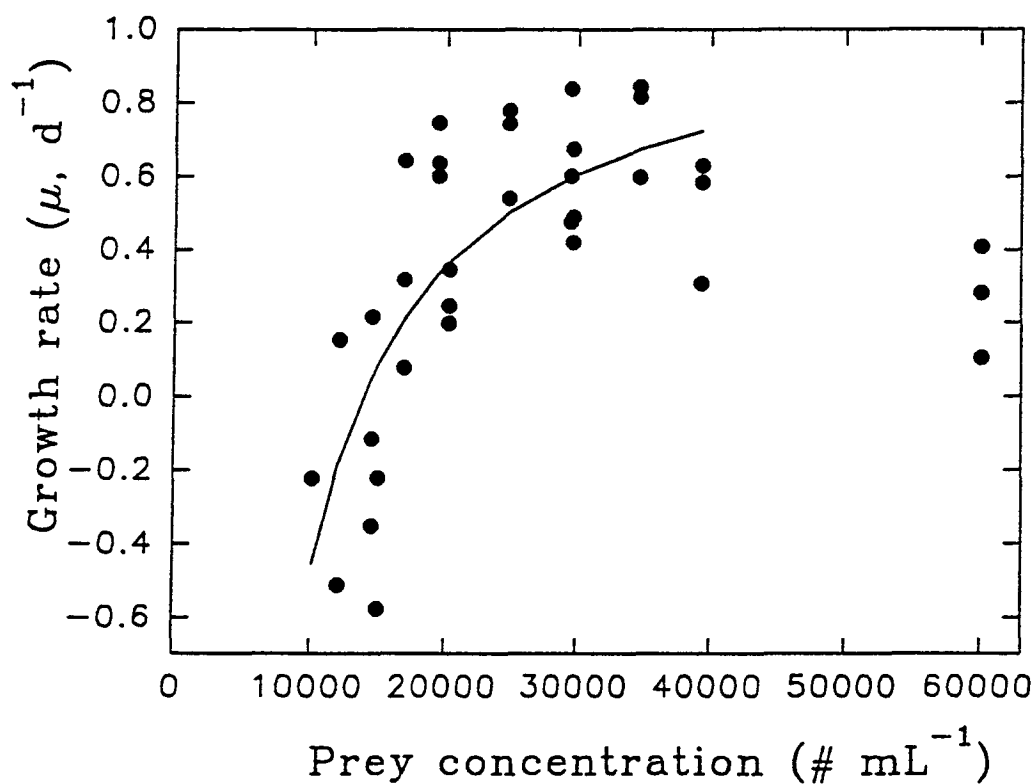


Fig. 7.1. The numerical response of *Strombidium capitatum* strain APAG grown on a 1:1 ratio of the two flagellates *Isochrysis galbana* and *Chroomonas salina*. The circles represent growth rates and the line represents the modified Michaelis-Menten fit to data (Eq. 1, Chapter 3). See Table 7.1 for the parameters and estimates of error associated with this curve.

## CHAPTER 8

### AN EXAMINATION OF THE FUNCTIONAL AND NUMERICAL RESPONSES OF OLIGOTRICHS

#### Introduction

In the past chapters I investigated the numerical and functional responses of 5 ciliate species. These responses were isolate specific (Figs. 8.1 and 8.2), ranging from the slowly growing and grazing *Strombidium acuminatum* strain BJLSC to the rapidly growing and grazing *Strombidium spiralis* strain IA. Now I will compare my results with similar work by others (Figs. 8.1 and 8.2, Tables 8.1 and 8.2) and evaluate my findings. There was no "typical" ciliate response to varied food concentrations (Figs. 8.1 and 8.2). This implies that ciliates cannot be considered a single functional group for food web modeling. The maximum differences between parameters (see Tables 8.1 and 8.2) were often greater than the differences suggested by the coefficients of variation of these parameters (Table 8.3). Thus, while some differences were undoubtedly artifactual, others were probably real. In the following sections I: 1) suggest reasons for variation in response between species and studies; 2) examine the effect of scaling growth and grazing responses to determine if a common size and/or temperature dependent response might be invoked for all ciliates; and 3) present three growth and grazing responses which were used to model ciliate blooms (Chapter 9).

#### 1.0 REASONS FOR RESPONSE VARIATION

##### 1.1 Methodological Biases and the Use of Steady State Measurements

###### 1.1.1 Methodological Biases

The variation in responses (Figs. 8.1, 8.2) can be partially attributed to methodological errors in data acquisition and manipulation. Errors in estimating prey abundance (see Fig. 3.2), cell volumes, and carbon quotas (Verity *et al.* 1993, Montagnes *et al.* submitted) would cause several fold errors on the independent axis. Error on the dependent axis might occur, as growth rate may not be constant over the incubation period (see Chapter 3).

It may also be inappropriate to universally apply the modified Michaelis-Menten kinetics to the data (Chapter 3 Eqs. 1 and 2). This model can be a good predictor of both

functional and numerical responses and is based on sound theoretical mechanisms (e.g. Holling 1959, Fenchel 1986, Appendix 2) which have been supported by direct observation (Taniguchi and Takeda 1988). However, these mechanisms vary due to external factors. The model assumes that predators are non-selective and have a constant encounter rate. Both these assumptions can be violated. Oligotrichs can be selective and may alter their behaviour (Blackbourn 1974, Stoecker 1988, Taniguchi and Takeda 1988, Verity 1991a). The model also assumes that the gross growth efficiency is constant, which it may not be (Stoecker and Evans 1985, Verity 1985). Further, my results indicate that: 1) there is deviation from the hyperbolic response at high food concentrations, indicating inhibition (see Chapters 3, 5, and 7, also see Verity 1985); 2) there may be switching in behaviour at lower food concentrations (see Chapter 4); and 3) Eq. 1 may not be applicable to mortality rate estimates (see Chapter 3). Finally, piecewise regression (Blackman kinetics) may, at times, fit functional and numerical response data better (Condrey 1982, Condrey and Fuller 1985). Thus, applying Eqs. 1 and 2 (Chapter 3) indiscriminately to all ciliates is inappropriate. However, given that: 1) Michaelis-Menten-like kinetics are a first approximation of grazing and growth responses for ciliates (see Holling 1959, Spain 1982, Fenchel 1986, Taniguchi and Takeda 1988, Legovic 1989, Appendix 2); 2) my data follow a rectangular hyperbolic response (rather than a piecewise, Blackman, response); and 3) from the parameters I measured, there was no means to determine the reasons for the deviant ciliate behaviour, I consider Eqs. 1 and 2 (Chapter 3) to adequately represent the responses for use in my food web model (see below).

### **1.1.2 The Use of Steady State Measurements**

The time over which experiments are run and the extent of the acclimation period can affect the results of both grazing and growth experiments (Verity 1985). Ciliates exhibit behavioural changes to variation in food concentration over minutes (e.g. Verity 1991b), but they exhibit morphological and physiological changes over hours to days (Lynn 1975, Lynn *et al.* 1987, Fenchel and Jonsson 1988, Fenchel 1990). Failure to acclimate ciliates, over a period of days, to steady state conditions may result in variable and inaccurate growth and grazing estimates. Because of the difficulty of maintaining such conditions, few studies have

established steady state estimates. Other than chemostat methodologies (e.g. Scott 1985), small containers and regular transferring of ciliates seems to be the only means to maintain ciliates at a constant prey concentration for extended periods. By virtue of their large surface area and shallow depth, small containers could increase microbial growth, facilitate the settling and accumulation of prey (on the bottom), and provide surfaces for cells to collide into (and possibly lyse). The 10 mL containers I used may therefore misrepresent natural conditions, and these potential errors should be considered when evaluating my results. However the methodology I used was the only practical means to acclimate and maintain these ciliates over extended periods. Therefore, the precision of such estimates is at present constrained by culturing logistics.

My estimates of growth responses may be better than previous ones on marine planktonic ciliates, as they were conducted for several days under steady-state conditions. Further, most studies of ciliate numerical responses have likely underestimated the threshold food concentration (the concentration where growth equals mortality), as ciliates may not immediately die at sub-threshold levels. For instance, Verity (1985) acclimated two tintinnids for 12-18 h prior to growth experiments at several food concentrations, but there was no (or little) indication of a threshold concentration (Verity 1985, Fig. 3). In another case, Heinbokel's (1978) response curves on tintinnids, which have been used in several models (e.g. Frost 1987, Frost and Franzen 1992), were based on ciliates that were only acclimated "overnight". In some of my experiments the threshold concentration may have been overestimated due to imprecision of prey concentration measurements (see previous chapters). However, these imprecise measurements should have been overcome to some extent by the multiple measurements that were made near the threshold levels (see previous chapters). Since I also made extensive measurements below the threshold concentrations (measurements which other methods are unable to make) these studies should provide more realistic (higher) estimates of mortality rate (see Fig. 8.1a and b, insets) and would be more appropriate for modeling systems where the ciliates deplete their food source.

My grazing rate estimates (except Chapter 4) are like those obtained by others, which were conducted on ciliates acclimated for short periods (several hours, see previous chapters). I expect these estimates are biased. For instance, the grazing rates may be overestimated at low food concentrations since these experiments often used ciliates maintained at higher food concentrations (Chapters 4 and 5). These ciliates would be larger and more active than those maintained on leaner diets, and therefore they might graze at higher rates. The problem of obtaining grazing estimates on prey-acclimated ciliates lies in the difficulty of maintaining large ciliates numbers (needed for grazing experiments) at constant food concentrations for extended periods. Therefore logistics limit the resolution of accurate grazing rates.

### 1.2 Use of Surrogate Particles to Determine Grazing Rates.

Surrogate particles, both beads and stained prey, have been extensively used to measure protozoan grazing rates in the laboratory and field (e.g. Jonsson 1986, Pace and Bailiff 1987, Stoecker 1988, Rublee and Galagos, 1989, Gonzalez *et al.* 1990, McManus and Okubo 1991, Putt 1991, Sherr and Sherr 1993), and there have been criticisms of this technique (e.g. ciliates may have prey preference, Stoecker 1988, Putt 1991; fixation may cause egestion of prey, Sieracki *et al.* 1987; particles may not be monodispersed, Pace and Baliff 1987, but see Putt 1990 and McManus and Okubo 1991). Based on a literature review and an assessment of available techniques I chose surrogate uptake to estimate grazing (see previous chapters). In retrospect, I now believe this methodology inadequately measured grazing rates, as there was considerable variation in my data (Chapters 3-6). Analysis of my data also indicated that the variability in grazing rates measured by surrogate uptake can significantly over- or underestimate the predicted grazing rates.

Assuming my growth rate estimates are accurate, the ingestion rate required to sustain growth can be calculated using the bioenergetic equation:

$$\text{Ingestion} = (\text{growth} + \text{respiration}) / \text{assimilation efficiency} \quad (3)$$

Respiration for ciliates and flagellates is dependent on cell size and follows the relation:  $\log_{10} R \text{ (nL O}_2 \text{ cell}^{-1} \text{ h}^{-1}) = \log_{10} \text{Vol (}\mu\text{m}^3) * 0.75 - 4.09$  (Fenchel and Finlay 1983). This respiration rate can be converted to carbon (ng) by converting nL O<sub>2</sub> to moles of O<sub>2</sub>,

converting this to moles of CO<sub>2</sub>, assuming a respiratory quotient ranging from 1 (for carbohydrate) to 0.7 (for fat) (Schmidt-Nielsen 1980), and then converting to mass of carbon (multiplying by 12 g C mole<sup>-1</sup>). Assimilation efficiencies, ranging from 0.65 to 0.9, have been established for protozoa (Laybourn-Parry 1984, Stoecker 1984, Verity 1985), although the accuracy of these measurements may be suspect (Caron and Goldman 1993). Using my growth rates and cell volumes (cell volume was determined from 30-100 growing cells, see Table 8.1) and a range of respiratory quotient and assimilation efficiencies and Eq. 3, I have compared the predicted ingestion rates to my direct estimates, for the ciliates examined in Chapters 3-6 (Fig. 8.3). This analysis indicates that the surrogate particle method: 1) underestimated the calculated (bioenergetically determined) grazing rate by up to an order of magnitude for *Strombidinopsis acuminatum* and *Strombidium acuminatum*; 2) overestimated calculated grazing by up to four-fold for *Strobilidium* sp. strain JERC; and 3) compared reasonably to the calculated grazing rate of *Strobilidium spiralis*.

The gross growth efficiency (carbon incorporated/carbon consumed, GGE) of ciliates, which is typically 0.3-0.6 (see Caron and Goldman 1990 for a review) can also be used to determine the accuracy of grazing estimates (although the GGE can vary with food concentration, Verity 1985, 1991). The observed growth rates of the ciliates described in Chapters 3-6 were divided by their observed and predicted (by Eq. 3) ingestion rates (Fig. 8.4). In all 4 cases the predicted GGE plateaued near 0.4-0.5 while in 3 of the 4 cases the observed GGE was far from this range. Thus, predicting grazing rates from growth rates appears to be a more accurate than using surrogate particles to estimate grazing.

Grazing rates can be affected by food quality (type of prey analog). Oligotrichs can be selective in their feeding (Blackbourn 1974, Stoecker 1988), and this will affect grazing estimates. *Strobilidium spiralis* consumed latex microspheres but not stained algae (Chapter 4), *Strobilidium* sp. strain JERC consumed stained algae but not microspheres (Chapter 5), and *Strombidium capitatum* consumed neither (Chapter 7). These data support the evidence of other researchers that prey analog choice influences grazing estimates, and it indicates that there is not a single "best" prey analog to use (e.g. Putt 1991). Thus, my grazing estimates



from surrogate uptake are likely inaccurate, and I have used Eq. 3 to establish grazing rate responses in the model presented in Chapter 9.

### 1.3 Physiological-Behavioural Variables

To simplify modeling, it would be convenient if all ciliates behaved in a similar fashion, but they do not (see Chapters 3-7 and Figs. 8.1 and 8.2). Still, it is possible that some factors might be used to scale growth responses and allow us to simplify the "ciliate" component of models. For instance, differences in ciliate cell size, prey type, and ambient temperature might affect the ciliates and alter the growth responses (Müller and Geller 1993).

Increases in temperature by 10°C may raise ciliate responses by 2-2.5 fold (i.e.  $Q_{10} = 2-2.5$ , Fenchel and Finlay 1983, Fenchel 1987, Caron *et al.* 1990). This relation can be stated as:

$$\log_{10}(\text{rate}_1/\text{rate}_2) = \log_{10}Q_{10} * \{(\text{temp}_1 - \text{temp}_2)/10\} \quad (4)$$

However, variation exists in  $Q_{10}$  estimates (Müller and Geller 1993, Verity 1985). The relationship between physiological rates and temperature may not be log-linear and may deviate significantly at high temperatures, where it is often strongly negative (Aelion and Chisholm 1985, Caron *et al.* 1990). Thus, differences in ambient temperature may explain some of the response variations seen in Figs. 8.1 and 8.2, but caution should be applied when using  $Q_{10}$  scaling.

Cell volume is another parameter used to scale growth rate. Dogma suggests that large cells grow slower than small ones, but there is variation, as ciliates can have "r" or "K" like strategies (Taylor and Shutter 1978, Turley *et al.* 1986). Generally, protozoa follow the allometric response  $\mu = aV^b$ , where  $\mu$  ( $\text{d}^{-1}$ ) is growth rate,  $V$  ( $\mu\text{m}^3$ ) is volume and "a" ( $\text{d}^{-1} V^{-1}$ ), and "b" are constants (Taylor and Shutter 1981, Fenchel and Finlay 1983). At 20°C the value of "a" ranges from 20 to 40  $\text{d}^{-1} V^{-1}$  (from Fig. 1, Taylor 1981 and Fig. 3, Fenchel and Finlay 1983) while "b" is approximately -0.25 (Taylor 1981, Fenchel and Finlay 1983, Fenchel 1987, Müller and Geller 1993).

Using the above relationships, differences in ambient temperature and cell volume may be accounted for. I have scaled the growth responses presented in Table 8.1 and Fig. 8.1b to

20°C (using  $Q_{10} = 2$ ) and standardizing growth rate by solving for "a" in the allometric equation  $\mu = aV^b$  (using  $b = -0.25$ ) (Fig. 8.5). Note that applying these transformations to the entire curve (rather than only to the maximum rate) may be inappropriate, as these relationships are typically calculated from maximum growth rates.

After scaling for temperature and cell volume, some conformity between the ciliates existed, but differences between the responses remained (Fig. 8.5). The transformed maximum growth rate generally fell within the previously observed range of 20-40 d<sup>-1</sup>  $\mu\text{m}^{-3}$ , with most of the ciliates exhibiting a volume specific growth of near 20 (Fig. 8.5, inset). Note that two of the three studies on *Strobilidium spiralis* (curves 2 and 8 vs. 9) gave a higher transformed growth rate (~40 d<sup>-1</sup>  $\mu\text{m}^{-3}$ , Fig. 8.5, inset). The response of three medium sized ciliates were also similar (Fig. 8.5, curves 6, 9, and 10). Thus, although differences in ambient temperature and cell size may account for some of the variation between responses, it is likely that other factors alter the response.

I have also scaled the grazing rates (Fig. 8.2a, Table 8.2) by dividing them by the square of the sum of the prey and predator radii ( $[r_{\text{ciliate}} + r_{\text{prey}}]^2$ ) and using a  $Q_{10} = 2$  (scaled to 20°C). The former manipulation was based on the assumption that ingestion is directly proportional to prey-predator encounters, and such encounters will vary directly with the cross-sectional areas of both prey and predator. These manipulations changed the relative position of the curves (cf. Fig. 8.2b vs. Fig. 8.6) but indicated that size and temperature did not control grazing rate.

Thus, differences between ciliate responses are not solely due to variation in ambient temperature and cell size. As indicated above (section 1.1), methodological biases likely contribute to these differences. However, species specific factors such as behavioural responses or possibly physiological responses to food processing may also cause the differences. For instance, swimming speed (Buskey and Stoecker 1988, 1989), prey rejection (Blackbourn 1978, Taniguchi and Takeda 1988), filtration efficiency (Bernard and Rassoulzadegan 1990), vacuole formation (summarized in Capriulo 1990), and prey detection (Verity 1988) could affect the ingestion rate.

Variation in food quality within and between experiments may have affected the growth rates presented in Figs. 8.1 and 8.2. Nutritional quality differs between and within prey species. This was discussed in Chapter 6, but see the data in Chapters 4, 5, and 7. The extent to which different prey species affect growth was qualitatively examined in Chapters 4-7 and has been shown by others (Capriulo 1990, Caron and Goldman 1990, Caron *et al.* 1990).

Initially, I examined the suitability of several algal species for maintaining ciliates:

*Thalassiosira pseudonana*, *Pavlova lutheri*, *Pyramimonas orientalis*, *Tetraselmis suecia*, *Tetraselmis* sp., *Croomonas salina*, *Isochrysis galbana*, *Heterocapsa triquetra*, *Scrippsiella trochoidea*, *Micromonas pusilla*, and *Rhodomonas lens*. These all proved to be adequate food for some ciliates, but not for all (data not shown). Ultimately, I chose to use the four species *Thalassiosira pseudonana*, *Isochrysis galbana*, *Croomonas salina* and *Rhodomonas lens*, as these algae stimulated growth for most ciliates that I isolated, and have been shown by others to be good food items (e.g. Repak 1983, Verity and Villareal 1986).

Variation of oligotrich growth rates may be in part due to food preferences (Verity 1991a and b). Not only does prey type affect ciliate growth but there are species specific growth responses to prey type (cf. Tables 4.1, 5.1, 6.1, and 7.1). My response curves were based on prey which elicited a maximum growth response, but I only examined 3-4 prey species. Possibly, other prey would produce higher rates.

From these studies, I suggest that food type is the primary factor affecting ciliate species composition and distribution in the plankton. Concomitantly, prey abundance is the primary factor affecting ciliate growth rate and therefore abundance in the plankton. The former suggestion may appear as an obvious platitude, but it is a concept often overlooked in plankton models. Recognition of such species specific responses should allow us to better assess the role of ciliates in the plankton. It also suggests that monospecific ciliate blooms could be caused by monospecific prey patches, if the optimum ciliate and prey combination coincide. Such an event is explored in Chapter 9.

## 1.4 Species Differences

Variations in growth and grazing rates are likely species specific, as implied by Figs. 8.1 and 8.2. Such differences in ciliate numerical responses may be due to a number of factors: 1) clonal decline (see Chapter 3 and 4); 2) clonal variation (see Chapter 3); 3) inclusion of both planktonic and semi-benthic species in analyses (both *Strombidium acuminatum* strain BJSCH and *Strombidium sulcatum* from Fenchel and Jonsson, 1988, Table 8.1 are likely semi-benthic); 4) inclusion of mixotrophic and non-mixotrophic species (oligotrichs range from non-mixotrophic to obligate mixotrophic species, e.g. Stoecker *et al.* 1988, Putt 1990, Stoecker and Silver 1990, Stoecker and Michaels 1991); and 5) tendencies toward r and K life strategies (Taylor 1978).

It would be presumptuous to pursue a discussion of species variations based on my research and the limited studies on planktonic oligotrichs. However, two comparisons from the data presented in Fig. 8.1 are exemplary of the response differences from similar ciliates. Curves 2, 8 and 9 in Fig. 8.1 are all from different studies on ciliates that appear to be *Strobilidium spiralis* (see Chapter 2), but all three responses are different. Further, curves 2 and 3 are from my studies on two species of *Strobilidium* of different size but similar morphology (see Chapter 2), and they are different. Thus, lumping ciliates into a single functional group, as has been done for past models, ignores the diversity of responses that ciliates may exhibit. This could inaccurately represent their role as microzooplankton.

## 2.0 Ciliate Growth and Grazing Responses for Food Web Modeling

Variation in grazing and growth responses exists between planktonic ciliates. Rather than devise a single numerical response to represent all ciliates, I have proposed three growth responses which cover a range (Fig. 8.7, Table 8.4): species A was based on (parameters were adjusted slightly, see previous chapters and Table 8.4) the growth rate of *Strombidinopsis acuminatum* strain SPJSC; species B was based on the growth rate of *Strobilidium spiralis* strain IA; and species C was based on the growth rate of *Strobilidium* sp. stain JERC. The grazing rates of these 3 ciliates were calculated as a function of growth rate, based on Eq. 3, a

respiratory quotient of 0.80, and an assimilation efficiency of 0.75. The latter two parameters gave a response near the middle of the expected range, see Figs. 8.3 and 8.4 (although a respiratory quotient of 0.9 has been suggested for tintinnids, Verity 1985). These 3 ciliate responses cover a large portion of the ranges in growth responses presented above and are used to examine the impact of ciliates on nanoplankton blooms (Chapter 9).

Table 8.1. A comparison of numerical response constants for 10 oligotrichs. The parameters are the same as those described in Eq. 1, Chapter 3. Cell volumes ( $\mu\text{m}^3$ ) and densities ( $\# \text{ mL}^{-1}$ ) are presented in bold type. Cell carbon quotas ( $\text{pg C cell}^{-1}$ ) and carbon concentrations ( $\text{ng C mL}^{-1}$ ) are presented in normal type. Prey carbon was estimated using the conversion: carbon (pg) =  $0.109 * \text{live cell volume } (\mu\text{m}^3)^{0.991}$  (from Montagnes *et al.* submitted), except for marked cases. <sup>1</sup>A value obtained from a figure rather than the text. <sup>2</sup>Recalculated from raw data graphically presented in Verity (1991a) but provided by the author. <sup>3</sup>Calculated using  $0.1 \text{ pg C } \mu\text{m}^{-3}$  (Borsheim and Bratbak 1987). <sup>4</sup>Ciliate carbon estimated using  $0.148 \text{ pg C } \mu\text{m}^{-3}$  from Putt and Stoecker (1989) except in marked cases (\*) where it was presented in the literature.

SPECIES	CILIATE volume & carbon ( $\mu\text{m}^3$ ) (pg C cell <sup>-1</sup> )	$\mu_{\text{max}}$ (d <sup>-1</sup> )	k (# mL <sup>-1</sup> ) (ng C mL <sup>-1</sup> )	x' (# mL <sup>-1</sup> ) (ng C mL <sup>-1</sup> )	SOURCE	°C	PREY SPECIES	PREY CARBON (pg C cell <sup>-1</sup> )	PREY RANGE CONC. (# mL <sup>-1</sup> ) (ng C mL <sup>-1</sup> )
<i>Strombidinopsis acuminatum</i> strain SPJSC	117193 17368	0.985	4091 24.30	1567 9.31	This study	16	<i>Thalassiosira pseudonana</i>	5.9	400 to 90000 2.38 to 534
<i>Strobilidium spiralis</i> strain IA	110000 16302	1.85	19070 617.87	10230 331.45	This study	16	<i>Chroomonas salina</i>	32.4	0 to 95000 0 to 3080
<i>Strobilidium</i> sp. strain JERC	19635 2910	0.721	10580 208.27	4075 80.22	This study	16	<i>Chroomonas salina</i> <i>Isochrysis galbana</i>	19.7	1700 to 57000 33.5 to 1120
<i>Strombidium</i> sp. strain BJLSC	28575 4235	0.612	5812 34.52	2709 16.09	This study	16	<i>Thalassiosira pseudonana</i>	6.0	100 to 50000 0.59 to 297
<i>Strombidium capitatum</i> strain APAG	64140 9506	1.07	12370 243.50	13860 272.90	This study	16	<i>Chroomonas salina</i> <i>Isochrysis galbana</i>	19.7	14000 to 60000 275 to 1181
<i>Strombidium</i> sp.	6500 963	2 <sup>1</sup>	6500 52 <sup>4</sup>	0 0	Fenchel & Jonsson 1988	20	<i>Pteridomonas danich</i>	8.0 <sup>3</sup>	0 to 20000 0 to 160
<i>Eutintinnus pectinis</i>	18000 2668	1.54	24530 24.530	1390 13.90	Heinbokel 1978	18	<i>Isochrysis galbana</i> <i>Monochrysis lutheri</i> <i>Dunaliella tertiolecta</i>	10.0	0 to 40000 0 to 400
<i>Strobilidium</i> (= <i>Lhomanniella</i> ) <i>spiralis</i>	150000 22230	1.18	5400 54.81	730 74.10	Jonsson 1986	12	<i>Pyramimonas</i> sp.	10.2	0 to 50000 0 to 507
<i>Strobilidium spiralis</i>	11494 <sup>2</sup> 3200*	1.79	11915 41.7	5025 17.56	Verity 1991	20	<i>Isochrysis galbana</i>	3.5	7000 to 1200000 25 to 420
<i>Strombidium reticulatum</i>	40000 5928	0.84	6300 63.95	800 8.12	Jonsson 1986	12	<i>Pyramimonas</i> sp.	10.2	0 to 100000 0 to 1015

Table 8.2. A comparison of functional response constants for 8 oligotrichs. The parameters are the same as those described in Eq. 2 (Chapter 3) or as modified in Eq. 1 (Chapter 3), which allows for a non-zero x-intercept. Cell volumes ( $\mu\text{m}^3$ ) and densities ( $\# \text{ mL}^{-1}$ ) are presented in bold type. Cell carbon quotas ( $\text{pg C cell}^{-1}$ ) and carbon concentrations ( $\text{ng C mL}^{-1}$ ) are presented in normal type. Prey carbon was estimated using the conversion: carbon (pg) =  $0.109 * \text{live cell volume } (\mu\text{m}^3)^{0.991}$  (from Montagnes *et al.* submitted), except for marked cases. <sup>1</sup>A value obtained from a figure rather than the text. <sup>2</sup>Recalculated from raw data graphically presented in Verity (1991a) but provided by the author. <sup>?</sup>No temperature was presented but 20°C was assumed.



SPECIES	$g_{\max}$ (# h <sup>-1</sup> ) (pg C h <sup>-1</sup> )	k (# mL <sup>-1</sup> ) (pg C mL <sup>-1</sup> )	x' (# mL <sup>-1</sup> ) (pg C mL <sup>-1</sup> )	SOURCE	°C	PREY SPECIES	PREY (pg C cell <sup>-1</sup> )	PREY RANGE CONC. (# mL <sup>-1</sup> ) (pg C mL <sup>-1</sup> )
<i>Strombidinopsis acuminatum</i> strain SPJSC	101.00 0.60	426300 2532	0 0	This study	16	<i>Thalassiosira pseudonana</i> and 5 µm beads	5.9	1800 to 70000 10.7 to 416
<i>Strobilidium spiralis</i> strain IA	45.45 1.47	4028 130.51	0 0	This study	16	<i>Chroomonas salina</i> and 5 µm beads	32.4	1000 to 95000 32 to 3080
<i>Strobilidium</i> sp. strain JERC	41.21 but max=24 <sup>4</sup> 1.34 but max = 0.78	3865 125.2	0 0	This study	16	<i>Chroomonas salina</i> and 5 µm beads	32.4	100 to 48000 3.24 to 1555
<i>Strombidium</i> sp. strain BJLSC	4.21 0.025	3401 20.20 <sup>3</sup>	0 0	This study	16	<i>Thalassiosira pseudonana</i> and 5 µm beads	5.9	450 to 30000 2.67 to 178
<i>Eutintinnus pectinis</i>	16 0.16	1628 16.28	1000 10	Heinbokel 1978	18	<i>Isochrysis galbana</i> <i>Monochrysis lutheri</i> <i>Dunaliella tertiolecta</i>	10.0	1000 to 40000 10 to 400
<i>Favella</i> sp.	13.55 <sup>1</sup> 1.49	452 <sup>1</sup> 49.76	0 0	Stoecker 1988	15	<i>Heterocapsa triquetra</i>	110	0 to 2500 0 to 275
<i>Strobilidium spiralis</i>	169.00 <sup>2</sup> 0.593	19849 <sup>2</sup> 69.47	4229 <sup>2</sup> 14.80	Verity 1991	20	<i>Isochrysis galbana</i>	3.5	7000 to 1200000 25 to 420
<i>Strombidium sulcatum</i>	34.40 0.11	4681 15.21	336 1.09	Bernard & Rassoulzadegan 1990	20 <sup>?</sup>	<i>Dunaliella minuta</i>	3.3	0 to 1200000 0 to 17520

Table 8.3. A comparison of error estimates of numerical and functional responses (coefficients of variation) from data of the five species presented in Chapters 3-7. The symbols ( $\mu_{\max}$ ,  $k$ ,  $x'$ ,  $G_{\max}$ ,  $k$ ) are the parameters used to fit data to Eqs. 1 and 2 (Chapter 3). No data (---).

Species	Coefficients of variation of				
	growth parameters			grazing parameters	
	$\mu_{\max}$	$k$	$x'$	$G_{\max}$	$k$
<i>Strombidinopsis acuminatum</i>	4.7	15.0	10.0	182.9	2169
<i>Strobilidium spiralis</i>	13.9	15.0	9.0	6.1	33.7
<i>Strobilidium</i> sp. strain JERC	15.2	32.2	13.4	7.4	22.0
<i>Strombidium acuminatum</i> strain BJLSC	11.6	21.1	12.4	17.7	81.1
<i>Strombidium capitatum</i>	27.8	51.8	6.5	---	---

Table 8.4. Parameters used to establish 3 different ciliate numerical response curves (for ciliates A, B, C) using Eq. 1, (Chapter 3). These are use in the model of ciliate-prey population dynamics in Chapter 9. The symbols ( $\mu_{\max}$ ,  $k$ ,  $x'$ ) are the parameters used to fit data to Eq. 1 (Chapter 3). Values are in units of ng carbon mL<sup>-1</sup> for concentrations ( $k_{\mu}$ ,  $x'_{\mu}$ ), and d<sup>-1</sup> for growth rate ( $\mu_{\max}$ ). Values in bold are the number (mL<sup>-1</sup>) of 8  $\mu$ m (diameter) particles that would be made from the respective carbon value (carbon particle<sup>-1</sup> was calculated from: carbon (pg) = 0.109 \* live cell volume ( $\mu$ m<sup>3</sup>)<sup>0.991</sup>, from Montagnes *et al.* submitted). These particle concentrations were used in the model discussed in (Chapter 9).

species	$\mu_{\max}$	$k_{\mu}$	$x'_{\mu}$
<hr/>			
A	0.99	24	10
		<b>921</b>	<b>380</b>
B	1.85	618	331
		<b>24436</b>	<b>13014</b>
C	0.72	208	80
		<b>8143</b>	<b>3105</b>

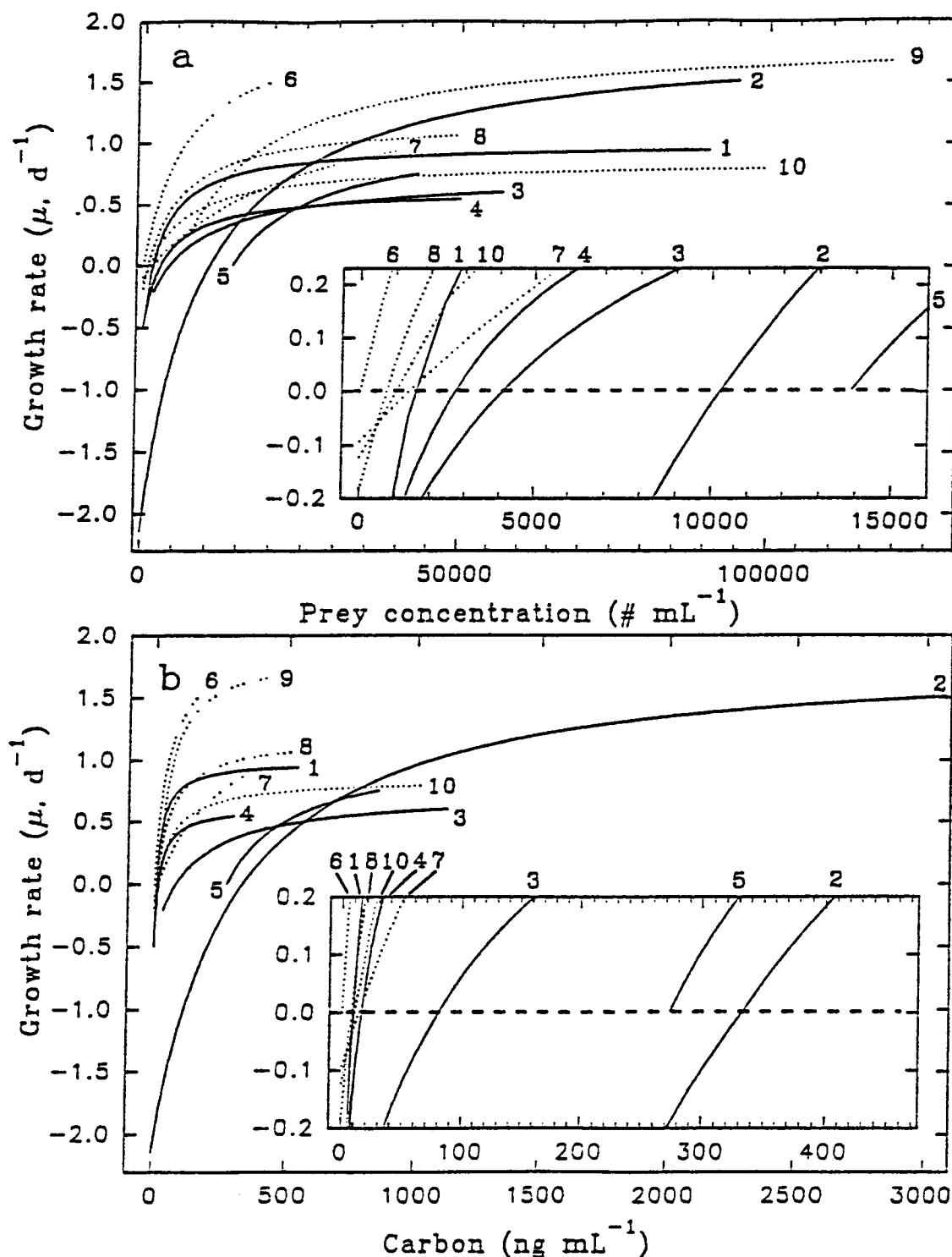


Fig. 8.1. The growth rates (numerical responses) of 10 oligotrichs in response to varied prey concentration as prey numbers (panel a) and prey carbon (panel b). The lines are the modified Michaelis-Menten fits (Eq. 1, Chapter 3) to the data; see Table 8.1 for the parameters associated with these curves and particulars associated with each study. The solid curves were obtained from this study and represent: *Strombidinopsis acuminatum* strain SPJSC (1); *Strombidium spiralis* strain IA (2); *Strombidium* sp. strain JERC (3); *Strombidium acuminatum* strain BJLSC (4); and *Strombidium capitatum* strain APAG (5). The broken curves were obtained from the literature and represent: *Strombidium sulcatum* (Fenchel and Jonsson 1988) (6); *Eutintinnus pectinis* (Heinbokel 1978) (7); *Strombidium* (= *Lohmanniella*) *spiralis* (Jonsson 1986) (8); *Strombidium spiralis* (Verity 1991a) (9); and *Strombidium reticulatum* (Jonsson 1986) (10). The insets are an enlargement of the region where the curves intercept the zero growth (threshold) concentrations; see Table 8.1 for the value ( $x'$ ) of these intercepts. Note, curve 9 is not in the insets as it does not extend to  $\mu = 0$ .

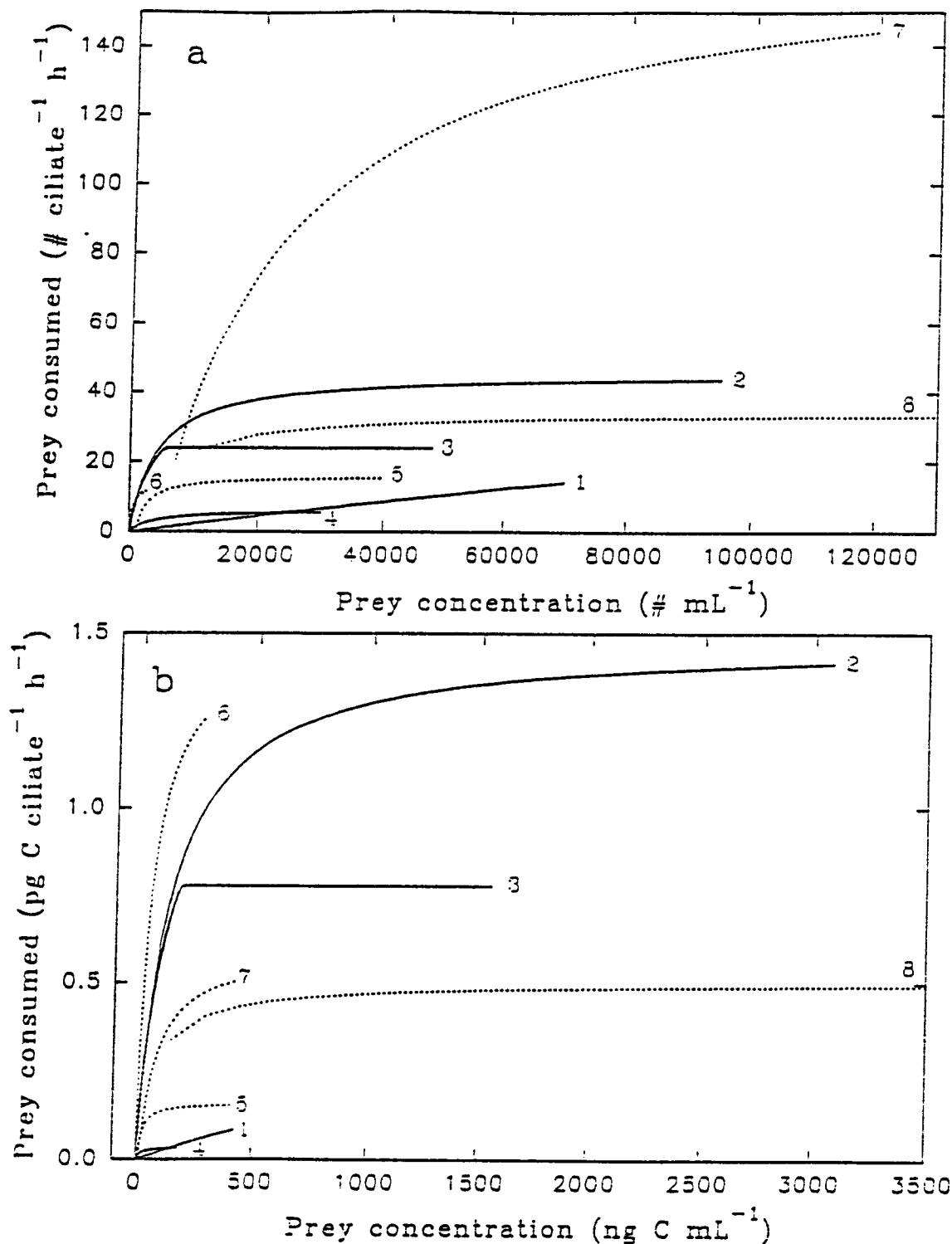


Fig. 8.2. The grazing rates (functional responses) of eight oligotrichs in response to varied prey concentration as numbers (panel a) and prey carbon (panel b). The lines are the Michaelis-Menten fits (Eq. 2, Chapter 3) to the data; see Table 8.2 for the parameters associated with these curves and particulars associated with each study. The solid curves were obtained from this study and represent: *Strombidinopsis acuminatum* strain SPJSC (1); *Strombidium spiralis* strain LA (2); *Strombidium* sp. strain JERC (3); and *Strombidium acuminatum* strain BJLSC (4). The broken curves were obtained from the literature and represent: *Eutintinnus pectinis* (Heinbokel 1978) (5); *Favella* sp. (Stoecker 1988) (6); *Strombidium spiralis* (Verity 1991a) (7); and *Strombidium sulcatum* (Bernard and Rassoulzadegan 1990) (8).

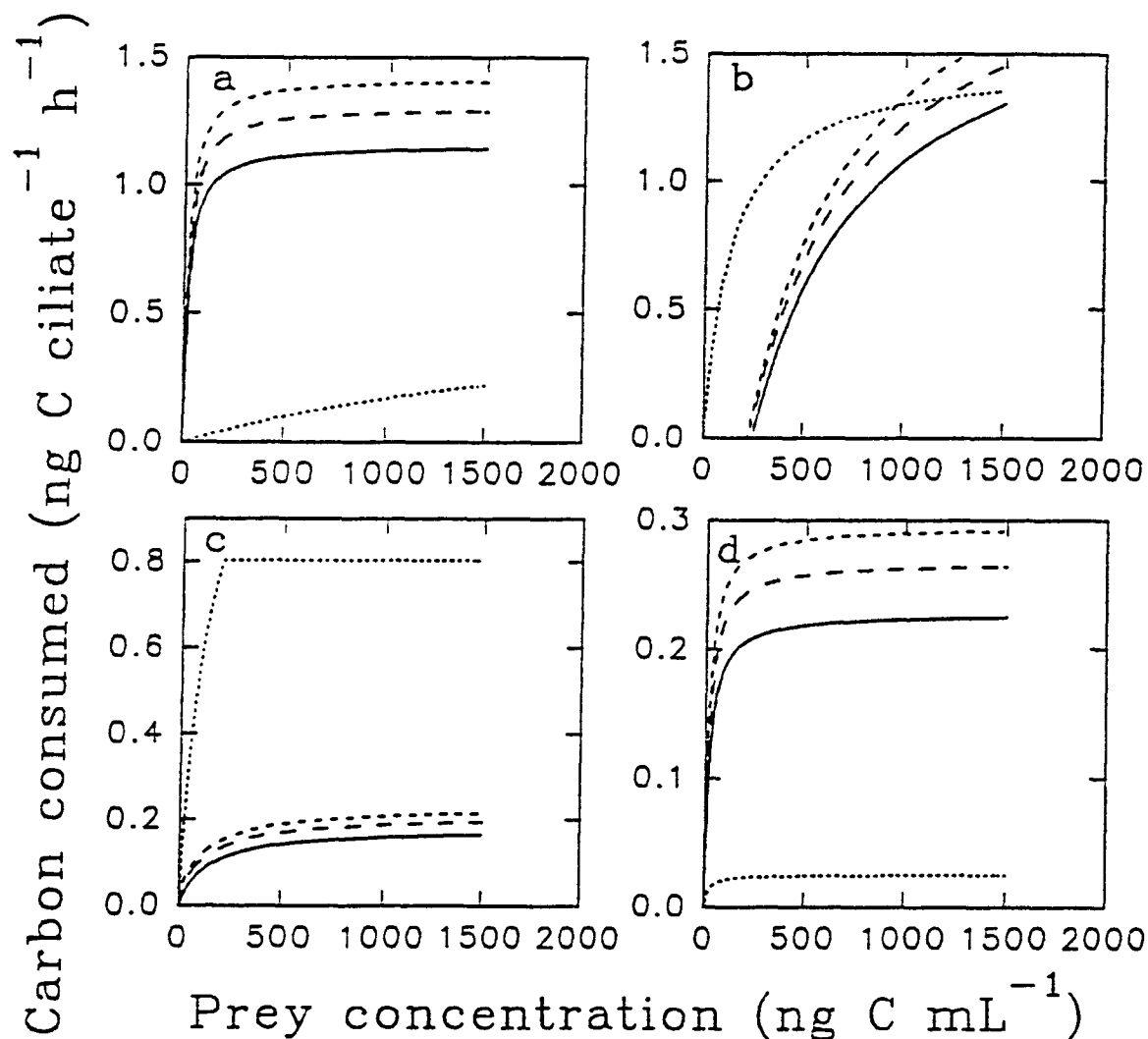


Fig. 8.3. A comparison of observed functional response rates (dotted lines) and those predicted from equation 3 (see section 1.2), using growth rates predicted by values presented in Chapters 3-6 and Eq. 1, Chapter 3. The 3 predicted rates used the following parameters: a respiratory quotient of 1 and an assimilation efficiency of 0.8 (short dashes); a respiratory quotient of 0.8 and an assimilation efficiency of 0.75 (medium dashes); a respiratory quotient of 0.75 and an assimilation efficiency of 0.7 (solid lines). Data were obtained from: *Strombidinopsis acuminatum* strain SPJSC, Chapter 3 (panel a); *Strombidium spiralis* strain IA, Chapter 4 (panel b); *Strombidium* sp. strain JERC, Chapter 5 (panel c); and *Strombidium acuminatum* strain BJLSC, Chapter 6 (panel d).

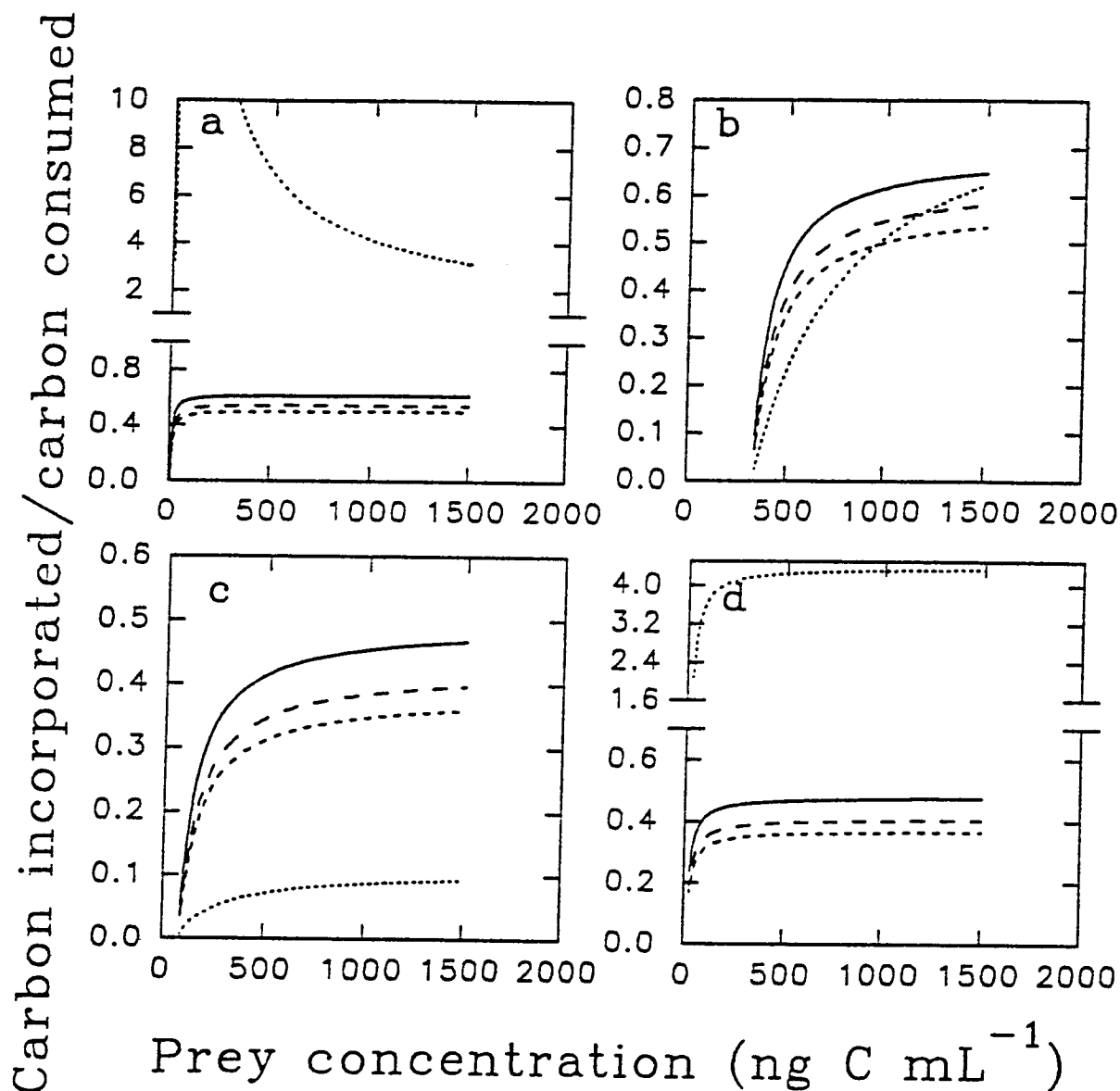


Fig. 8.4. A comparison of gross growth efficiencies (carbon incorporated/carbon consumed) based on observed growth and grazing data (dotted line lines) and those based on observed growth and predicted grazing rates (predicted grazing rate was determined using Eq. 3 (see section 1.2) and growth rates predicted by values presented in Chapters 3-6 and Eq. 1, Chapter 3). The three predicted grazing rates used the following parameters: a respiratory quotient of 1 and an assimilation efficiency of 0.8 (short dashes); a respiratory quotient of 0.8 and an assimilation efficiency of 0.75 (medium dashes); a respiratory quotient of 0.75 and an assimilation efficiency of 0.7 (solid lines). Data were obtained from: *Strombidinopsis acuminatum* strain SPJSC, Chapter 3 (panel a); *Strobilidium spiralis* strain IA, Chapter 4 (panel b); *Strobilidium* sp. strain JERC, Chapter 5 (panel c); and *Strombidium acuminatum* strain BJLSC, Chapter 6 (panel d).

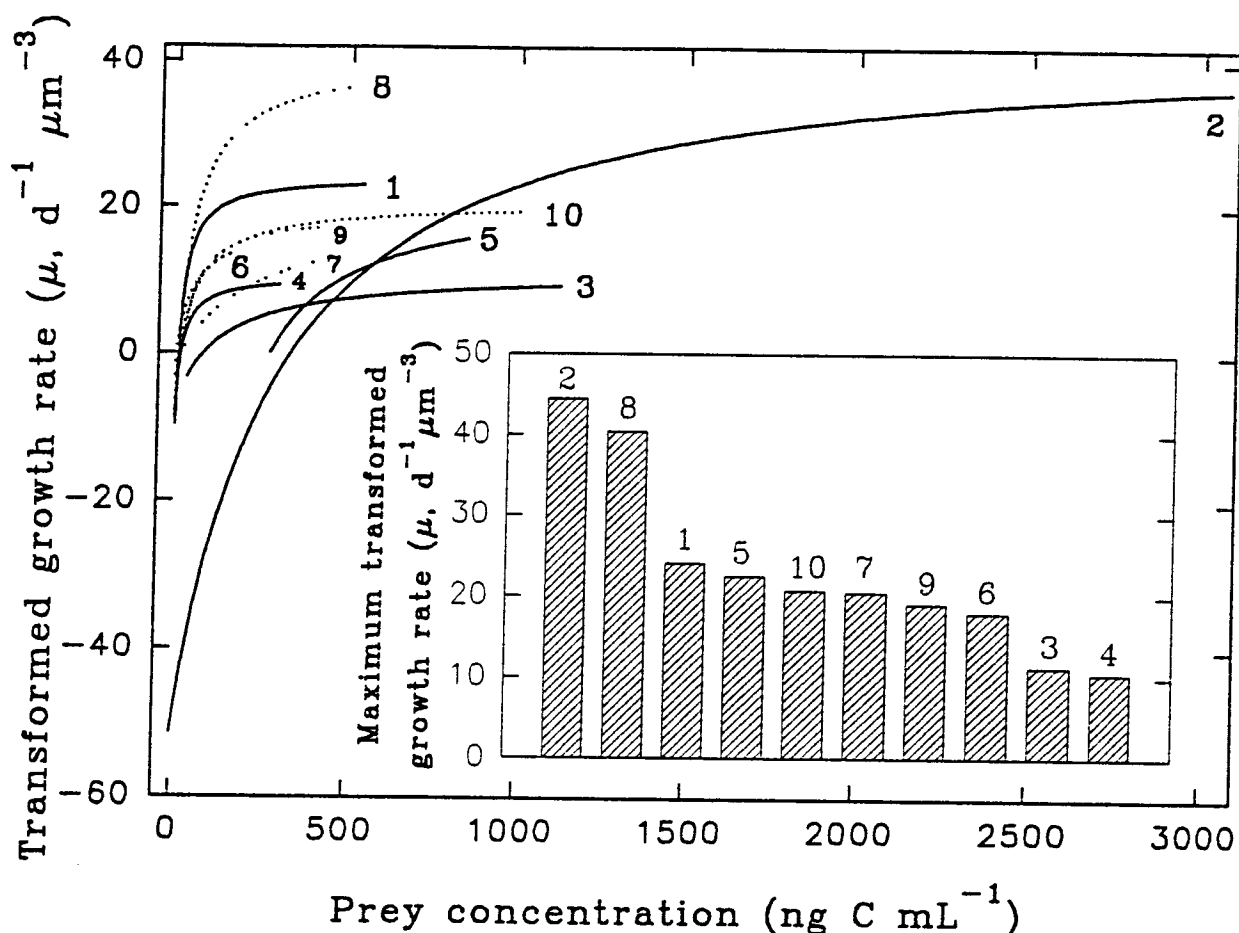


Fig. 8.5. The growth rate of 10 oligotrichs in response to varied prey concentration, corrected for differences in cell volume and ambient temperature (to 20°C). The lines are the transformed modified Michaelis-Menten fits (see Fig. 8.1) to the data; see Table 8.1 for the particulars associated with each study and the text (Chapter 8 section 1.3) for the specific transformations. The solid curves were obtained from this study and represent: *Strombidinopsis acuminatum* strain SPJSC (1); *Strobilidium spiralis* strain IA (2); *Strobilidium* sp. strain JERC (3); *Strombidium acuminatum* strain BJLSC (4); and *Strombidium capitatum* strain APAG (5). The broken curves were obtained from the literature and represent: *Strombidium sulcatum* (Fenchel and Jonsson 1988) (6); *Eutintinnus pectinis* (Heinbokel 1978) (7); *Strobilidium* (= *Lohmanniella*) *spiralis* (Jonsson 1986) (8); *Strobilidium spiralis* (Verity 1991a) (9); and *Strombidium reticulatum* (Jonsson 1986) (10). The inset is a comparison of the transformed maximum growth rates predicted by Eq. 1, Chapter 3 (the untransformed maximum growth rates are presented in Table 8.1).



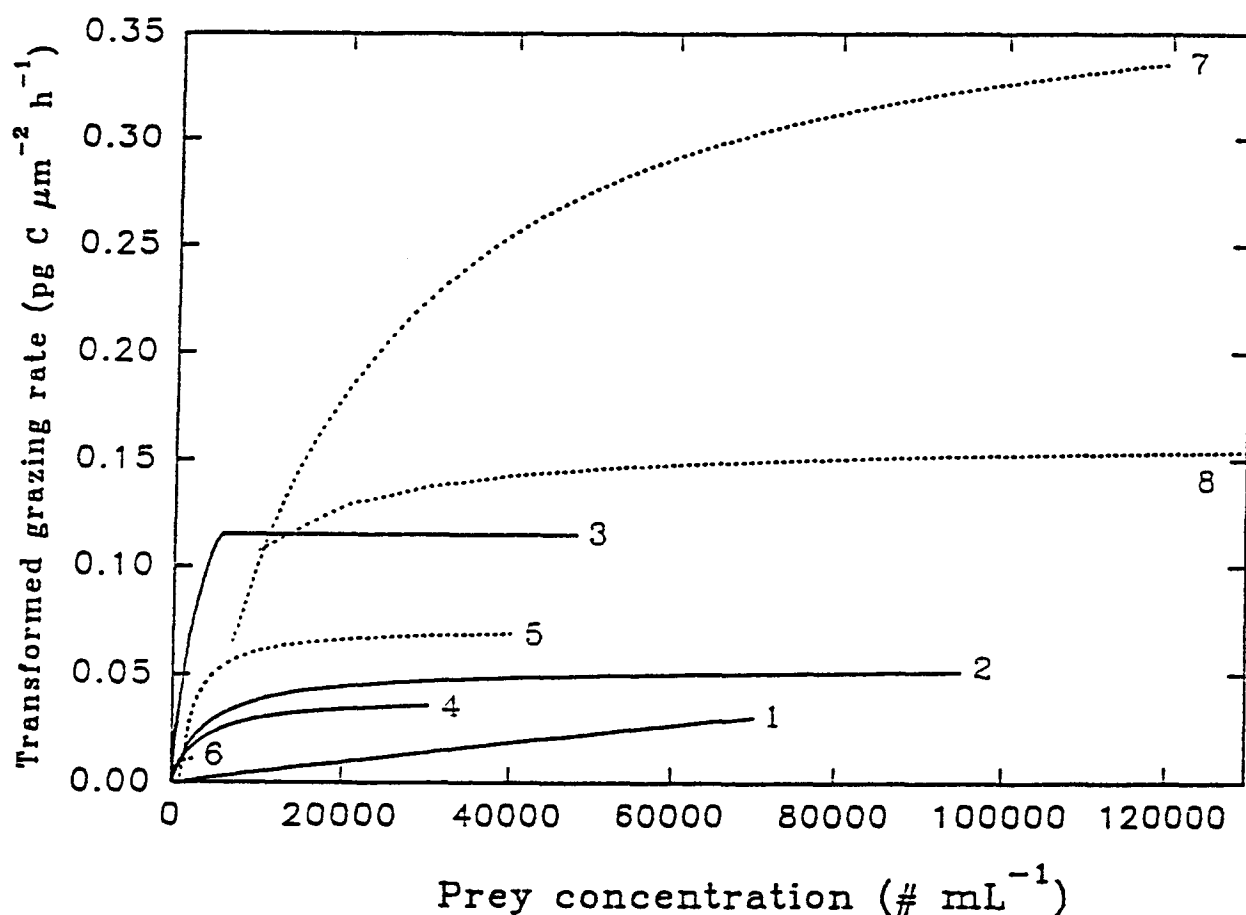


Fig. 8.6. The grazing rate of 8 oligotrichs in response to varied prey concentration, corrected for differences in cell size and ambient temperature (to 20°C). The lines are the transformed Michaelis-Menten fits (see Fig. 8.2) to the data; see Table 8.2 for the particulars associated with each study and the text (Chapter 8 section 1.3) for the specific transformations. The solid curves were obtained from this study and represent: *Strombidinopsis acuminatum* strain SPJSC (1); *Strombidium spiralis* strain LA (2); *Strombidium* sp. strain JERC (3); and *Strombidium acuminatum* strain BJLSC (4). The broken curves were obtained from the literature and represent: *Eutimninus pectinis* (Heinbokel 1978) (5); *Favella* sp. (Stoecker 1988) (6); *Strombidium spiralis* (Verity 1991a) (7); and *Strombidium sulcatum* (Bernard and Rassoulzadegan 1990) (8).

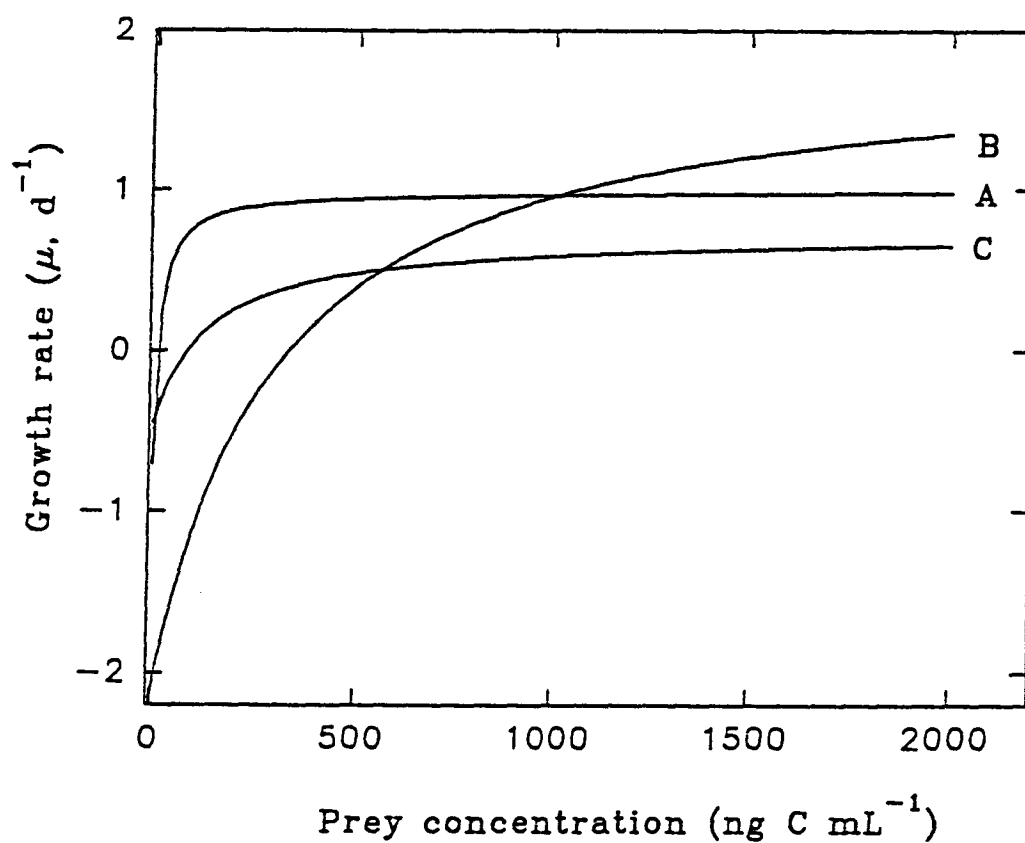


Fig. 8.7. Three growth responses used to represent different ciliate types (A-C) (see section 2.0 for details). These responses are used to model ciliate-nanoplankton prey interactions in Chapter 9. The parameters for these curves are presented in Table 8.4.

## CHAPTER 9

### A MODEL OF CILIATE AND PHYTOPLANKTON POPULATION DYNAMICS

#### Introduction

In this chapter I investigate short-term and small-scale ciliate-phytoplankton bloom dynamics using the BASIC model presented in Appendix 4. The goal of this exercise was to use the data, collected in the previous chapters, to answer the following general questions about ciliate blooms. 1) Can ciliates control blooms of small ( $< 10 \mu\text{m}$ ) phytoplankton by grazing them down over short periods (several days)? 2) Are ciliates a link or a sink for phytoplankton biomass (i.e. are they important in the transfer of biomass to higher trophic levels)? 3) Can ciliates and copepods compete for the same food source? 4) Can different ciliate species cause different types of algal and ciliate blooms (i.e. are species differences important)? I then examined a phytoplankton-ciliate-copepod food web, to determine how ciliate blooms could influence the flow of carbon to copepods. These questions were designed to determine if ciliate blooms could be an important component of marine food webs.

The phytoplankton and/or ciliate blooms I have considered are mono-specific, rapid increases in numbers or biomass, visible as transient peaks (Legendre 1990, Lynn and Montagnes 1991). In coastal waters, short term phytoplankton blooms could be stimulated by a number of factors: tidal or wind mixing events, changes in irradiance, or by allochthonous nutrient inputs from terrestrial run off (Mackas *et al.* 1985, Harris 1986, Legendre 1990). Such blooms probably do not exist for more than 2-3 weeks, as mixing processes (e.g. wind and tides) dissipate them, and mesozooplankton populations (e.g. copepods) can respond to them if they do persist. For the model, I have assumed that over periods of  $< 20$  days, phytoplankton blooms are not influenced by increases in mesozooplankton populations (Raymont 1983) and that advection of organisms and nutrients in or out of the system would be negligible. These are the conditions where ciliate blooms might occur and where ciliates could have a selective advantage over mesozooplankton due to ciliates' rapid growth rates. Blooms with these parameters are probably meters to kilometers in size and fall into the "fine"

scale patches described by Haury *et al.* (1978). Mackas *et al.* (1985) suggested that patches of this magnitude persist for 1-10 days and are dominated by "episodic predation stress".

## 1.0 The Model (see Appendix 4)

### 1.1 General Description

The model simulated the population dynamics of ciliates and phytoplankton in a non-steady state situation, where the ciliates and copepods encountered a patch of water with a defined initial phytoplankton (algal) concentration. There were 5 types of organisms in the system (Fig. 9.1): algae, 3 ciliate species (A, B, C, see Table 8.4, Fig. 8.7), and a copepod species (data obtained from Frost, 1972 for *Calanus pacificus*, see section 1.3.2). The algae were small (8  $\mu\text{m}$  in diameter) and during the simulation grew at a constant rate of  $\mu = 0.7 \text{ d}^{-1}$ , or  $\mu = 0 \text{ d}^{-1}$  when algal abundance reached its maximum level (see below). Algal mortality was by predation from the ciliates (see section 2.0, Chapter 8) and the copepods. Ciliate growth rates were species specific functions of algal concentration (as illustrated in previous chapters). For all 3 ciliates, mortality was due to starvation (a function of algal concentration, Table 8.4, Fig. 8.7) and to predation by the copepod (a function of ciliate concentration and size). There was no growth or mortality of the copepods over the simulation period, as 20 days is less than the gestation period for many mesozooplankton (Raymont 1983).

The model was designed to examine the dynamics of nanoplankton-ciliate blooms that were grazed by a copepod. This was a test of the potential impact and temporal extent of ciliate blooms. In no way should the following analysis be extended to assess the role of ciliates under more complex conditions. In the future, more elaborate, models may do this; these would likely include: advection terms, dispersal of ciliates and prey, migration terms, more predators, estimates of nutrient regeneration, and cohort analysis of the zooplankton.

## 1.2 Constraints

Algal concentration was always  $\leq 5 \times 10^4$  cells  $\text{mL}^{-1}$ . This maximum was based on the assumption that algae can be nutrient-limited, and nitrogen, which may be the limiting nutrient (e.g. Harrison *et al.* 1983, Harris 1986), can have pre-bloom concentrations of 10-20  $\mu\text{M}$  (140-280  $\mu\text{g L}^{-1}$ , e.g. Takahashi *et al.* 1977, Harrison *et al.* 1983, Haigh *et al.* 1992). An average 8  $\mu\text{m}$  (diameter) algal cell has 5.24 pg N in it (based on the relation: nitrogen (pg) =  $0.0172 * (\text{volume in } \mu\text{m}^3)^{1.023}$ , from Montagnes *et al.* submitted). Thus, a 20  $\mu\text{M}$  nitrogen source would allow the maximum production of  $\sim 5 \times 10^4$  cells  $\text{mL}^{-1}$ . Algal production was zero when the maximum concentration of  $5 \times 10^4$  cells  $\text{mL}^{-1}$  was reached, but as soon as this maximum concentration was depressed, by grazing, there was algal growth.

## 1.3 Parameters and Rate Equations

### 1.3.1 Ciliates

The ciliate growth parameters (Table 9.1) were established in Chapter 8 (Table 8.4) and were used in a Eq. 1 (Chapter 3) to determine ciliate growth rate for a given algal concentration.

Ciliate grazing rates were calculated using Eq. 3 (Chapter 8), assuming growth rate estimates were accurate, a respiratory quotient of 0.8, and an assimilation efficiency of 0.75 (see Chapter 8). Growth and grazing rates were converted to similar units (carbon  $\text{time}^{-1}$ ) using the equations: ciliate carbon = 0.148 pg C  $\mu\text{m}^{-3}$  (Putt and Stoecker 1989) and algal carbon (pg) =  $0.109 * \text{live cell volume } (\mu\text{m}^3)^{0.991}$  (Montagnes *et al.* submitted).

### 1.3.2 Copepod

The parameters for the copepod were obtained from work conducted on *Calanus pacificus* by Frost (1972) and modified by Mullin *et al.* (1975). Frost (1972) established piecewise numerical responses for *C. pacificus* feeding on diatoms that were 11  $\mu\text{m}$  (*Thalassiosira fluviatilis*), 35  $\mu\text{m}$  (*Coscinodiscus angustii*), and 75  $\mu\text{m}$  (*Coscinodiscus eccentricus*) in mean diameter. Mullin *et al.* (1975) reanalyzed Frost's data for *T. fluviatilis* using a modified Michaelis-Menten equation (with a non-zero intercept, similar to Eq. 1,

(Chapter 3). In the model, I have used the parameters established by Mullin *et al.* (1975) to determine the copepod grazing rate on the 8  $\mu\text{m}$  algae (i.e. assuming that 11  $\approx$  8  $\mu\text{m}$  algae). From Frost (1972, Fig. 4), I estimated (by eye) the half-saturation concentration ( $k$ ) and maximum grazing rate ( $G_{\text{max}}$ ) for *Cal. pacificus* capturing *Cos. angustii* (35  $\mu\text{m}$ ) and *Cos. eccentricus* (75  $\mu\text{m}$ ) (Table 9.1). In the model I used these two sized organisms to establish Michaelis-Menten like responses (with zero intercepts, Eq. 2, Chapter 3) for ciliate C (which is 25  $\mu\text{m} \approx$  35  $\mu\text{m}$ ) and ciliates A and B (which are  $\sim$ 75  $\mu\text{m}$ ).

I assumed that ciliates would be grazed at the same rate as diatoms of a similar size. There are studies which support and refute this assumption (Stoecker and Egloff 1987, Gifford and Dagg 1988, 1991, Tiselius 1989, Wiadnyana and Rassoulzadegan 1989, Jonsson and Tiselius 1990). Copepods may sense ciliates and preferentially capture them, but some ciliates "jump" and may avoid capture. Ciliate A, in the model, was based on a species of *Strombidinopsis* (which does not jump) while ciliates B and C were based on species of *Strobilidium* (which do jump). These variable behaviours could reduce the validity of the model. However, as there are conflicting data in the literature, and I have no data on the grazing rates of copepods on these ciliates, I have assumed that ciliates and diatoms would be grazed in a similar fashion by *C. pacificus*.

Copepod grazing of ciliates A, B, and C and algae followed Eq. 5. This equation is used for a single predator consuming  $n$  prey types, when the predation rates have been determined from separate experiments on single prey types using Michaelis-Menten-like kinetics (see Appendix 2, Legovic 1989).

$$G_i = (G_{\text{max}i} * P_i / k_i) / (1 + \sum P_j / k_j) \quad (5)$$

where,

$G_i$  = grazing rate on prey  $i$  (prey  $\text{d}^{-1}$ )

$G_{\text{max}i}$  = the maximum grazing rate on prey  $i$  (prey  $\text{d}^{-1}$ )

$P_i$  = the concentration of prey  $i$  ( $\text{mL}^{-1}$ )

$k_i$  = the half-saturation concentration for prey  $i$  ( $\text{mL}^{-1}$ )

$\sum P_j/k_j$  = the sum of all prey concentrations divided by their respective half-saturation constants

#### 1.4 Variables (Table 1)

I have varied the initial abundance of algae ( $.05\text{-}25 \times 10^3 \text{ mL}^{-1}$ ), the invariant (i.e. unchanging during the simulation) abundance of copepods ( $0.01\text{-}5 \text{ L}^{-1}$ ), and the initial abundance of the 3 ciliates ( $0\text{-}1 \text{ mL}^{-1}$ ), to examine the effect of these variables on population dynamics and carbon flow.

#### 1.5 A Summary of Assumptions

The following assumptions were made: 1) the time for a potential ciliate bloom to occur was limited to 20 days, and blooms occurring after 20 days were ignored; 2) advection was considered negligible during the bloom period, and there were no terms associated with it; 3) only small phytoplankton, ciliates, and copepods were considered in the system (e.g. no larger phytoplankton, metazoan microzooplankton, or fish were included); 4) copepods grazed ciliates at the same rate they would graze diatoms of similar size (i.e. predation was strictly size dependent); 5) nutrient regeneration was considered only in terms of phytoplankton maximum abundance (i.e. phytoplankton growth was limited by nutrient availability only when the maximum phytoplankton density was reached, and when phytoplankton density dropped below this maximum, growth resumed); and 6) the algal species elicited maximum ciliate growth rates.

#### 1.6 Equations

The following equations were numerically integrated over a 20 d period (time step = 0.05 days) using an iterated fourth order Runge-Kutta procedure (see Appendix 4). Cell abundances were converted to carbon using the relationships of Putt and Stoecker (1989) and Montagnes *et al.* (submitted), stated above.

Rate of change in abundance of ciliate species  $i$  ( $C_i$ ) at time  $t$  was modeled as:

$$dC_i/dt = (\mu_{C_i} * C_i) - (ZG_{C_i} * Z)$$

Rate of change in abundance of algae (P) at time  $t$  was modeled as:

$$dP/dt = (\mu_P * P) - (ZG_P * Z) - \Sigma(CG_{ip} * C_i)$$

where  $P \leq 5 \times 10^4$  cells mL<sup>-1</sup>, otherwise  $P = 5 \times 10^4$  cells mL<sup>-1</sup>

The gross production of ciliate  $i$  ( $CP_i$ ) over the 20 day period was

$$CP_i = \int_0^{20} \mu_{C_i}(t) * C_i * dt$$

where  $\mu_{C_i}(t) = \mu_{C_i}$  if  $\mu_{C_i} \geq 0$ , otherwise  $\mu_{C_i}(t) = 0$

The gross production of algae (PP) over the 20 day period was

$$PP = \int_0^{20} \mu_P(t) * P * dt$$

where  $\mu_P(t) = \mu_P$  if  $P \leq 5 \times 10^4$ , otherwise  $\mu_P(t) = 0$

The total number of algae grazed by the copepod (PZG) over the 20 day period was

$$PZG = \int_0^{20} ZG_P(t) * Z * dt$$

The total number of ciliate  $i$  grazed by the copepod ( $C_iZG$ ) over the 20 day period was

$$C_iZG = \int_0^{20} ZG_{C_i}(t) * Z * dt$$

The total number of algae grazed by the ciliate  $i$  ( $PC_iG$ ) over the 20 day period was

$$PC_iG = \int_0^{20} CG_{ip}(t) * C_i * dt$$

where,

$$t = 0.05 \text{ (d)}$$

$\mu_{C_i}$  = the growth rate of ciliate  $i$  (d<sup>-1</sup>), determined by Eq. 1 (Chapter 3), parameters stated in

Table 9.1 for each ciliate, and the algal concentration at time  $t$ .

$\mu_P$  = the growth rate of the algae (d<sup>-1</sup>) = 0.7 d<sup>-1</sup>

$Z$  = the copepod concentration (mL<sup>-1</sup>), set as a constant at the start of each simulation

$ZG_{C_i}$  = the grazing rate of the copepods on ciliate  $i$  (cells mL<sup>-1</sup> d<sup>-1</sup>), determined by Eq. 4

(Chapter 9), the parameters in Table 9.1, and the concentration of ciliate  $i$  at time  $t$

$ZG_P$  = the grazing rate of the copepods on the algae (cells mL<sup>-1</sup> d<sup>-1</sup>), determined by Eq. 4

(Chapter 9), the parameters in Table 9.1, and the concentration of ciliate  $i$  at time  $t$



$CG_{ip}$  = the grazing rate of ciliate  $i$  on the algae ( $\text{cells mL}^{-1} \text{ d}^{-1}$ ), determined by Eq. 1 (Chapter 3), Eq. 3 (Chapter 8), the parameters stated in Table 9.1 for each ciliate, and the algal concentration at time  $t$ .

## 2.0 Results of the Model and Discussion of Their Implications

### 2.1 Ciliate Blooms Control Blooms of Small Phytoplankton

The model (Appendix 4) predicted that ciliates can bloom under conditions where copepods are rare and phytoplankton are initially abundant (Figs. 9.2). Under these conditions, the copepod population was unable to control primary production, phytoplankton bloomed, and blooms of ciliates grazed down the phytoplankton; Fig. 9.3c-e illustrates some of these bloom conditions.

Copepod abundance may vary in coastal and oceanic waters from  $0\text{--}10 \text{ L}^{-1}$  (e.g. Harrison *et al.* 1983, Raymont 1983, Landry and Lehner-Fournier 1988, Nielsen and Richardson 1989, Nielsen and Kiorboe 1991). The model indicated that at an invariant concentration of  $0.5\text{--}1$  copepods  $\text{L}^{-1}$  and initial algal concentrations of near  $10^3 \text{ mL}^{-1}$ , ciliate blooms do not occur, although there were minor oscillations in ciliate A abundance (Fig. 9.3a and b). These low algal levels were because the copepod population was large enough to graze the algae down to the copepod's threshold concentration of  $\sim 800$  algae  $\text{mL}^{-1}$  (i.e. this is the concentration where copepods stop eating algae, Table 9.1).

Copepod and nano-phytoplankton levels of  $0.5\text{--}1$  copepods  $\text{L}^{-1}$  and  $10^3$  algal  $\text{mL}^{-1}$  are near average conditions for many coastal waters (e.g. Harrison *et al.* 1983, Raymont 1983, Middlebrook and Roff 1986). Thus, ciliate blooms probably do not occur under "typical" coastal conditions, and copepods are the dominant grazers of small phytoplankton. This conclusion supports Banse's (1982) argument that on average ciliates consume little food relative to copepods because the concentrations of suitable food particles tend to be too low.

One of the ciliates (A) survived under "typical" conditions but the other ciliates (B and C) did not (Fig. 9.3a and b). The mortality rates of ciliates B and C resulted from their high growth-threshold levels (i.e. they need high concentrations of algae to survive, Table 8.4).

How then can ciliates B and C persist? Likely, they persist by existing in a patchy environment.

Plankton distributions are patchy in both time and space (Haury *et al.* 1978, Harrison *et al.* 1983, Mackas *et al.* 1985, Harris 1986, Owen 1989, Sime-Ngando 1992). Therefore, conditions should exist where ciliates will bloom and A and B will persist. Ciliates bloomed when algae were initially abundant and/or copepods are rare (Fig. 9.3). Such conditions might exist in the summer (post-spring bloom) or in the winter when mesozooplankton abundance can be low. They might also occur at any time if mesozooplankton distribution is patchy and phytoplankton are abundant (e.g. Fig 9.3c-e). Such blooms would fall into the "fine" scale patches (tens to thousands of meters, Haury *et al.* 1978) which can exist for several days under unperturbed conditions.

Ciliate and nanophytoplankton blooms occur in British Columbian waters (Blackbourn 1974, Takahashi *et al.* 1977, Harrison *et al.* 1983, Appendix 3) and in other waters (Guillard and Ryther 1962, Verity 1986, Dale and Dahl 1987, Lynn and Montagnes 1991, Gallegos 1992). In Sechart Inlet, British Columbia (Appendix 3), ciliate and  $< 10 \mu\text{m}$  phytoplankton abundances occasionally exhibited relatively high levels that could be considered blooms, but rarely achieved the high levels predicted by the model. In contrast, blooms of ciliates occur that are higher than those predicted by the model (Dale and Dahl 1987, Lynn and Montagnes 1991). Thus, there are factors other than those employed in the model which affect bloom development.

British Columbian waters, unlike the model, typically contain more than 3 ciliates species (Martin and Montagnes 1993). A greater diversity of ciliate responses might alter the formation of blooms, as other responses likely exist. Also, to examine the maximum potential for ciliate blooms, I established an upper (but atypical) limit for the phytoplankton bloom ( $5 \times 10^4$  cells  $\text{mL}^{-1}$ ). Field data on phytoplankton abundances (Appendix 3) and observed nitrogen pulses of  $\sim 10 \mu\text{M}$  (Takahashi *et al.* 1977) suggest that maximum algal levels of  $1 - 2.5 \times 10^4 \text{ mL}^{-1}$  are more representative for small scale blooms. Limiting the phytoplankton

biomass does decrease the size of ciliate blooms in the model. Thus, the simulations I have presented can be viewed as a maximum for ciliate blooms.

High abundances of ciliates may result from concentration by physical factors (Mackas *et al.* 1985). An aggregation of up to  $2 \times 10^3$  ciliates  $\text{mL}^{-1}$  observed by Dale and Dahl (1987) in a Norwegian bay was probably due in part to concentration from wind mixing, and the subsequent dispersal of the ciliates was probably due to flushing of the bay. Dale and Dahl (1987) argue that the bloom could only have occurred without mixing if the ciliates divided  $\sim 3$  times  $\text{d}^{-1}$  (at  $9\text{-}10^\circ\text{C}$ ). This is unlikely, but not impossible, as I found a maximum of 3 divisions  $\text{d}^{-1}$  for one ciliate at  $16^\circ\text{C}$  (Chapter 4).

These differences between the model output and field data do not diminish the likelihood that ciliate blooms exist or that they graze down phytoplankton blooms. The differences do suggest though, that blooms are more complex than the model simulates. Of some interest, and of possible consequence to aquaculture, is the observation that blooms of small phytoplankton and ciliates often occur in enclosures (Grice *et al.* 1980, Smetacek 1984, Sheldon 1986, Riemann *et al.* 1990, Turner and Granéli 1992, Granéli *et al.* 1993). Enclosures, by removing some physical and biological components (e.g. loss of ciliates through advection and mesozooplankton grazing), are simplifications of larger planktonic systems (Steele and Gamble 1982). Therefore, it is not surprising that ciliate blooms are seen in them. Since the aquaculture of marine organisms often employs small enclosures, such blooms might be expected there.

The primary goal of this dissertation was to substantiate the claim that planktonic ciliates bloom and graze down algal blooms over short periods. This section has indicated that ciliates can graze down prey populations. Below I show that these blooms occur over short periods of several days.

## 2.2 Ciliates Can Bloom Over 10 to 20 Day Periods

The model predicted that ciliate booms typically occurred over a 5-10 day period and were always less than 20 days, when the 3 ciliates (species A, B, C) were present at initial concentrations of  $0.3 \text{ mL}^{-1}$  (e.g. Fig. 9.3c-e). However, when only one species was

introduced (at  $1 \text{ mL}^{-1}$ , see section 2.4), some blooms developed after 20 days. Typically, blooms after 20 days occurred when there were low initial algal and low copepod conditions (under these conditions net algal growth was not limited by copepod grazing, but the initial concentrations were insufficient to immediately stimulate rapid ciliate growth). When blooms occurred after 20 days, I did not consider them to be plausible, as conditions, not accounted for in the model, would likely occur (e.g. mixing events, Mackas *et al.* 1985 and copepod growth and migration, Raymont 1983).

Blooms of ciliates often do occur over 10 to 20 days: natural populations of small autotrophic flagellates and the ciliate *Strobilidium* (= *Lohmanniella*) were placed in  $1 \text{ m}^3$  containers, and over 6 days the ciliates bloomed, grazed down the flagellates and then died (Smetacek 1984); a 16-32 day cycle of ciliates and flagellates existed in the Mediterranean Sea (Ibanez and Rassoulzadegan 1977); and ciliate peaks followed heterotrophic flagellate peaks within 4-6 days in Danish coastal waters (Andersen and Sorensen 1986). These studies were only able to establish such relationships by sampling every 1-2 days. Unfortunately, logistic and financial constraints limit most field studies to less regular sampling. For instance, although peaks of ciliates and small phytoplankton occurred in Sechart Inlet (Appendix 3), the monthly to weekly sampling did not provide information on the formation of these blooms. The model and field data indicate that ciliates can bloom over <20 day periods. As will be shown below, ciliate blooms may be important in the transfer of carbon to upper trophic levels. Therefore, sampling regimes should be designed to capture these short blooms. This would likely require daily sampling.

### **2.3 Ciliates Are Both a Link and Sink, and Ciliates Can Compete With Copepods**

For the last two decades it has been argued that microzooplankton (20-200  $\mu\text{m}$ ) can be an important link between nanoplankton (2-20  $\mu\text{m}$ ) and mesozooplankton (>200  $\mu\text{m}$ ) (e.g. Pomeroy 1974, Porter *et al.* 1979, Gifford and Dagg 1988, 1991). However, this paradigm does not consider that ciliates can bloom in the fashion described above. This was possibly an oversight, as considerable production occurs during ciliate-nanoplankton blooms (see below),

and ciliates are probably not important in food webs at "typical" concentrations of food and copepods (see above).

Ciliates may not be a link if they graze down their prey and die (due to starvation), before they are captured by mesozooplankton. As was shown in previous chapters, planktonic ciliates do not survive when food concentrations are low. The half life of ciliate cultures in the absence of food is generally much less than 1 d (Chapters 3-7, Wickham *et al.* 1993). Using the model, I have examined the effect of different copepod concentrations and initial algal concentrations on carbon flow in the food web depicted in Fig. 9.1. The simulations for this analysis were conducted with an initial ciliate concentration of  $0.3 \text{ mL}^{-1}$  of each of the three ciliates (A, B, and C) and the parameters described in section 1.0. Since the outcome of the model was affected by both the proportion of the different ciliates initially introduced (see section 9.2.4) and variation in algal growth rate (data not shown) the following analysis would not apply to all situations. However, it does illustrate the general response of ciliates to average conditions.

As was shown above (Fig. 9.2), ciliate blooms occurred when copepods were rare and/or initial algal concentrations were high. Under these conditions, both ciliate and primary production were also high (Figs. 9.3e, 9.4), and the majority of algae were consumed by ciliates (Figs. 9.3e, 9.5a and b). In contrast, at high copepod concentrations and/or low initial algal concentrations the majority of algae were consumed by copepods (Fig. 9.5a and b). Between these two extremes there was an abrupt transition (Fig. 9.5a and b): the point where copepod grazing became insufficient to deplete phytoplankton to the copepod threshold concentration of  $\sim 800 \text{ cells mL}^{-1}$  (Table 9.1). Thus, under some conditions ciliate populations had a greater impact than copepod populations on small phytoplankton (Fig. 9.3 cf. a and b vs. c and e). This is also illustrated in Fig 9.6, where at low copepod and/or high algal conditions, ciliates consumed more of the algae than copepods, over the 20 day period. However, the ciliates may then have been eaten by the copepods and are therefore not simply competitors.

At high copepod concentrations and/or low initial algal concentrations, ciliate production was low (Fig. 9.4a), but the majority of ciliates produced were consumed by copepods (Fig. 9.5c). In contrast, at low copepod concentrations and/or high initial algal concentrations (bloom conditions where ciliate production was high, Figs. 9.2, 9.4a) the majority of ciliates died (due to starvation, e.g. Fig. 9.3e) without being consumed by copepods (Fig. 9.5c). This is also illustrated in Fig. 9.6a, where the number of ciliates ingested by the copepod population decreased at low copepod concentrations, but ciliate production remained high (Fig. 9.4a). Not surprisingly, the proportion of ciliate carbon transferred to upper trophic levels decreased as the number of copepods decreased.

However, during bloom conditions, ciliates were a link in the transfer of carbon to copepods: at low copepod concentrations and high initial algal concentrations, 40 to 50% of the carbon ingested by copepods was from ciliates (Fig. 9.5d). Gifford and Dagg (1988) also found that when ciliates were abundant, they constituted a significant fraction of the diet of the copepod *Acartia tonsa*, even though phytoplankton were also abundant. In contrast, at high copepod concentrations and low initial algal concentrations, virtually all the carbon ingested by copepods was from phytoplankton (Fig. 9.5d).

In summary, under ciliate bloom conditions in the model ciliates were a link, providing 40-50% of the carbon available to copepods (Fig. 9.5d). It was only when copepods were abundant and initial algal levels were low that ciliates were not an important carbon source. Field data support these conclusions: after a storm, in coastal waters off Denmark, where mixing caused increased primary production of the  $< 11 \mu\text{m}$  fraction, ciliate abundance remained between  $0.05\text{-}0.3 \text{ mL}^{-1}$  (Nielsen and Kiorboe 1991). This low ciliate abundance was attributed to the high mesozooplankton abundance ( $5\text{-}10 \text{ L}^{-1}$ ). However, in other Danish coastal waters, where copepod abundance is typically low (often  $< 1 \text{ L}^{-1}$ , Blanner 1982), there were ciliates blooms of up to  $160 \text{ mL}^{-1}$  (Andersen and Sorensen 1986). In another case, the copepod *Neocalanus plumchrus* was an efficient grazer of  $2\text{-}30 \mu\text{m}$  phytoplankton and, at densities of  $1 \text{ animal L}^{-1}$  it was able to control small ( $4\text{-}10 \mu\text{m}$ ) phytoplankton over 6 day incubations (Landry and Lehner-Fournier 1988). But, in the open Pacific ocean, where this

study was conducted, *N. plumchrus* is likely not to be abundant enough to control phytoplankton, as it was typically found at concentrations of  $0.2 \text{ L}^{-1}$  (Landry and Lehner-Fournier 1988). Thus, as suggested by others (e.g. Frost 1987, Strom and Welschmeyer 1991), this is a region where microzooplankton may be important grazers. A study in mesocosms also indicated that when copepods were less abundant (due to introduction of a planktivorous fish), flagellates and then ciliates began to bloom over 10 days (Granéli *et al.* 1993).

Under "typical" coastal conditions ( $10^3$  algae  $\text{mL}^{-1}$  and 1 copepod  $\text{L}^{-1}$ ), the model indicated that ciliates act as a link (Figs. 9.3a, 9.5d), but under these "typical" conditions there was little primary production, as a low phytoplankton biomass was maintained by copepod grazing (see Fig. 9.3a, 9.4b). This supports the view that on average, ciliates are not an important component of coastal planktonic systems (Banse 1982, Montagnes *et al.* 1988a).

Although ciliates were a link under bloom conditions, a large proportion of the ciliates died of starvation in post-bloom conditions and were therefore not available to mesozooplankton (Fig. 9.3a, 9.5c). Incidental observations from my experiments (Chapters 3-7) suggest that starved and dead ciliates do not remain intact (data not shown). If this is so, ciliates would not sink from the water column and would fuel the microbial loop, remineralizing nutrients to the primary producers (Azam *et al.* 1983).

## 2.4 Species Differences Are Important

In the model, when the initial concentration of the 3 ciliates was kept constant (1:1:1, at  $0.3$  ciliates  $\text{mL}^{-1}$ ), variations of both initial algal and invariant copepod concentrations caused changes in the species composition of the blooms (Fig. 9.2). For instance, when copepods were rare and algae abundant, ciliates A and B both bloomed and had similar peak abundances, but at slightly lower algal concentrations only ciliate A bloomed (Fig. 9.2a and b). When only one species was introduced into the model, the species differences were more pronounced (Fig. 9.7); examples of these are illustrated in Fig. 9.8. Ciliate C was an exceptional example of these differences: it reaches peak abundances of only  $6 \text{ mL}^{-1}$  when the other two species were present, but it bloomed to  $500 \text{ mL}^{-1}$  when introduced alone (Fig. 9.2,

9.7b). These differences in model results were caused by differences in threshold concentrations, half-saturation constants, and maximum rates of the 3 ciliates (Table 9.1) and illustrate the uniqueness of species specific responses. As mentioned above, the values of ciliate abundance may be unreasonably high, but the relative differences between the results is instructive: the abundance of species in a bloom is affected by the type and relative proportion of ciliates encountering the phytoplankton bloom.

Bloom dynamics and the flow of carbon through the food web also depended on the ciliate species present. Examples of these differences are depicted in Fig. 9.8. For instance, when only ciliate A was present or it was present in equal concentrations with the other two species (Fig. 9.8a and d), primary production was low, and copepods consumed a relatively large portion of the ciliates. However, when only ciliates B or C were present, primary production was high, relatively few of the ciliates were eaten by copepods, and many of the ciliates died due to starvation when algae were depleted (Fig 9.8b and c).

In summary, the differences between numerical responses, presented in Chapter 8, can be of consequence in terms of ciliate bloom dynamics and carbon flow. Such differences are likely species dependent (see Chapters 2 and 8). Thus, both species-level analysis of field samples and laboratory examination of species differences will be warranted if we wish to understand the range of influence that ciliates could have on planktonic food webs. An obvious corollary to this is that we must also continue taxonomic studies on oligotrichs, which are still a poorly studied group of organisms (Martin and Montagnes 1993).

## **2.5 How Ciliate Blooms Influence Carbon Flow to Copepods**

Ciliate blooms occur when there were initially many algae and copepods were rare (see above). The model provided an indication of the flow of carbon through the food web and can offer some information on the relative importance of ciliate blooms.

Under bloom conditions, both ciliate and algal production, over a 20 day period, increased from non-bloom conditions by an order of magnitude (Figs. 9.3, 9.4). At the region where both algae and ciliate production begin to increase (Fig. 9.4a and b), the carbon flow (total, ciliate, or algae) to the copepod population was maximized (Figs. 9.6a, 9.9a and c).



Thus, this transition region appears to be important in terms of maximum mesozooplankton production. However, the maximum benefit in terms of carbon ingestion by individual copepods lay in the entire region where ciliates bloomed (Figs. 9.9b and d). Therefore, during ciliate blooms the flow of carbon to individual copepods was high, even when copepod abundance was low. This suggests that while ciliate blooms do not enhance the production of mesozooplankton populations over short periods, they may be a food source for individuals. Thus, ciliate blooms which are <20 days may aid in the long term production of mesozooplankton.

The predictions of the model agree with field data. During a phytoplankton bloom, when copepods were abundant, copepods controlled the ciliate population, and ciliates contributed ~10% to the copepod diet (Nielsen and Kiorboe 1991). Under these conditions, ciliates were not a link between the microbial and classical (phytoplankton-copepod) food webs. A similar situation existed in coastal waters with the copepod *Acartia clausi* grazing on ciliates (Tiselius 1989): at low ciliate concentrations ( $< 1 \text{ mL}^{-1}$ ), ciliates were a minor component of the copepod's diet. However, in other coastal waters, where ciliates were abundant (as a result of grazing on nanoplankton) they were a significant portion of the diet of *Acartia tonsa* (Gifford and Dagg 1988). Similar results were also found in the North Bering/Chukchi Seas, where the link from nanoplankton to copepods, through ciliates, increased at regions of higher nanoplankton biomass (Andersen 1988). Thus, ciliates are not an important component of copepod production when nano-phytoplankton are rare, but they may be when these autotrophs bloom.

## CONCLUDING REMARKS

Assuming that the ciliates used in the model (Table 8.4, Fig. 8.7) are representative of coastal ciliates, the above analysis suggests that, over a 5-20 day period, ciliates can act as "bloom and bust" organisms in a "feast and famine" situation. During blooms the ciliates are able to graze down populations of small phytoplankton, and subsequently the ciliate population crashes due to predation by copepods and starvation. Ciliate blooms are a link in the flow of

carbon from phytoplankton to individual copepods but channel much of the carbon away from upper trophic levels. It also appears that the species composition of the ciliate assemblage can affect the bloom dynamics.

We must therefore rethink our understanding of ciliates in planktonic systems. They may not be a constant link between small phytoplankton and mesozooplankton, as previous analyses implied (e.g. Pomeroy 1974, Conover 1982, Laval-Peuto *et al.* 1986). Rather, they can be, under transient conditions, important as both links and sinks of carbon, but under "typical" coastal conditions ( $10^3$  algae  $\text{mL}^{-1}$  and 1 copepod  $\text{L}^{-1}$ ) ciliates may not be important components of food webs. One of the most important findings of my studies was that the threshold food concentration (where ciliates began to die due to starvation) was often higher than "typical" food concentrations (Chapter 8 and Appendix 3). This means that ciliates can not survive at "typical" concentrations and rely on patches and/or blooms of phytoplankton. The question then arises: how do ciliates survive between patches?

There are few data explaining how planktonic ciliates survive periods of starvation. My studies indicated that oligotrichs die within 2-3 days of starvation (Chapters 3-7), and at no time did these ciliates form resting cysts. However, tintinnids can form cysts (Reid and John 1978, 1983, Takahashi and Aizawa 1990) and naked oligotrichs may also (Reid 1987). It is surprising that encystment has never been reported for cultured planktonic oligotrichs. This is one area that requires more work if we are to understand the germination of ciliate blooms. Mixotrophy may also be a mechanism that allows some ciliates to survive periods of starvation, as they can derive nutrition from enslaved chloroplasts and may maintain them for hours to days (Stoecker and Silver 1990, Stoecker and Michaels 1991). Finally, micro-scale patchiness (Owen 1989) is another mechanism that may allow ciliates to survive between blooms. If phytoplankton are concentrated in small patches (centimeters to meters), then ciliates may be moving from one patch to another. Such associations have been shown for tintinnids and dinoflagellates (Stoecker *et al.* 1984) and ciliates may migrate (Jonsson 1989). Again, this is an area that requires study.

There is also a lack of information on where ciliates go when they die. If after a bloom ciliates are not ingested by upper trophic levels (e.g. mesozooplankton), what is the fate of their biomass? There is good evidence that ciliates decrease in cell size as they starve (e.g. Lynn *et al.* 1987, Fenchel 1990). Thus, a substantial portion of ciliate biomass may be respired in post bloom periods, and ciliates would act as a carbon sink (i.e. a loss of carbon from the system). It is also possible that starved cells eventually lyse and their contents become available to bacterial degradation. Thus, ciliates blooms may contribute to the microbial loop (Azam *et al.* 1983). The fate of such blooms may be important in our understanding of carbon cycling, especially in regions like the subarctic Pacific where microzooplankton may be the dominant grazers.

Finally, now that I have supported the notion that ciliates can bloom, it would be constructive to investigate these blooms in the field. The problems with doing this are obvious: if ciliate blooms are transient and brief, then observing an entire bloom will require exhaustive sampling. My studies suggest ways to simplify such a search by narrowing the range of conditions where blooms should occur. Ciliates should bloom when: mesozooplankton are not abundant; small phytoplankton are abundant; conditions allow small phytoplankton to bloom; and lack of mixing processes provide stable conditions over 1-3 weeks. Where are these places? Ciliate blooms should occur in small embayments and inlets where there is little mixing but nutrient enrichment may occur, either through periodic mixing or allochthonous processes. Blooms may also occur in enclosures such as aquaculture tanks or experimental mesocosms. Finally, blooms may occur in the open water column if conditions allow for patches in the 100 m to 10 km range, which persist for days to weeks. Such patches could, for instance, be caused by fronts or vertical shear (Haury *et al.* 1978, Mackas *et al.* 1985). Daily examination of ciliate distributions over several weeks may reveal that ciliate blooms are in fact a regular but ephemeral occurrence in many planktonic systems.

Table 9.1. Parameters and variables used in the model of ciliate-phytoplankton (algal) interactions.

Parameter in model	Value	Units	Description
dt	0.05	days	time step
Ciliates			
P1	0.99	d <sup>-1</sup>	Ciliate A, maximum growth rate ( $\mu_{\max}$ )
P2	380	algae mL <sup>-1</sup>	Ciliate A, growth threshold concentration (x)'
P3	921	algae mL <sup>-1</sup>	Ciliate A, growth half-saturation constant (k)
P4	1.85	d <sup>-1</sup>	Ciliate B, maximum growth rate ( $\mu_{\max}$ )
P5	13014	algae mL <sup>-1</sup>	Ciliate B, growth threshold concentration (x)'
P6	24436	algae mL <sup>-1</sup>	Ciliate B, growth half-saturation constant (k)
P7	0.72	d <sup>-1</sup>	Ciliate C, maximum growth rate ( $\mu_{\max}$ )
P8	3105	algae mL <sup>-1</sup>	Ciliate C, growth threshold concentration (x)'
P9	8143	algae mL <sup>-1</sup>	Ciliate C, growth half-saturation constant (k)
P10	0.8	CO <sub>2</sub> /O <sub>2</sub>	respiratory quotient for ciliates
P11	0.75	none	assimilation efficiency for ciliates
P12	0.7	d <sup>-1</sup>	algal growth rate ( $\mu$ )
Copepod			
	3312000	algae d <sup>-1</sup> copepod <sup>-1</sup> day <sup>-1</sup>	the maximum grazing rate on the algae
	767	algae mL <sup>-1</sup>	the grazing threshold concentration for the algae (x)'
	785	algae mL <sup>-1</sup>	the grazing half-saturation constant for the algae (k)
	30000	ciliates d <sup>-1</sup> copepod <sup>-1</sup> day <sup>-1</sup>	the maximum grazing rate on ciliate C
	100	algae mL <sup>-1</sup>	the grazing half-saturation constant for ciliate C (k)
	14400	ciliates d <sup>-1</sup> copepod <sup>-1</sup> day <sup>-1</sup>	the maximum grazing rate for ciliates A and B
	45	algae mL <sup>-1</sup>	the grazing threshold concentration for ciliates A and B (x)'
	921	algae mL <sup>-1</sup>	the grazing half-saturation constant for the algae (k)
Variables in model	Range	Units	Description
x1	50-25x10 <sup>3</sup>	# mL <sup>-1</sup>	initial algal concentration
x2	0-1	# mL <sup>-1</sup>	initial concentration of ciliate A
x3	0-1	# mL <sup>-1</sup>	initial concentration of ciliate B
x4	0-1	# mL <sup>-1</sup>	initial concentration of ciliate C
zoo	0.01-5	# L <sup>-1</sup>	invariant copepod concentration

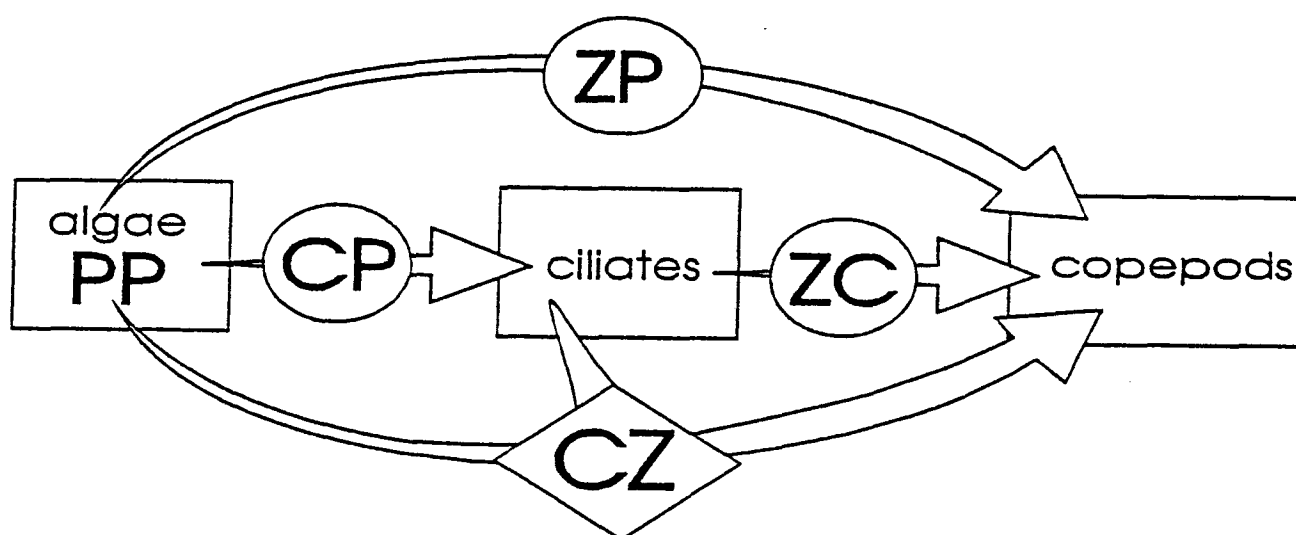


Fig. 9.1. A schematic diagram of the model described in Appendix 4. There are five types of organisms in the model: small ( $8\ \mu\text{m}$ ) phytoplankton (algae), ciliate species A, B, C, (see Table 8.4, Fig. 8.7) and a copepod species (data obtained from Frost, 1972 for *Calanus pacificus*). During the 20 day simulation, the algae had a constant growth rate of  $\mu = 0.7\ \text{d}^{-1}$  (but see text). Algal mortality was by predation from the ciliates and the copepod. Ciliate growth rates were functions of algal concentration. For all three ciliates, mortality was due to starvation and to predation by the copepod. There was no growth or mortality of the copepods over the simulation period. Four calculations of carbon transfer, over the 20 day simulation period, are presented in subsequent examples of this diagram (Figs 9.3 and 9.8). These values were determined from the integrated production (carbon  $\text{time}^{-1}$ ) over the 20 day simulation. They are represented here as: PP, the amount of autotrophic carbon produced; ZP, the percentage of autotrophic carbon produced that was consumed by the copepods; CP, the percentage of autotrophic carbon produced that was consumed by the ciliates; ZC, the percentage of ciliate carbon produced that was consumed by the copepods; and CZ, the percentage of the copepod diet contributed by ciliates (i.e. ciliate carbon ingested / [ciliate carbon ingested + algae carbon ingested]).

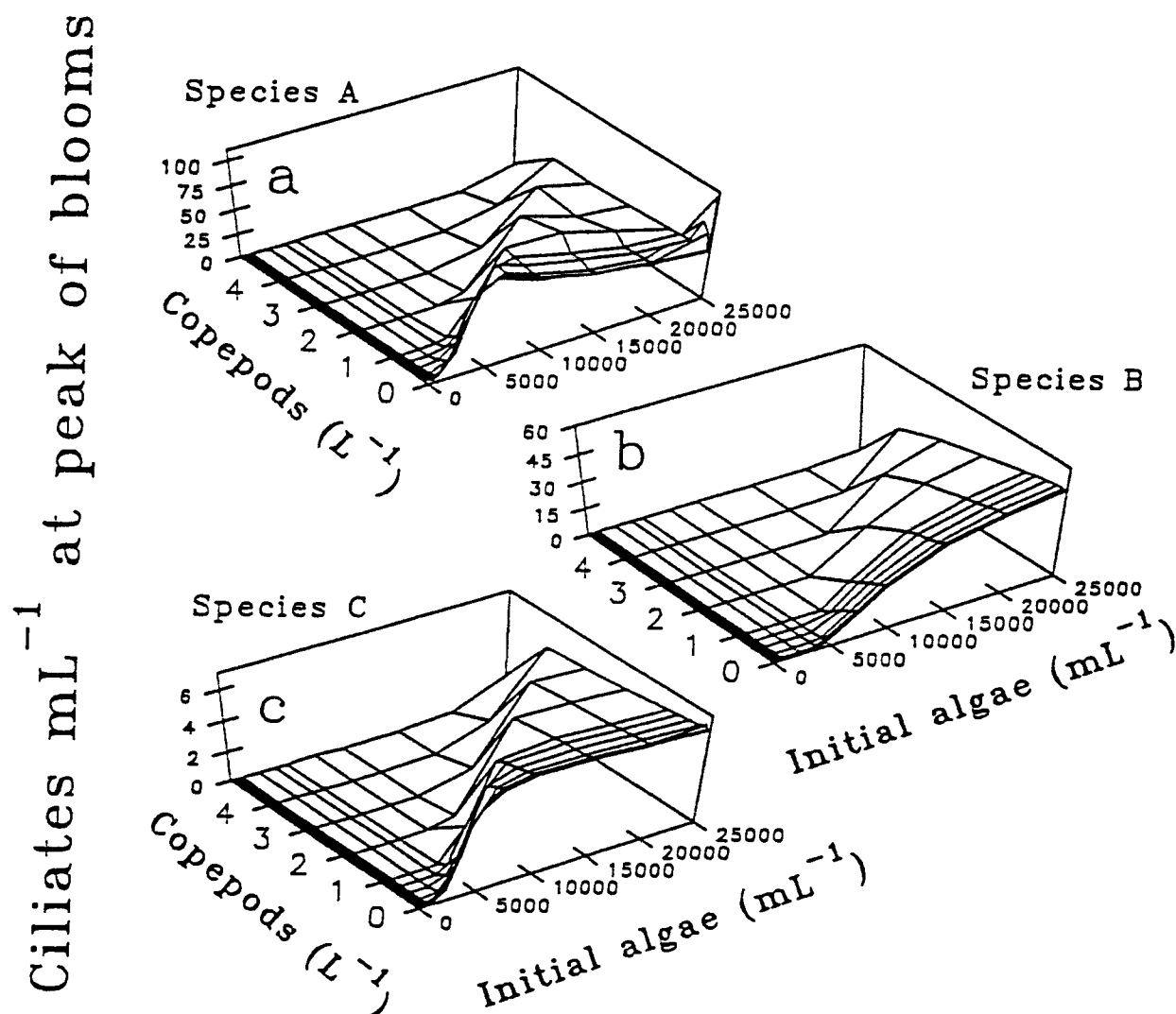


Fig. 9.2. Output from the model of ciliate-phytoplankton dynamics (Appendix 4): the effect of variations in initial algal concentration and constant copepod abundance (i.e. it did not change during the simulation) on the formation and peak magnitude of ciliate blooms. a, b, c, peak numbers of ciliates A, B, and C, respectively (Table 8.4), respectively. All the simulations for these panels were initiated with a total of  $0.9 \text{ ciliates mL}^{-1}$  ( $0.3$  of each ciliate). The initial algal concentration was varied from  $25$  to  $2.5 \times 10^4 \text{ mL}^{-1}$  and the constant copepod abundance was varied from  $0.025$  to  $5 \text{ L}^{-1}$ .

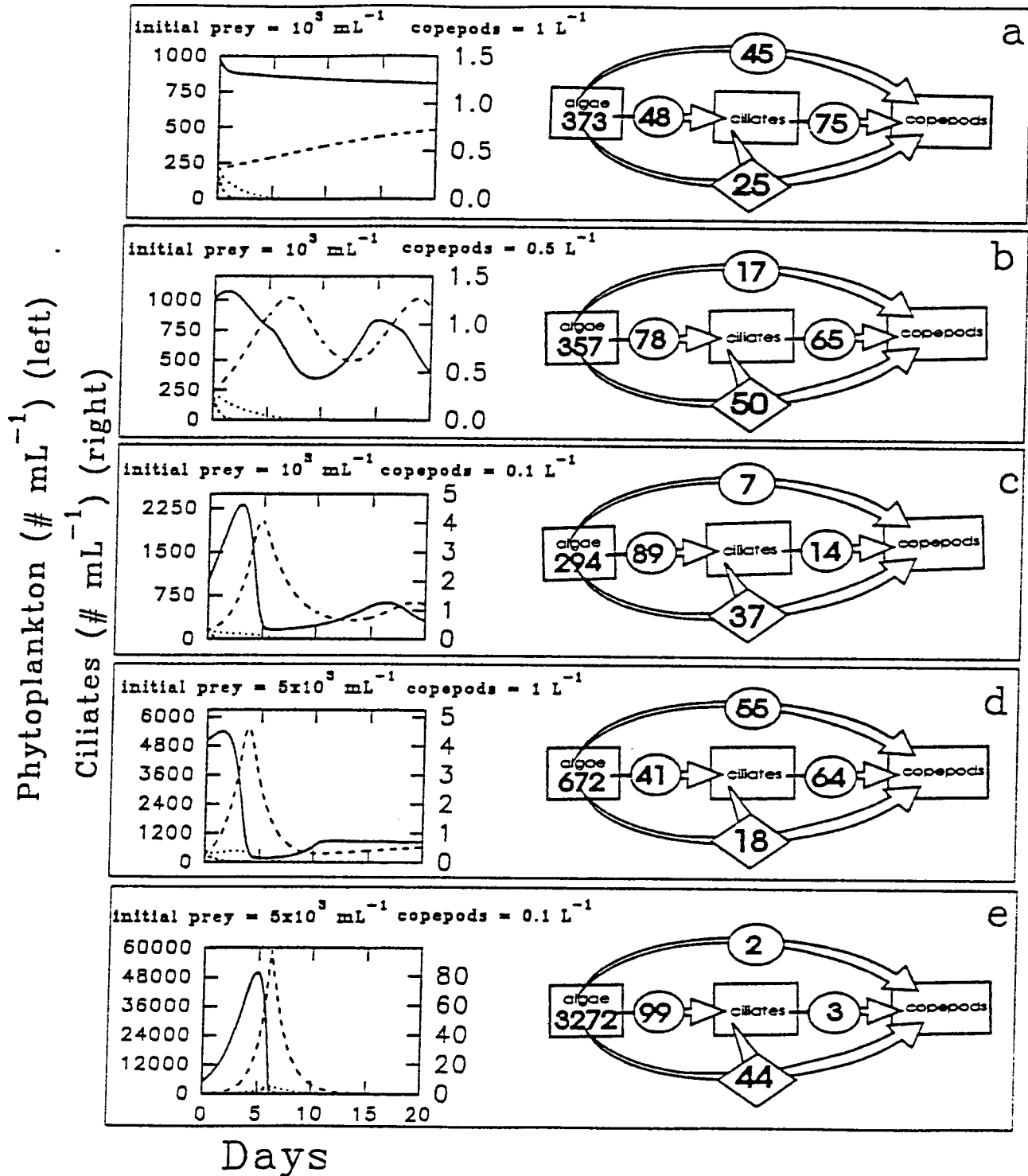


Fig. 9.3. Output from the model of ciliate-phytoplankton dynamics (Appendix 4): five examples of bloom development over 20 days and the flow of carbon during those 20 days: a, initial algal concentration =  $10^3 \text{ mL}^{-1}$  and constant copepod concentration =  $1 \text{ L}^{-1}$ ; b, initial algal concentration =  $10^3 \text{ mL}^{-1}$  and constant copepod concentration =  $0.5 \text{ L}^{-1}$ ; c, initial algal concentration =  $10^3 \text{ mL}^{-1}$  and constant copepod concentration =  $0.1 \text{ L}^{-1}$ ; d, initial algal concentration =  $5 \times 10^3 \text{ mL}^{-1}$  and constant copepod concentration =  $1 \text{ L}^{-1}$ ; e, initial algal concentration =  $5 \times 10^3 \text{ mL}^{-1}$  and constant copepod concentration =  $0.1 \text{ L}^{-1}$ . Phytoplankton, solid line. Ciliate A, large dashed line. Ciliate B, small dashed line. Ciliate C, dotted line. All the simulations for these panels were initiated with a total of  $0.9 \text{ ciliates mL}^{-1}$  ( $0.3$  of each ciliate). The calculation of values in circles, ovals, and diamonds are described in Fig 9.1.

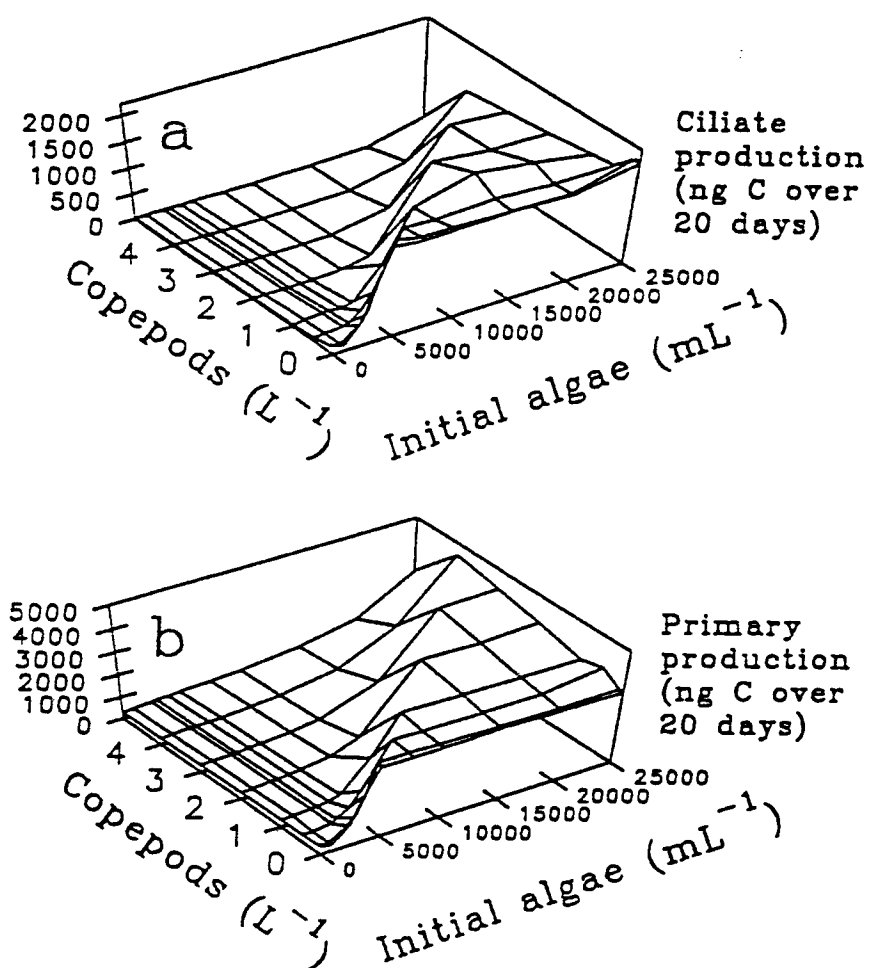


Fig. 9.4. Output from the model of ciliate-phytoplankton dynamics (Appendix 4): the effect of variations of initial algal concentration and constant copepod abundance on 2 bloom parameters: a, gross ciliate (ng C) production over the 20 day simulation and b, gross primary (algae) production (ng C) over the 20 day simulation. The simulations for these panels were initiated with a total of  $0.9 \text{ ciliates } mL^{-1}$  (0.3 of each ciliate). The initial algal concentration was varied from 100 to  $2.5 \times 10^4 \text{ mL}^{-1}$  and the constant copepod abundance was varied from 0.01 to  $5 \text{ L}^{-1}$ .



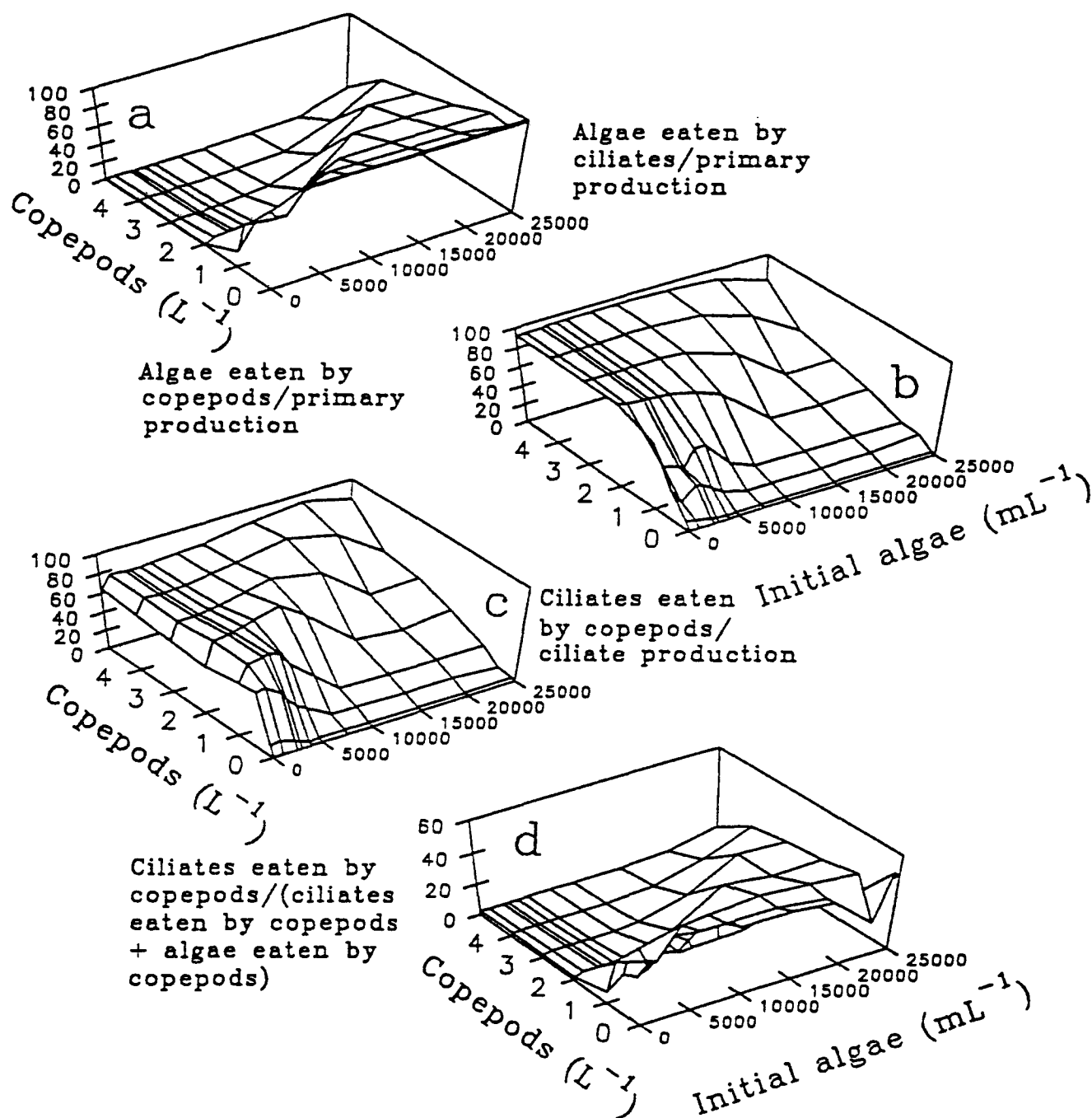


Fig. 9.5. Output from the model of ciliate-phytoplankton dynamics (Appendix 4): the effect of variations in initial algal concentration and constant copepod abundance on 4 bloom parameters measured over the 20 day simulation: a, (algal carbon consumed by copepods)/(algal carbon produced); b, (algal carbon consumed by ciliates)/(algal carbon produced); c (ciliate carbon consumed by copepods)/(ciliate carbon produced); d, (ciliate carbon consumed by copepods)/(ciliate carbon consumed by copepods + algal carbon consumed by copepods). All the simulations for these panels were initiated with a total of  $0.9 \text{ ciliates mL}^{-1}$  (0.3 of each ciliate). All production and consumption measurements are the integrated value over the 20 day simulation. The initial algal concentration was varied from 100 to  $2.5 \times 10^4 \text{ mL}^{-1}$  and the constant copepod abundance was varied from 0.01 to  $5.0 \text{ L}^{-1}$ .

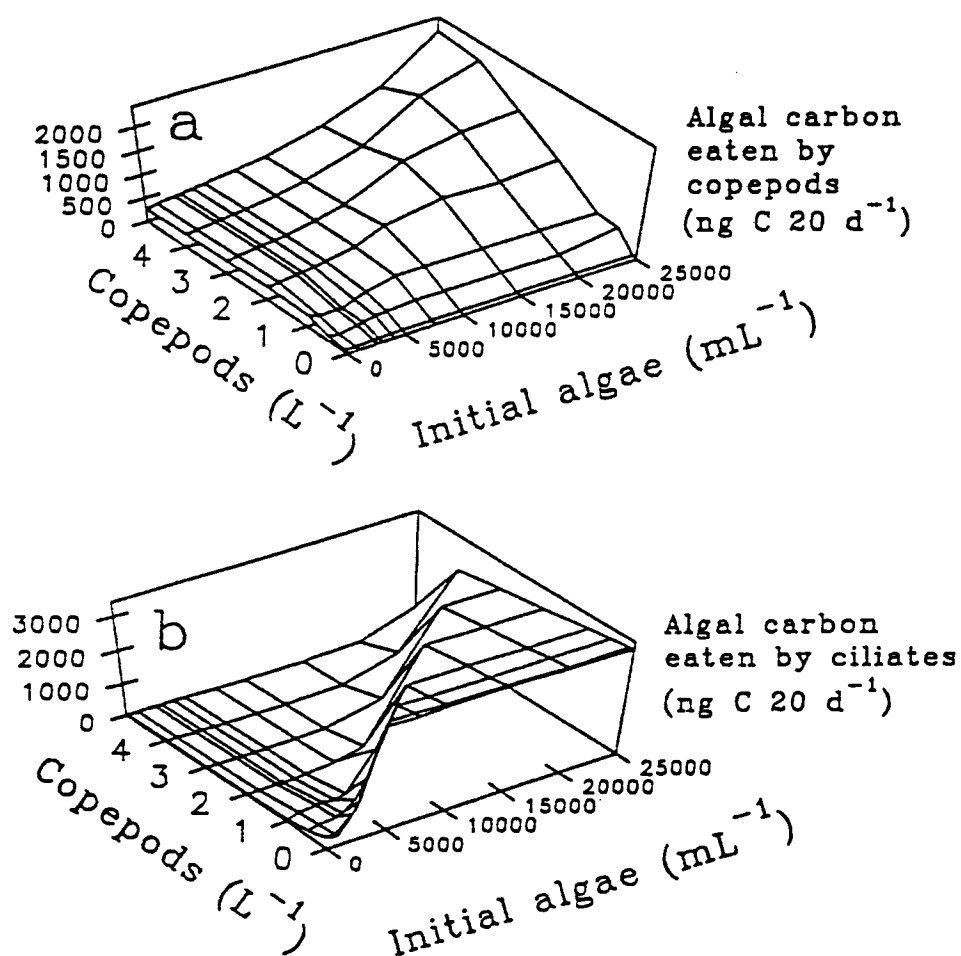


Fig. 9.6. Output from the model of ciliate-phytoplankton dynamics (Appendix 4): the effect of variations in initial algal concentration and constant copepod abundance on 2 bloom parameters: a, algal carbon (ng) eaten by copepods over the 20 day simulation and b, algal carbon (ng) eaten by ciliates over the 20 day simulation. The simulations for these panels were initiated with a total of  $0.9 \text{ ciliates mL}^{-1}$  (0.3 of each ciliate). The initial algal concentration was varied from 100 to  $2.5 \times 10^4 \text{ mL}^{-1}$ , and the constant copepod abundance was varied from 0.01 to  $5 \text{ L}^{-1}$ .

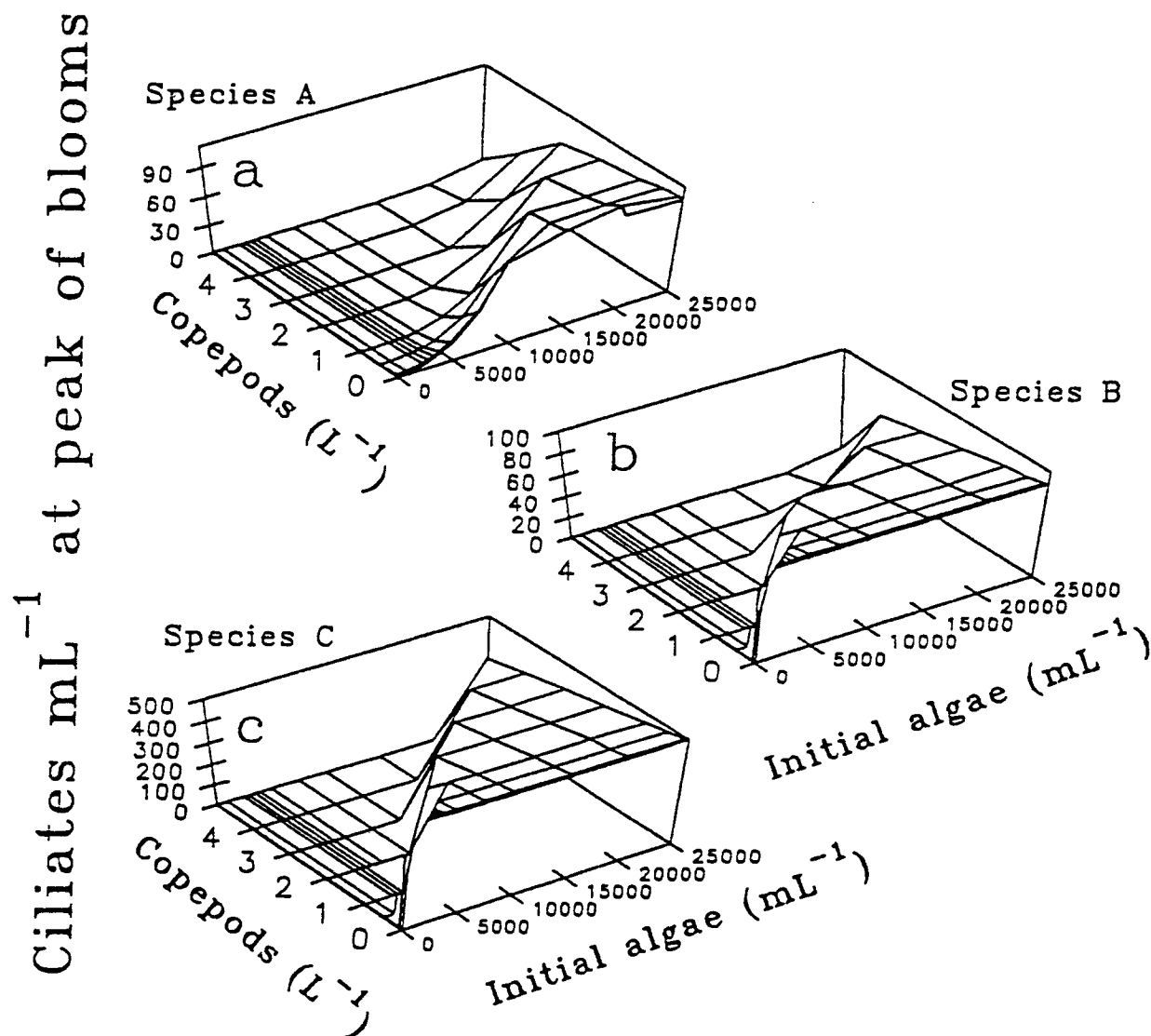


Fig. 9.7. Output from the model of ciliate-phytoplankton dynamics (Appendix 4): the effect of variations in initial algal concentration and constant copepod abundance on the formation and peak magnitude of ciliate blooms when only one species (A, B, or C, Table 8.4) was included in the model: a, only ciliate A present; b, only ciliate B present; c, only ciliate C present. All three simulations were initiated with an algal concentration of  $25 \times 10^3$  mL<sup>-1</sup> and one ciliate mL<sup>-1</sup>. A constant copepod concentration of  $0.5$  L<sup>-1</sup> was maintained throughout the simulations.

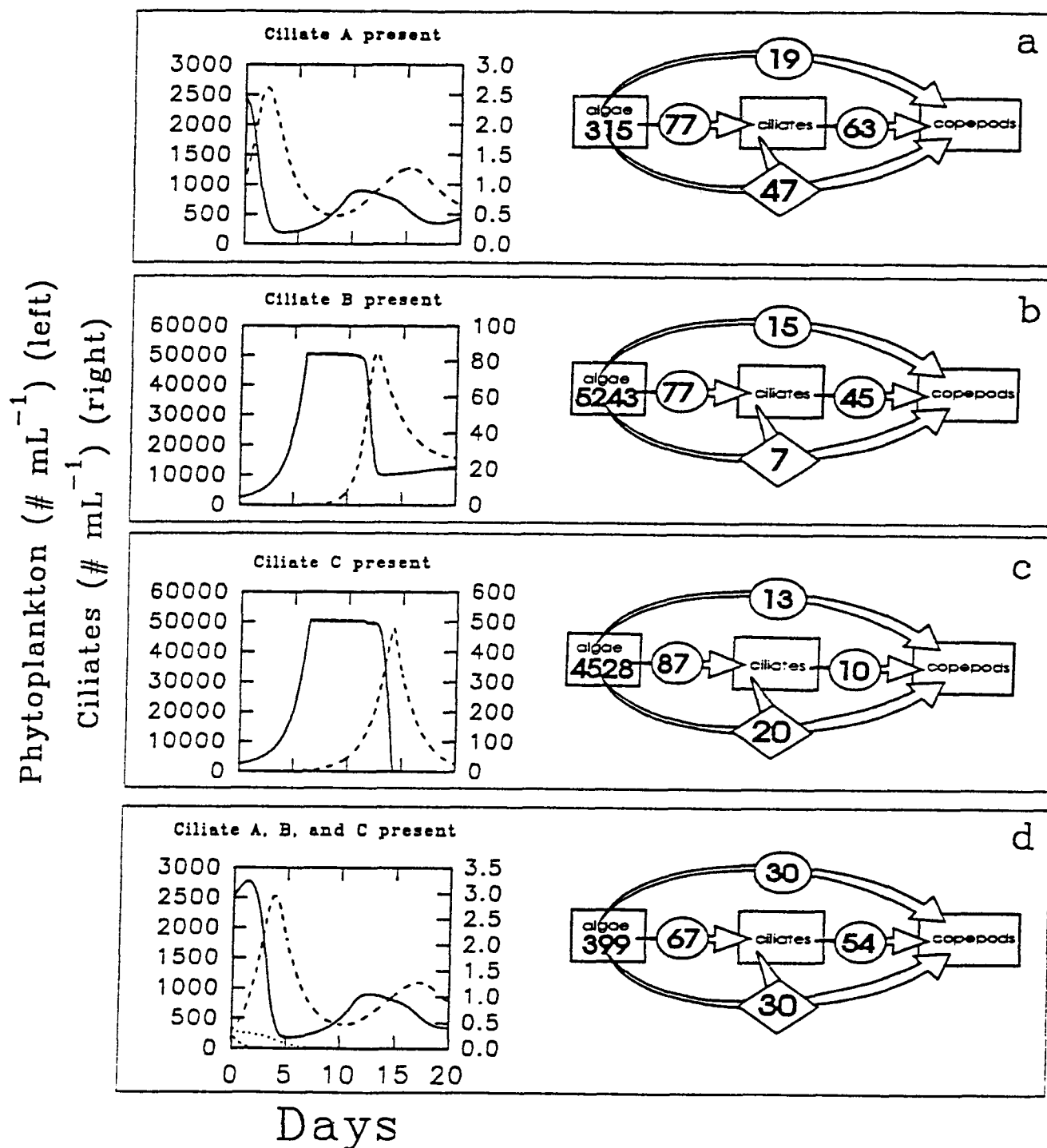


Fig. 9.8. Output from the model of ciliate-phytoplankton dynamics (Appendix 4): the effect of 3 ciliate species (A, B, and C, Table 8.4) on bloom development over 20 days and the flow of carbon during those 20 days: a, only ciliate A present; b, only ciliate B present; c, only ciliate C present; d, ciliates A, B, and C present. For panels a-c dashed lines are ciliates. For all panels solid lines are algae. For panel d: ciliate A, large dashed line; ciliate B, small dashed line; and ciliate C, dotted line. All four simulations were initiated with an algal concentration of  $25 \times 10^3 \text{ mL}^{-1}$  and one ciliate  $\text{mL}^{-1}$  ( $0.333 \text{ mL}^{-1}$  of each ciliate in panel d). A constant copepod concentration of  $0.5 \text{ L}^{-1}$  was maintained throughout the simulations. The calculation of values in circles, ovals, and diamonds are described in Fig 9.1.

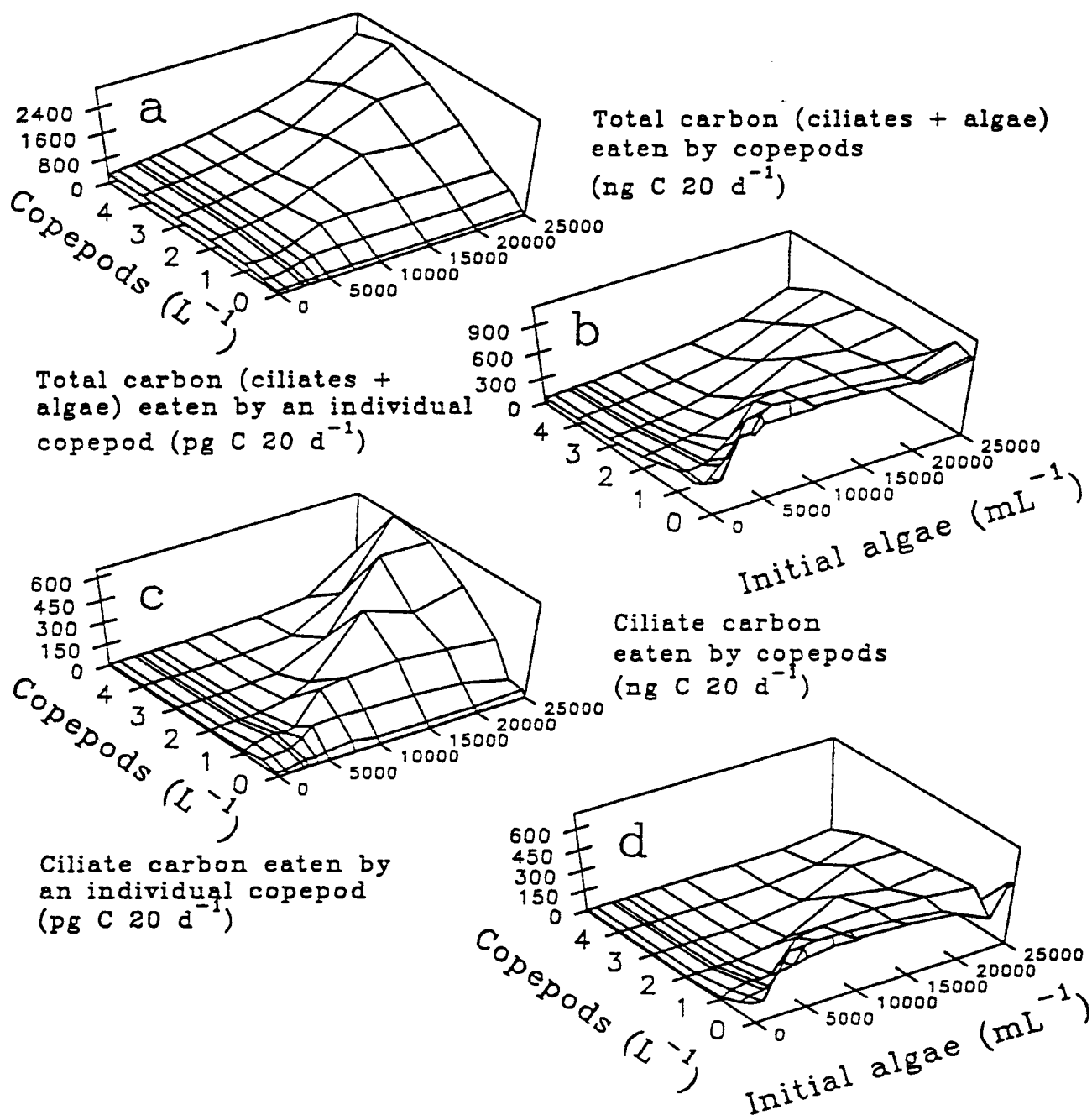


Fig. 9.9. Output from the model of ciliate-phytoplankton dynamics (Appendix 4): the effect of initial algal concentration and constant copepod abundance on 4 bloom parameters: a, total (algae + ciliates) carbon (ng) eaten by copepods over the 20 day simulation; b, total (algae + ciliates) carbon (pg) eaten by an individual copepod over the 20 day simulation; c, ciliate carbon (ng) eaten by copepods over the 20 day simulation; d, ciliate carbon (pg) eaten by an individual copepod over the 20 day simulation. The simulations for these panels were initiated with a total of 0.9 ciliates mL<sup>-1</sup> (0.3 of each ciliate). The initial algal concentration was varied from 100 to 2.5 × 10<sup>3</sup> mL<sup>-1</sup>, and the constant copepod abundance was varied from 0.01 to 5 L<sup>-1</sup>.

## LITERATURE CITED

- Adl, S. M., Berger, J. D. (1991). Timing of oral morphogenesis and its relation to commitment to division in *Paramecium tetraurelia*. *Exp. Cell Res.* 192: 497-504
- Aelion, C. M., Chisholm, S. W. (1985). Effect of temperature on growth and ingestion rates of *Favella* sp. *J. Plank. Res.* 7: 821-830
- Andersen, P. (1988). The quantitative importance of the "microbial loop" in the marine pelagic: a case study from the North Bering/Chukchi seas. *Arch. Hydrobiol.* 31: 243-251
- Andersen, P., Sorensen, H. M. (1986). Population dynamics and trophic coupling in pelagic microorganisms in eutrophic coastal waters. *Mar. Ecol. Prog. Ser.* 33: 99-109
- Azam, F., Fenchel, T., Field, J. G., Gray, J. S., Meyer-Reil, L. A., Thingstad, F. (1983). The ecological role of water column microbes in the sea. *Mar. Ecol. Prog. Ser.* 10: 257-263
- Banse, K. (1982). Cell volume, maximal growth rates of unicellular algae and ciliates, and the role of ciliates in the marine pelagial. *Limnol. Oceanogr.* 27: 1059-1071
- Bell, G. (1988). *Sex and death in Protozoa*. Cambridge Univ. Press, Cambridge
- Bernard, C., Rassoulzadegan, F. (1990). Bacteria or microflagellates as a major food source for marine ciliates: possible implications for the microzooplankton. *Mar. Ecol. Prog. Ser.* 64: 147-155
- Berger, J. D. (1976). Gene expression and phenotypic change in *Paramecium tetraurelia* exconjugants. *Genet. Res. Camb.* 27: 123-134
- Blackbourn, D. J., Taylor, F. J. R., Blackbourn, J. (1973). Foreign organelle retention by ciliates. *J. Protozool.* 20: 286-288
- Blackbourn, D. J. (1974). The feeding biology of tintinnid protozoa and other inshore microzooplankton. Ph.D. thesis. Univ. British Columbia
- Blanner, P. (1982). Composition and seasonal variation of the zooplankton in the Limfjord (Denmark) during 1973-1974. *Ophelia* 21: 1-40
- Borsheim, K. Y., Bratbak, G. (1987). Cell volume to cell carbon conversion factors for a bacterivorous *Monas* sp. enriched from seawater. *Mar. Ecol. Prog. Ser.* 36: 171-175
- Buskey, E. J., Stoecker, D. K. (1988). Locomotory patterns of the planktonic ciliate *Favella* sp.: adaptations for remaining within food patches. *Bull. Mar. Sci.* 43: 783-796
- Buskey, E. J., Stoecker, D. K. (1989). Behavioral responses of the marine tintinnid *Favella* sp. to phytoplankton: influence of chemical, mechanical and photic stimuli. *J. Exp. Biol. Ecol.* 132: 1-16
- Capriulo, G. M. (1990). Feeding-related ecology of marine protozoa. In: Capriulo, G. M. (ed.) *Ecology of marine protozoa*. Oxford Univ. Press, Oxford, p. 186-259
- Caron, D. A., Goldman, J. C. (1990). Protozoan nutrition regeneration. In: Capriulo, G. M. (ed.) *Ecology of marine protozoa*. Oxford Univ. Press, Oxford, p. 283-306

- Caron, D. A., Goldman, J. C., Fenchel, T. (1990) Protozoan respiration and metabolism. In: Capriulo, G. M. (ed.) Ecology of marine protozoa. Oxford Univ. Press, Oxford, p. 307-322
- Caron, D. A., Goldman, J. C. (1993). Predicting excretion rates of protozoa: reply to comment by Landry. *Limnol. Oceanogr.* 38: 472-474
- Condrey, R. E. (1982). Ingestion-limited growth of aquatic animals: the case for Blackman kinetics. *Can. J. Fish. Aquat. Sci.* 39: 1585-1595
- Condrey, R. E., Fuller, D. A. (1985). Testing equations of ingestion-limited growth. *Arch. Hydrobiol.* 21: 257-267
- Conover, R. J. (1982). Interrelations between microzooplankton and other organisms. *Ann. Inst. océanogr.* 58(S): 31-46
- Corliss, J. O. (1979). The ciliated protozoa: characterization, classification and guide to the literature, Second edition. Pergamon Press, London
- Corliss, J. O., Esser, S. C. (1974). Comments on the role of the cyst in the life cycle and survival of free living protozoa. *Trans. Am. Microsc. Soc.* 93: 578-593
- Dale, T., Dahl, E. (1987). Mass occurrence of planktonic oligotrichous ciliates in a bay in southern Norway. *J. Plank. Res.* 9: 871-879
- Fauré-Fremiet, E. (1924). Contributions à la connaissance des infusoires planktoniques. *Bulletin Biologique de la France et de la Belgique*, Supplement no. 6, p 1-171
- Fauré-Fremiet, E. (1969). Remarques sur la systématique des ciliés oligotrichida. *Protistologica* 5: 345-352
- Fenchel, T. (1982). Ecology of heterotrophic microflagellates. III. Adaptations to heterogeneous environments. *Mar. Ecol. Prog. Ser.* 9: 25-33
- Fenchel, T., Finlay, B. J. (1983). Respiration rates in heterotrophic, free-living protozoa. *Microb. Ecol.* 9: 99-122
- Fenchel, T. (1986). Protozoan filter feeding. In: J. O. Corliss, Patterson, D. J. (ed.) *Progress in Protistology* Vol. 1. Biopress Ltd., Bristol, p. 66-113
- Fenchel, T. (1987). Ecology of Protozoa, the biology of free-living phagotrophic protists. Springer-Verlag, New York
- Fenchel, T., (1990). Adaptive significance of polymorphic life cycles in Protozoa: responses to starvation and refeeding in two species of marine ciliates. *J. Exp. Mar. Biol. Ecol.* 136: 159-177
- Fenchel, T. Finlay, B. J. (1983). Respiration rates in heterotrophic, free-living protozoa. *Microb. Ecol.* 9: 99-122
- Fenchel, T., Jonsson, P. R. (1988). The functional biology of *Strombidium sulcatum*, a marine oligotrich ciliate (Ciliophora, Oligotrichina). *Mar. Ecol. Prog. Ser.* 48: 1-15
- Foissner, W., Skogstad, A., Pratt, J. R. (1988). Morphology and infraciliature of *Trochiliopsis australis* n. sp., *Pelagohalteria viridis* (Fromentel, 1876) n. g., n. comb., and *Strobilidium lacustris* n. sp. (Protozoa, Ciliophora). *J. Protozool.* 35: 489-497

- Frost, B. W. (1972). Effects of size and concentration of food particles on the feeding behavior of the marine planktonic copepod *Calanus pacificus*. *Limnol. Oceanogr.* 17: 805-815
- Frost, B. W. (1987). Grazing control of phytoplankton stock in the open subarctic Pacific Ocean: a model assessing the role of mesozooplankton, particularly the large calanoid copepods *Neocalanus* spp. *Mar Ecol. Prog. Ser.* 39: 49-68
- Frost, B. W., Franzen, N. C. (1992). Grazing and iron limitation in the control of phytoplankton stock and nutrient concentration: a chemostat analogue of the Pacific equatorial upwelling zone. *Mar. Ecol. Prog. Ser.* 83: 291-303
- Gallegos, C. L. (1992). Phytoplankton photosynthesis, productivity, and species composition in a eutrophic estuary: comparison of bloom and non-bloom assemblages. *Mar. Ecol. Prog. Ser.* 81: 257-267
- Gifford, D. J. (1985). Laboratory culture of marine planktonic oligotrichs (Ciliophora, Oligotrichida). *Mar. Ecol. Prog. Ser.* 23: 257-267
- Gifford, D. J. (1988). Impact of grazing by microzooplankton in the Northwest arm of Halifax Harbour, Nova Scotia. *Mar. Ecol. Prog. Ser.* 47: 249-258
- Gifford, D. J., Dagg, M. J. (1988). Feeding of the estuarine copepod *Acartia tonsa* Dana: carnivory vs. herbivory in natural microplankton assemblages. *Bull. Mar. Sci.* 43: 458-468
- Gifford, D. J., Dagg, M. J. (1991). The microzooplankton- mesozooplankton link: consumption of planktonic protozoa by the calanoid copepods *Acartia tonsa* Dana and *Neocalanus plumchrus* Murukawa. *Mar. Microb. Food Webs* 5: 161-177
- Granéli, E., Olsson, P., Carlsson, P., Granéli, W., Nylander, C. (1993). Weak "top-down" control of dinoflagellate growth in the coastal Skagerrak. *J. Plank. Res.* 15: 213-237
- Grice, G. D., Harris, R. P., Reeve, M. R., Heinbokel, J. F., Davis, C. O. (1980). Large-scale enclosed water column ecosystems. An overview of foodweb I, the final CEPEX experiment. *J. mar. biol. Ass. U.K.* 60: 401-414
- Grim, J. N. (1987). The kinetid structures of the Choreotrichous ciliate *Strobilidium velox* and an assessment of its evolutionary lineage. *J. Protozool.* 34: 117-123
- Gold, K. (1970). Cultivation of marine ciliates (Tintinnida) and heterotrophic flagellates. *Helgoländer wiss. Meeresunters* 20: 264-271
- Gonzalez, J. M., Sherr, E. B., Sherr, B. F. (1990). Size-selective grazing on bacteria by natural assemblages of estuarine flagellates and ciliates. *App. Environ. Microbiol.* 56: 583-589
- Guillard, R. L., Ryther, J. H. (1962). Studies of marine planktonic diatoms, I. *Cyclotella nanna*, and *Detonula confervacea* (Cleve) Gran. *Can. J. Microbiol.* 8: 229-239
- Haigh, R., Taylor, F. J. R., Sutherland, T. E. (1992). Phytoplankton ecology of Sechart Inlet, a fjord system on the British Columbia coast. I. General features of the nano- and microplankton. *Mar. Ecol. Prog. Ser.* 89: 117-134
- Harris, G. P. (1980). Temporal and spatial scales in phytoplankton ecology. Mechanisms, methods, models, and management. *Can. J. Fish. Aquat. Sci.* 37: 877-900



- Harris, G. P. (1986). *Phytoplankton ecology*. Chapman and Hall, New York
- Harrison, P. J., Waters, R. E., Taylor, F. J. R. (1980). A broad spectrum artificial medium for coastal and open ocean phytoplankton. *J. Phycol.* 16: 28-35
- Harrison, P. J., Fulton, J. D., Taylor, F. J. R., Parsons, T. R. (1983). Review of the biological oceanography of the Strait of Georgia: pelagic environment. *Can. J. Fish. Aquat. Sci.* 40: 1064-1094
- Harrison, P. J., Thompson, P. A., Calderwood, G. S. (1990). Effects of nutrient and light limitation on the biochemical composition of phytoplankton. *J. Appl. Phycol.* 2: 45-56
- Haury, L. R., McGowan, J. A., Wiebe, P. H. (1978). Patterns and processes in the time-space scales of plankton distributions. In: Steele, J. H. (ed.) *Spatial patterns in plankton communities*. Plenum Press, New York, p. 277-327
- Heinbokel, J. F. (1978). Studies on the functional role of tintinnids in the southern California Bight. I. Grazing and growth rates in laboratory cultures. *Mar. Biol.* 4: 177-189
- Holling, C. S. (1959). Some characteristics of simple types of predation and parasitism. *Can. Entomol.* 41: 385-399
- Ibanez, F., Rassoulzadegan, F. (1977). A study of the relationships between pelagic ciliates (Oligotrichina) and planktonic nanoflagellates of the neritic ecosystem of the Bay of Villefranche-Sur-Mer. Analysis of chronological series. *Ann. Inst. océanogr.* 53: 17-30
- Jackson, K. M., Berger, J. (1984). Survival of ciliated protozoa under starvation conditions and at low bacterial levels. *Microb. Ecol.* 10: 47-59
- Jackson, K. M., Berger, J. (1985). Survivorship curves of ciliate protozoa under starvation conditions and at low bacterial levels. *Protistologica* 21: 17-24
- Jerome, C. A., Montagnes, D. J. S., Taylor, F. J. R. (1993). The effect of the quantitative protargol stain and Lugol's and Bouin's fixatives on cell size: a more accurate estimate of ciliate species biomass. *J. Euk. Microbiol.* 40: 254-258
- Johannes, R. E. (1965). Influence of marine protozoa on nutrient regeneration. *Limnol. Oceanogr.* 10: 434-443
- Jonsson, P. R. (1986). Particle size selection, feeding rates and growth dynamics of marine planktonic oligotrichous ciliates (Ciliophora: Oligotrichina). *Mar. Ecol. Prog. Ser.* 33: 265-277
- Jonsson, P. R. (1989). Vertical distribution of planktonic ciliates- an experimental analysis of swimming behaviour. *Mar. Ecol. Prog. Ser.* 52: 39-53
- Jonsson, P. R., Tiselius, P. (1990). Feeding behaviour, prey detection and capture efficiency of the copepod *Acartia tonsa* feeding on planktonic ciliates. *Mar. Ecol. Prog. Ser.* 60: 35-44
- Kofoed, C. A., Campbell, A. S. (1939). Reports on the scientific results of the expedition to the eastern tropical Pacific. The Ciliates. The Tintinninoidea. *Bull. Mus. Comp. Zool., Harvard* 84: 1-473

- Krainer, K. H. (1991). Contributions to the morphology, infraciliature and ecology of the planktonic ciliates *Strombidium pelagicum* n. sp., *Pelagostrombidium mirabile* (Penard, 1916) n. g., n. comb., and *Pelagostrombidium fallax* (Zacharias, 1896) n. g., n. comb. (Ciliophora). Euro. J. Protistol. 27: 60-70
- Landry, M. R., Lehner-Fournier, J. M. (1988) Grazing rates and behaviors of *Neocalanus plumchrus*: implications for phytoplankton control in the subarctic Pacific. Hydrobiologia 167/168: 9-19
- Laval-Peuto, M., Brownlee, D. C. (1986). Identification and systematics of the Tintinnina (Ciliophora): evaluation and suggestions for improvement. Ann. Inst. océanogr. 62: 69-84
- Laval-Peuto, M., Heinbokel, J. F., Anderson, R. O., Rassoulzadegan, F., Sherr, B. (1986). Role of micro- and nanozooplankton in marine food webs. Insect Sci. Applic. 7: 387-395
- Laybourn-Parry, J. (1984). A functional biology of free-living protozoa. Univ. California Press, Berkeley
- Lee, J. J., Small, E. B., Lynn, D. H., Bovee, E. C. (1985). Some techniques for collecting, cultivating and observing protozoa. In: Lee, J. J., Hutner, S. H., Bovee, E. C. (ed.) An illustrated guide to the Protozoa. Soc. Protozool. Special Publ. Allen Press, Kansas, p. 1-7
- Leegaard, C. (1915). Untersuchungen über einige planktonciliaten des Meeres. Nyt Mag. f. Naturv. 53: 1-37
- Legendre, L. (1990). The significance of microalgal blooms for fisheries and for the export of particulate organic carbon in the oceans. J. Plank. Res. 12: 681-699
- Legovic, T. (1989). Predation in food webs. Ecol. Model. 48: 267-276
- Lochte, K. (1991). Protozoa as makers and breakers of marine aggregates. In: Reid, P. C., Turley, C. M., Burkill, P. H. (ed.) Protozoa and their role in marine processes, NATO ASI publication, Springer Verlag, New York, p. 237-246
- Lynn, D. H. (1975). The life cycle of the histophagous ciliate *Tetrahymena corlissi* Thompson, 1955. J. Protozool. 22: 188-195
- Lynn, D. H., Montagnes, D. J. S., Riggs, W. (1987). Divider size and the cell cycle after prolonged starvation of *Tetrahymena corlissi*. Microb. Ecol. 13: 115-127
- Lynn, D. H., Montagnes, D. J. S. (1988). Taxonomic description of some conspicuous species of Strobilidiine ciliates (Ciliophora: Choreotrichida) from the Isles of Shoals, Gulf of Maine. J. mar. biol. Ass. U.K. 68: 639-658
- Lynn, D. H., Montagnes, D. J. S., Small, E. B. (1988). Taxonomic descriptions of some conspicuous species in the family Strombidiidae (Ciliophora: Oligotrichida) from the Isles of Shoals, Gulf of Maine. J. mar. biol. Ass. U.K., 68: 259-276
- Lynn, D. H., Montagnes, D. J. S., Dale, T., Gilron, G. L., Strom, S. L. (1991). A reassessment of the genus *Strombidinopsis* Kent 1881 (Ciliophora, Choreotrichida) with descriptions of four new planktonic species and remarks on its taxonomic phylogeny. J. mar. biol. Ass. U.K. 71: 597-612
- Lynn, D. H., Corliss, J. O. (1991). Ciliophora: Chapter 5. In: Harrison, F. W. (ed.) Microscopic anatomy of invertebrates Vol. 1, 7. Wiley-Liss Inc., New York, p. 333-46

- Lynn, D. H., Montagnes, D. J. S. (1991). Global production of heterotrophic marine planktonic ciliates. In: Reid, P. C., Turley, C. M., Burkill, P. H. (ed.) *Protozoa and their role in marine processes*. NATO ASI publication, Springer Verlag, New York, p. 281-307
- Mackas, D. L., Denman, K. L., Abbott, M. R. (1985). Plankton patchiness: biology in the physical vernacular. *Bull. Mar. Sci.* 37: 652-674
- Maeda, M., Carey, P. G. (1985). An illustrated guide to the species of the family Strombidiidae (Oligotrichida, Ciliophora), free swimming protozoa common in the aquatic environment. *Bull. Ocean Res. Inst., Univ. Tokyo* 19: 1-68
- Maeda, M. (1986). An illustrated guide to the species of the Families Halteriidae and Strobiliidae (Oligotrichida, Ciliophora), free swimming protozoa common in the aquatic environment. *Bull. Ocean Res. Inst., Univ. Tokyo* 21: 1-67
- Martin, A. J., Montagnes, D. J. S. (1993). Winter ciliates and their putative prey in a British Columbian fjord: with descriptions of six species. *J. Euk. Microbiol.* in press
- McManus, G. B., Okubo, A. (1991). On the use of surrogate food particles to measure protistan ingestion. *Limnol. Oceanogr.* 36: 613-617
- Middlebrook, K., Roff, J. C. (1986). Comparison of methods for estimating annual productivity of the copepods *Acartia hudsonica* and *Eurytemora herdmanni* in Passamaquoddy Bay, New Brunswick. *Can J. Fish. Aquat. Sci.* 43: 656-664
- Montagnes, D. J. S., Lynn, D. H. (1987). A quantitative protargol stain (QPS) for ciliates: method description and test of its quantitative nature. *Mar. Microb. Food Webs* 2: 83-93
- Montagnes, D. J. S., Lynn, D. H., Roff, J. C., Taylor, W. D. (1988a). The annual cycle of heterotrophic planktonic ciliates in the waters surrounding the Isles of Shoals, Gulf of Maine: an assessment of their trophic role. *Mar. Biol.* 99: 21-30
- Montagnes D. J. S., Lynn, D. H., Stoecker, D. K., Small, E. B. (1988b). Taxonomic descriptions of one new species and redescription of four species in the family Strombidiidae (Ciliophora, Oligotrichida). *J. Protozool.* 35: 189-197
- Montagnes, D. J. S., Taylor, F. J. R., Lynn, D. H. (1990). *Strombidium inclinatum* n. sp. and a reassessment of *Strombidium sulcatum* Claparede and Lachmann (Ciliophora). *J. Protozool.* 37: 318-323
- Montagnes, D. J. S., Lynn, D. H. (1991). The taxonomy of the Choreotrichs, the major marine planktonic ciliates with emphasis on the aloricate forms. *Mar. Microb. Food Webs* 5: 59-74
- Montagnes, D. J. S., Lynn, D. H. (1993). A quantitative protargol stain (QPS) for ciliates and other protists. In: Kemp, P., Cole, J., Sherr, B., Sherr, E. (ed.) *Current methods in aquatic microbial ecology*. Lewis Publishers, Boca Raton, p. 229-240
- Montagnes, D. J. S., Berges, J. A., Harrison, P. J., Taylor, F. J. R. (1993). Estimating carbon, nitrogen, protein and chlorophyll *a* from cell volume in marine phytoplankton: a comparison of microscopic and electronic particle counting techniques and the effect of fixation with acid Lugol's iodine. *Limnol. Oceanogr.* (submitted)
- Müller, H., Geller, W. (1993). Maximum growth rates of aquatic ciliated protozoa: the dependence on body size and temperature reconsidered. *Arch. Hydrobiol.* 126: 315-327

- Mullin, M. M., Stewart, E. F., Fuglister, F. J. (1975). Ingestion by planktonic grazers as a function of concentration of food. *Limnol. Oceanogr.* 20: 259-261
- Nanny, D. L., (1980). Experimental ciliatology, and introduction to genetic and developmental analysis on ciliates. John Wiley and Sons, Toronto
- Nielsen, T. G., Richardson, K. (1989). Food chain structure of the North Sea plankton communities: seasonal variations of the role of the microbial loop. *Mar. Ecol. Prog. Ser.* 56: 75-87
- Nielsen, T. G., Kiorboe, T. (1991). Effects of a storm event on the structure of the pelagic food web with special emphasis on planktonic ciliates. *J. Plank. Res.* 13: 35-51
- Ohman, M. D., Snyder, R. A. (1991). Growth kinetics of the omnivorous oligotrich ciliate *Strombidium* sp. *Limnol. Oceanogr.* 36: 922-935
- Owen, R. W. (1989). Microscale and finescale variations of small plankton in coastal and pelagic environments. *J. Mar. Res.* 47: 197-240
- Pace, M. L., Bailiff, M. D. (1987). Evaluation of a fluorescent microsphere technique for measuring grazing rates of phagotrophic microorganisms. *Mar. Ecol. Prog. Ser.* 40: 185-193
- Paranjape, M. A. (1980). Occurrence and significance of resting cysts in a hyaline tintinnid, *Helicostomella subulata* (Ehre.) Jorgesen. *J. exp. mar. Biol. Ecol.* 48: 23-33
- Petz, W., Foissner, W. (1992). Morphology and morphogenesis of *Strobilidium caudatum* (Fromentel), *Meseres corlissi* n. sp., *Halteria grandinella* (Müller), and *Strombidium rehwaldi* n. sp. (Protozoa, Ciliophora). *J. Protozool.* 39: 159-176
- Pomeroy, L. (1974). The ocean's food web: a changing paradigm. *Biosci.* 24: 499-504
- Porter, K. G., Pace, M. L., Nauwerck, A. (1979). Ciliate protozoa as links in planktonic food chains. *Nature* 279: 563-565
- Putt, M., Stoecker, D. K. (1989). An experimentally determined carbon:volume ratio for marine "oligotrichous" ciliates from estuarine and coastal waters. *Limnol. Oceanogr.* 34: 333-355
- Putt, M. (1990). Metabolism of photosynthate in the chloroplast-retaining ciliate *Laboea strobila*. *Mar. Ecol. Prog. Ser.* 60: 271-282
- Putt, M. (1991). Development and evaluation of tracer particles for use in microzooplankton herbivory studies. *Mar. Ecol. Prog. Ser.* 77: 27-37
- Rassoulzadegan, F. (1982). Dependence of grazing rate, gross growth efficiency and food size range on temperature in a pelagic oligotrichous ciliate *Lohmanniella spiralis* Leeg., fed on naturally occurring particulate matter. *Ann. Inst. océanogr.* 58(S): 177-184
- Raymont, J. E. G. (1983) Plankton and productivity in the oceans 2nd ed., Vol. 2 Zooplankton. Pergamon Press, Oxford
- Reid, P. C., John, A. W. (1978). Tintinnid cysts. *J. mar. biol. Ass. U.K.* 58: 551-557
- Reid, P. C., John, A. W. G. (1983). Resting cysts in the ciliate class Polyhymenophorea: phylogenetic implications. *J. Protozool.* 30: 710-713

- Reid, P. C. (1987). Mass encystment of a planktonic oligotrich ciliate. *Mar. Biol.* 95: 221-230
- Repak, A. J. (1983). Suitability of selected marine algae for growing the marine heterotrich ciliate *Fabrea salina*. *J. Protozool.* 30: 52-54
- Riemann, B., Sorensen, H. M., Bjornsen, P. K., Horsted, J. S., Jensen, L. M., Nielsen, T. G., Sondergaard, M. (1990). Carbon budgets of the microbial food web in estuarine enclosures. *Mar. Ecol. Prog. Ser.* 65: 159-170
- Rivier, A., Brownlee, D. C., Sheldon, R. W., Rassoulzadegan, F. (1985). Growth of microzooplankton: a comparative study of bacterivorous zooflagellates and ciliates. *Mar. Microb. Food Webs* 1: 51-60
- Rublee, P. A., Gallagose, G. L. (1989). Use of fluorescently labeled algae (FLA) to estimate microzooplankton grazing. *Mar. Ecol. Prog. Ser.* 51: 221-227
- Schmidt-Nielsen, K. (1980). *Animal physiology: adaptation and environment*. Cambridge Univ. Press, New York
- Scott, J. M. (1985). The feeding rates and efficiencies of a marine ciliate, *Strombidium* sp., grown under chemostat steady-state conditions. *J. Exp. Mar. Biol. Ecol.* 90: 81-95
- Sheldon, R. W., Nival, P., Rassoulzadegan, F. (1986). An experimental investigation of a flagellate-ciliate-copepod food chain with some observations relevant to the linear biomass hypothesis. *Limnol. Oceanogr.* 31: 184-188
- Sherr, E. B., Sherr, B. F., McDaniel, J. (1991). Clearance rates of  $< 6 \mu\text{m}$  fluorescently labeled alga (FLA) by estuarine protozoa: potential grazing impact of flagellates and ciliates. *Mar. Ecol. Prog. Ser.* 69: 81-92
- Sherr, E. B., Sherr, B. F. (1993). Protistan grazing rates via uptake of fluorescently labeled prey. In: Kemp, P., Cole, J., Sherr, B., Sherr, E. (ed.) *Handbook of methods in aquatic microbial ecology*. Lewis Publishers, Boca Raton
- Sieracki, M. E., Hass, L. W., Caron, D. A., Lessard, E. J. (1987). Effects of fixation on particle retention by microflagellates: underestimation of grazing rates. *Mar. Ecol. Prog. Ser.* 38: 251-258
- Silver, M. W., Gowing, M. M., Brownlee, D. C., Corliss, J. O. (1984). Ciliated protozoa associated with oceanic sinking detritus. *Nature* 309: 246-248
- Sime-Ngando, T., Juiper, K., Vézina, A. (1992). Ciliated protozoan communities over Cobb Seamount: increase in biomass and spatial patchiness. *Mar. Ecol. Prog. Ser.* 89: 37-51
- Skogstad, A., Granskog, L., Klaveness, D. (1987). Growth of freshwater ciliates offered planktonic algae as food. *J. Plank. Res.* 9: 503-512
- Small, E. B., Lynn, D. H. (1985). Phylum Ciliophora. In: Lee, J. J., Hutner, S. H., Bovee, E. C. (ed.) *An illustrated guide to the Protozoa*. Soc. Protozool. Special Publ. Allen Press, Lawrence, Kansas, p. 395-575
- Smetacek, V. (1981). The annual cycle of protozooplankton in Kiel Bight. *Mar. Biol.* 63: 1-11
- Smetacek, V. (1984). Growth dynamics of a common Baltic protozooplankton: the ciliate genus *Lohmanniella*. *Limnologica* 15: 371-376
- Smith-Sonneborn, J. (1981). Genetics and aging in protozoa. *Int. Rev. Cytology* 73: 319-354

- Snyder, R. A., Ohman, M. O. (1991). Description of a new species of Strombidinopsidae (Ciliophora: Choreotrichida) from coastal waters of Southern California, U. S. A. Trans. Am. Microsc. Soc. 110: 237-243
- Spain, J. D. (1982). BASIC microcomputer models in biology. Addison-Wesley Publishing Co., London
- Steele, J. H., Gamble, J. C. (1982). Predation control in enclosures. In: Grice, G. D, Reeve, M. R., (ed.) Marine mesocosms, biological and chemical research in experimental ecosystems. Springer-Verlag, New York
- Stoecker, D. K. (1984). Particle production by planktonic ciliates. Limnol. Oceanogr. 29: 930-940
- Stoecker, D. K. (1988). Are marine planktonic ciliates suspension-feeders? J. Protozool. 35: 252-255
- Stoecker, D. K., Davis, H. L., Anderson, D. M. (1984). Fine scale spatial correlations between planktonic ciliates and dinoflagellates. J. Plank. Res. 6: 829-842
- Stoecker, D. K., Evans, G. T. (1985). Effects of protozoan herbivory and carnivory in a microplankton food web. Mar. Ecol. Prog. Ser. 25: 159-167
- Stoecker, D. K., Sunda, W. G., Davis, L. H. (1986). Effects of copper and zinc on two ciliates. Mar. Biol. 92: 21-29
- Stoecker, D. K., Egloff, D. A. (1987). Predation by *Acartia tonsa* Dana on planktonic ciliates and rotifers. J. Exp. Mar. Biol. Ecol. 110: 53-68
- Stoecker, D. K., Silver, M. W., Michaels, A. E., Davis, L. H. (1988). Obligate mixotrophy in *Laboea strobila*, a ciliate which retains chloroplasts. Mar. Biol. 99: 415-423
- Stoecker, D. K., Silver, M. W. (1990). Replacement and aging of chloroplasts in *Strombidium capitatum* (Ciliophora: Oligotrichida). Mar. Biol. 107: 491-502
- Stoecker, D. K., Michaels, A. E. (1991). Respiration, photosynthesis and carbon metabolism in planktonic ciliates. Mar. Biol. 108: 441-447
- Stout, J. D. (1980). The role of protozoa in nutrient cycling and energy flow. In: Alexander (ed.), Advances in microbial ecology Vol. 4, New York, Plenum Press, p. 1-50
- Strom, S. L., Welschmeyer, N. A. (1991). Pigment-specific rates of phytoplankton growth and microzooplankton grazing in the open subarctic Pacific Ocean. Limnol. Oceanogr. 36: 50-63
- Takahashi, K., Aizawa, Y. (1990). Excystment of tintinnid ciliates from marine sediment. Bull. Plankk. Soc. Japan 36: 137-139
- Takahashi, M., Seibert, D. L., Thomas, W. H. (1977). Occasional blooms of phytoplankton during summer in Saanich Inlet, B. C., Canada. Deep Sea Res. 24: 775-780
- Taniguchi, A., Takeada, Y. (1988). Feeding rate and behavior of the tintinnid ciliate *Favella taraikaensis* observed with a high speed VTR system. Mar. Microb. Food Webs 3: 21-34
- Taylor, G. T. (1982). The role of pelagic heterotrophic protozoa in nutrient cycling: a review. Ann. Inst. océanogr. 58(S): 227-241

- Taylor, W. D. (1978). Maximum growth rate, size and commonness in a community of bacterivorous ciliates. *Oecologia* 36: 263-272
- Taylor, W. D., Shuter, B. J. (1981). Body size, genome size, and intrinsic rate of increase in ciliated protozoa. *Amer. Nat.* 118: 160-172
- Thompson, P. A., Harrison, P. J. (1992). Effects of monospecific algal diets of varying biochemical composition on the growth and survival of Pacific oyster (*Crassostrea gigas*) larvae. *Mar. Biol.* 113: 645-654
- Tiselius, P. (1989). Contribution of aloricate ciliates to the diet of *Acartia clausi* and *Centropages hamatus* in coastal waters. *Mar. Ecol. Prog. Ser.* 56: 49-56
- Turley, C. M., Newell, R. C., Robins, D. B. (1986). Survival strategies of two small marine ciliates and their role in regulating bacterial community structure under experimental conditions. *Mar. Ecol. Prog. Ser.* 33: 59-70
- Turner, J. T., Granéli, E. (1992). Zooplankton feeding ecology: grazing during enclosure studies of phytoplankton blooms from the west coast of Sweden. *J. Exp. Mar. Biol. Ecol.* 157: 19-31
- Verity, P. G. (1985). Grazing, respiration, excretion, and growth rates of tintinnids. *Limnol. Oceanogr.* 30: 1268-1282
- Verity, P. G. (1986). Grazing of phototrophic nanoplankton by microzooplankton in Narragansett Bay. *Mar. Ecol. Prog. Ser.* 29: 105-115
- Verity, P. G. (1988). Aggregation patterns of ciliates from natural assemblages in response to different prey. *Mar. Microb. Food Webs* 5: 115-128
- Verity, P. G. (1991a). Measurement and simulation of prey uptake by marine planktonic ciliates fed plastidic and aplastidic nanoplankton. *Limnol. Oceanogr.* 36: 729-750
- Verity, P. G. (1991b). Aggregation patterns of ciliates from natural assemblages in response to different prey. *Mar. Microb. Food Webs* 5: 115-128
- Verity, P. G., Villareal, T. A. (1986). The relative food value of diatoms, dinoflagellates, flagellates and cyanobacteria for tintinnid ciliates. *Arch. Protistenkd.* 131: 71-84
- Verity, P. G., Robertson, C. Y., Tronzo, C. R., Andrews, M. G., Nelson, J. R., Seracki, M. E. (1993). Relationships between cell volume and the carbon and nitrogen content of marine photosynthetic nanoplankton. *Limnol. Oceanogr.* 37: 1434-1446
- Wailles, G. H. (1943). Canadian Pacific Fauna 1. Protozoa 1f Ciliata 1g Suctorina. *Fish. Res. Bd. Can.* 1-46
- Wiadnyana, N. N., Rassoulzadegan, F. (1989). Selective feeding of *Acartia clausi* and *Centropages typicus* on microzooplankton. *Mar. Ecol. Prog. Ser.* 53: 37-45
- Wichterman, R. (1986). The biology of *Paramecium*. Plenum Press, New York
- Wickham, S. A., Gilbert, J. J., Berninger, U. G. (1993). Effects of rotifers and ciliates on the growth and survival of *Daphnia*. *J. Plank. Res.* 15: 317-334

## APPENDIX 1

## THE GROWTH MEDIUM USED IN THIS STUDY TO GROW BOTH CILIATES AND PHYTOPLANKTON

Below is the recipe for HESNW<sup>1</sup> medium (modified) used by the Northeast Pacific Culture Collection (NEPCC, Department of Oceanography, University of British Columbia, Vancouver, British Columbia) to grow their phytoplankton stocks. It was also the medium I used for all my ciliates and phytoplankton cultures (unless otherwise stated). The sea water used to make the medium was obtained from West Vancouver Laboratory, Biological Science Branch, Department of Fisheries and Oceans, 4160 Marine Dr., West Vancouver; the water was pumped from Burrard Inlet, 100 m from the shore at a depth of 15 m. The final salinity of the medium was between 27-29 ‰.

ENRICHMENT STOCKS	Stock Conc. (g L <sup>-1</sup> )	Final Conc.(micromoles L <sup>-1</sup> )
1) NaNO <sub>3</sub>	46.67	549.09
2) Na <sub>2</sub> glycerophosphate	6.67	21.79
3) Na <sub>2</sub> SiO <sub>3</sub> .9H <sub>2</sub> O	30.00	105.60
* 4) Na <sub>2</sub> EDTA.2H <sub>2</sub> O	3.64	9.81
Fe(NH <sub>4</sub> ) <sub>2</sub> (SO <sub>4</sub> ) <sub>2</sub> .6H <sub>2</sub> O	2.34	5.97
FeCl <sub>3</sub> .6H <sub>2</sub> O	0.16	5.92 x 10 <sup>-1</sup>
5) MnSO <sub>4</sub> .4H <sub>2</sub> O	0.54	2.42
ZnSO <sub>4</sub> .7H <sub>2</sub> O	0.073	2.54 x 10 <sup>-1</sup>
CoSO <sub>4</sub> .7H <sub>2</sub> O	0.016	5.69 x 10 <sup>-2</sup>
Na <sub>2</sub> MoO <sub>4</sub> .2H <sub>2</sub> O	0.126	5.2 x 10 <sup>-1</sup>
** Na <sub>2</sub> EDTA.2H <sub>2</sub> O	1.89	5.05
6) H <sub>3</sub> BO <sub>3</sub>	3.80	61.46
7) Na <sub>2</sub> SeO <sub>3</sub>	0.00173	1.0 x 10 <sup>-2</sup>
VITAMIN STOCK		
Thiamine	0.1	2.97 x 10 <sup>-1</sup>
Vitamin B <sub>12</sub>	0.002	1.47 x 10 <sup>-3</sup>
Biotin	0.001	4.09 x 10 <sup>-3</sup>



Vitamin Stock should be stored frozen. Enrichment stocks can be refrigerated.

\* Add before the trace metals. Heat solution 4) to dissolve the iron. Adjust pH to 6.

#### Preparation of medium

- 1) Filter natural seawater through a 0.45 micrometer filter.
- 2) Autoclave medium flask with distilled water before first use.
- 3) Add 1 mL of each enrichment stock and 1 mL of vitamin stock L<sup>-1</sup> of seawater.
- 4) To prevent precipitation during autoclaving add: 0.12 g NaHCO<sub>3</sub> and 1.44 mL 1N HCl L<sup>-1</sup> of seawater.
- 5) Autoclave 20 min (for 1 L medium).
- 6) Let stand for at least 2 d before use (pH should be 8.2).
- 7) Medium may be filtered aseptically through a glass fiber filter to remove orange-brown precipitate.

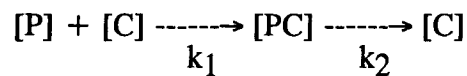
<sup>1</sup>Harrison, P. J., Waters, R. E., Taylor, F. J. R. (1980). A broad spectrum artificial medium for coastal and open ocean phytoplankton. J. Phycol. 16: 28-35

## APPENDIX 2

### CONSUMPTION AND FILTRATION: THEIR DERIVATION AND APPLICATION.

Below is a description of the derivation of Michaelis-Menten-like kinetics and their application to ciliate feeding. I have only described ciliate feeding. However, assuming that growth rate is a constant function of grazing (i.e. a constant gross growth efficiency, then this derivation should also apply to growth rate. The only modification to this would be that unlike feeding rate, growth rates may be negative (net mortality). Therefore, growth rates are likely to have non-zero intercepts.

Ciliate feeding has been modeled using Michaelis-Menten type equations to describe the "basic functional response curve" (Fenchel 1986, but see Holling 1959). Consumption rate (E) is the number of prey (P) consumed by a ciliate (C) per unit time ( $PC^{-1}T^{-1}$ ). If consumption is a combined process of non-selective prey encounter and ingestion then, it is controlled by two rate constants: encounter rate and ingestion rate. Assuming that: 1) particle capture is directly proportional to particle concentration; 2) encounter area and particle retention are invariant with particle concentration; and 3) ingestion takes a finite time during which further ingestion can not take place, then the consumption of particles may be depicted as



where [P] is prey concentration, [C] is ciliate concentration,  $k_1$  ( $VC^{-1}t^{-1}$ ) and  $k_2$  ( $PC^{-1}t^{-1}$ ) are rate constants (where t is time and V is volume).

In a steady state at concentration [P] each ciliate has a constant probability of capturing a prey. Then the velocities of these reactions are  $V_1$  and  $V_2$

$$V_1 = k_1[P][C] \text{ or } [C] = V_1/k_1[P]$$

$$V_2 = k_2[PC]$$

$$[P_{\text{total}}] = [P] + [PC]$$

$$[C_{\text{total}}] = [C] + [PC]$$

Assume  $[P_{\text{total}}] \approx [P]$  thus, [PC] is a small portion of  $[P] + [PC]$

In a steady state  $V_1 = V_2 = V = \text{consumption rate (E)}$

$$E = k_2([C_{\text{total}}] - [C])$$

$$E = k_2([C_{\text{total}}] - E/k_1[P])$$

$$E + k_2E/k_1[P] = k_2([C_{\text{total}}]) \text{ or } E(1 + k_2/k_1[P]) = k_2([C_{\text{total}}])$$

$$E = k_2([C_{\text{total}}]/((1 + k_2/k_1[P])))$$

multiplying by  $k_1[P]$

$$E = k_1[P]k_2([C_{\text{total}}]/(k_2 + k_1[P]))$$

dividing by  $k_1$

$$E = [P]k_2([C_{\text{total}}]/(k_2/k_1 + [P]))$$

dividing by total ciliates to get E as "per ciliate"

$$E = [P]k_2/(k_2/k_1 + [P])$$

where  $k_2 = E_m$  = maximum ingestion rate and  $k$  is  $k_2/k_1$

$$E[P] = E_m [P]/(k + [P]) \quad (\text{A2.1})$$

If there is a minimum threshold on food (i.e. at a certain low food concentration ( $[P']$ ))

where feeding stops, then

$$E[P] = E_m([P] - [P'])/(k + ([P] - [P'])) \quad (\text{A2.2})$$

Jonsson (1986) has conducted feeding experiments on the ciliate *Strobilidium* (= *Lohmanniella*) *spiralis*; his results can be explained using the above terminology. Typically, the velocity of the first reaction, determined by  $k_1$ , was much slower than the second reaction, determined by  $k_2$ . However, when food concentration was high  $k_2$  determined the rate of ingestion. For *S. spiralis*, eating 14.4  $\mu\text{m}$  prey, ingestion rate was one cell  $\sim 15 \text{ s}^{-1}$  ( $k_2 = 0.067 \text{ prey C}^{-1}\text{s}^{-1}$ ). Jonsson found that the maximum clearance rate varied with prey size. Therefore, the "filter" did not have the same efficiency for all prey.

Equation A2.1 is based on the assumptions that  $k_1$  and  $k_2$  are invariant. For a particular prey it is likely that  $k_2$ , the time it takes a ciliate to ingest ("handle" and phagocytose) prey is constant; at least it is for *Favella* (Taniguchi and Takeda 1988). However,  $k_1$ , the rate at which filtration occurs may change.

Of course, the whole notion of filtration rate may be erroneous since oligotrichs may not filter feed. The presence of striae (Capriulo *et al.* 1986) and other extrusomes (Montagnes

*et al.* 1988) used for prey capture suggests raptorial feeding. Chemosensory abilities also suggest a selectivity, and thus non-filtering, mechanisms (Verity 1988). Therefore, the amount of food ingested could have little to do with the amount of medium "filtered". Non-filter feeding does not necessarily discount the model developed above (Eq. A2.1). It does however, imply that  $k_1$  may vary.

Studies have examined the clearance rates ( $k_1$ ?) for planktonic ciliates. They range from 1 to 100  $\mu\text{l h}^{-1}$  (see Jonsson 1986, Stoecker 1988). For the tintinnid *Favella* the time between prey capture and complete engulfment ( $k_2$ ?) was ~700 ms (Taniguchi and Takeda 1988). Jonsson (1988) has recommended that more data are needed to estimate these parameters; especially for the small,  $<20 \mu\text{m}$ , oligotrichs which seem to be ubiquitous. In general, more studies need to be conducted to determine if the Michaelis-Menten relation holds true and to determine if  $k_1$  and  $k_2$  vary.

#### LITERATURE CITED

- Capriulo, G. M., Traveras, J., Gold, K. (1986). Ciliate feeding: effect of food presence or absence on occurrence of striae in tintinnids. *Mar. Ecol. Prog. Ser.* 30: 145-158
- Fenchel, T. (1986). Protozoan filter feeding. In: Corliss, J. O., Patterson, D. J. (ed) *Progress in Protistology Vol. 1*, Biopress Ltd., Bristol, p. 66-113
- Holling, C. S. (1959). Some characteristics of simple types of predation and parasitism. *Can. Entomol.* 41: 385-399
- Jonsson, P. R. (1986). Particle size selection, feeding rates and growth dynamics of marine planktonic oligotrichous ciliates (Ciliophora: Oligotrichina). *Mar. Ecol. Prog. Ser.* 33: 265-277
- Montagnes D. J. S., Lynn, D. H., Stoecker, D. K., Small, E. B.. (1988). Taxonomic descriptions of one new and redescription of four species in the family Strombidiidae (Ciliophora, Oligotrichida). *J. Protozool.* 35: 189-197
- Stoecker, D. K. (1988). Are marine planktonic ciliates suspension-feeders? *J. Protozool.* 35: 252-255
- Taniguchi, A., Takeada, Y. (1988). Feeding rate and behavior of the tintinnid ciliate *Favella taraiakaensis* observed with a high speed VTR system. *Mar. Microb. Food Webs* 3: 21-34
- Verity, P. G. (1988). Aggregation patterns of ciliates from natural assemblages in response to different prey. *Mar. Microb. Food Webs* 5: 115-128

### APPENDIX 3

#### THE ANNUAL CYCLE OF OLIGOTRICHS AND $<10\ \mu\text{m}$ PHYTOPLANKTON IN SECHELT INLET, A BRITISH COLUMBIAN FJORDAL SYSTEM

Work conducted in conjunction with: R. Haigh<sup>1</sup>, F. J. R. Taylor<sup>1</sup>, and T. F. Sutherland<sup>2</sup>

<sup>1</sup>Department of Oceanography, University of British Columbia, Vancouver, B.C., V6T 1Z4, Canada. <sup>2</sup>Dept. Oceanography, Dalhousie University, Halifax, N.S., B3H 4J1, Canada

#### INTRODUCTION

This appendix provides a description of the changes in abundance and biomass of ciliates and their putative prey ( $<10\ \mu\text{m}$  phytoplankton) over 1.3 years, in Sechelt Inlet. Sechelt Inlet is typical of many fjordal inlets and should therefore provide representative estimates of ciliate and prey abundance and biomass for much of British Columbia's waters. This analysis is strictly exploratory; its goals were to establish initial ("typical") ciliate and prey concentrations for the population model presented in Chapter 9 and to recognize the naturally occurring range of these two trophic groups.

Sechelt Inlet (Fig. A3.1) is a southern British Columbian fjord located 40 km northwest of Vancouver. It consists of a main inlet and two adjoining ones, Narrows and Salmon Inlets; these are collectively referred to as the Sechelt Inlet complex. The main inlet is 29 km long, on average 1.2 km wide, has a maximum depth of 300 m, and has a shallow (14 m) sill at its entrance. Three distinct water layers exist in the inlet: a surface layer (~5 m) of low-salinity water (due to precipitation and river runoff); an intermediate layer occupying a depth between ~5 and 65 m; and a deep layer of resident water, characterized by uniform temperature and salinity (Lazier 1963). Estuarine circulation in Sechelt Inlet is slight due to the relatively low freshwater drainage ( $110\ \text{m}^3\ \text{s}^{-1}$ , Pickard 1961), and depends largely on the intrusion of a tidal jet that flushes the indigenous deep water zone (Lazier 1963).

Temperature, salinity, chlorophyll *a*, nitrate, ammonium and phosphate were measured over the 18 months of this study. The method of analysis and results of these measurements are presented elsewhere (Haigh *et al.* 1992).

## MATERIALS AND METHODS

Water samples were collected from 6 stations in Sechart Inlet (49° 40' N, 123° 45' W, Fig. A3.1) between April 1989 and September 1990. Samples were taken using the segmented integrated pipe sampler (SIPS, Sutherland *et al.* 1992). This system is composed of eight segments of PVC tubing (inside diameter 3.75 cm). The segments are connected by snap-together joints and have a closing device at the bottom of each segment. The two surface segments are 1.5 m long and the remaining six tubes are 3.0 m (total length 21 m). The segments were connected together and lowered into the water to collect eight integrated samples. Each segment's contents were released into a bucket for sub-sampling aboard the boat. A sample was also taken from 30 m with a 1 L Niskin bottle. For details of the sampling procedure see Haigh *et al.* (1992) and Sutherland *et al.* (1992)

Subsamples (125 mL) from the bucket were preserved with 1 % acid Lugol's and ciliate and phytoplankton abundances were analyzed using the Utermöhl technique (Hasle 1978). Depending on the biomass, 2.5 to 10 mL were settled in a counting chamber for  $\geq 12$  h. Ciliate prey ( $< 10 \mu\text{m}$ ) were counted at 500x along one or two 10-20 mm transects. Ciliates were counted at either 240x along six transects across the chamber diameter (25-26 mm) or at 95x, examining the entire chamber bottom. Oligotrich ciliates (see Chapter 2) were divided into three groups:  $< 25 \mu\text{m}$ , 25-50  $\mu\text{m}$ , and  $> 50 \mu\text{m}$  in diameter. The counts were then transformed to cells  $\text{mL}^{-1}$  and were integrated over depths, assuming that samples from segments of the SIPS were representative of the entire depths sampled and the sample bottle represented the bottom 9 m.

The plankton data were converted to carbon using species specific cell volumes. Where possible, representative cells were measured for each species and the volume was calculated using equations for simple geometric shapes. For a number of the less common species, dimensions were extracted from the literature (dinoflagellates: Dodge 1982; nanoflagellates: Watanabe 1976, Throndsen 1988). Phytoplankton volumes were converted to carbon using the relation:  $\text{C (pg)} = 0.109 * (\text{live cell volume, } \mu\text{m}^3)^{0.991}$  and recognizing that

Lugol's fixed cells are 80% of live volume, from Montagnes *et al.* (submitted). Ciliate volumes were converted to carbon using the relation:  $C \text{ (pg)} = 0.19 * (\text{volume, } \mu\text{m}^3)$ , from Putt and Stoecker (1989).

The data were presented in two ways: 1) as the change with time of average abundance (cells  $\text{mL}^{-1}$ ) or biomass (pg carbon  $\text{mL}^{-1}$ ) from the integrated water column (either 6 or 30 m, see below) and 2) as correlations between prey and ciliate abundance or biomass for every sample taken over the 18 month sampling period ( $n = 1056$ ). As stated above, these data were used as baseline estimates for the model presented in Chapter 9.

## RESULTS AND DISCUSSION

Ciliate and prey abundance and biomass were fairly constant throughout the year, although they both tended to be higher in the summer (Figs. A3.2, A3.3). Both prey and ciliate abundance and biomass occasionally increased by one or two orders of magnitude above seasonal averages (Figs. A3.2, A3.3, A3.4). Possibly these ciliate pulses were due to population growth (blooms).

Since the top ~5 m of the inlet was probably physically distinct from the deeper waters (see Materials and Methods), the abundance and biomass of organisms were exclusively examined from the top 3 segments of the SIPS (top 6 m), to better elucidate population dynamics. Average integrated ciliate and prey abundance and biomass in the top 6 m were typically higher than those in the top 30 m but showed similar seasonal trends (Figs. A3.5, A3.6).

The abundance and biomass of ciliates that were 25-50  $\mu\text{m}$  in diameter (similar in size to those examined in Chapters 3-7) were examined. Over the top 30 m of the inlet, both abundance and biomass of 25-50  $\mu\text{m}$  ciliates varied by up to 3 orders of magnitude (Fig. 3A.4). However, in the top 6 m the average integrated biomass and abundance of 25-50  $\mu\text{m}$  ciliates rarely varied by more than one order of magnitude (Figs. A3.7-8).

On average the ratios of total ciliate:prey abundance and biomass were near 10:1000  $\text{mL}^{-1}$  and  $10^4:10^4$  ng C, respectively. The ratios of 25-50  $\mu\text{m}$  ciliate:prey abundance and

biomass were near  $1:1000 \text{ mL}^{-1}$  and  $3 \times 10^3:10^4$ , respectively (Fig. A3.4). These may be considered "typical" levels for modeling (see Chapter 9).

Many of the parameters observed in this study (e.g. the ciliate:prey ratio, the ciliate and prey concentrations, and the higher ciliate numbers in upper waters) agree with those observed in other cold water studies (Revelante and Gilmartin 1987, Andersen and Sorensen 1986, Haigh and Taylor 1991, Lynn and Montagnes 1991 [and references within], Verity and Vernet 1992, Martin and Montagnes 1993).

Since ciliates have rapid numerical responses, they may potentially exhibit a positive correlation with their prey (Stoecker *et al.* 1984). Studies support this notion: significant correlations existed between abundances of naked ciliates and  $< 20 \mu\text{m}$  prey in an estuary in Maine (Revelante and Gilmartin 1987), and on a global level ciliate and phytoplankton biomass were positively correlated (Lynn and Montagnes 1991). The Sechelt data also show significant ( $\alpha = 0.05$ ) positive correlations (but not good predictors  $r^2 = 0.38-0.55$ ) between ciliate abundance and biomass and their prey (Fig. A3.4). Further, there were some instances where ciliate and prey populations simultaneously increased, but there did not appear to be regular coupling in the abundance or biomass of ciliates and prey (Figs. A3.2-3, A3.5-8), as might be expected (Andersen and Sorensen 1986). As there are undoubtedly periods where blooms of ciliates have grazed down their prey, but have not crashed themselves, there should also be times when ciliates and their prey are negatively correlated. Such situations can be seen in the output of the model presented in Chapter 9. Given that the Sechelt data were collected weeks to months apart and ciliate-prey interactions likely occur on the order of days (Andersen and Sorensen 1986, Chapter 9), it is not surprising that such coupled trends, if they existed, were not obvious. The data do provide an indication of the range and "typical" concentrations of these two trophic groups in British Columbian coastal waters. In Chapter 9, these values have been compared to the output of the model.



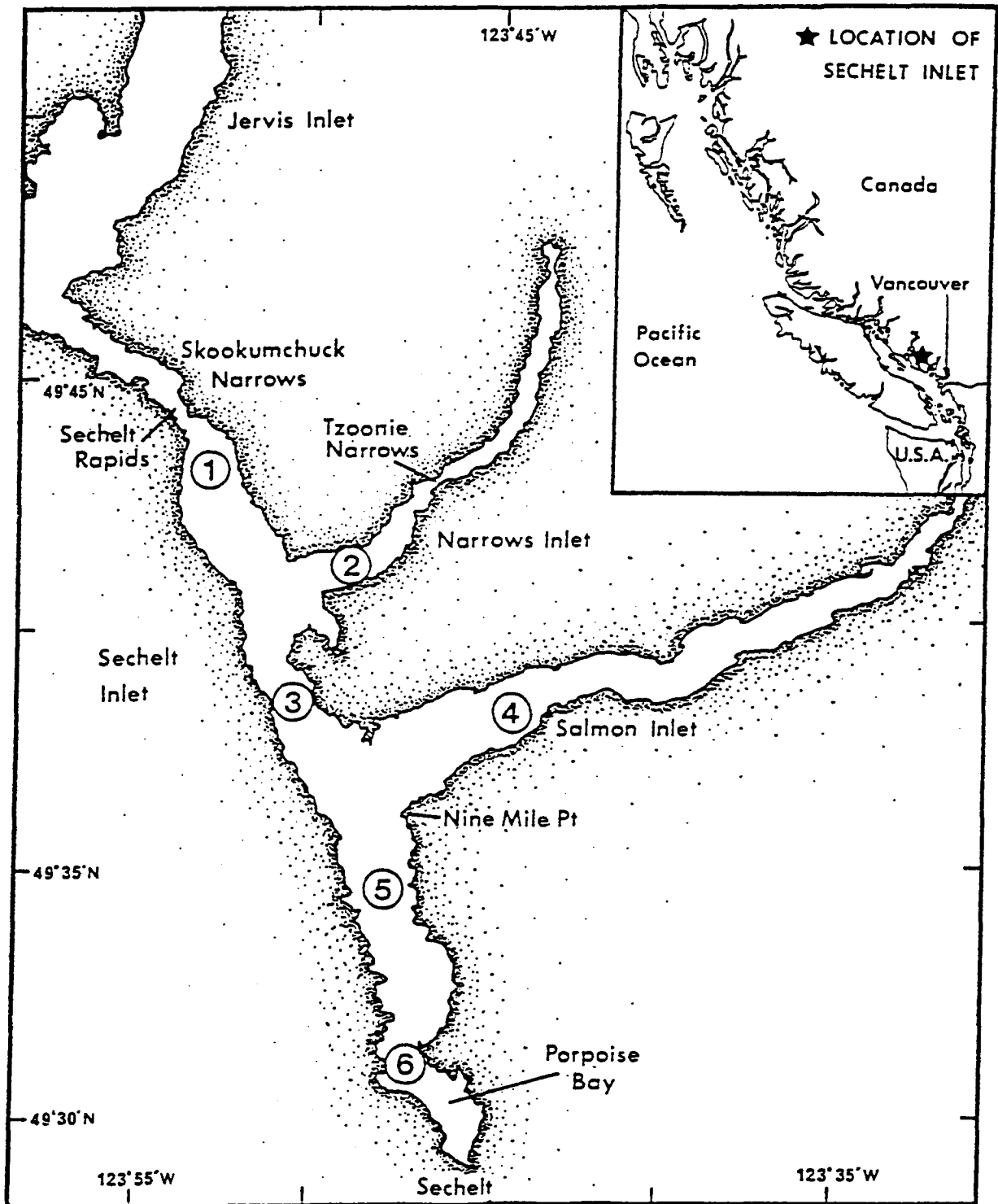


Fig. A3.1. Sechelt Inlet Complex with station locations (1-6).

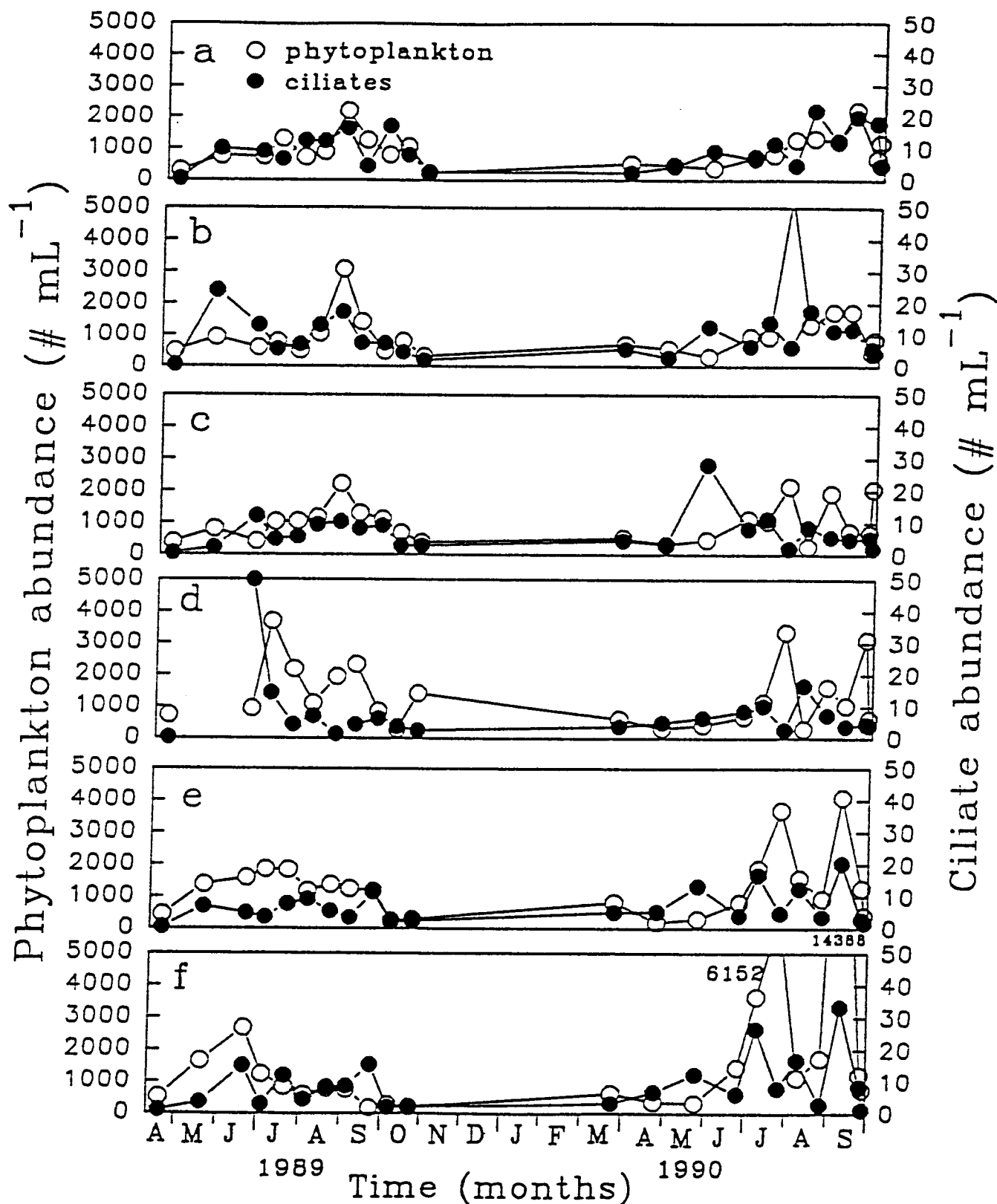


Fig. A3.2. The seasonal cycle of ciliate and small ( $<10\ \mu\text{m}$ ) phytoplankton abundance (numbers  $\text{mL}^{-1}$  as an average from integrating a 30 m water column) at 6 sites in Sechart Inlet (a-f = 1-6, respectively; see Fig. A3.1). Open circles represent phytoplankton numbers. Solid circles represent ciliate numbers. Values above or beside peaks off the panel indicate the magnitude of these measurements.

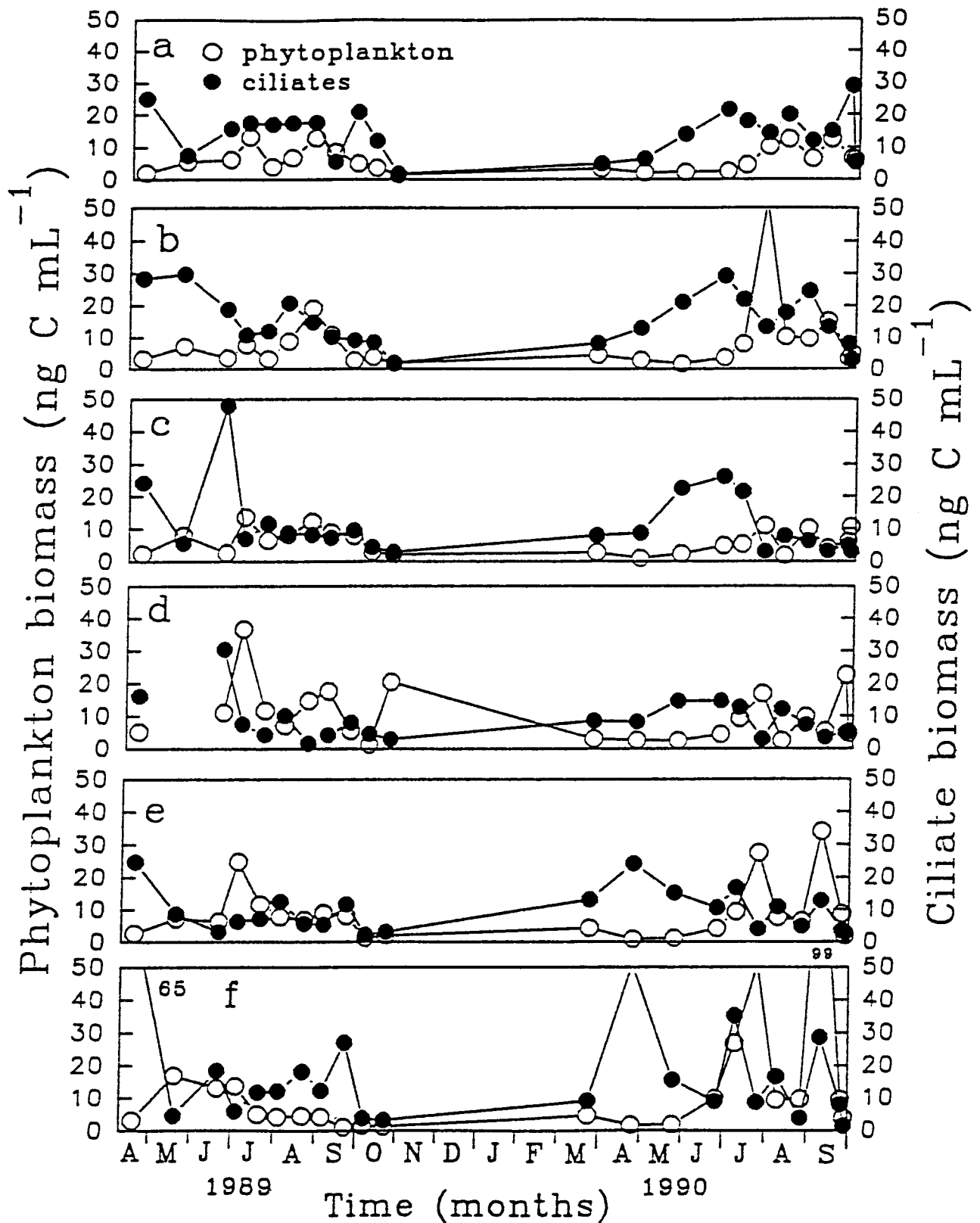


Fig. A3.3. The seasonal cycle of ciliate and small ( $< 10 \mu\text{m}$ ) phytoplankton biomass (ng carbon mL<sup>-1</sup>) as an average from integrating a 30 m water column) at 6 sites in Sechart Inlet (a-f = 1-6, respectively; see Fig. A3.1). Open circles represent phytoplankton numbers. Solid circles represent ciliate numbers. Values above or beside peaks off the panel indicate the magnitude of these measurements.

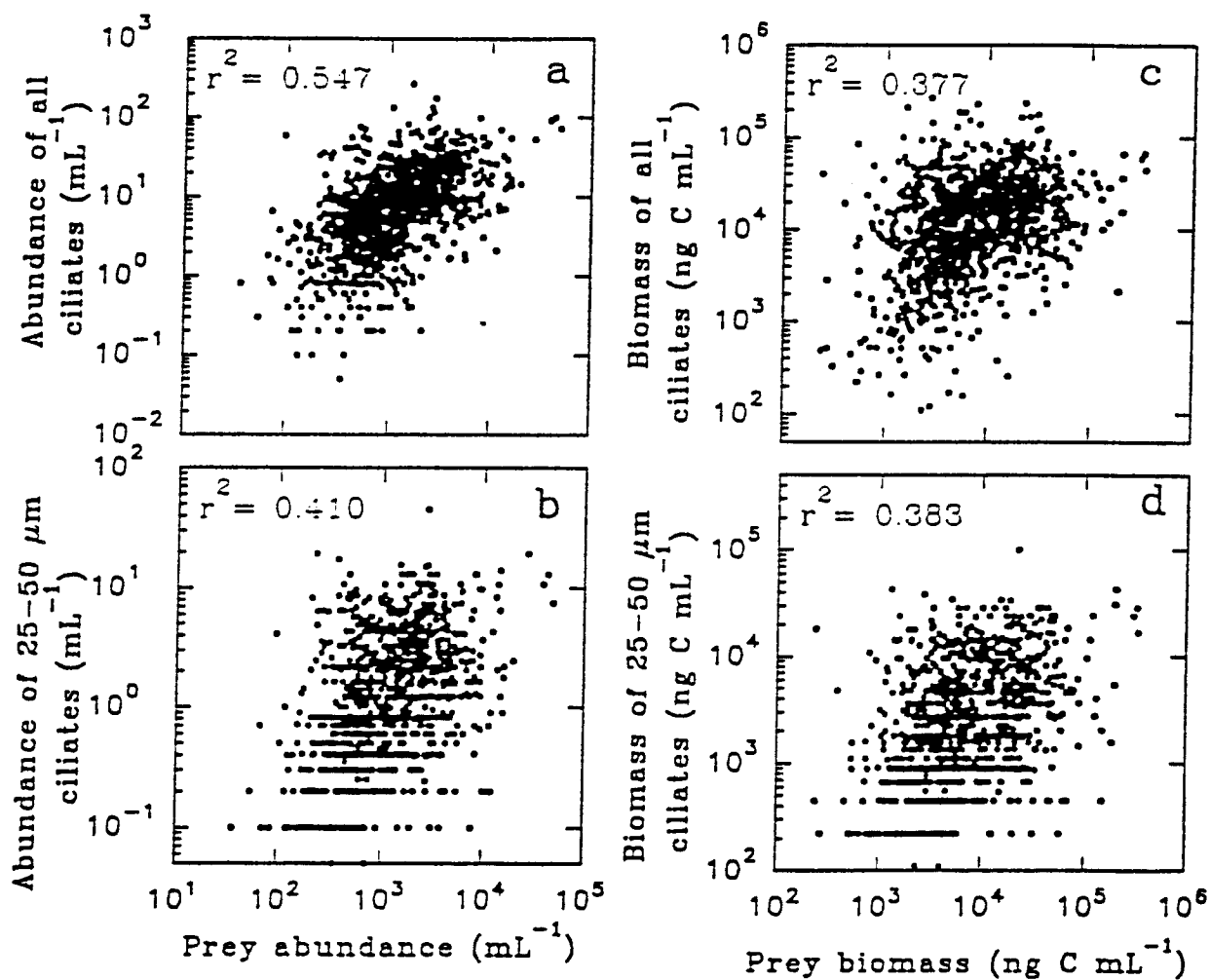


Fig. A3.4. Four correlations between ciliates and their putative prey ( $< 10 \mu\text{m}$  phytoplankton) using data from every sample taken over the 18 month sampling period ( $n = 1056$ ). a, the abundance of all oligotrich ciliates vs. the prey abundance; b, the abundance of 25-50  $\mu\text{m}$  (diameter) oligotrich ciliates vs. the prey abundance; c, the biomass of all oligotrich ciliates vs. the prey biomass; the biomass of 25-50  $\mu\text{m}$  (diameter) oligotrich ciliates vs. the prey biomass. The  $r^2$  values for each regression are presented in the appropriate panels; all four correlations were significant at  $\alpha = 0.05$ .

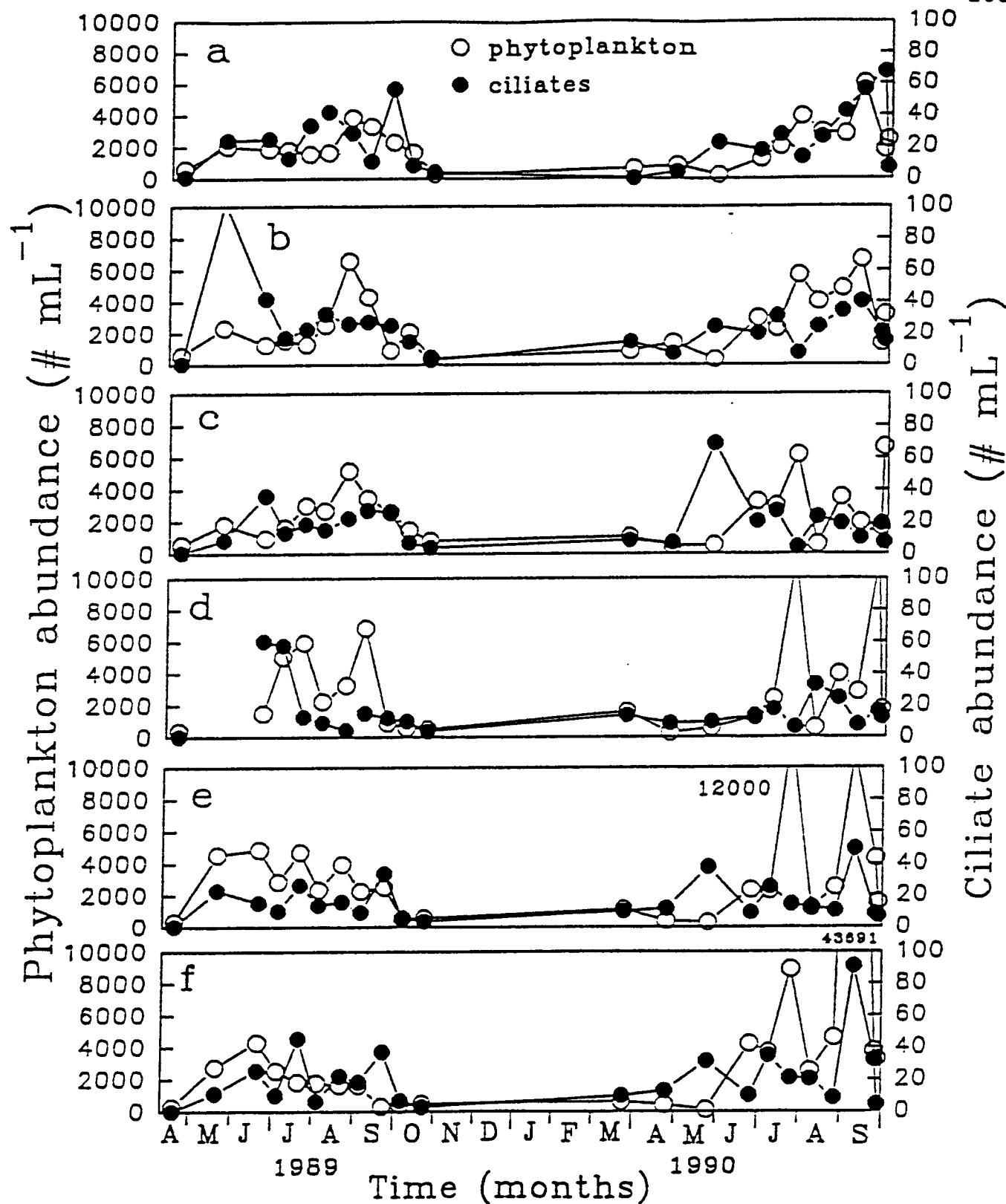


Fig. A3.5. The seasonal cycle of ciliate and small ( $<10\ \mu\text{m}$ ) phytoplankton abundance (numbers  $\text{mL}^{-1}$  as an average from integrating a 6 m water column) at 6 sites in Sechart Inlet (a-f = 1-6, respectively; see Fig. A3.1). Open circles represent phytoplankton numbers. Solid circles represent ciliate numbers. Values above or beside peaks off the panel indicate the magnitude of these measurements.

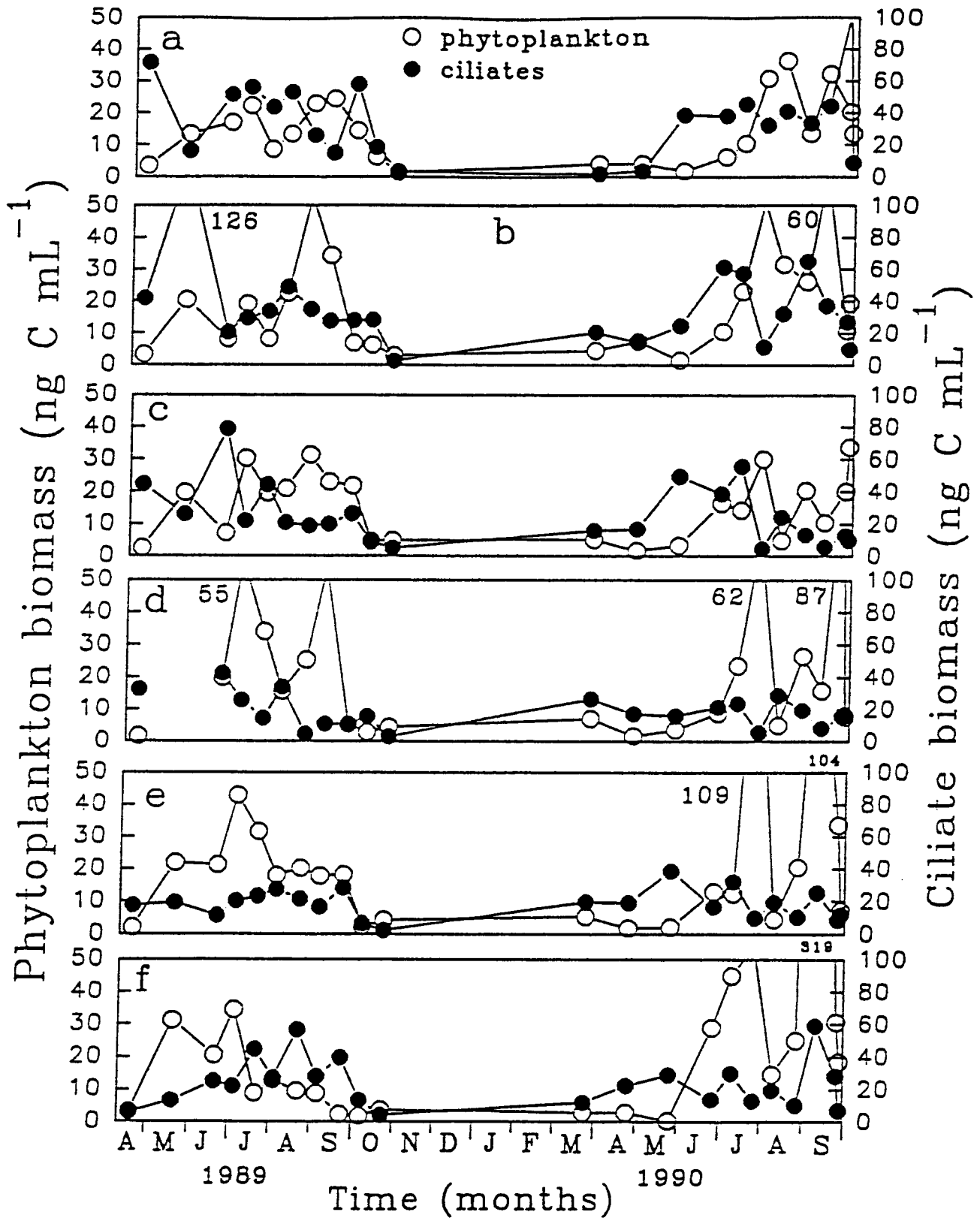


Fig. A3.6. The seasonal cycle of ciliate and small ( $<10\ \mu\text{m}$ ) phytoplankton biomass ( $\text{ng carbon mL}^{-1}$  as an average from integrating a 6 m water column) at 6 sites in Sechart Inlet (a-f = 1-6, respectively; see Fig. A3.1). Open circles represent phytoplankton numbers. Solid circles represent ciliate numbers. Values above or beside peaks off the panel indicate the magnitude of these measurements.

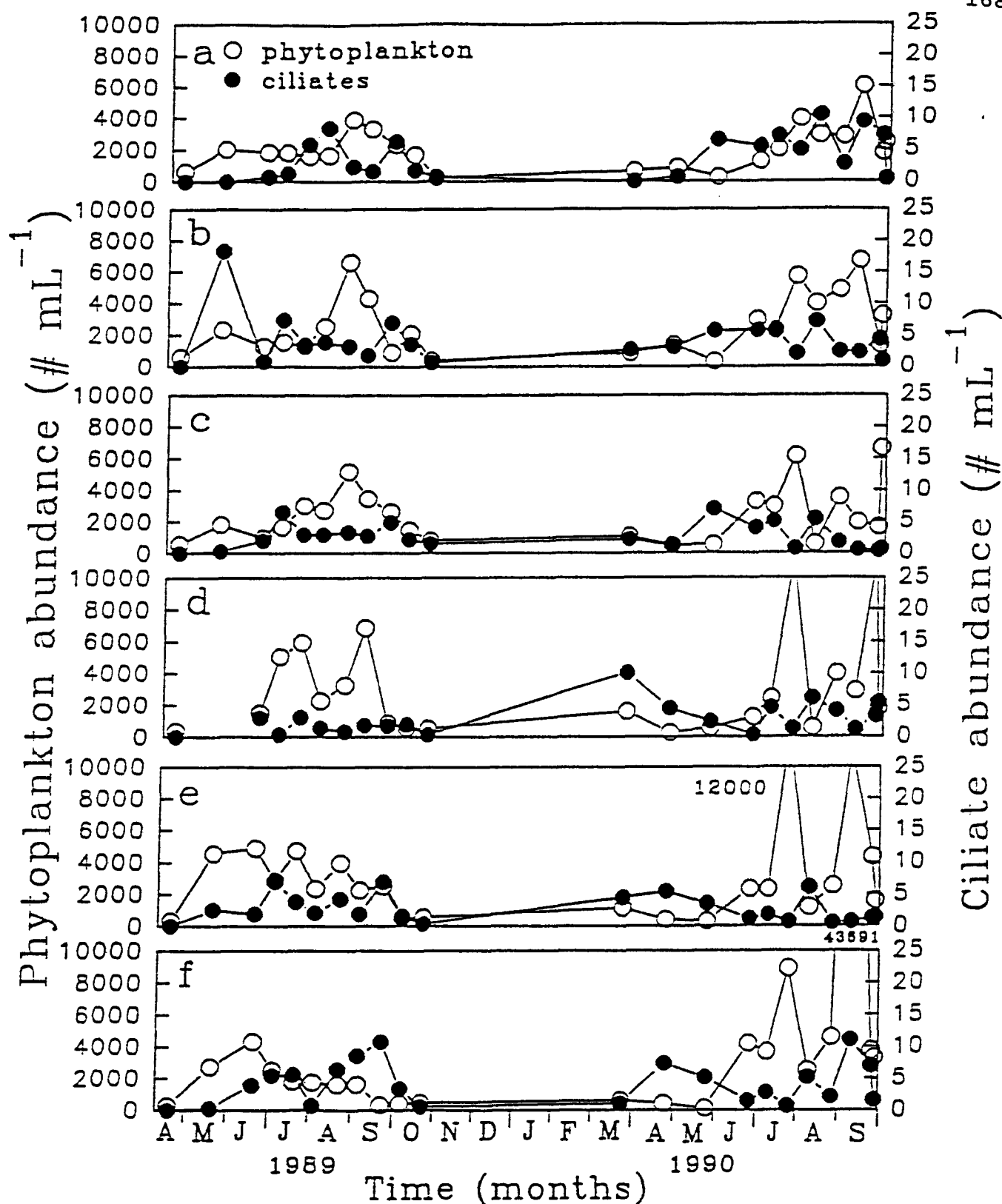


Fig. A3.7. The seasonal cycle of 25-50  $\mu\text{m}$  (diameter) ciliate and small ( $< 10 \mu\text{m}$ ) phytoplankton abundance (numbers  $\text{mL}^{-1}$  as an average from integrating a 6 m water column) at 6 sites in Sechart Inlet (a-f = 1-6, respectively; see Fig. A3.1). Open circles represent phytoplankton numbers. Solid circles represent ciliate numbers. Values above or beside peaks off the panel indicate the magnitude of these measurements.

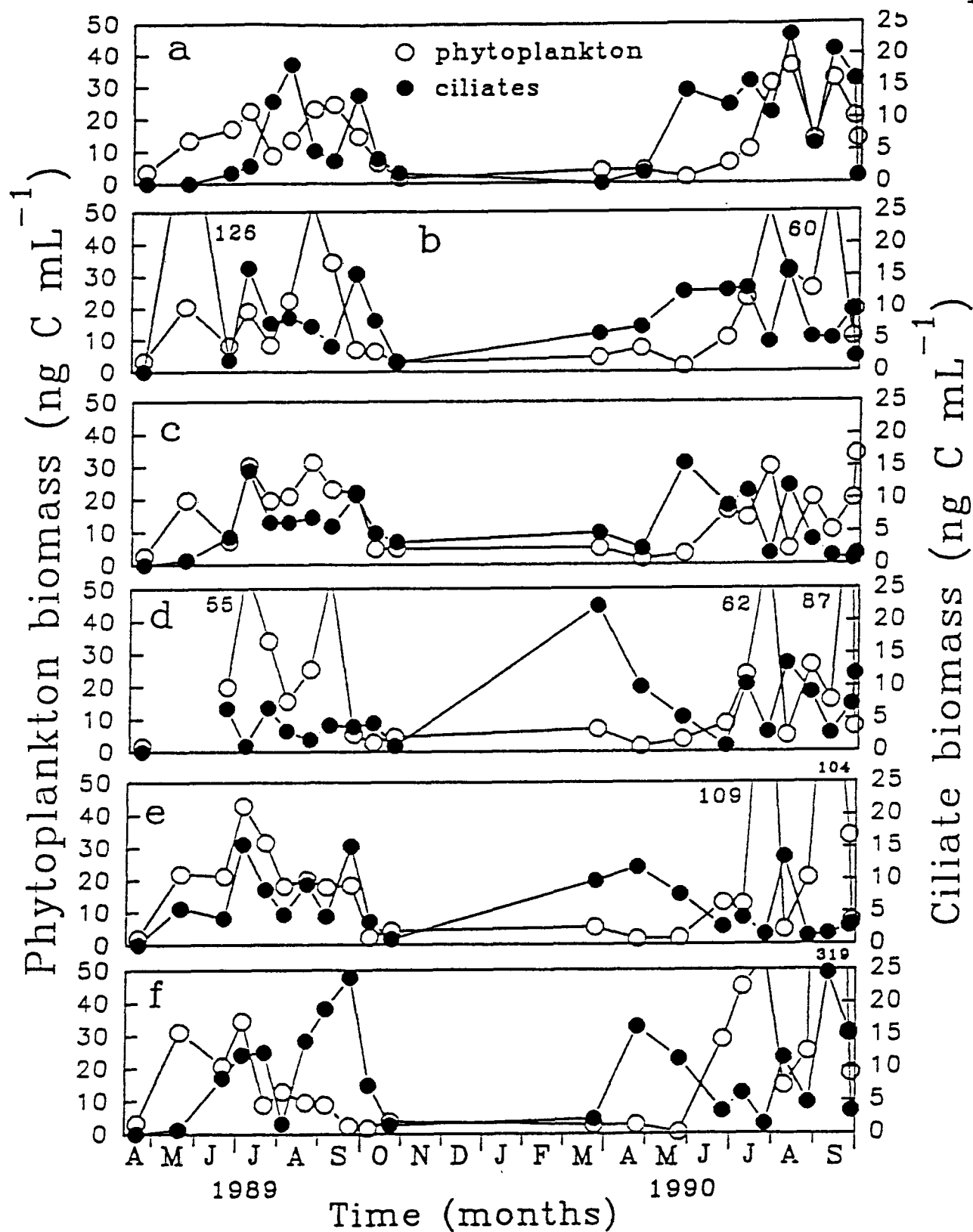


Fig. A3.8. The seasonal cycle of 25-50  $\mu\text{m}$  (diameter) ciliate and small ( $< 10 \mu\text{m}$ ) phytoplankton biomass (ng carbon  $\text{mL}^{-1}$ ) as an average from integrating a 6 m water column) at 6 sites in Sechart Inlet (a-f = 1-6, respectively; see Fig. A3.1). Open circles represent phytoplankton numbers. Solid circles represent ciliate numbers. Values above or beside peaks off the panel indicate the magnitude of these measurements.



## LITERATURE CITED

- Andersen, P., Sorensen, H. M. (1986). Population dynamics and trophic coupling in pelagic microorganisms in eutrophic coastal waters. *Mar. Ecol. Prog. Ser.* 33: 99-109
- Dodge, J. D. (1982). *Marine dinoflagellates of the British Isles*. Her Majesty's Stationery Office, London
- Haigh, R., Taylor, F. J. R. (1991). Mosaicism of microplankton communities in the northern Strait of Georgia, British Columbia. *Mar. Biol.* 110: 301-314
- Haigh, R., Taylor, F. J. R., Sutherland, T. E. (1992). Phytoplankton ecology of Sechart Inlet, a fjord system on the British Columbia coast. I. General features of the nano- and microplankton. *Mar. Ecol. Prog. Ser.* 89: 117-134
- Hasle, G. R. (1978). Using the inverted microscope. In: Sournia, A. (ed.) *Phytoplankton Manual*. Monographs on Oceanographic Methodology 6, UNESCO, p. 191-196
- Lazier, J. R. N. (1963). Some aspects of the oceanographic structure in the Jervis Inlet system. M. Sc. thesis, Univ. British Columbia
- Lynn, D. H., Montagnes, D. J. S. (1991). Global production of heterotrophic marine planktonic ciliates. In: Reid, P. C., Turley, C. M., Burkill, P. H. (ed.) *Protozoa and their role in marine processes*, NATO ASI publication, Springer Verlag, New York p. 281-307
- Martin, A. J., Montagnes, D. J. S. (1992). Winter ciliates and their putative prey in a British Columbian fjord: with descriptions of six species. *J. Euk. Microbiol.* in press
- Montagnes, D. J. S., Berges, J. A., Harrison, P. J., Taylor, F. J. R. (1993). Estimating carbon, nitrogen, protein and chlorophyll *a* from cell volume in marine phytoplankton: a comparison of microscopic and electronic particle counting techniques and the effect of fixation with acid Lugol's iodine. *Limnol. Oceanogr.* (submitted)
- Pickard, G. L. (1961). Oceanographic features of inlets in the British Columbia mainland coast. *J. Fish. Res. Board Can.* 18: 907-999
- Putt, M., Stoecker, D. K. (1989). An experimentally determined carbon:volume ratio for marine "oligotrichous" ciliates from estuarine and coastal waters. *Limnol. Oceanogr.* 34: 333-355
- Revelante, N., Gilmartin, M. (1987). Seasonal cycle of the ciliated protozoan and micrometazoan biomass in a Gulf of Maine Estuary. *Estuar. Coast. Shelf Sci.* 25: 581-598
- Stoecker, D. K., Davis, H. L., Anderson, D. M. (1984). Fine scale spatial correlations between planktonic ciliates and dinoflagellates. *J. Plank. Res.* 6: 829-842
- Sutherland, T. A., Leonard, C., Taylor, F. J. R. (1992). A segmented integrating pipe sampler for profiling the upper water column. *J. Plankton Res.* 14: 915-923
- Thronsdon, J. (1988). *Cymbomonas* Schiller (Prasinophyceae) reinvestigated by light and electron microscopy. *Arch. Protistenkd.* 136: 327-336
- Verity, P. G., Vernet, M. (1992). Microzooplankton grazing, pigment, and composition of communities during late spring in two Norwegian fjords. *Sarsia* 77: 263-274

Watanabe, L. N. (1976). Theoretical and practical aspects of nanophytoflagellate taxonomy and ecology on the British Columbia coast. Unpubl. Manusc.

## APPENDIX 4

### THE CODE FOR A BASIC MODEL TO INVESTIGATE THE ROLE OF CILIATES AS GRAZERS OF SMALL PHYTOPLANKTON

#### Model Description

There were five types of organisms in the system I have modeled (Fig. 9.1, Chapter 9): phytoplankton (prey), ciliate A, B, C, (see Table 8.4, Chapter 8) and a copepod species (see Chapter 9). The prey were small (8  $\mu\text{m}$  in diameter) and during the simulation had a constant growth rate of  $\mu = 0.7 \text{ d}^{-1}$  (near one division day<sup>-1</sup>). Algal mortality was by predation from the ciliates (see section 2.0, Chapter 8) and the copepod (see Chapter 9). Ciliate growth rates were functions of prey concentration (see Chapters 8 and 9). For all three ciliates, mortality was due to starvation (a function of prey concentration, Table 8.4) and to predation by the copepod (a function of ciliate concentration and size). There was no growth or mortality of the copepods over the simulation period. For a full explanation of the model see Chapter 9.

#### The Model in BASIC code

```

DECLARE SUB model ()
DIM SHARED x(20), d(20), z1(20), z2(20), z3(20), z4(20), z5(20), z6(20),
z7(20), p(15), zoo
DIM z(15, 900), zm(5)
SCREEN 9
COLOR 1, 63
INPUT "enter time step, as fraction of a day (eg .05):", dt

OPEN "c:\user\david\link3.dat" FOR OUTPUT AS #10

'this sets the time step and numerical integration constants
IF dt = 0 THEN dt = .1
z2 = dt / 2: z6 = dt / 6
zoo = 0: icount = 0: p(12) = .6

'number of variables
nd = 18:

'this opens a file and imports growth and grazing parameters
g$ = COMMAND$
IF g$ = "" THEN LOCATE 1, 1: INPUT "enter ciliate parameter file name (e.g.
ciliate.dat):", g$
OPEN g$ FOR INPUT AS 1
FOR i = 1 TO 11: INPUT #1, p(i), id$: NEXT

```

CLOSE 1

```

LOCATE 2, 1: INPUT "enter number of days to simulate for (e.g. 18 or 36):",
ndays
start:
LOCATE 24, 1: PRINT "
";
LOCATE 24, 1: INPUT "enter prey  $\mu$ , initial algae, ciliates and copepods (e.g.
0.6,1000,1,1,1,0.001):", p(12), x(5), x(1), x(2), x(3), zoo
labu = p(12): labp = x(5): lab1 = x(1): lab2 = x(2): lab3 = x(3)
IF p(12) = 0 THEN END

'this set initial state of (ciliates=1, algae=input value * this value) for
maximum value output and gross phytoplankton output
zm(1) = 0: zm(2) = 0: zm(3) = 0: zm(5) = 0: x(4) = 0: x(6) = 0: x(7) = 0: x(8)
= 0: x(9) = 0: x(10) = 0: x(11) = 0: x(12) = 0
x(13) = 0: x(14) = 0: x(15) = 0
d(1) = 0: d(2) = 0: d(3) = 0: d(4) = 0: d(5) = 0: d(6) = 0: d(7) = 0: d(8) =
0: d(9) = 0: d(10) = 0: d(11) = 0: d(12) = 0
d(13) = 0: d(14) = 0: d(15) = 0

'this integrates the equations for "ndays" days using the 5th order Runge-
Kutta method
FOR time = 0 TO ndays / dt
t = time * dt: Z9 = t: model
  FOR i = 1 TO nd: Z1(i) = d(i): Z7(i) = x(i): z2(i) = x(i) + Z1(i) * z2: x(i)
= z2(i): NEXT: t = Z9 + z2: model
  FOR i = 1 TO nd: Z3(i) = d(i): Z4(i) = Z7(i) + Z3(i) * z2: x(i) = Z4(i):
NEXT: model
  FOR i = 1 TO nd: Z5(i) = d(i): z6(i) = Z7(i) + Z5(i) * dt: x(i) = z6(i):
NEXT: t = Z9 + dt: model
  FOR i = 1 TO nd: x(i) = Z7(i) + (Z1(i) + 2 * Z3(i) + 2 * Z5(i) + d(i)) * z6:
NEXT

'this prevents prey numbers from becoming negative and should not be necessary
if the time step is small enough
IF x(1) < 0 THEN x(1) = 0
IF x(2) < 0 THEN x(2) = 0
IF x(3) < 0 THEN x(3) = 0
IF x(5) < 0 THEN x(5) = 0

'this places the data into a matrix z(1,2,3,5 time)
z(1, time) = x(1): z(2, time) = x(2): z(3, time) = x(3): z(4, time) = x(4):
z(5, time) = x(5)
z(6, time) = x(6): z(7, time) = x(7): z(8, time) = x(8): z(9, time) = x(9):
z(10, time) = x(10)
z(11, time) = x(11): z(12, time) = x(12): z(13, time) = x(13): z(14, time) =
x(14): z(15, time) = x(15)

'this prints the daily output to the screen
IF icount > 1 / dt THEN PRINT z(1, time); z(2, time); z(3, time); z(4, time);
z(5, time)
icount = icount + 1: IF icount > 1 / dt + 1 THEN icount = 0

'this records the maximum number [zm(i)] of prey and ciliates
IF x(1) > zm(1) THEN zm(1) = x(1)
IF x(2) > zm(2) THEN zm(2) = x(2)

```



```

17.368) + ((z(14, (ndays / dt)) + lab2) * 16.302) + ((z(15, (ndays / dt)) +
lab3) * 2.91))))
'LOCATE 20, 33: PRINT "3"; citocp
'link = INT(100 * (((17.368 * z(7, (ndays / dt))) + (16.302 * z(8, (ndays /
dt))) + (2.91 * z(9, (ndays / dt)))) / ((17.368 * z(7, (ndays / dt))) +
(16.302 * z(8, (ndays / dt))) + (2.91 * z(9, (ndays / dt))) + (z(6, (ndays /
dt)) * .027778))))
'LOCATE 21, 33: PRINT "4"; link
tcopeat = INT(((17.368 * z(7, (ndays / dt))) + (16.302 * z(8, (ndays / dt))) +
(2.91 * z(9, (ndays / dt))) + (z(6, (ndays / dt)) * .027778))
ccopeat = INT(((17.368 * z(7, (ndays / dt))) + (16.302 * z(8, (ndays / dt))) +
(2.91 * z(9, (ndays / dt)))) * 100) / 100
pcopeat = INT((z(6, (ndays / dt)) * .027778) * 100) / 100
cileat = INT(((z(10, (ndays / dt)) + z(11, (ndays / dt)) + z(12, (ndays /
dt))) * .027778) * 100) / 100
pp = INT(((z(4, (ndays / dt)) + labp) * .027778) * 100) / 100
FOR i = 1 TO 5
FOR time = 0 TO ndays / dt
    t = time * dt
    x = t / ndays * 300
    y = 200 * (1 - z(i, time) / (zm(i) + .00001))
    IF time = 0 THEN PSET (x, y) ELSE LINE -(x, y)
    IF i = 1 THEN CIRCLE (x, y), 1
    IF i = 2 THEN CIRCLE (x, y), 2
    IF i = 3 THEN CIRCLE (x, y), 3
    IF i = 4 THEN CIRCLE (x, y), 4
NEXT
NEXT
PRINT #10, zoo, labp, ((z(13, (ndays / dt))) + lab1) * 17.368, ((z(14, (ndays
/ dt))) + lab2) * 16.302, ((z(15, (ndays / dt))) + lab3) * 2.91, (((z(13,
(ndays / dt))) + lab1) * 17.368) + ((z(14, (ndays / dt)) + lab2) * 16.302) +
((z(15, (ndays / dt)) _
) + lab3) * 2.91)
'PRINT #10, zoo, labp, pp, tcopeat, ccopeat, pcopeat, cileat
'PRINT #10, zoo, labp, pptocp, pptoci, citocp, link, INT(((z(4, (ndays / dt))
+ labp) * .027778) * 100) / 100
'this section allows the data to be printed to a file
'LOCATE 24, 3: INPUT "type the file name for output or `0' for no
output"; fileout$
'OPEN fileout$ FOR OUTPUT AS #2
'PRINT #2, "time", "ciliate A", "ciliate B", "ciliate C", "prey"
'FOR outi = 0 TO ndays / dt
'PRINT #2, outi, z(1, outi), z(2, outi), z(3, outi), z(5, outi)
'NEXT outi
'CLOSE #2
GOTO start
'CLOSE #10

SUB model

'this section calculates the derivatives of ciliate [x(1), x(2) and x(3) etc.]
'it then place these derivatives in d(1), d(2) and d(3)
'Note that p(i)'s are from the ciliate parameter file (e.g. cili.dat)

'these are the formulae for ciliate A
'Ciliate A growth rate as function of prey x(5)
xcl = x(5) - p(2)

```

```

    ucil1 = (p(1) * xc1) / (p(3) + xc1)
    'Ciliate A grazing rate as function of its growth rate
    gcil1 = x(1) * (((ucil1 * 625) + (176 / p(10))) / p(11))
    IF gcil1 < 0 THEN gcil1 = 0
    IF x(5) <= 0 THEN gcil1 = 0

    'these are the formulae for ciliate B
    'Ciliate B growth rate as function of algae x(5)
    xc2 = x(5) - p(5)
    ucil2 = (p(4) * xc2) / (p(6) + xc2)
    'Ciliate B grazing rate as function of its growth rate
    gcil2 = x(2) * (((ucil2 * 587) + (170 / p(10))) / p(11))
    IF gcil2 < 0 THEN gcil2 = 0
    IF x(5) <= 0 THEN gcil2 = 0

    'these are the formulae for ciliate C
    'Ciliate C growth rate as function of algae x(5)
    xc3 = x(5) - p(8)
    ucil3 = (p(7) * xc3) / (p(9) + xc3)
    'Ciliate C grazing rate as function of its growth rate
    gcil3 = x(3) * (((ucil3 * 105) + (48 / p(10))) / p(11))
    IF gcil3 < 0 THEN gcil3 = 0
    IF x(5) <= 0 THEN gcil3 = 0

    xcop = x(5) - 767: IF xcop < 0 THEN xcop = 0
    DEN = 1 + ((1 / 785) * xcop) + ((1 / 45) * x(1)) + ((1 / 45) * x(2)) + ((1 / 100) * x(3))
    'these are the formulae for the copepods grazing prey as a function of prey
    x(5) concentration
    gcopp = ((3312000 / 785) * xcop) / DEN

    'this is the formula for the copepods grazing ciliate A as a function of
    ciliate A x(1) concentration
    gcopc1 = ((14400 / 45) * x(1)) / DEN

    'this is the formula for the copepods grazing ciliate B as a function of
    ciliate B x(2) concentration
    gcopc2 = ((14400 / 45) * x(2)) / DEN

    'this is the formula for the copepods grazing ciliate C as a function of
    ciliate C x(3) concentration
    gcopc3 = ((30000 / 100) * x(3)) / DEN

    'these are the derivatives combining growth and grazing rates
    d(1) = (ucil1 * x(1)) - (d(7))
    d(2) = (ucil2 * x(2)) - (d(8))
    d(3) = (ucil3 * x(3)) - (d(9))
    d(4) = p(12) * x(5)
    d(5) = (p(12) * x(5)) - ((gcil1) + (gcil2) + (gcil3) + (gcopp * zoo))
    IF x(5) >= 50000 THEN d(5) = 0 - (gcil1) - (gcil2) - (gcil3) - (gcopp
* zoo)
    IF x(5) >= 50000 THEN d(4) = 0
    d(6) = (gcopp * zoo)
    d(7) = (gcopc1 * zoo)
    d(8) = (gcopc2 * zoo)
    d(9) = (gcopc3 * zoo)

```

```
d(10) = gcil1  
d(11) = gcil2  
d(12) = gcil3  
d(13) = (ucil1 * x(1)): IF d(13) < 0 THEN d(13) = 0  
d(14) = (ucil2 * x(2)): IF d(14) < 0 THEN d(14) = 0  
d(15) = (ucil3 * x(3)): IF d(15) < 0 THEN d(15) = 0
```

```
END SUB
```